

Copyright statement

This copy of the thesis has been supplied on condition that anyone who consults it is understood to recognize that its copyright rests with the author and due acknowledgement must always be made of the use of any material contained in, or derived from, this thesis.

Validation and application of the MERIS
Terrestrial Chlorophyll Index

Samuel Almond

Conservation Science
Bournemouth University

A thesis submitted for the partial fulfillment of the requirements
of Bournemouth University for the Degree of Doctorate of
Philosophy

October 2009

Abstract

Climate is one of the key variables driving ecosystems at local to global scales. How and to what extent vegetation responds to climate variability is a challenging topic for global change analysis. Earth observation provides an opportunity to study temporal ecosystem dynamics, providing much needed information about the response of vegetation to environmental and climatic change at local to global scales. The European Space Agency (ESA) uses data recorded by the Medium Resolution Imaging Spectrometer (MERIS) in red / near infrared spectral bands to produce an operational product called the MERIS Terrestrial Chlorophyll Index (MTCI). The MTCI is related to the position of the red edge in vegetation spectra and can be used to estimate the chlorophyll content of vegetation. The MTCI therefore provides a powerful product to monitor phenology, stress and productivity.

The MTCI needs full validation if it is to be embraced by the user community who require precise and consistent, spatial and temporal comparisons of vegetation condition. This research details experimental investigations into variables that may influence the relationship between the MTCI and vegetation chlorophyll content, namely soil background and sensor view angle, vegetation type and spatial scale. Validation campaigns in the New Forest and at Brooms Barn agricultural study site reinforced the strong correlation between chlorophyll content and MTCI that was evident from laboratory spectroscopy investigations, demonstrating the suitability of the MTCI as a surrogate for field chlorophyll content measurements independent of cover type. However, this relationship was significantly weakened where the leaf area index (LAI) was low, indicating that the MTCI is sensitive to the effects of soil background.

In the light of such conclusions, this project then assessed the MTCI as a tool to monitor changes in ecosystem phenology as a function of climatic variability, and the suitability of the MTCI as a surrogate measure of photosynthetic light use efficiency, to model ecosystem gross primary productivity (GPP) at various sites in North America with contrasting vegetation types. Changes in MTCI throughout the growing season demonstrated the potential of the MTCI to estimate vegetation dynamics, characterising the temporal characteristics in both phenology and gross primary productivity.

Table of contents

| | |
|--|-----------|
| Acknowledgements | 15 |
| List of acronyms | 17 |
| | |
| CHAPTER 1: INTRODUCTION | 19 |
| 1.1 The need for monitoring of terrestrial vegetation..... | 21 |
| 1.2 Effects of climate change upon terrestrial vegetation | 22 |
| 1.3 Phenology and productivity..... | 22 |
| 1.4 Carbon budgets | 23 |
| 1.5 Chlorophyll..... | 24 |
| 1.6 The role of remote sensing | 24 |
| | |
| CHAPTER 2: THE REMOTE SENSING OF CANOPY CHLOROPHYLL | |
| CONTENT | 27 |
| 2.1 Reflectance at the leaf scale..... | 28 |
| 2.1.1 Photosynthetic pigments and their radiometric signature..... | 28 |
| 2.1.2 Leaf structure | 30 |
| 2.1.3 The red edge | 33 |
| 2.1.4 Middle-infrared region | 34 |
| 2.2 Spectral properties of the vegetated canopy | 34 |
| 2.2.1 Canopy variables that influence observed reflectance | 34 |
| 2.2.2 Non-canopy variables influencing observed canopy reflectance | 35 |
| 2.3 Remote sensing of terrestrial vegetation | 41 |
| 2.3.1 The role of ‘Moderate’ spatial resolution satellite sensors..... | 41 |
| 2.3.2 Imaging spectrometry | 42 |
| 2.4 Methods for the estimation of content using remote sensing | 44 |
| 2.4.1 Vegetation indices | 44 |
| 2.4.2 Red edge position techniques | 47 |
| 2.4.3 Modelling approaches..... | 48 |
| 2.5 The MERIS Sensor | 50 |
| 2.6 The MERIS Terrestrial Chlorophyll Index (MTCI)..... | 52 |
| 2.6.1 Evaluation of the MTCI..... | 54 |

Contents

| | |
|--|-----------|
| 2.6.2 MTCI operational uncertainties | 55 |
| 2.7 Chapter Summary | 56 |
| 2.8 Research Objectives | 58 |
| 2.9 Thesis plan | 60 |
| | |
| CHAPTER 3: EVALUATION OF THE RELATIONSHIPS BETWEEN CANOPY CHLOROPHYLL CONTENT AND THE MTCI AND THE EFFECT OF VIEW ANGLE AND SOIL BACKGROUND | 61 |
| 3.1 Introduction | 62 |
| 3.2 Chapter aims | 63 |
| 3.3 Method..... | 64 |
| 3.3.1 Spectral measurement..... | 65 |
| 3.3.2 Chlorophyll measurement..... | 68 |
| 3.3.3 Spectral indices..... | 72 |
| 3.3.4 Statistical analysis..... | 73 |
| 3.4 Results and discussion | 74 |
| 3.4.1 Relationship between chlorophyll content and the MTCI..... | 76 |
| 3.4.2 The effects of soil reflectance on the MTCI..... | 82 |
| 3.4.3 Effect of view angle on the MTCI..... | 84 |
| 3.4.4 Evaluating the performance of spectral indices to infer chlorophyll content | 85 |
| 3.4.5 The effect of soil background upon the relationship between chlorophyll and vegetation indices | 87 |
| 3.4.6 The influence of view angle on the relationship between chlorophyll and vegetation indices | 88 |
| 3.5 Conclusions | 92 |
| | |
| CHAPTER 4: MULTI-SCALE ANALYSIS AND VALIDATION OF THE MERIS TERRESTRIAL CHLOROPHYLL INDEX IN WOODLAND AND ARABLE STUDY SITES | 94 |
| 4.1 Introduction | 95 |
| 4.2. Chapter aims | 96 |
| 4.3 Study Areas..... | 97 |
| 4.3.1 New Forest..... | 97 |

Contents

| | |
|---|-----|
| 4.3.2 Brooms Barn..... | 98 |
| 4.4 Methods | 101 |
| 4.4.1 Sampling design | 101 |
| 4.4.2 Remote sensing data | 104 |
| 4.4.3 Ground data collection..... | 104 |
| 4.4.4 Data processing at the New Forest | 108 |
| 4.4.4.1 CASI-2 data processing..... | 108 |
| 4.4.4.2 Ground data processing | 112 |
| 4.4.4.3 Chlorophyll map production..... | 112 |
| 4.4.4.4 Assessing the relationship between chlorophyll content and MTCI | 113 |
| 4.4.8 Data processing at Brooms Barn | 115 |
| 4.5 Results and discussion | 117 |
| 4.5.1 New Forest..... | 117 |
| 4.5.2 Brooms Barn..... | 124 |
| 4.6 Discussion of chapter aims | 127 |
| 4.7 Limitations of the study | 133 |
| 4.8 Conclusions | 135 |

CHAPTER 5: MTCI AS A TOOL TO MONITOR PHENOLOGICAL CHANGE

| | |
|---|------------|
| | 137 |
| 5.1 Introduction | 138 |
| 5.1.1 Vegetation phenology and productivity | 138 |
| 5.1.2 Remote sensing and phenology | 139 |
| 5.1.3 Vegetation phenology..... | 141 |
| 5.1.4 Determining phenological phases using remote sensing..... | 142 |
| 5.1.5 The relationship between MTCI and phenology | 143 |
| 5.2 Chapter aims | 143 |
| 5.3 The study areas | 144 |
| 5.3.1 The New Forest | 144 |
| 5.3.2 Ancillary study areas | 145 |
| 5.4 Methods | 150 |
| 5.4.1 Study area selection | 150 |
| 5.4.2 Remotely sensed data | 151 |
| 5.4.3 Auxiliary data | 153 |

Contents

| | |
|--|-----|
| 5.4.4 Estimating phenological phases from MTCI time series data..... | 154 |
| 5.4.5 Predicting MTCI using mean temperature observations..... | 156 |
| 5.5 Results and Discussion..... | 156 |
| 5.5.1 Woodlands..... | 156 |
| 5.5.2 Grass and heathlands..... | 160 |
| 5.5.3 Accounting for inter-annual variation..... | 161 |
| 5.5.4 Variation in phenological transition dates..... | 165 |
| 5.5.5 Comparison of MTCI and MOD13 phenological profiles..... | 169 |
| 5.5.6 Predicting MTCI using temperature data..... | 173 |
| 5.6 Conclusions..... | 175 |

CHAPTER 6: EXAMINATION OF THE RELATIONSHIP BETWEEN GROSS PRIMARY PRODUCTIVITY AND MTCI IN VARIOUS ECOSYSTEMS..... 177

| | |
|---|-----|
| 6.1 Introduction..... | 178 |
| 6.2 Chapter aims..... | 181 |
| 6.3 Study sites..... | 182 |
| 6.3.1 Grassland site..... | 182 |
| 6.3.2 Coniferous boreal site..... | 183 |
| 6.3.3 Deciduous study site..... | 183 |
| 6.3.4 Mixed woodland site..... | 183 |
| 6.4 Method..... | 184 |
| 6.4.1 Flux and site data..... | 184 |
| 6.4.2 Remotely sensed data..... | 185 |
| 6.4.3 Calculation of site specific light use efficiency..... | 186 |
| 6.5 Results and discussion..... | 187 |
| 6.5.1 Inter-annual variability in the relationship between flux tower GPP and MTCI..... | 187 |
| 6.5.2 The relationship between flux tower GPP estimates, MTCI and PAR.... | 193 |
| 6.5.3 The relationship between GPP and MTCI and APAR..... | 193 |
| 6.5.4 Accounting for the relationship between expected and actual GPP using LUE..... | 199 |
| 6.5.5 Comparison of developed models with MODIS GPP product..... | 203 |
| 6.5.6 Potential limitations and further work..... | 206 |
| 6.6 Conclusions..... | 208 |

| | |
|--|------------|
| CHAPTER 7: THESIS SUMMARY..... | 210 |
| 7.1 Summary of work..... | 211 |
| 7.2 Objectives of the thesis..... | 213 |
| 7.3 Limitations and uncertainties | 217 |
| 7.4 Principal contributions..... | 218 |
| 7.5 Further Research..... | 219 |
| 7.6 Concluding comments | 220 |
| | |
| REFERENCES | 221 |
| APPENDICES..... | 257 |
| Appendix 1 – Wet chemistry assay results..... | 258 |
| Appendix 2 – AZGCORR code..... | 260 |
| Appendix 3 – Radiometric variation between MERIS and CASI-2..... | 261 |
| Appendix 4 - Publications | 262 |
| Appendix 5 - SPSS results | 261 |

List of figures

Figure 2.1. Cross-section of a typical leaf. Major structural leaf components are highlighted and their interaction with light in the visible – NIR domain identified.31

Figure 2.2. Spectral reflectance of a green vegetation and dry bare soil in the visible – NIR region of the reflectance spectrum derived from laboratory spectroscopy of spinach leaves. 32

Figure 2.3. Angular effect caused by sensor characteristics, orbital patterns and illumination geometry. Note that figures quoted in (a) are based on the MERIS sensor. 39

Figure 2.4. Vegetation reflectance spectra at four chlorophyll contents, increasing content 1-4, together with the location of the MERIS bands 8, 9 and 10, located in the red edge region of the spectra. 52

Figure 3.1. Diagrammatic representation of the set up of the apparatus used in the laboratory experiment. 67

Figure 3.2. The Minolta SPAD to estimate chlorophyll concentration in spinach leaves. 68

Figure 3.3. Illustration of the flow line that is used in ArcGIS to derive LAI. 71

Figure 3.4. The growth of spinach grown in non-fertilised soil. 74

Figure 3.5. Mean spectral reflectance profiles for spinach grown on non-fertilised soils (NF), weeks 1-4. 75

Figure 3.6. Variation in MTCI (a), and chlorophyll content (b) for spinach grown in various soils as derived from GER 1500 reflectance 77

Figure 3.7. Change in LAI (a) chlorophyll concentration (b) over the duration of the laboratory experiment for spinach plants. 78

Figure 3.8. The relationship between MTCI and chlorophyll content (a), chlorophyll concentration (b) and LAI for all soil backgrounds. 79

Figure 3.9. The relationship between MTCI and total chlorophyll content for spinach grown on various soil backgrounds. 81

Figure 3.10. Relationship between total chlorophyll content and MTCI was improved when removing results from white soils. 3

Figure 3.11. The spectral reflectance profiles of a variety of bare soil sample used in this investigation..... 3

Figure 3.12. MTCI at seven different sensor view angles for spinach: week 1 (▲); week 2 (◆); week 3 (■) and week 4 (+) 85

Figure 3.13. Comparison of the performance of vegetation indices for the estimation of chlorophyll content..... 86

Figure 3.14. The effect of soil background upon the relationship with chlorophyll content and spectral indices..... 88

Figure 3.15. The change in observed canopy reflectance in visible and NIR wavelengths due to changing viewing geometry from ±30 degrees of nadir in the principle plane. 89

Figure 3.16. Change in spectral vegetation index values as a function of view angle ... 90

Figure 4.1. Frame Wood, New Forest, MTCI validation study area in southern England showing the location of individual sampling units (ISU) used to derive ground chlorophyll content..... 99

Figure 4.2. Brooms Barn study area, Suffolk England showing the location of the individual sampling units (ISU) used to derive ground chlorophyll content. 3

Figure 4.3. Sampling procedures used in the New Forest and Brooms Barn study sites to account for variation within each ISU..... 103

Figure 4.4. Variation in top of canopy reflectance between adjacent CASI-2 flight lines prior to normalising reflectance gradient in the cross track direction (a), (b) after correction..... 110

Figure 4.5. CASI-2 RGB mosaic comprised of seven geo-referenced flight scans that have been corrected for the effects of the atmosphere and radiometric variation. 111

Figure 4.6. Up-scaling process used in this study aggregated the original 2m CASI-2 chlorophyll map to derive the 300m-chlorophyll map. 114

Figure 4.7. The method used to identify and extract MTCI field pixels in the Brooms Barn validation exercise 116

Figures 4.8. The variation in LAI (a), chlorophyll concentration (b) and chlorophyll content (c) between sampling units in New Forest study area..... 118

Figure 4.9. The local variability in canopy closure, which is representative of the New Forest study site and shown on CASI-2 2-metre RGB mosaic. 119

Figure 4.10. The effect of scene component aggregation as a function of spatial resolution. In an open canopy, at 20-metre resolution, pixels are composed of crown, understory and soil..... 119

Figure 4.11. Relationship between CASI MTCI and chlorophyll content derived from ground data for all ISU in the study area..... 120

Figure 4.12. Chlorophyll content map of the study area derived from the modelled relationship between CASI MTCI data and chlorophyll. Black areas represent no data, where a binary mask was applied to remove missing data or areas covered by heathland or non-vegetated areas. 122

Figure 4.13. The relationship between CASI MTCI and CASI-2 chlorophyll map, both were resampled to a spatial resolution of 300m. 123

Figure 4.14. Relationship between ‘full resolution’ MTCI imagery and field derived chlorophyll content for the study area at 300m spatial resolution..... 123

Figure 4.15. The relationship between chlorophyll content and MTCI for all cover types. 125

Figure 4.16. Photographs showing the stage of crop development of a typical onion (a) and sugar beet crop (b). Images were taken during the Brooms Barn validation campaign during May 2008..... 125

Figure 4.17. The relationship between chlorophyll content for agricultural crops and MTCI where LAI \Rightarrow 0.3. Error bars indicate the standard deviation for a particular cover type to which that pixel relates. 126

Figure 4.18. The relationship between MTCI and chlorophyll content in agricultural crops as determined at the Dorchester study site (a) from Dash and Curran (2007), and (b) Brooms Barn validation. 130

Figure 4.19. The relationship between chlorophyll content and MTCI for various cover types..... 131

Figure 4.20. The relationship between MTCI and chlorophyll content as a function of LAI..... 131

Figure 4.21. Relationship between MERIS MTCI and that derived from CASI-2 imagery 134

Figure 5.1. Field and satellite sensor studies have demonstrated that vegetation growth exhibits distinct temporal trends..... 141

Figure 5.2. Photographs illustrating the species composition at a number of study areas in the New forest. 145

Figure 5.3. Woodland and heath and grassland study areas used in the phenology study in the New Forest, Hampshire, UK. 149

Figure 5.4. Vector layers used to select MTCI pixels located within the boundary of each study area in the New Forest. Also shown are the locations of the homogenous coniferous and deciduous woodland pixels..... 149

Figure 5.5. Diagrammatic representation of the layer stacked MTCI 8-day composites. 152

Figure 5.6. Discrete Fourier Transformation (DFT) was used to remove noise (smooth) from the MTCI phenological profile. 155

Figure 5.7. Phenology transition dates were determined using maximum and minimum values in the rate of change of the (DTF smoothed) MTCI phenology profile..... 155

Figure 5.8. Seasonal MTCI phenological profiles for woodland study areas in the New Forest National Park; 2003 - 2007..... 158

Figure 5.9. Comparison between deciduous and coniferous woodland MTCI profiles in the New Forest study site for growing seasons 2003 - 2007..... 159

Figure 5.10. Seasonal MTCI phenological profile for heath and grassland sites in the New Forest National Park; 2003 - 2007..... 160

Figure 5.11. Variation between the long term CET (1669-2002) monthly mean temperature and the years 2003-2008. 161

Figure 5.12. Relationship between MTCI and local T_{mean} for woodland and heath and grassland sites, New Forest, using 2003 - 2007 data; woodland sites (a) 2003-2007; grass and heathland sites (b)..... 163

Figure 5.13. Variation in MTCI and mean monthly temperature (CET_{mean}) in 2006 compared to the running average 2003 –2005 and 2007 for both woodland and heath and grassland study areas at all three study areas. 164

Figure 5.14. Variation in key phenological transition dates through the growing season as determined by the rate of change in curvature in the MTCI profile for the New Forest woodland study areas..... 165

Figure 5.15. Comparison between MTCI and the phenological profiles derived from MODIS NDVI (a), and MODIS EVI (b)..... 170

Figure 5.16. The relationship between temperature ($T_{\text{mean local}}$) and MTCI at the New Forest woodland sites, 2003-2007..... 173

Figure 5.17. The linear relationship observed between MTCI and temperature ($T_{\text{mean local}}$) 2003 – 2007 for all study areas..... 174

Figure 6.1. The location of the flux tower sites that were used in this study. 184

Figure 6.2. The temporal variation in flux tower GPP as measured using eddy covariance techniques for UCI 1850 (a), Harvard Forest (b), Fort Peck (c) and Fort Dix (d) sites and corresponding MTCI values..... 188

Figure 6.3. The relationship between tower GPP and MTCI for UCI 1850 (a), Harvard Forest (b), Fort Peck (c) and Fort Dix (d).. 191

Figure 6.4. Relationship between flux tower GPP and MTCI*PAR for all sites and both years where data were available. 193

Figure 6.5. The relationship between flux tower GPP measurements and MTCI*APAR at UCI 1850 (a) Harvard Forest (b), Fort Peck (c) and Fort Dix (d) (2005 only) 196

Figure 6.6. The relationship MTCI*APAR using all data..... 198

Figure 6.7. Relationship between predicted GPP based on the MTCI*APAR model and flux tower GPP for all four sites..... 199

Figure 6.8. Variation in LUE as defined by Monteith (1972) and Gitelson *et al* (2006) across the 2005 growing season at Fort Dix (a). Variation in APAR and MTCI throughout the growing season of 2005 for the Fort Dix study site (b). 201

Figure 6.9. Variation in photosynthetic LUE for UCI 1850 site for 2004 and 2005 growing seasons (a). The relationship between predicted GPP (MTCI*APAR) and LUE (b)..... 202

Figure 6.10. The relationship between flux tower GPP and MOD17 estimates at UCI 1850 (a), Harvard Forest (b), Fort Peck (c) and Fort Dix (d)..... 204

List of tables

| | |
|--|-----|
| Table 2.1. Relationship between the reflectance and absorption characteristics of green vegetation at visible – NIR wavelengths | 32 |
| Table 2.2. MERIS band properties adapted from Curran and Steele (2005)..... | 51 |
| Table 3.1. Summary of the spinach trays used in this experiment. | 65 |
| Table 3.2. Soil reflectance properties as measured in MERIS bands 8, 9 and 10 and the MTCI of bare soil as used in this experiment..... | 84 |
| Table 3.3. Results from one-way ANOVA assessing the significant of the influence of variation in view angle on the MTCI – chlorophyll content relationship. Levenes significance was included to show the data did not violate the assumption of heterogeneity of variance..... | 91 |
| Table 4.1. Summary of the data and method used in the MTCI validation at the New Forest and Brooms Barn sites | 107 |
| Table 4.2 The variability in chlorophyll content according to crop type in the Brooms Barn study site. | 124 |
| Table 4.3. Surface reflectance from onion, sugar beet and bare soil as measured in MERIS bands 8, 9 and 10 that are used to derive the MTCI..... | 126 |
| Table 5.1a. Location and composition of woodland study areas within the New Forest | 146 |
| Table 5.1b. Locations and estimated composition of grass and heathland study areas within the New Forest..... | 147 |
| Table 5.2. Location, area and vegetation type of the auxiliary study areas..... | 148 |
| Table 5.3. Location of weather stations in relation to the study areas..... | 153 |
| Table 5.4. Phenological transition dates derived from the UK Phenology Network.... | 166 |
| Table 5.5. Inter-annual variability in phenological transition dates as derived from the MTCI time series for woodland study areas in the New Forest. | 167 |
| Table 5.7. Comparison between estimated transition dates derived from NDVI, EVI and MTCI time series. | 171 |
| Table 6.1 Comparison of the coefficients between predicted and flux tower GPP for each study site as determined by the various methods used to estimate GPP in this investigation..... | 206 |

Acknowledgements

First, I would like to thank my supervisors at Bournemouth University: Professor Paul Curran, who as well as being Vice-Chancellor of Bournemouth University, found time to supervise my research and correct my grammar. Dr. Ross Hill who has done a sound job of getting up to speed with my research and reading numerous drafts of work in various stages of completion (at short notice). I would also like to thank second supervisors, past, present and surrogate. Thanks to Dr. Doreen Boyd for being a mentor after her official duties were over following a move to the University of Nottingham. A special thanks to Dr. Jadunandun Dash of the University of Southampton, who has provided priceless assistance on a number of occasions.

Special thanks must go to my family, including the new addition, Wilfred Barnaby. Thank you for your support and encouragement when things got difficult and unrelenting confidence in me throughout my studies.

This work was carried out under a full PhD. Studentship at Bournemouth University. Many thanks to the University for providing me with this opportunity.

To my Granddad

List of acronyms

| | |
|-----------------|--|
| ACCP | Accelerated Canopy Chemistry Program |
| ACRM | Markov Chain Canopy Reflectance Model |
| AMERIFLUX | American Flux Tower Network |
| ANOVA | Analysis of Variance |
| APAR | Absorbed Photosynthetic Active Radiation |
| ARSF | NERC Airborne Research and Survey Facility |
| ARVI | Atmospheric Resistant Vegetation Index |
| ATBD | Algorithm Theoretical Basis Document |
| ATSR | Along-Track Scanning Radiometer |
| AVHRR | Advanced Very High Resolution Radiometer |
| AVIRIS | Airborne Visible/Infrared Imaging Spectrometer |
| BOREAS | Boreal Ecosystem-Atmosphere Study |
| BRDF | Bidirectional Reflectance Distribution Function |
| CASI | Compact Airborne Spectrographic Imager |
| CCD | Charged Coupled Device |
| CEH | Centre of Ecology and Hydrology |
| CEOS | Committee on Earth Observation Satellites |
| CET | Central England Temperature |
| CO ₂ | Carbon Dioxide |
| CV-MVC | Constrained View Angle Maximum Value Composite |
| DAO | Data Assimilation Office |
| DEM | Digital Elevation Model |
| DFT | Discrete Fourier Transformation |
| DMF | Dimethylformamide |
| Envisat | ESA Environmental Satellite |
| EO | Earth Observation |
| ERTS-1 | Earth Resources Technology Satellite-1 |
| ESA | European Space Agency |
| EUROFLUX | European Flux Tower Network |
| EVI | Enhanced Vegetation Index |
| FLAASH | Fast Line-of-sight Atmospheric Analysis of Spectral Hypercubes |
| FLUXNET | Flux Tower Network |
| FOV | Field-of-View |
| fPAR | Fraction Photosynthetic Active Radiation |
| GPS | Global Positioning System |
| IFOV | Instantaneous Field-of-View |
| IPCC | Inter-government Panel on Climate Change |
| ISU | Individual Sampling Unit |
| LAI | Leaf Area Index |
| LIBERTY | Leaf Incorporating Biochemistry Exhibiting Reflectance and Transmittance Yield |
| LIBSAIL | Coupled LIBERTY and SAIL models |
| LPV | Land Product Validation |
| LUE | Light Use Efficiency |
| LUT | Look-Up Table |
| MCARI | Modified Chlorophyll Absorption Ratio |
| MERIS | Medium Resolution Imaging Spectrometer |
| METEOSAT | Meteorological Satellite |

| | |
|----------|--|
| MISR | Multi Angular Spectra Radiometer |
| MODIS | Moderate resolution Imaging Spectroradiometer |
| MODLAND | MODIS Land Discipline Team |
| MODTRAN | Moderate Resolution Atmospheric Transmission Model |
| MSAVI | Modified Soil Adjusted Vegetation Index |
| MTCI | MERIS Terrestrial Chlorophyll Index |
| MSR | Multispectral Radiometer |
| MSS | Multispectral Scanner |
| MVC | Maximum Value Compositing |
| NASA | National Aeronautics and Space Administration |
| NDVI | Normalised difference vegetation index |
| NEODC | NERC Earth Observation Data Centre |
| NERC | Natural Environment Research Council |
| NIR | Near Infrared |
| NOAA | National Oceanic and Atmospheric Administration |
| NSF | National Science Foundation (US) |
| OSAVI | Optimised soil-adjusted vegetation index |
| OSGB | Ordnance Survey Great Britain |
| PAR | Photosynthetic Active Radiation |
| Pixel | Picture element |
| POLDER | Polarisation and Directionality of Earth Radiance |
| PRI | Photochemical Reflectance Index |
| PROSAIL | Coupled PROSPECT and SAIL models |
| REP | Red Edge Position |
| RGB | Red Green Blue |
| ROI | Region of Interest |
| RTM | Radiative Transfer Model |
| SAIL | Scattering by Arbitrary Inclined Leaves |
| SAVI | Soil Adjusted Vegetation Index |
| SMOS | Soil Moisture and Ocean Salinity Sensor |
| SPAD | Soil Plant Analysis Division |
| SPOT | Satellite pour l'Observation de la Terre |
| SPOT-HRV | SPOT High Resolution Visible |
| TM | Thematic Mapper |
| UKPN | UK Phenology Network |
| USDA | US Department of Agriculture |
| USGS | U.S. Geological Survey |
| UV | Ultra-Violet |
| VALERI | Validation of Land European Remote Sensing Instruments |
| VI | Vegetation Index |
| WGCV | Working Group on Calibration and Validation |
| WGS | World Geodetic System |
| WIST | Warehouse Inventory Search Tool |

CHAPTER 1: INTRODUCTION

Chapter 1: Introduction

1.1 The need for monitoring of terrestrial vegetation

The Earth's atmosphere is strongly influenced by the biophysical state of the Earth's surface and the atmospheric abundance of trace greenhouse gases, including carbon dioxide (Denman *et al.*, 2007). Carbon dioxide (CO₂) is a key greenhouse gas and its concentration in the atmosphere is influenced by complex interactions of natural fluctuations in geochemical cycles, anthropogenic release through the combustion of fossil fuels and the burning of biomass, and the uptake by sinks such as terrestrial ecosystems and the oceans (Matthews, 2007). The global atmospheric CO₂ concentration is currently c.370 μmol⁻¹, and is expected to reach c.700 μmol⁻¹ by the end of the Century (Lawson *et al.*, 2001). Increasing atmospheric CO₂ concentration affects the nature of the climate system, resulting in increased global mean temperatures and increased climate variability, including changes in precipitation distribution and frequency and the occurrence of extreme weather events (IPCC 2007). The latest IPCC report (2007) highlighted the trend of increasing of global surface temperatures and stated that eleven of the previous twelve years (1995-2006) were amongst the warmest since 1850. However, the rise in global temperatures is not uniform in time or space, with a near two-fold increase in global mean temperatures being observed over the fifty years from 1956 – 2005 compared with the period 1906-2005 (IPCC 2007). Geographically, there is a clear trend of increased warming at higher northern latitudes, where average mean temperatures rises are almost double the global mean over the past 100 years (IPCC 2007).

The observed and predicted change to the climate system has a marked impact upon the Earth's physical cycles and biological systems, which will vary in magnitude in space and time in accordance with the regional variability in climate. The analysis and prediction of the effects of global climate change are very difficult to quantify due to feedback mechanisms and complex relationships between the chemical cycles, climate and biological cycles in oceanic and terrestrial ecosystems (IPCC 2007).

1.2 Effects of climate change upon terrestrial vegetation

Documented changes in climatic conditions since the middle of the last century, coupled with our knowledge of the environmental controls that influence vegetation physiology, namely temperature, precipitation, atmospheric CO₂ concentration and the associated availability of nutrients (Denman *et al.*, 2007), may mean that the conditions under which vegetation has developed in the past will have changed now (Boisvenue and Running, 2006). Therefore, climatic variation may have an important bearing on growth, composition and structure of terrestrial ecosystems, influencing the timing and duration of growing seasons, plant vigor and productivity. The response of terrestrial vegetation to climate change is complex as physiological effects will be location and species specific (Hanhong and Sicher, 2004). CO₂ fertilisation, warmer winter weather and longer growing season conditions may enhance growth. However, unfavorable conditions, such as drought and limiting temperatures, may increase physiological stress, consequently reducing productivity and growth rates and effecting the natural seasonal development of terrestrial ecosystems (Watkiss, 2009).

1.3 Phenology and productivity

The seasonal development of vegetation, or its phenology, refers to the natural growth or development of vegetation. Phenological timing and events, such as leaf development or greening up, senescence and growing season length, have the capacity to influence the productivity of terrestrial vegetation. The length of the growing season corresponds to the period when photosynthetic activity (and carbon assimilation) can occur (Xiao *et al.*, 2004; Piao *et al.*, 2007). The timing of phenological events has been shown to vary in relation to changes in local climate. Therefore, vegetation phenology is an important bio-indicator of the impact of climate change on ecosystem productivity (Schleip *et al.*, 2006).

Our current understanding of climate forcing on vegetation phenology is largely limited to a few locations where extensive records exist (Fisher and Mustard, 2007). The climate–phenology models developed at such locations are often non-transferable to other locations either regionally or globally (Badeck *et al.*, 2004). Therefore there is a pressing need to provide temporal observations of vegetation productivity and health, establishing phenological change and developing transferable phenological models.

1.4 Carbon budgets

Vegetation covers almost three quarters of the Earth's terrestrial surface, so an understanding of the effects of climate variation upon the functioning of vegetation and the timing of phenological events are critical to model ecosystem and energy cycles, such as the carbon cycle (Dixon, 1976; Dixon *et al.*, 1994). Due to the uncertainty of the response of the Earth's vegetation to future climatic conditions, changes to terrestrial ecosystem carbon sinks caused by climatic variations are poorly understood (Coa and Woodward, 1998; Matthews, 2007).

Uncertainty of the relationship of vegetation productivity to climate has led to political debate, international discussion and treaties (Wylie *et al.*, 2003). Terrestrial ecosystems have become an important economic commodity not only due to commercial practices, such as farming and timber production, but also as major sinks of carbon (especially forests). The global initiative of reducing carbon emissions through the Kyoto Protocol places a strong emphasis on the role of vegetation as a major carbon sink (Pfaff *et al.*, 2000; Clevers *et al.*, 2001; Wylie *et al.*, 2003). Therefore, understanding the processes effecting vegetation phenology and productivity, and determining the response of vegetation to variations in climate will have a direct bearing upon the goals set out in the Kyoto Protocol (Van Vilet *et al.*, 2003).

Global economic growth and an ever-increasing human population exert demands on the Earth's natural and managed vegetated resources. Identifying, analyzing and interpreting the physical changes to terrestrial ecosystems that are occurring spatially and temporally are significant for land use management and securing food provision (at local to global scales) (Thomas, 2006). Moreover, vegetation phenology and productivity are also fundamental inputs into global climate and biochemical models (Kokaly and Clark, 1999; Coppin *et al.*, 2001).

1.5 Chlorophyll

Plant productivity depends on leaf photosynthetic rate and the leaf life duration as well as the availability of such factors as nitrogen, water and temperature (Bindi *et al.*, 2002). Research has confirmed that foliar biochemistry, including both photochemicals (including chlorophyll) and nitrogen, are closely related to maximum photosynthetic rates (Martin and Aber, 1997; Bacour *et al.*, 2006). Chlorophyll is one of the most important and abundant photosynthetic pigments. The amount of chlorophyll within a canopy is positively correlated with vegetation productivity and plant health (Dash and Curran, 2007). Leaf chlorophyll content is also an indicator of stress at the leaf-to-canopy-scale (Bacour *et al.*, 2006), providing us with vital information regarding the response of terrestrial vegetation to unfavourable change in climate and associated nutrient provision. When a plant is under stress, small changes in chlorophyll content are evident in the initial stages. As the stress increases, chlorophyll content decreases more quickly than the other pigments. These changes in chlorophyll content are indicative of stress of a plant (Bannari *et al.*, 2007). Chlorophyll content is therefore likely to decrease as a response of plant stress prior to observed physiological changes, such as leaf area. Field studies have also shown a close relationship between foliar leaf chemistry and litter decomposition rates (Demarez and Gastellu-Etchegorry, 2000), providing detail regarding the flux of carbon from the vegetation to the soil system, which is of vital importance in carbon sequestration studies.

The ability to determine the photosynthetic pigment content of vegetation will therefore yield important information about vegetation productivity and health status and produce accurate estimates of plant vigour and environmental quality (Carter and Spiering, 2002).

1.6 The role of remote sensing

The unique viewpoint offered by remote sensing can help develop our understanding of the importance and dynamic nature of the fragile environment that supports all life on Earth. The field of remote sensing, and subsequently our understanding of the processes that shape and influence our planet, has improved with subsequent developments in technology and our understanding of the interactions of electromagnetic radiation with the Earth's surface and atmosphere.

Understanding vegetation / ecosystem dynamics has long been a priority of the scientific community with emphasis on the effects of land cover change on ecological processes and cycles as well as on Earth-atmosphere systems. Measurements from satellites provide the only feasible means of observing large portions of the Earth's surface at a high temporal frequency in a consistent manner; therefore remote sensing is a key technology for quantifying landscape patterns and processes (Newton *et al.*, 2009).

Remote sensing provides an opportunity to study vegetation condition and observe seasonal vegetation dynamics, and offers the potential to understand vegetation – climate system interactions (Reed 2006). Remote sensing provides the unique opportunity to observe vegetation over large areas over time, giving us the potential to understand the effects of climatic change and management practices from local to global scales.

An integrated observation strategy allows us to quantitatively understand the links and feedback mechanisms associated in the exchange of energy and matter between the vegetation canopy, atmosphere and soil on a variety of temporal and spatial scales. Furthermore, such understanding is essential for local to global scale applications related to vegetation monitoring and climate change (Houborg *et al.*, 2007). Temporal and spatial monitoring on such scales enables us to understand the functioning of vegetated ecosystems (Demarez and Gastellu-Etchegorry, 2000).

Remotely sensed data have been used in the study of vegetation condition and seasonal vegetation dynamics for many years (Reed, 2006). The ability to observe vegetation phenology remotely provides a unique opportunity to monitor temporally the effects of climatic change on vegetated canopies at local to global scales. The vast majority of studies have used data from the Advanced Very High Resolution Radiometer (AVHRR) sensor (Zhang *et al.*, 2006). A new generation of remote sensing data sources are now available and they improve greatly our ability to identify changes in ecosystem phenology. Phenology observed using a time-series of satellite sensor data together with ground-based phenological observations could provide vital information about vegetation responses to climate forcing and changing geochemical and water regimes (Reed *et al.*, 1994).

There has been an intensive global effort in recent years to measure and model carbon

exchanges between the terrestrial ecosystems and the atmosphere using a combination of modelling, remote sensing and *in-situ* measurements. Earth observation is needed to derive global vegetation properties (Myneni *et al.*, 2002) and combined with biogeochemical models to provide carbon exchange variables (Hill *et al.*, 2006). Such variables are fundamental inputs to models of global climate and biogeochemical cycles (Coppin *et al.*, 2004).

CHAPTER 2: THE REMOTE SENSING OF CANOPY CHLOROPHYLL CONTENT

Chapter 2

Chapter 1 has documented the potential effects of global climate change on vegetation phenology, productivity, health and the terrestrial carbon cycle. The use of remote sensing to monitor terrestrial vegetation dynamics through the estimation of canopy chlorophyll content at the regional - global scale is an emerging research area. The discussion in chapter 2 outlines the current understanding and methods for the estimation of chlorophyll content using remote sensing methods. Chapter 2 then introduces the Medium Resolution Imaging Spectrometer (MERIS), onboard the European Space Agency's (ESA) environment monitoring Envisat platform, and the only operational product to estimate chlorophyll content in terrestrial vegetation; the MERIS Terrestrial Chlorophyll Index (MTCI). The focus of this thesis is to explore the potential of the MTCI as a tool to monitor vegetation dynamics at local – global scales. The principal aims of this research are detailed in section 2.8 following detailed discussion specific to the methods used to estimate chlorophyll content.

2.1 Reflectance at the leaf scale

Remote sensing of foliar bio-chemicals has developed rapidly since the 1980s and 1990s (Curran *et al.*, 2001), utilising laboratory analysis, field measurements, and imaging spectrometers (Haboudane *et al.*, 2008). Specialist programmes, such as NASA's Accelerated Canopy Chemistry Program (ACCP), with the aim of understanding the interaction of radiation with leaves and canopies have made tremendous progress in developing approaches and methods to estimate chlorophyll content at both the leaf and canopy scale.

2.1.1 Photosynthetic pigments and their radiometric signature

The reflectance of vegetation in the visible region of the spectrum (400-700 nm) is dominated by the absorption properties of photosynthetic pigments (Asrar *et al.*, 1989; Curran *et al.*, 1991). Each photosynthetic pigment absorbs light more efficiently in a different part of the electromagnetic spectrum, Chlorophyll *a* absorbs strongly at wavelengths between 400-450 nm and 650-700 nm; chlorophyll *b* between 450-500 nm. However, none of the pigments absorb well in the green-yellow region, which is responsible for the high reflectance in the green region of the spectrum for vegetation

Chapter 2. The remote sensing of canopy chlorophyll content

(Asrar, 1998). Chlorophyll *a* is the most common of the five photosynthetic pigments present in each plant.

If chlorophyll concentrations are low then the leaf is unable to maximise its photosynthetic potential and reflectance in the visible region of the spectrum will be high. Conversely, at high chlorophyll concentrations there is increased absorption in visible wavelengths. According to the Beer - Lambert Law, a negative exponential relationship exists between chlorophyll concentration and absorption by chlorophyll. Thus, an increase in foliar chlorophyll content leads to an increase in absorption, leading to a broadening and deepening of the absorption feature (Filella and Peñuelas, 1994).

Leaf reflectance is influenced by the ratio of the concentration of chlorophyll *a* and chlorophyll *b* as well as other pigments (Curran *et al.*, 1991; Asner, 1998), and chlorophyll fluorescence (Blackburn and Milton, 1995). Typically, the concentration of chlorophyll *a* is approximately two to three times that of *b*, although this differs between species. Other than the photosynthetic pigments, various structural factors and biochemicals influence reflectance; for example, lignin, nitrogen, cellulose and sugar concentrations have been shown to influence reflectance at the leaf scale (Curran *et al.* 2001). Minor absorption features located between 400-2400 nm are the result of harmonics and overtones of the stronger absorption bands at longer wavelengths (Curran, 1989).

During photosynthesis part of the energy captured by chlorophyll is displaced, re-emitted as light at a longer wavelength than the excitation energy (Grace *et al.*, 2007). The emitted energy is in the waveband 650-800nm, with peaks at 690 and 740nm. Foliar fluorescence is a measure of light use efficiency in the photosynthetic process and is used as a diagnostic tool for the detection of stress. The fluorescence signal effectively represents 'wasted energy', surplus energy that is not used in photosynthesis (Zarco-Tejada *et al.*, 2000). Typically, the fluoresced signal is less than 3% of the reflected signal. Modelling offers the potential to separate the fluoresced energy to determine photosynthetic rate and CO₂ assimilation.

2.1.2 Leaf structure

Visible light reflectance from a leaf is linked directly to chlorophyll concentration, whilst near infrared (NIR) reflectance is independent of chlorophyll concentration and governed by the internal structure of the leaf (Gausman, 1977). At the leaf scale various factors affect the reflectance in both the visible and NIR wavelengths. In the NIR spectral domain (701-1300 nm), leaf structure explains the optical properties. The NIR spectral region can be divided into two spectral sub-regions: (i) 701 - 1100 nm, where reflectance is high, bar two minor water-related absorption bands (centered at 960 and 1100 nm) and (ii) between 1100 - 1300 nm, which corresponds to the transition between high NIR reflectance and water-related absorption bands of the middle infrared. The intensity of NIR reflectance from vegetation is commonly greater from vegetation than from most non-vegetated surfaces, so allowing vegetation to be discriminated against the 'darker' surrounding matter (soil, urban areas etc).

Epidermis cells that make up the upper layers of the leaf are penetrable by all wavelengths (Figure 2.1). Internally, Palisade cells, that contain the chloroplasts, absorb strongly across all visible wavelengths, but to a lesser extent for visible green, reflecting approximately 10-30% of the total amount of visible radiation arriving at the leaf surface. Infrared wavelengths penetrate the Palisade cells into the underlying mesophyll. The mesophyll cells scatter much of the NIR radiation (approx 60%) reaching the leaf layer (Figure 2.2). This internal photon scattering at the air-cell interface leads to strong reflectance in the NIR region of the spectrum from a healthy vegetation canopy (Table 2.1) (Woolley 1971).

Chapter 2. The remote sensing of canopy chlorophyll content

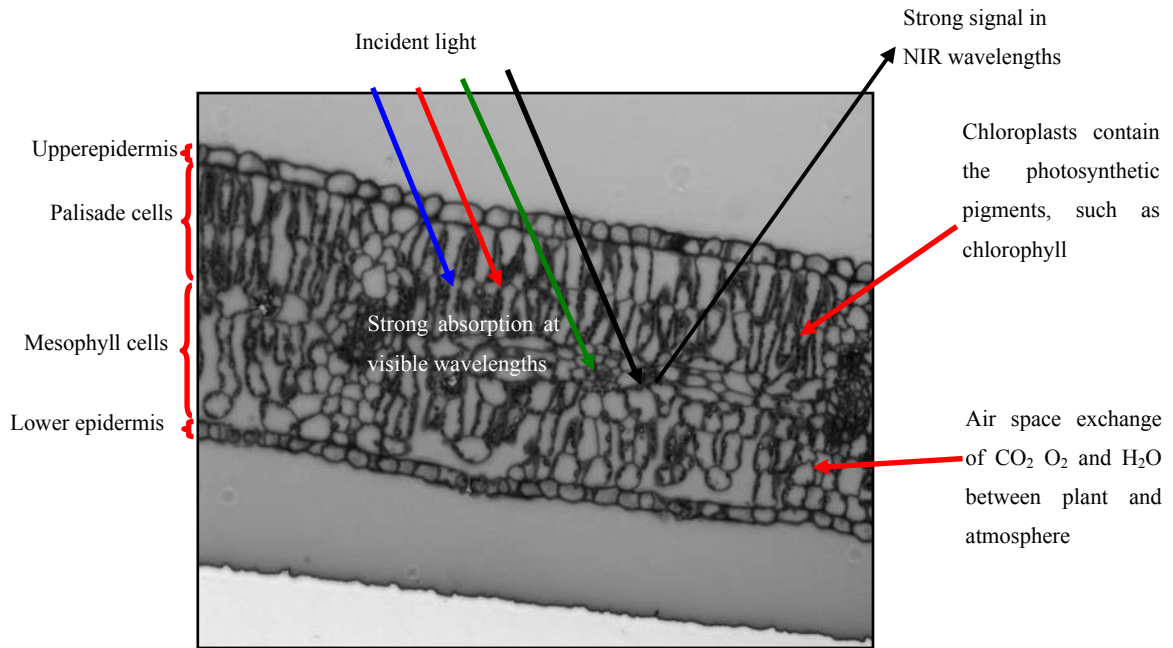


Figure 2.1. Cross-section of a typical leaf. Major structural leaf components are highlighted and their interaction with light in the visible – NIR domain identified.

For a leaf reflectance spectra, the absorption features corresponding to 400 nm and 700 nm, in the green and red wavelengths (approx) are attributed to chlorophyll, whilst the troughs in the NIR wavelengths are due to absorption of water contained in the leaf mesophyll layers.

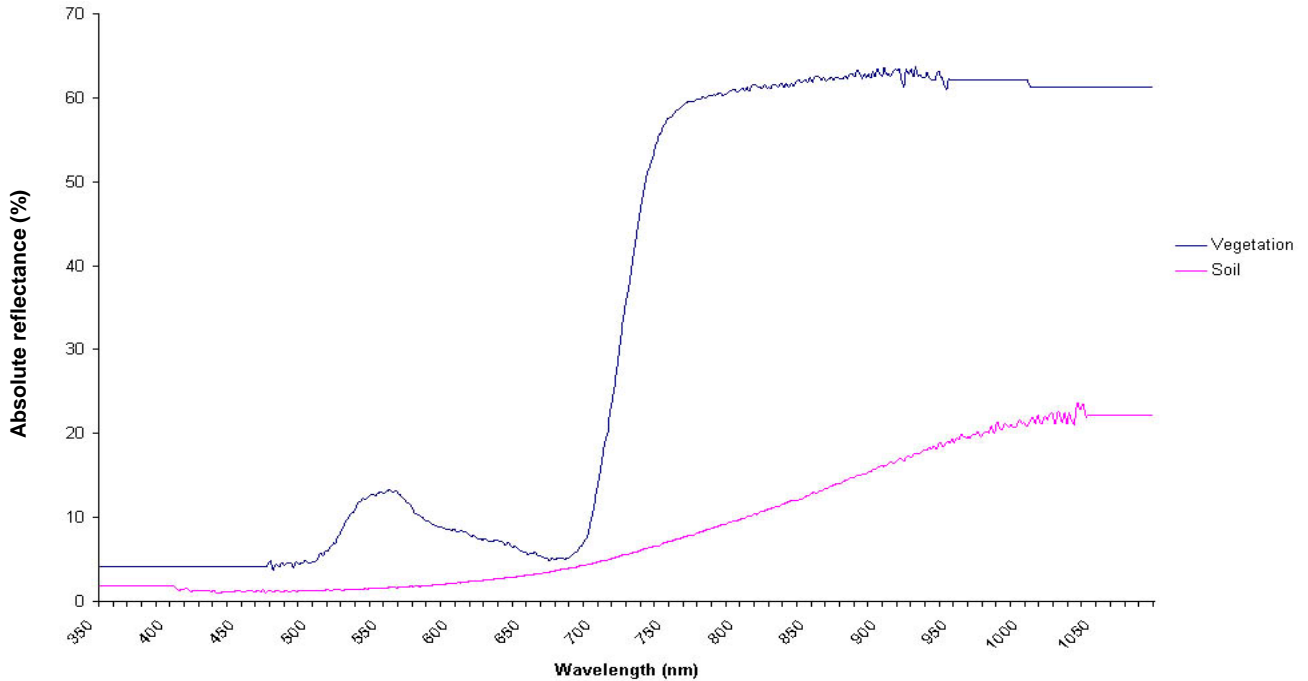


Figure 2.2 Spectral reflectance of a green vegetation and dry bare soil in the visible – NIR region of the reflectance spectrum derived from laboratory spectroscopy of spinach leaves.

| Region of spectrum | Wavelength (nm) | Characteristics | Relation to vegetation amount |
|--------------------|-----------------|---|-------------------------------|
| Green | 350-500 | Reduced pigment absorption | Weak positive |
| Red | 600-700 | Strong chlorophyll absorption | Strong negative |
| Red edge | 700-740 | Transition between strong absorption and strong reflectance | Weak negative |
| NIR | 740-1300 | High reflectance | Strong positive |

Table 2.1. Relationship between the reflectance and absorption characteristics of green vegetation at visible – NIR wavelengths

2.1.3 The red edge

The red edge marks the boundary between red and NIR wavelengths and is a result of the combined effects of strong absorption in the visible red region by chlorophyll and the reflectance maxima in the NIR region due to scattering caused by internal leaf structure (Horler *et al.*, 1983, Dawson and Curran, 1998; Haboudane *et al.*, 2008). An increase in foliar chlorophyll concentration produces molecular aggregation by chlorophyll molecules resulting in polymerization, or other forms of aggregation (Jago *et al.*, 1999). The effect of increasing the amount of foliar chlorophyll is a minor deepening and significant broadening of the chlorophyll absorption feature, shifting the boundary of the red edge to longer wavelengths (Dash and Curran, 2004; Jago *et al.*, 1999). The amount of chlorophyll within the leaf / vegetation canopy has been shown to be positively related to the point of maximum slope at wavelengths between 690-740nm in the reflectance spectra (Horler *et al.*, 1983; Jago *et al.*, 1999). This change in red edge position (REP) can be used to estimate the amount of chlorophyll content at both the leaf and canopy scales (Munden *et al.*, 1994). Thirty years after defining the relationship between the red edge and the chlorophyll concentration, research determining chlorophyll concentration using the red edge remains active.

A strong correlation exists between the concentration of foliar photosynthetic pigments and a shift in the red edge position towards blue spectrum in stressed vegetation (Carter and Spiering, 2002). The total chlorophyll content in leaves decreases in stressed vegetation, changing the proportion of light-absorbing pigments and leading to less overall absorption due to lower chlorophyll *a* and *b* concentrations at the leaf level (Zarco-Tejada *et al.*, 2004). Both the position and the slope of the red edge change under stress conditions (Clevers *et al.*, 2001), inducing shifts in the long wavelength edge of the chlorophyll absorption feature to shorter wavelengths (Ustin *et al.*, 2001). This suggests that the red edge position is a useful indicator of vegetation stress (Smith *et al.*, 2004), senescence, photosynthetic capacity and vegetation productivity (Davids and Tyler, 2003). Differences in reflectance between healthy and stressed vegetation due to changes in pigment content have been detected in the reflectance green peak and along the red edge. These difference provide the opportunity to derive remote detection methods to map and quantify vegetation stress through the influence of chlorophyll content variation

2.1.4 Middle-infrared region

In the middle-infrared region (1300 - 2500 nm) absorption features are a function of bending and stretching vibrations of bonds between hydrogen-carbon and nitrogen-oxygen atoms (Moorthy *et al.*, 2003). This reflectance region provides information about the absorption of leaf components such as water, cellulose and lignin. Nitrogen status of vegetation can be inferred through the study of absorption features in this region of the electromagnetic spectrum (Baret and Fourty, 1997).

2.2 Spectral properties of the vegetated canopy

2.2.1 Canopy variables that influence observed reflectance

Canopy reflectance is a function of Leaf Area Index (LAI), defined as the single sided area of the green elements per unit of ground area (Morisette *et al.*, 2006). LAI strongly influences the reflectance signature of a vegetation canopy; with a significant effect in NIR and a smaller influence in visible reflectance. Of the many types of biophysical property that influence the radiation at optical wavelengths from a forest canopy, LAI is the most important (Boyd and Danson, 2005). An increase in canopy LAI leads to an increase in NIR scattering and enhanced canopy absorption at around 680nm and 780 nm. Unlike chlorophyll concentration, LAI generates weak variations of the reflectance spectrum at 550 and 720 nm. LAI is therefore related negatively to red reflectance and positively related to NIR; therefore an increase in LAI will consequently increase NIR reflectance. It can be seen that high differences in the red (685–690 nm) to NIR (701 – 1300 nm) region are observed at low LAI (0.1, 0.5, and 1.0) (Haboudane *et al.*, 2008). This trend could be in connection with the influence of non-photosynthetic materials and leaf litter on canopy reflectance when the green biomass is represented in weak proportions. In open canopies, radiation will penetrate to the lower levels of the canopy and the response from the upper layers will not be as strong. Therefore, open canopies (typically with an LAI < 2) will reflect more visible and less NIR wavelengths. As the canopies close the contribution to reflectance from underlying canopy structure and surface material is reduced.

Experimental approaches and canopy radiative transfer models (RTM) have been utilised to explore the contribution and affect of non-photosynthetic biomass on canopy reflectance (Asner, 1998). The structural component of the vegetation (stems, branches,

etc.) influences the reflectance characteristics by determining the orientation and spatial arrangement of the leaves and therefore the extent to which the photons interact with the understory, ground (litter, soil) and structural components of the vegetation. It can therefore be summarised that vegetation reflectance is a function of tissue optical properties (leaf, woody stem and standing litter) and canopy biophysical properties (such as leaf and stem area, leaf orientation and foliar clumping). Leaf angle and distribution play an important role in influencing the reflectance from a vegetative canopy, whereby overlapping leaves cause shadowing effects on underlying and adjacent leaf layers. Shadowing can result in a reduction in overall reflectance as great as 50% in the visible and 75% in the NIR wavelengths (Gibson and Power, 2000). Unlike visible wavelengths, NIR wavelengths are able to penetrate through the upper canopy layers to the lower leaves, and depending upon canopy thickness, to the understory. Although transmittance will vary with vegetation species and canopy structure, generally, thinner canopies will have lower NIR reflectance than a canopy that consists of numerous layers (Gibson and Power, 2000). Therefore the NIR reflectance from a thin canopy is likely to be composed of the signal from the vegetation as well as understory vegetation and soil.

2.2.2 Non-canopy variables influencing observed canopy reflectance

Remote sensing at the aircraft or satellite level will commonly involve complications caused by the exposure of the underlying soil surface and the understory, especially where the vegetation cover is less than 100% (Kokaly and Clark, 1999). Rock *et al.* (1994) have shown that the change of background reflectance affects the reflectance slope between 550 and 700 nm. This reflectance region is closely linked to the variations of reflectance characteristics of background materials (soil and canopy structural components). Therefore it can be expected that a decrease in canopy LAI (i.e. to less than 1) will consequently lead to an increase in the reflectance slope between 550 and 700nm. The reflectance and bi-direction reflectance from a vegetation canopy can be significantly affected by soil background conditions (Price, 1990). Soil type and moisture content can affect the spectral signature of a vegetated scene. In a less densely vegetated area, ground surface (i.e. rock and soil type) will affect the signature. For example, basalt will increase the amount of red reflectance. It has also been demonstrated that moisture decreases the reflectance in all wavelengths, therefore the

time lag between a precipitation event and image acquisition will influence the returning reflectance for a given canopy (Price, 1990).

As vegetation grows (leading to a corresponding increase in LAI), the contribution of the soil background to the observed reflectance signature decreases. However, according to vegetation type, seasonality, agricultural practices, vegetation density, amongst other variables, the contribution of the soil may prove to be significant. The wide variation in soils by nature leads to problems of classification and interpretation. Typically, soil reflectance is low at shorter visible wavelengths, increasing at the longer NIR wavelengths. Reflectance characteristics vary with soil type and mineral content and organic composition. Organic matter can strongly influence reflectance characteristics. Increasing the organic component of the soil is shown to 'darken the soil' throughout the spectrum. This trend is also made more complex by the degree of decomposition of the organic matter, with litter in the early stages of decomposition having higher reflectance in the NIR (Rondeaux *et al.*, 1996). Water content also plays an important role in influencing soil reflectance by decreasing the reflectance in the visible and NIR spectrum with increasing water content. Remote sensing in the optical domain has been shown to be sensitive to soil roughness (Baret *et al.*, 1993). Rough, coarse soils have the effect of decreasing reflectance throughout the visible region of the electromagnetic spectrum due to multiple photon scattering and shadowing effects (Jacquemound *et al.*, 1992).

Atmospheric path radiance can be a significant part of the observed canopy spectra (Kokaly and Clark, 1999). Path radiance contributions are an additive to the observed canopy reflectance. Detailed understanding of such contribution is paramount to successfully derive surface reflectance. In vegetation monitoring, the effects of the atmosphere are particularly important. The atmosphere degrades the remotely sensed signal by reducing the contrast in the red and NIR reflected signals. The red signal normally increases as a result of scattered, upwelling path radiance contributions from the atmosphere. The NIR signal tends to decrease as a result of atmospheric attenuation associated with scattering and water vapour absorption. The net result is a drop in reflectance signals and an underestimation of the amount of vegetation at the surface (Huete and Justice, 1994). The degradation of the signal is dependent on the aerosol

content of the atmosphere, with turbid atmospheres having the greatest effect. Atmospheric influences on remotely sensed vegetation canopies include the incomplete reflectance or removal of wavebands due to atmospheric absorptions. Such residual information is due to water, carbon dioxide and other trace gases in the atmosphere.

Another effect of the atmosphere is the adjacency effect. The adjacency effect is a physical phenomenon caused by atmospheric scattering of radiation between fields of different surface reflectance, whereby reflected background radiation is scattered into the instantaneous field of view (IFOV) of the sensor contributing to the measured signal from the surface target. The effects of this can be observed in medium-high spatial resolution (<100 m) imagery, especially in the 400–1000nm region (Richter and Schläpfer, 2002). The influence decreases with wavelength because atmospheric scattering efficiency decreases.

2.2.3 Anisotropic Reflectance of the Earth's Surface

Canopy reflectance is further complicated by changes in viewing and solar geometry. Viewing geometry of the sensor and solar changes due to seasonality and time of day can cause statistically significant effects in the amount of reflectance from a vegetated canopy (Treitz and Howarth, 1999). Changes in the viewing geometry and higher solar zenith angle that are an issue in the higher latitudes during winter months will affect the spectral reflectance from a given canopy.

In reality the Earth's surface is a non-Lambertian reflector, a characteristic that means radiation is not reflected in all directions equally, and therefore is a function of viewing and illumination geometry. The nature of the reflectance and its direction is controlled by the physical and optical properties of the surface being illuminated. In reality the direction of the scattering is linked to radiation wavelength and the nature of the three dimensional surface; object spacing, shape and size will produce distinct shadows as a function of viewing and illumination angle (Liang *et al.*, 2000).

As has been outlined in a previous section, over a vegetative canopy, the reflectance is a function of the interaction of the radiation and the canopy structure. The proportion of the leaves and canopy that are in direct sunlight as well as the amount of background in

view will lead to variation in the observed canopy reflectance. Reflectance will vary with the size, orientation and spacing of the scattering objects (leaves) as well as the orientation of the satellite and the position of the Sun. This relationship causes a complex interaction of scatterers and shadowing as a function of illumination and viewing angles. As satellites take measurements of the Earth's surface from various view angles under differing illumination geometry, an understanding of these factors on the influence on a scene and surface anisotropy is needed in order to understand the true reflectance and subsequently the surface properties.

Sensors with a large instantaneous field-of-view (IFOV), such as AVHRR or MERIS are ideal for global vegetation studies (Walter Shea *et al.*, 1997). However, a low repeat image acquisition period due to large swath width is coupled with multiple look angles and that results in enhanced directional effects (Bacour *et. al.*, 2006). Typically, the processing of data from the aforementioned sensors consists of sensor calibration and both geometric and atmospheric correction. However, there has been an increased focus within the field of vegetation remote sensing on the bidirectional reflectance properties of the surface. This effect on the MERIS sensor is largely absent from the research literature. The bidirectional reflectance distribution function (BRDF) describes the scattering of a parallel beam of incident light from one direction into another direction in the hemisphere (Schaepman-Strub *et al.*, 2006) and accounts for the dependence of surface spectral reflectance on the geometry at which the surface is illuminated and viewed (Nicodemus *et al.*, 1977).

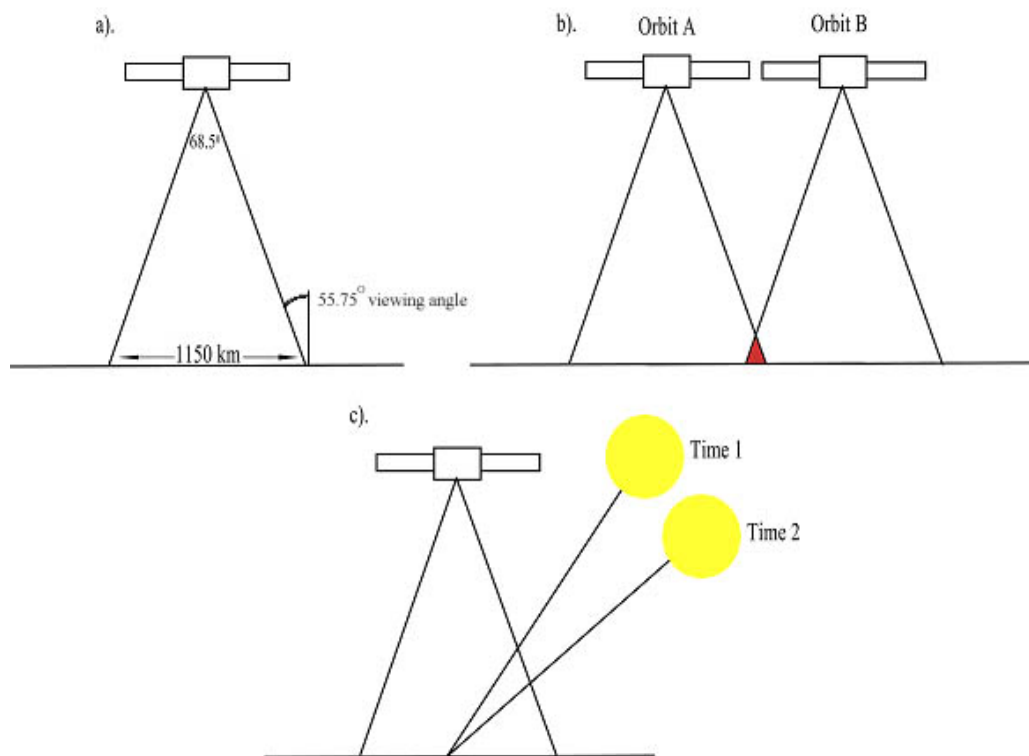


Figure 2.3. Angular effect caused by sensor characteristics, orbital patterns and illumination geometry. Note that figures quoted in (a) are for the MERIS sensor.

The IFOV of MERIS at the satellite results in viewing angles with a range between 0° at nadir to angles in excess of 55° at the edge of a single scene (refer to Figure 2.3 a). This angular effect is further amplified by the curvature of the Earth. Angular variations will also be present in data acquired from MISR (Multi Angular Spectra Radiometer) and MODIS (Moderate resolution Imaging Spectroradiometer). Research using POLDER (Polarisation and Directionality of Earth Radiance) imagery, determined that vegetation indices exhibited variations in the range of 20-50% as a result of variation in spectral reflectance caused by changing viewing geometry (Leroy and Hautecoeur, 1999). Bi-directional reflectance is one of the major sources of variation in short wavelength AVHRR imagery (Duchemin, 1999), whereby off-nadir viewing introduces sensor and geometry effects. Research into the effect of off-nadir viewing upon NDVI measurement demonstrated that increasing relative solar zenith angles increased the NDVI. Smaller solar zenith angles increased the NDVI, increasing the contrast between vegetation and background (Galvão *et al.*, 2004). Angular variations will also be present in data acquired from a geographical location during different orbital phases.

Wide swath imagery means the same location can be imaged without a direct overpass (Figure 2.3 b shows this area highlighted in red.)

Images sensed over the same area at a constant viewing angle but at different times of the day (for example by a geostationary sensor such as MSR onboard METEOSAT), or at different times of the year, will be affected by variations in the angle of illumination (as illustrated in Figure 2.3 c). These effects make the comparison of temporal series of remote sensing data or the analysis of data within a wide swath problematic (Blackburn and Pitman, 1999).

As sensors with a large IFOV build up a series of views of the same location on the Earth's surface over a period of hours or days, the directional observations can be used to help investigate the issues that arise due to viewing and solar geometry. Semi-empirical models can be based upon the angular information to describe the bi-directional reflectance distribution function of a particular viewing geometry (Hu *et al.*, 1997). This function may be fitted using empirical or physical models (Liang *et al.*, 2000). Such models are used to correct viewing and illumination geometry and the associated effects of shadowing. The outcome of such models allows the scene to be viewed without the effects of solar and sensor changes, thus providing the surface reflectance at nadir observations (Schaaf *et al.*, 2002). Applying empirical techniques (e.g. compositing algorithms) to index-derived data can normalise bidirectional reflectance effects. Numerous methods have been used to normalise reflectance; for example Holben (1986) used maximum value compositing to normalise view direction to nadir and thereby normalise surface reflectance in time series AVHRR.

2.3 Remote sensing of terrestrial vegetation

This section will outline the types of imaging sensors that have significantly contributed to developing our understanding of terrestrial vegetated ecosystems, and more specifically, the monitoring of temporal vegetation dynamics and vegetation condition.

Remote sensing has been used to determine vegetation spatial extent, cover type and biophysical and chemical properties. However, despite the different generations of remote sensing satellite sensors that have been launched since ERTS-1 in 1972, not one series of sensors provides the capacity to fully meet the requirements of the user community investigating temporal vegetation dynamics (Boyd and Danson, 2005).

2.3.1 The role of ‘Moderate’ spatial resolution satellite sensors

Satellite remote sensing can contribute to the field of terrestrial global change monitoring by providing a macroscopic view of the Earth’s vegetated ecosystems and systematically monitoring change over time and space. Coarse spatial resolution sensors have been defined as those with a spatial resolution between 250 m and 5km and until recently such sensors were referred to as ‘moderate’ resolution (Justice and Tucker, 2009). ‘Moderate’ resolution sensors provide a unique perspective of Earth. Due to the characteristic wide IFOV (Figure 2.3 a) they allow repeat observations of the same point on the Earth’s surface within the desired maximum period for information updates (repeat pass) of around 10 days. Such a revisit period is necessary due to the potentially dynamic nature of vegetation (Gond *et al.*, 1999).

The drive for an alternative source of data to Landsat MSS in the mid 1980s explored the possibility of adopting the NOAA AVHRR sensor for vegetation. With a spatial resolution of 1.1km (in Local Area Coverage mode), and 4.4 km (in Global Area Coverage mode) and daily global observations, the AVHRR sensor, a system designed to support weather applications, operating broad bands in the visible – thermal infrared domain (400-2500nm), offered a unique way to monitor terrestrial surfaces over local to global scales (Baret *et al.*, 2006). The successful application of vegetation index time series approach to grassland monitoring (Justice *et al.*, 1985) meant AVHRR became a unique source of information characterising and detailing the temporal variability in land surface properties and vegetated ecosystems (Bacour *et al.*, 2006).

Chapter 2. The remote sensing of canopy chlorophyll content

The potential of deriving vegetation index time series from a sensor with a high temporal resolution was widely recognised. AVHRR NDVI time series were used to explore inter-annual variability of vegetation, coupling for the first time regional phenology with climate variation. Tucker *et al.* (1986) linked global photosynthetic rates to fluctuation in atmospheric CO₂. The ability to determine vegetation phenology and temporal variation of productivity using vegetation indices has led to the adoption of ‘moderate’ spatial resolution sensors as a tool for the measurement and monitoring of terrestrial environments at the regional to global scale.

Deriving time series vegetation analysis from AVHRR data introduced a number of obstacles to the development of useable datasets (Justice and Tucker, 2009). The wide swath width of AVHRR meant that pixels at the scenes’ edge were viewed at large off nadir viewing angles (up to 55°). The lack of on-board calibration also meant that methods were needed to correct satellite sensor performance. Such issues led the way for the development of MODIS and other ‘moderate’ resolution sensors, which were designed, in part, to exploit the potential demonstrated by AVHRR NDVI time series data.

To date a number of ‘moderate’ resolution sensors have been launched, including the Along-Track Scanning Radiometer (ATSR), SPOT Vegetation Program, and the Medium Resolution Imaging Spectrometer (MERIS). However, of the current sensors most of the terrestrial research activity has concentrated on MODIS data. This can be explained by the availability of information supporting the MODIS instrument and the availability of products, which have been extensively validated (Justice and Tucker 2009).

2.3.2 Imaging spectrometry

Remote sensing has been used extensively to monitor and quantify changes in terrestrial vegetation across a broad range of spatial and temporal scales. What has become clear is that the type of remotely sensed data required for the monitoring of vegetation depends on the ecological questions being asked (Curran, 2001). Typically, terrestrial vegetation research can be categorised into three themes:

Chapter 2. The remote sensing of canopy chlorophyll content

1. “What is the type of vegetation that is there?”
2. “How much vegetation is there?”
3. What is the condition of the vegetation?”

Vegetation type and quantity investigations usually incorporate broad waveband remotely sensed data, whereas assessing vegetation condition typically utilises reflectance data acquired in narrow wavebands (Dash *et al.*, 2008). Vegetation condition can be assessed by estimating foliar chlorophyll content from data recorded in narrow visible / NIR wavebands by imaging spectrometers.

Spectrometry is the science of measuring the intensity of optical radiation in narrow, contiguous wavelength intervals (Schaepman, 2009). Imaging spectrometers, or hyperspectral sensors, are instruments used to acquire a spectrally resolved image of a scene in fine spectral and spatial resolution, whereby for each registered pixel radiance spectrum can be derived (Goetz *et al.*, 1985).

The application of narrow-band spectral methods for pigment detection using airborne and spaceborne spectrometers has been the intended goal of much of the leaf level research since the time of the (Advanced Canopy Chlorophyll Program) ACCP program (Ustin *et al.*, 2009). Imaging spectrometers have been used to estimate foliar biochemical content of vegetation canopies due to contiguous narrow bands in wavelengths that sample individual absorption and reflectance features that are characteristic of green vegetation (Dash *et al.*, 2008). A number of methods have been developed to exploit the reflectance properties of green leaves in the ‘red edge’ region of the reflectance spectrum.

However, at present there are only two operational spaceborne imaging spectrometers, the Moderate Resolution Imaging Spectrometer (MODIS) onboard NASA’s Terra and Aqua satellites, and MERIS onboard ESA’s Envisat satellite.

2.4 Methods for the estimation of content using remote sensing

Photosynthetic pigments have different spectral behaviour, with specific absorption features at different wavelengths, which permit remote sensing techniques to potentially discriminate their respective effects on vegetation reflectance spectra. Using laboratory analysis, field measurements, and remotely sensed data, scientists have made tremendous progress in developing approaches and methods to estimate chlorophyll content at both leaf and canopy levels, and over diverse vegetation species (Haboudane *et al.*, 2008).

Existing methods of extracting quantitative biophysical and biochemical information from optical imagery suggests that there are a limited range of methods (McDonald *et al.*, 1998). Such methods can be physically based, including inversion of canopy models, or use empirical and semi-empirical methods, including vegetation indices to estimate the chlorophyll content at both the leaf and canopy scale (Haboudane *et al.*, 2002). Both techniques have been used successfully and have captured the geographical and temporal variations in biochemical canopy content.

2.4.1 Vegetation indices

Vegetation Indices (VI) are designed to emphasise the differences in spectral reflectance, between the wavelengths and variables under study, which for vegetation applications are usually in the red and NIR regions of the reflectance spectrum. Indices based on optical wavebands exploit the fact that green vegetation absorbs radiation in the red wavelengths, due to the presence of chlorophyll and other photosynthetic pigments in leaves, and strongly scatters solar radiation in the NIR wavelength because of internal leaf structure. The output of such indices is an empirical measure of the biophysical variable being investigated. Due to their simplicity, ease of application and widespread familiarity, vegetation indices have a wide range of usage within the user community.

During the past four decades vegetation indices using band combinations in the visible spectrum have been used to estimate total pigments. Based on simple combinations of visible and NIR reflectance, vegetation indices have been used to define vegetation status and condition. Such indices as the Normalised Difference Vegetation Index (NDVI) (Rouse *et al.*, 1973) or the Simple Ratio (SR) (Jordan, 1969) have been

Chapter 2. The remote sensing of canopy chlorophyll content

extensively used to monitor vegetation at local to global scales (Rondeaux *et al.*, 1996). The NDVI is essentially a measure of ‘greenness’ and has been used to infer the LAI as well as casually linked to canopy chlorophyll content (Ustin *et al.*, 2009). The NDVI bears a near linear relationship with LAI, the fraction of photosynthetically active radiation (*f*PAR) (Mynemi and Williams, 1994) and photosynthetic biochemical content (Jones *et al.*, 2007). Generally, vegetation indices and normalised ratios have been shown to be a strong indicator of photosynthetically active biomass (Van Der Meer *et al.*, 2001), and therefore show a correlation with canopy chlorophyll content.

In reality, the shape of the reflectance spectra from a vegetated canopy will be a function of the scene characteristics and is influenced by leaf and canopy biochemical content composition, canopy structure, soil characteristics as well as view and solar geometry. Some research has shown that indices are not solely responsive to changes in the vegetation cover. For example, research into the response of six vegetation indices and a simple ratio concluded that indices did not respond linearly to vegetation cover change (McDonald *et al.*, 1998). Vegetation indices have been shown to be sensitive to the effects of topography, LAI variations, solar and viewing geometry, background variation, and stand structure (McDonald *et al.*, 1998). Vegetation indices such as the NDVI are particularly sensitive to atmospheric conditions and soil background, as well as solar and viewing geometry. A number of alternative methods utilising VI were developed to account for non-vegetation effects. Indices such as Soil Adjusted Vegetation Index (SAVI) (Huete, 1988) and Modified Soil Adjusted Vegetation Index (MSAVI) (Qi *et al.*, 1994) attempt to compensate for the effects of soil background and soil moisture respectively. The ARVI (Atmospheric Resistant Vegetation Index) (Kaufman and Tanré, 1992) has been developed to reduce the contribution of atmospheric affects, with less associated noise than the NDVI (Rondeaux *et al.*, 1996). The spectral position and breadth of the bands used in each VI significantly influence the suitability of the use of each vegetation index.

The influence of sub-canopy soil background can be pronounced on intrinsic vegetation indices, such as the SR or NDVI, in instances where vegetation cover is low and the soil reflectance is unknown. The established linear relationship between NIR and visible reflectance from bare soils allows the influence of soils upon the vegetation reflectance

spectra to be minimised through assuming this linear relationship. Although significantly reducing the effects of soil background, soil adjusted vegetation indices required knowledge of the study area (such as LAI or soil reflectance characteristics). However, due to the variability in soil reflectance characteristics, because of the aforementioned mineral, roughness, organic matter and soil water content influences, case to case studies are always necessary to ensure soil effects are minimised (Roundeaux *et al.*, 1996).

The inherent problem with broad waveband vegetation indices based on the red and NIR region of the electromagnetic spectrum is the saturation that arises due to the asymptotic relationship with LAI and biomass (Mutanga and Skidmore, 2004). NDVI has been shown in numerous studies to provide poor estimates of biomass where vegetation cover is equal to or greater than 100%. The use of NDVI as a monitoring tool is limited in tropical areas, high biomass ecosystems and in peak growing seasons for forested and agricultural areas, where LAI is underestimated due to saturation of NDVI (Zarco – Tajada *et al.*, 2001).

The problem of asymptotic saturation is common with vegetation products derived from multispectral imagery due to the broad wavebands in which reflectance is acquired. Studies using imaging spectrometers, evaluating the reflectance in individual narrow bands, have reduced biomass saturation issues (Blackburn, 1999). Narrow band VIs designed to estimate chlorophyll content use different combinations of spectral bands to minimise variations in non-foliar photosynthetic pigments, whilst maximising sensitivity to chlorophyll content (Haboudane *et al.*, 2002). Such wavelengths are based upon the robust relationship between chlorophyll content and the red edge position (REP). The spectral regions that are identified as the most suitable to study chlorophyll effects are those around 680 nm, corresponding to the absorption peak of chlorophyll *a*, and around the red edge, 700 – 750 nm. Such wavelengths have been shown to provide significant correlations with LAI, biomass (Eitel *et al.*, 2007) and chlorophyll content (Zarco–Tejada *et al.*, 2005). Detailed discussions and reviews concerning appropriate optimal wavelengths and chlorophyll indices can be found in publications such as those by Blackburn (1999).

Several narrow waveband leaf-level optical indices have been suggested for chlorophyll content estimation from contiguous reflectance data. Red Edge Reflectance Indices such as (R_{740}/R_{720}) and $(R_{734}+R_{747}) / (R_{715} + R_{726})$ (Vogelmann *et al.*, 1993); (R_{750}/R_{700}) (Gitelson and Merzlyak, 1996); (R_{695}/R_{760}) (Carter, 1994); (R_{750}/R_{710}) (Zarco-Tejada *et al.*, 2001), have been developed to estimate chlorophyll concentration. The aforementioned indices, however, do not show the same relationship at the leaf and at the canopy levels, due to the effects of scene components, such as soil, shadows and non photosynthetic biomass. Indices such as red edge and spectral and derivative indices were shown to be the best indicators for total chlorophyll content estimation at the leaf scale and canopy levels (Zarco-Tajada *et al.*, 2004). Such narrow waveband indices were successfully tested on closed canopies with potentially large shadow effects and minimal influences of soil background, demonstrating insensitivity to the influence of shadows.

An inherent issue with the application of VI to estimate canopy biophysical and biochemical variables is their transferability. The shape and form of canopy reflectance spectra depend on a complex interaction of several canopy variables (e.g., vegetation structure, leaf biochemical composition, soil background) and viewing and illumination geometry and atmospheric factors (Baret and Guyot, 1991) that will vary over time and space and from one vegetation type to another. As a result, the relationship between a sought vegetation variable and a VI is likely to be a function of canopy characteristics, soil background effects and external conditions.

2.4.2 Red edge position techniques

The REP has been shown to be highly correlated with foliar chlorophyll concentration (Zarco - Tejada and Miller, 1999), and can be derive mathematically by

$$D_{\lambda(i)} = R_{\lambda(i)} - R_{\lambda(i-1)} / \Delta\lambda \quad (2.1)$$

Where $D_{\lambda(i)}$ is the REP derivative spectrum, $R_{\lambda(i)}$ and $R_{\lambda(i-1)}$ are reflectances at wavelength i and $(i-1)$ respectively (Curran and Dash, 2005). The application of the first derivative method to estimate REP requires continuous reflectance spectra measured by a sensor with fine spectral resolution. To overcome the dependency on continuous spectra

numerous methods have been proposed for determining the slope and position of the REP including, linear interpolation (Guyot *et al.*, 1988), Lagrangian interpolation (Dawson and Curran, 1998), polynomial fitting (Baret *et al.*, 1992) and inverted Gaussian fitting (Bonham-Carter, 1998). However, each curve fitting technique derives a different location for the REP and therefore estimation of chlorophyll content (Dash and Curran, 2007; Cho and Skidmore, 2006).

Curve-fitting techniques to derive the REP are complex, non-automated procedures (Verstraete *et al.*, 1999) and time consuming for large data sets (Dash and Curran, 2007). REP techniques are not suitable for the estimation of chlorophyll content in high chlorophyll content canopies due to the asymptotic relationship between REP and chlorophyll content (Jago *et al.*, 1999). In such instances, REP techniques saturate, therefore they are not suitable for global terrestrial vegetation monitoring in areas of high biomass. Moreover, REP methods are inappropriate for the use on current spaceborne sensors where reflectance is recorded in distinct bands (Dawson and Curran, 1998).

2.4.3 Modelling approaches

This section briefly introduces the theory of modelling as it has been used to estimate canopy chlorophyll content. Remotely sensed vegetation reflectance models can be used to derive canopy biophysical variables (both structural and optical properties), or to describe or correct the reflectance variation caused by geometry (Lucht and Lewis, 2000). Vegetation models are based upon a number of variables that simplify canopy components to make estimation computationally efficient. Canopy reflectance modelling takes one of two approaches, physical or empirical. Compared to (semi-) empirical regression models based on vegetation indices, physically based Radiative Transfer Models (RTM) have the advantage that they can be adapted to the prevailing observation geometry (viewing / illumination geometry) and site specific characteristics such as local background reflectance, atmospheric conditions, crop type, and phenology (Dorigo and Gerighausen, 2008). Physical models describe the transfer and interaction of radiation inside the canopy based on physical laws and thus provide an explicit connection between the biophysical variables, canopy structure and canopy reflectance (Houborg *et al.*, 2009) and have proven to be an alternative to empirical–statistical

approaches that link VI and vegetation variables using experimental data.

Inversion methods are one way in which to determine or derive biophysical and biochemical variables at the leaf and canopy scale. Such inversion can be achieved through utilizing look-up-tables, neural networks (Bacour *et al.*, 2006b), and genetic algorithms amongst others (Myneni *et al.*, 1992, Houborg *et al.*, 2009). The goal of such models is to determine reflectance characteristics for a given view and illumination geometry and use this to account for surface characteristics.

The canopy reflectance models, such as the turbid medium Markov chain canopy reflectance model (ACRM) (Kuusk, 1996) make assumptions regarding stand geometry and vegetation structure. ACRM assumes the canopy consists of a homogeneous layer of vegetation and a thin layer of vegetation on the ground surface. Similarly, the physically based PROSPECT is an example of an RTM based on the plate model that simplified the optical properties of plant leaves (in the region of the spectrum between 400-2500nm) (Jacquemoud and Baret, 1990). Within this model scattering is defined and variables are individually mathematically described (such as photosynthetic pigments, pigment concentration, water content and mesophyll structure) and the model has been evaluated using independent datasets on a local scale successfully (Jacquemoud *et al.*, 1996). Many RTM are available at different scales, from leaf level (1-D PROSPECT) to the canopy level (e.g. SAIL).

Model inversion techniques, based on linked leaf-canopy radiative transfer models, have been shown to be a feasible method for biochemical estimation from canopy-level reflectance in closed canopies (Jacquemoud, 1993; Jacquemoud *et al.*, 2000). However, complex modelling techniques when used on regional and global scales are more problematic. Issues of scaling, surface irregularities and difficulties in obtaining multi-angular datasets limit the use in vegetation modelling (Asrar *et al.*, 1992). Model applications have shown to be viable when defining biochemical and biophysical characteristics on relatively homogenous and spatially continuous vegetation. The estimation of leaf biochemistry in open vegetation canopies from remote sensing data requires modelling strategies which account for soil background and shadows which dominate the bidirectional reflectance (BRDF) signature.

Computation modelling allows the plant to be expressed as a geometric shape, which interacts with a series of others to make up a model of a vegetated canopy. Such models incorporate the physical scattering between the components of the plant (leaves, stems) and between soil and other adjoining plants. Such models are useful to interpret reflectance from open vegetation canopies, where information within a pixel is a combination of soil, shadow and vegetation. The simulated reflectance at different wavelengths and pixel sizes can be useful in the study of the effect of up-scaling on spectral vegetation indices (Zarco – Tejeda *et al.*, 2001). Inversions of 3-D vegetation models allow canopy variables, such as LAI and chlorophyll content, to be estimated (Justice *et al.*, 1998). Such models are complex, and like REP curve fitting techniques, time consuming for large data sets which means they are not suitable for monitoring vegetation dynamics at regional to global scales.

2.5 The MERIS Sensor

MERIS has been described in detail in a number of publications (Curran and Steele, 2005; Delward *et al.*, 2007). In this literature review details relating to the sensor's role of monitoring terrestrial vegetation will be recalled. The MERIS sensor onboard the ESA Envisat satellite is potentially a valuable sensor for monitoring the Earth's terrestrial environments at regional and global scales due to its moderate spatial resolution and three day repeat cycle (Curran and Dash, 2004). The MERIS repeat cycle is within the desired maximum period for information updates (repeat pass) of around 10 days, due to the potentially dynamic nature of vegetation, where growth can be rapid in some ecosystems according to season (Gond *et al.*, 1999).

MERIS was originally designed for oceanographic applications (the measurement of phytoplankton and suspended matter) and atmospheric applications (including cloud properties, measurement of water vapor column content and aerosols) (Van Der Meer, 2001). With a unique fine radiometric resolution MERIS is the most radiometrically accurate sensor in space (Curran and Steele, 2005) (Table 2.2). Unlike many spaceborne sensors, the MERIS platform has good spectral sampling in the visible / NIR wavelengths coupled with narrow wavebands that theoretically improve the accuracy of vegetation monitoring. MERIS is a push broom imager that acquires reflectance in 15 programmable bands, 2.5 nm – 20 nm wide in the region of the spectrum between 390

Chapter 2. The remote sensing of canopy chlorophyll content

nm – 1040 nm (Dawson, 2000) (Table 2.2). The radiometric requirement (fully programmable potential) and accuracy (maintained through on-board band-to-band calibration) of the MERIS sensor are far in excess of that of any sensor orbiting the Earth (Van Der Meer *et al.*, 2001). The high radiometric accuracy will allow potential pigment identification and quantification in both oceanic and terrestrial applications. In the standard setting, MERIS has 5 discontinuous bands in the red and NIR wavelengths, nominally set to 665, 681.25, 705, 753.75 and 760 nm (Table 2.2).

| Band | | | |
|---------------|--------------------|-------------------|--|
| Number | Centre (nm) | Width (nm) | Environmental variables of interest |
| 1 | 412.5 | 10 | Yellow substance turbidity |
| 2 | 442.5 | 10 | Chlorophyll absorption |
| 3 | 490 | 10 | Chlorophyll, other pigments |
| 4 | 510 | 10 | Turbidity, suspended sediment, red tides |
| 5 | 560 | 10 | Chlorophyll reference, suspended sediment |
| 6 | 620 | 10 | Suspended sediment |
| 7 | 665 | 10 | Chlorophyll absorption |
| 8* | 681.25 | 7.5 | Chlorophyll fluorescence |
| 9* | 708.75 | 10 | Atmospheric correction |
| 10* | 753.75 | 7.5 | Oxygen absorption reference |
| 11 | 760.625 | 3.75 | Oxygen absorption R-branch |
| 12 | 778.75 | 15 | Aerosols, vegetation |
| 13 | 865 | 20 | Aerosols correction over ocean |
| 14 | 885 | 10 | Water vapour absorption reference |
| 15 | 900 | 10 | Water vapour absorption, vegetation |

*Indicates bands for calculating MTCI.

Table 2.2. MERIS band properties adapted from Curran and Steele (2005).

The pixel size at nadir are 260m across track by 300m along track. The sensor has a field-of-view (FOV) of 68.5° and a swath width of 1150 km on the ground. The FOV is divided between five cameras, each with a FOV of 14°. MERIS is in a Sun synchronous orbit, with a local time overpass at the Equator (descending limb of orbit) of 10.00 am (Dewald *et al.*, 2007; Gao *et al.*, 2004). Due to the wide swath, important consideration

should be given to the fact that MERIS imagery will compose of reflectance obtained at differing view and illumination angles (section 2.3.3).

Prior to the launch of Envisat, the potential of the MERIS sensor as a valuable tool for monitoring terrestrial ecosystems was recognised. The radiometric resolution and narrow band width of the MERIS sensor were considered appropriate to derive the red edge position which marks the boundary between the chlorophyll absorption feature at red wavelengths and the NIR reflectance maxima due to leaf internal scattering (Gobron *et al.*, 1999; Dawson, 1999).

2.6 The MERIS Terrestrial Chlorophyll Index (MTCI)

Methods used to determine chlorophyll content from remote sensing data have focused on locating the red edge position between the red absorption feature and the NIR reflectance maxima of a vegetation reflectance spectrum (Curran *et al.*, 2007). However, such methods are time-consuming and are not accurate indicators of chlorophyll content at high contents. The MERIS Terrestrial Chlorophyll Index (MTCI) was designed to monitor vegetation condition via an estimation of chlorophyll content by exploiting the MERIS band positions in the chlorophyll absorption feature and the red edge.

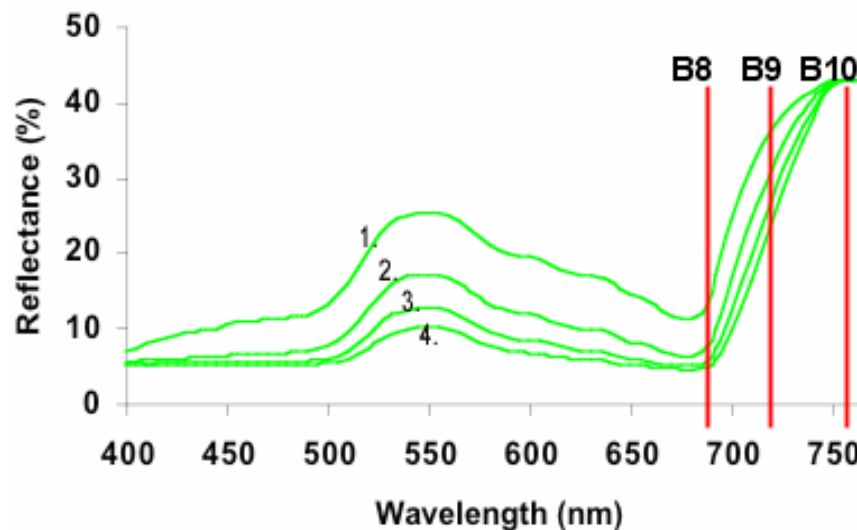


Figure 2.4. Vegetation reflectance spectra at four chlorophyll contents, increasing content 1-4, together with the location of the MERIS bands 8, 9 and 10, located in the red edge region of the spectra.

Chapter 2. The remote sensing of canopy chlorophyll content

With an increase in chlorophyll content the difference in reflectance between band 8 and 9 decreases (Figure 2.4), whilst the difference in reflectance between bands 9 and 10 increases. The MTCI is very simple to calculate, overcoming the potential limitations of using REP methods to derive chlorophyll content. It is calculated using the ratio of the difference in reflectance between band 10 and band 9 and the difference in reflectance between band 9 and band 8 of the MERIS standard band setting:

$$\text{MTCI} = R_{753.75} - R_{708.75} / R_{708.75} - R_{681.25} \quad (2.1)$$

Or

$$\text{MTCI} = R_{\text{band } 10} - R_{\text{band } 9} / R_{\text{band } 9} - R_{\text{band } 8} \quad (2.2)$$

Where $R_{753.75}$, $R_{708.75}$, $R_{681.25}$ are reflectance in the centre wavelengths (nm) of the MERIS standard band setting in bands 10, 9 and 8 respectively (Table 2.2). The MTCI may be used to derive an estimate of the relative location of the reflectance ‘red edge’ of vegetation, yet it is sensitive to all values of chlorophyll content, unlike REP techniques that suffer from saturation problems at high chlorophyll contents. The MTCI combines information on leaf area index and foliar chlorophyll concentration to produce a metric for chlorophyll content (Dash *et al.*, 2008).

The MTCI has been adopted as an ESA Level 2 land product, whereby MTCI 8-day and monthly global composites are produced in near real time (Curran *et al.*, 2007). Given that the MTCI is the only available chlorophyll index from a spaceborne sensor there is now a real opportunity for monitoring vegetation function and condition systemically and reliably.

2.6.1 Evaluation of the MTCI

The Algorithm Theoretical Basis Document (ATBD) (Curran and Dash, 2005) outlines the criteria for the design of the MTCI as follows:

1. Sensitive to a wide range of chlorophyll contents
2. Estimation of the MTCI values, unlike REP techniques, requires minimal computational costs in terms of processing capacity.
3. Estimation of chlorophyll with MTCI is independent of soil and atmospheric condition, spatial resolution and observation geometry.

Data from model, laboratory and field measurements as well as MERIS data were used in the initial indirect evaluation of the MTCI to assess the MTCI in relation to points 1-3 listed above. Modelling the reflectance spectra, using LIBSAIL (a combination of Leaf Incorporating Biochemistry Exhibiting Reflectance and Transmittance Yield (LIBERTY) and Scattering by Arbitrary Inclined Leaves (SAIL) (Curran and Dash, 2005)), simulated MERIS band positions over a wide range of chlorophyll contents. The modelled data revealed a near linear relationship between chlorophyll content and MTCI. The angle of the regression line between chlorophyll content and MTCI suggested sensitivity to high chlorophyll contents. Such sensitivity was confirmed using canopy reflectance spectra from Douglas-fir (*Pseudotsuga menziesii*) and big leaf maple (*Acer macrophyllum*) (Curran and Dash, 2005). The relationship between MTCI and chlorophyll content for Douglas-fir and big leaf maple had a coefficient of determination (R^2) of 0.64 and 0.72 respectively (Dash and Curran, 2007).

Further evaluation of the MTCI, again carried out by Dash and Curran (2007), using field derived chlorophyll content from various crops, demonstrated a strong positive relationship with 'full resolution' MTCI (R^2 of 0.8). The MTCI has now been used with success to estimate foliar and canopy chlorophyll content in several applications. To date, the MTCI has been used in a growing body of research to estimate chlorophyll content in a variety of environmental applications: estimating crop productivity (Dash and Curran, 2007) and GPP based upon the relationship between chlorophyll content and MTCI in six species of wheat (Wu *et al.*, 2009). The MTCI has also been used as a surrogate to infer salt stress in coastal zones that were affected by the Indian Ocean

tsunami (Dash and Curran, 2006) and estimate environmentally induced stress in oak forests (Rossini *et al.*, 2007). Dash *et al.*, (2007) show that the MTCI may also be used in land cover classification, whereby the variation in leaf chlorophyll content between high and low chlorophyll season was used to map eleven broad land cover classes.

2.6.2 MTCI operational uncertainties

Although modeled vegetation spectra and initial evaluation have demonstrated a strong relationship between chlorophyll content and MTCI, there are still several of uncertainties that need to be addressed if the MTCI is to be embraced by the user community. The MTCI, by design is sensitive to chlorophyll content, which is a function of foliar chlorophyll concentration and LAI. Therefore the MTCI will change in response to both the foliar concentration of chlorophyll and the amount of vegetation present. If chlorophyll concentration is constant, an increase in LAI will therefore increase chlorophyll content. However, a positive change in LAI is known to increase NIR reflectance, if chlorophyll content is controlled, there is uncertainty regarding the effect of LAI on the MTCI. Similarly, vegetation structure has been shown to influence canopy reflectance, particularly in NIR wavelengths (Soudani *et al.*, 2006). The effect of canopy structure will be particularly relevant assessing the transferability of the MTCI between cover types and will have implications for estimating chlorophyll content in heterogeneous areas.

The initial MTCI design and investigation process removed non-vegetated pixels from MERIS scenes (Curran and Dash, 2005). The process removed those pixels with high red reflectance to allow the interpretation of the vegetated reflectance spectra. As a result of this process the effect of non-vegetated areas has not been considered. As an operational product, an understanding of the effect of non-vegetated areas on the MTCI is of vital importance to permit the successful interpretation of scene properties.

Although modeled data suggest the MTCI is insensitive to both viewing geometry and background reflectance, an operational understanding of both variables is required to lead to the further adoption of the MTCI as a tool for the monitoring of vegetation dynamics at local to global scales.

2.7 Chapter Summary

This chapter reviewed a range of variables and techniques that are typically associated with the estimation of chlorophyll content. Particular reference has been made to the intrinsic problems associated with estimating chlorophyll content and the methods used to estimate it. Figure 2.5 summarises the variables that contribute to the observed reflectance recorded at the sensor. To successfully estimate chlorophyll content, all variables that may contribute to pixel reflectance need to be understood and accounted for.

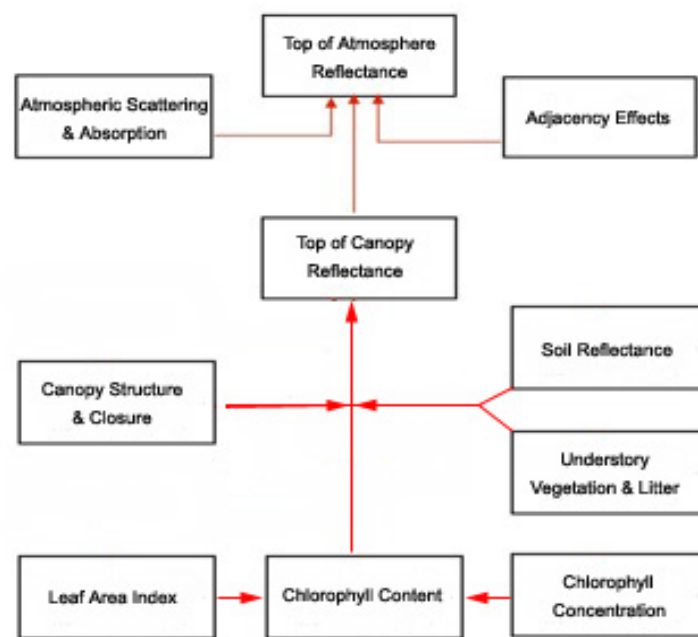


Figure 2.5. This flowline summarises the relationship between chlorophyll content and each factor that contributes to canopy reflectance observed at the sensor.

Although chlorophyll content has been successfully estimated at local to regional scales utilising REP, indices and modelling techniques, such approaches are not feasible at the regional to global scale for use in environmental monitoring. Various limitations are associated with each method and these are summarised as follows:

Vegetation Indices

Vegetation indices, such as the NDVI are designed to exploit the difference in reflectance between the visible and NIR in the vegetation reflectance spectra. The linear relationship between NDVI, LAI and chlorophyll breaks down where the LAI / chlorophyll content of the canopy is high due to saturation caused by the asymptotic relationship with LAI. Furthermore, research has demonstrated that vegetation indices, such as the NDVI, are sensitive to background variation as well as changes in illumination and viewing geometry.

Red Edge Position

REP techniques require hyperspectral or continuous spectra to determine the maximum slope and exact location of the point of maximum slope at wavelengths between 690-740 nm in the reflectance spectra. REP techniques are non-automated, computationally inefficient and therefore would be inappropriate for use on large datasets (e.g. spatial and temporal time series). Due to the current multi-spectral satellite sensors in orbit, REP is not feasible in estimating regional – global chlorophyll content.

Modelling

Computation modelling techniques have been shown to estimate canopy chlorophyll content accurately. Although modelling techniques have been proven to account for the non-Lambertian nature of the Earth's surface, such methods do require prior knowledge of surface characteristics. Complex modelling techniques are limited when used on regional and global scales due to the non-homogeneity of the Earth's surface and difficulties in obtaining multi-angular datasets.

The MTCI

In light of the limitations of existing techniques designed to estimate canopy chlorophyll content at the local – global scale the MTCI was proposed. Based on the unique radiometric characteristics of the MERIS sensor, acquiring reflectance in three narrow bands in the REP, the MTCI has been shown to be sensitive to all values of chlorophyll content, unlike REP techniques and the NDVI that suffer from saturation problems. Coupled with the orbiting characteristics of the Envisat platform, the MTCI offers the potential to monitor global vegetation health and condition every three days.

2.8 Research Objectives

Chlorophyll content is a key canopy variable that is related to quantity, productivity and canopy health. However, prior methods used to estimate chlorophyll content were computationally inefficient, time consuming and required reflectance measured in contiguous bands. The MTCI utilizes the unique bands (width and position) of the MERIS sensor that are located in the red edge region of the reflectance spectra to provide an estimation of canopy chlorophyll content. The preceding literature review highlighted the role that medium resolution sensors such as MERIS may play in providing a pivotal role to monitor global change in terrestrial ecosystems. Therefore there is true potential to monitor globally vegetation status with high temporal resolution. Such data is of vital importance to understanding global carbon cycles and the influence of climate change on terrestrial ecosystems. The challenge now is how to validate the MTCI, and understand the capacity to which global monitoring of chlorophyll content can provide information on local - global vegetation dynamics. There is a potential to define the MTCI's operational use in routine monitoring programs and develop our understanding of terrestrial ecosystem.

The Committee on Earth Observation Satellites (CEOS) established the Working Group on Calibration and Validation (WGCV) to drive the validation of land products to produce higher-level global land products that can be embraced by the user community. Full validation is key to ensure a robust and widely used product that fulfils the users' needs. As the MTCI is the only available chlorophyll index from a spaceborne sensor, comprehensive validation is mandatory to determine the reliability of the index (Baret *et al.*, 2005). The criteria of a global vegetation index includes (after Huete and Justice, 1999):

1. The index should maximize sensitivity to plant biophysical variables (in this instance, chlorophyll content), preferably with a linear response in order that some degree of sensitivity is available for a wide range of vegetation conditions and to facilitate validation and calibration of the index.
2. The index should normalise external effects such as Sun angle, viewing angle, and atmosphere for consistent spatial and temporal comparisons.

Chapter 2. The remote sensing of canopy chlorophyll content

3. The index should normalize canopy background (brightness) variations for consistent spatial and temporal comparisons.
4. The index should be applicable to the generation of a global product, allowing precise and consistent, spatial and temporal comparisons of vegetation conditions.
5. The index should be coupled to key biophysical parameters as part of the validation effort, performance, and quality control.

The principal aims of this research are defined in the context of the above requirements.

These are stated as three objectives:

1. *Assessing the MTCI – chlorophyll content relationship. This thesis will explore not only the relationship between chlorophyll content and MTCI for different vegetation types, but will investigate through laboratory and field experiment the potential influence of non canopy variables on such a relationship. Laboratory based field spectroscopy was used to investigate the influence of illumination and viewing geometry and soil background reflectance on the MTCI – chlorophyll content relationship.*
2. *The development and application of a validation procedure to assess the relationship between MTCI and chlorophyll content in sites with contrasting cover types, canopy structure and architecture (open and closed woodland and agricultural canopies).*

Only through understanding the relationship between MTCI – chlorophyll can the MTCI be used as a tool to monitor vegetation dynamics and environmental change. In the light of 1 & 2, the MTCI will be used to;

3. *Characterise and critically explore the role of the MTCI to monitor vegetation dynamics. The thesis will explicitly investigate the potential role the MTCI may*

Chapter 2. The remote sensing of canopy chlorophyll content

play in characterising vegetation phenology and gross primary productivity. Through exploring the MERIS data archive, 2002 – date, vegetation dynamics can be characterized over a six growing seasons for a variety of contrasting land cover types.

The overriding aim of this thesis is to establish whether the MTCI meets the requirements related to prediction accuracy and consistency, regarding the need for specific spectral indices that are sensitive exclusively to a vegetation/canopy descriptor of interest, i.e. chlorophyll content.

2.9 Thesis plan

Chapter 3 investigates the relationship between chlorophyll content and MTCI using field spectroscopy and investigates the potential influence non-canopy variables may have on such a relationship. Experimental evaluation of factors that may influence the relationship between the MTCI and chlorophyll content involves the *in situ* measurement the MTCI from different vegetation types, soil background and illumination and view angles. Chapter 3 addresses research objective 1.

The aim of Chapter 4 is to examine the methodological issues associated with aggregating chlorophyll content acquired from ground-based point measurements to the ‘full resolution’ of the MTCI at 300m. The validation campaign assessed the MTCI as a tool for estimating chlorophyll in woodland and arable farming locations. Chapter 4 addresses research objective two.

Chapters 5 and 6 assess the temporal variability and sensitivity of the MTCI to estimate vegetation dynamics; addressing the suitability of the MTCI as a tool to monitor vegetation phenology and productivity across a variety of vegetation land cover types. As a benchmark, the sensitivity of the MTCI was compared against validated MODIS products. Conclusions in Chapter 5 and 6 will fulfill research objective three.

Chapter 7 discusses the main findings made in the previous chapters, provides conclusions of the research objectives and identifies the potential for further work.

**CHAPTER 3: EVALUATION OF THE RELATIONSHIPS
BETWEEN CANOPY CHLOROPHYLL CONTENT AND
THE MTCI AND THE EFFECT OF VIEW ANGLE AND
SOIL BACKGROUND**

Chapter 3

3.1 Introduction

Spectroscopy is widely used as a means of scaling up our understanding of the interactions between energy and vegetation canopies, from the scale of individual leaves, to coarser canopy-scale studies (Milton *et al.*, 2007). Understanding the relationship between canopy and incident radiation can be thoroughly investigated through spectroscopy in the laboratory environment, which can provide meaningful insight into the observed reflectance recorded with airborne and satellite sensors. Field measurements may suffer from the effects of unstable atmospheric conditions (cloud cover, humidity etc), as well as consistently changing solar geometry. However, laboratory based spectroscopy allows better control over environmental conditions, allowing control of incoming radiation, atmospheric conditions, radiation geometry and canopy and sub canopy variables (Dangel *et al.*, 2005). This approach allows thorough investigation of the effects of view angle and radiation geometry on canopy reflectance.

As has been previously discussed (Chapter 2), canopy reflectance can be significantly affected by canopy background (Price, 1990). The effects of canopy background is relevant for vegetation monitoring since 70% of the Earth's terrestrial surface consists of open canopies with significant canopy background signals exerting some effect on the canopy reflectance properties (Graetz, 1990). These open canopies include deserts, tundra, grasslands, shrub lands, savannas, woodlands, wetlands, and many open forested areas. One major contribution to canopy reflectance in open canopies can be attributed to the optical properties of the soil.

Large field-of-view (FOV) sensors, such as MERIS, have the advantage of increasing spatial and temporal coverage. However, off-nadir viewing introduces changes in sensor signal in response to variations in Sun and view angles (Galvaõ *et al.*, 2004). As a result of this spectral dependence, these effects are not removed by the calculation of vegetation indices.

At present little work has been carried out to determine the influences of soil background and viewing geometry upon on the MTCI. Therefore, there is a pressing need to

evaluate the effect of these variables on the MTCI – chlorophyll content relationship. To understand the performance of the index and its utility in the provision of robust measures of canopy chlorophyll content there is a need to validate the index across a range of acquisition and environmental conditions.

3.2 Chapter aims

The aim of this chapter is to investigate the factors that may influence the relationship between the MTCI and chlorophyll content. The objectives of this investigation were to:

- (i) Evaluate the relationship between chlorophyll content and the MTCI and five other spectral indices and REP that can be derived from current, moderate spatial resolution spaceborne sensors.
- (ii) Evaluate the effect of two major non-canopy variables: soil background and view angle on the relationship between chlorophyll content and the MTCI.

A series of spectral measurements employing laboratory-based spectroscopy were used to calculate the MTCI. The variability in MTCI as a result of the following variables was explored:

(a) Chlorophyll content: As a global product the MTCI will be used to estimate across a broad range of chlorophyll contents. In this experiment spinach, *Spinacia oleracea* (planophile type) was studied and grown under different fertilisation regimes to control chlorophyll content allowing the assessment of the sensitivity of the MTCI.

(b) Soil background: The effect of vegetation cover on the MTCI may be dependent on the type of scene background. A robust global product will need to derive chlorophyll content across a range of soil types and background colours. A range of different soil types and moisture content was explored.

(c) Sensor view angle: Little research has been undertaken into the influence of shadowing or illumination and viewing geometry on either MERIS data or the MTCI. With a FOV of 68.5° and a swath width of 1150km (Gao *et al.*, 2004) MERIS can only provide limited angular observations at large view zenith angles. It would therefore not be feasible to create BRDF MERIS products to examine the effect of viewing and

illumination geometry on the MTCI. Therefore a range of reflectance measurements was used to examine the effect of sensor view angle on the MTCI.

3.3 Method

A series of experiments were undertaken in a greenhouse located at the School of Biological Sciences, University of Southampton. Spinach (*Spinacia oleracea*) was grown with different levels of fertilisation and soil backgrounds in twenty-one growing trays (measuring 30 cm x 50 cm). The climate-controlled greenhouse had a maximum temperature of 20 °C, a minimum temperature of 12 °C and daylight duration of 16 hours.

For the purpose of this experiment, four soil types were used in twelve trays:

- (i) Standard bare soil (mixture of $\frac{2}{3}$ topsoil and $\frac{1}{3}$ compost),
- (ii) Grey soil (same as standard bare soil but covered with silver sand),
- (iii) White soil (same as standard bare soil but covered in talc layer),
- (iv) Moist soil (standard bare soil that had a controlled amount of water applied prior to spectral measurements being taken).

Two weeks after sowing and several days after germination the first set of measurements (SPAD, digital images and spectral reflectance) were undertaken and immediately after these measurements fertilisation was carried out using a foliar feed containing Nitrogen, Phosphorus and Potash.

Spinach plants were manipulated to provide variation in scene properties, including chlorophyll concentration and leaf area. Using the standard soil mixture three trays were subjected to high fertilisation (100% foliar feed), low fertilisation (50% diluted foliar feed) treatment and three were unfertilised (Table 3.1). Trays were placed on a perforated elevated platform to reduce cross contamination from the seepage of water. Fertilisation was then carried out at weekly intervals up to a week before the end of the experiment. Spectral reflectance, chlorophyll concentration and LAI were measured weekly at the canopy level for four weeks.

| Tray code | Soil type | Fertilisation regime | Addition wetting prior to spectral measurements |
|-----------|------------------------|----------------------|---|
| NF | Standard bare soil | No fertilisation | None |
| MF | Standard bare soil | 50% foliar feed | None |
| HF | Standard bare soil | 100% foliar feed | None |
| GS | Grey soil | No fertilisation | None |
| BS | Standard bare soil | No fertilisation | None |
| WBS | Standard wet bare soil | No fertilisation | Yes, 500ml prior to measurements |
| WS | White soil | No fertilisation | None |

Table 3.1. Summary of the spinach trays used in this experiment.

3.3.1 Spectral measurement

A laboratory experiment was undertaken in which reflectance spectra were measured, four times over a period of four weeks, under controlled illumination conditions. The reflectance spectra were obtained using the Geophysical and Environmental Research Corporation's single beam GER-1500 field spectrometer (on loan from the NERC Field Spectroscopy Facility). The GER 1500 had an angular FOV of 4°, the spectrometer was positioned on a tripod at 1.0m above the target, at nadir, giving a sampling area within the FOV of 10.6 cm diameter and area of 88.2 cm². The illumination source was a 500W Kaiser video light positioned on another tripod, 2.0m away from the target at an inclination angle of 60° (Figure 3.1). Compared with sunlight, laboratory illumination is highly heterogeneous (Sandmeier *et al.*, 1998). Therefore, maintaining a consistent illumination source was of vital importance, minimising methodological error in the reflectance measurements. The chosen illumination source, the 500W Kaiser video lamp, provides consistent spectral radiance, whilst minimising laboratory set-up costs (Malthus, personal communication, March 2007). To minimise the effects of stray light and inter laboratory reflectance from equipment, surfaces in the laboratory were covered in a black felt cloth. Spectroscopy was used to select a cloth based on its spectral

Chapter 3. Evaluation of the canopy chlorophyll content and MTCI relationship

properties, i.e., it was important to select a suitable covering material that minimised reflectance in the visible and NIR regions of the reflectance spectra.

The 50 cm growing trays allowed a maximum of 3 measurements per tray; therefore 3 points were positioned 10 cm apart and were permanently marked on the tray at the centre of each FOV using a visible marker. The spectral reflectance of each data point was an average of 10 spectral measurements. One non-Lambertian Spectralon panel was used as a reference target and spectral measurements were undertaken at regular intervals during the experiment to ensure consistency. Spectral measurements at seven sensor view angles (between -30° and $+30^{\circ}$) were also recorded in the principle plane for weeks 1-4 for Spinach grown in medium fertilised soil (Figure 3.1).

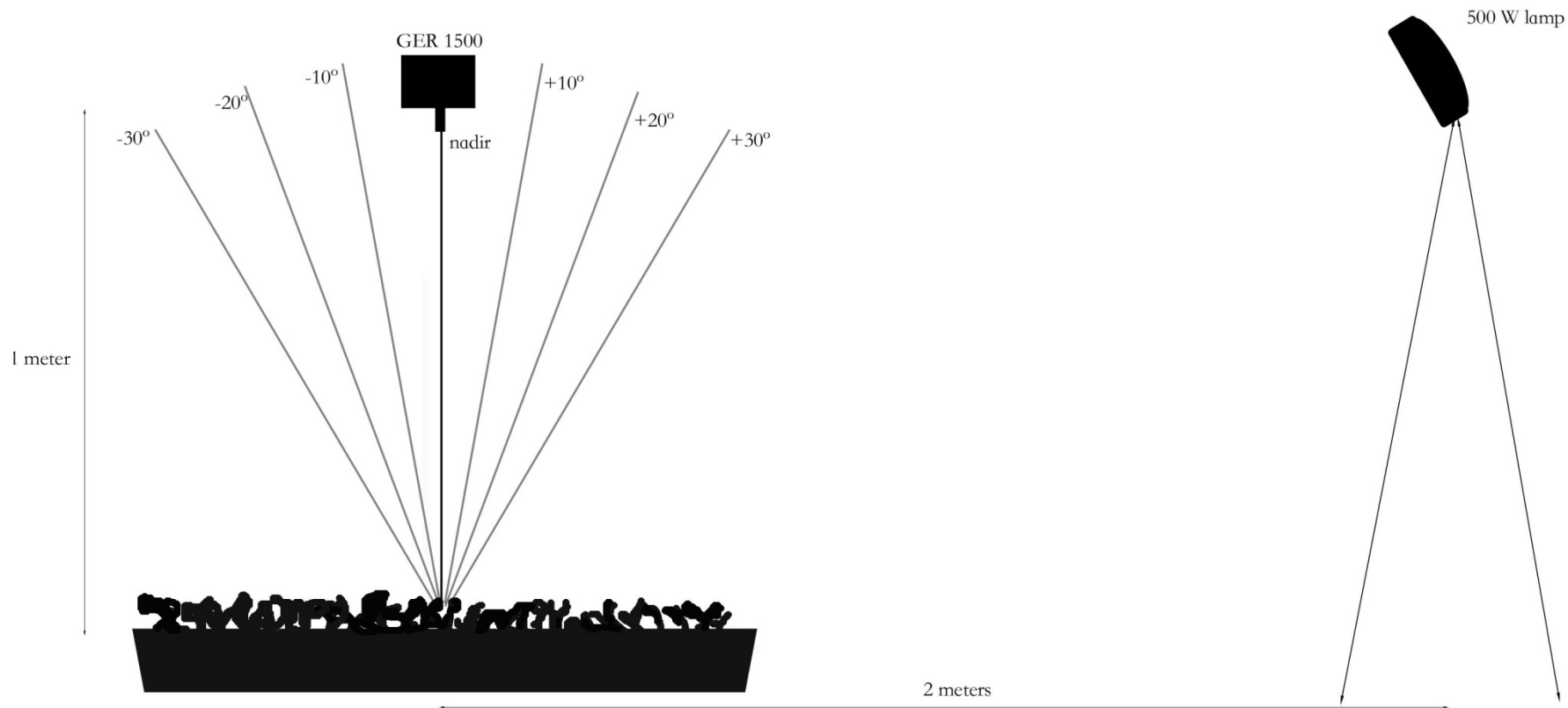


Figure 3.1. Diagrammatic representation of the set up of the apparatus used in the laboratory experiment.

3.3.2 Chlorophyll measurement

Chlorophyll concentration was measured instantaneously and non-destructively using the Minolta SPAD (Soil Plant Analysis Division) 502 chlorophyll metre. The Minolta SPAD 502 was used to estimate chlorophyll concentration in spinach due to the compact design, allowing quick and easy measurements in both the laboratory and field environment (Markwell *et al.*, 1995) (Figure 3.2). Primarily designed for agricultural crop science applications, with a focus of measuring crop health, the Minolta SPAD measures leaf transmittance at two wavelengths: red (650 nm) where light absorption by chlorophyll is efficient and NIR (940 nm) where absorption by chlorophyll is insignificant. The SPAD-502 meter calculates a non-dimensional, relative chlorophyll content in SPAD units at a range of 0-99 (lowest – highest) according to:

$$\text{SPAD} = k \cdot \log_{10} \left(\frac{T_{940}}{T_{650}} \right)$$

where T is the transmittance and k is a calibration coefficient determined by the manufacturer (Uddling *et al.*, 2007). The claimed accuracy of the meter output is ± 1 SPAD units (or $\pm 1\%$).



Figure 3.2. The Minolta SPAD to estimate chlorophyll concentration in spinach leaves.

Chapter 3. Evaluation of the canopy chlorophyll content and MTCI relationship

Wet chemistry assay procedures were used for the conversion and calibration of the Minolta SPAD-502 readings to chlorophyll concentrations. For each leaf 5 discs were cut and their dimensions recorded, usually this equated to an area of 316.14mm² for spinach leaves, and five SPAD measurements taken per leaf disc. Discs were immediately immersed in 1 ml of analytical grade N, N-dimethylformamide (DMF) to facilitate the complete extraction of the chlorophyll pigments. DMF overcomes the problems of incomplete extraction of chlorophyll (Wellburn, 1994) and eliminates the need of further sample preparation. Direct immersion in DMF is an equally efficient extraction procedure as pre-grinding of the samples and immersion (Moran and Porath, 1980). All samples were kept refrigerated at 4°C in the dark to reduce pigment breakdown and for the extraction of leaf pigments.

After refrigeration, samples were diluted 1:5 with DMF, allowing two samples to be taken from each original sample and to fall within the sensitivity and linear range of the spectrophotometer. The mean of three spectrophotometer readings was used to represent the sum of both chlorophyll *a* and *b* (µg ml⁻¹) determined using the specific extinction coefficients for a spectrophotometer with a spectral resolution of 1nm (Wellburn, 1994).

$$\text{Chlorophyll } a = 11.65 * A_{664} - 2.69 * A_{647} \quad (3.1)$$

$$\text{Chlorophyll } b = 20.81 * A_{647} - 4.53 * A_{664} \quad (3.2)$$

Where A_{664} and A_{647} are the recorded absorptions at 664 nm and 647 nm measured with a Cary 50, version 3.0, UV/VIS spectrophotometer. As samples had a known area chlorophyll concentration could be expressed as mg m⁻².

Chlorophyll concentrations corresponding to each SPAD value were plotted and correlated, with the coefficient of determination (R^2) used to indicate the strength of relationship. A regression model was used to describe the relationship between SPAD values and both chlorophyll *a* and *b* concentration. The regression models were then used to estimate spinach foliar chlorophyll concentrations based on SPAD results. In this instance, total chlorophyll concentration (mg m⁻²) in spinach can be estimated by the following regression equation:

Chapter 3. Evaluation of the canopy chlorophyll content and MTCI relationship

$$\text{Chlorophyll-}a \text{ concentration (mg m}^{-2}\text{)} = 0.36 * \text{SPAD}^2 - 12.44 * \text{SPAD} + 276.64 \quad (3.3)$$

$$\text{Chlorophyll-}b \text{ concentration (mg m}^{-2}\text{)} = 0.11 * \text{SPAD}^2 - 4.30 * \text{SPAD} + 100.22 \quad (3.4)$$

$$\text{Total chlorophyll concentration} = \text{chlorophyll-}a + \text{chlorophyll-}b \quad (3.5)$$

Using the calibration equations spinach foliar chlorophyll concentration was monitored throughout weeks 1- 4 of the laboratory experiment. For each of the GER 1500 FOV measurements (three per tray), 10 leaves were chosen representing the variation in chlorophyll concentration and 10 SPAD measurements were taken for each leaf.

The size, distribution and height of spinach plants were not suitable for LAI determination with the Delta-T Sunscan instrument. Therefore, digital photography was used to estimate LAI. An image of each tray was taken using a Panasonic LUMIX DMC-FZ10 digital camera and the regions of interest (ROI) corresponding to each of the trays three FOV were extracted. Individual leaves within the ROI were digitized, taking care to include those that were overlapping. After the digitisation, total leaf area was calculated using ArcGIS software (Figure 3.3).

Chlorophyll content was calculated as;

$$\text{Chlorophyll content} = \text{LAI} * \text{chlorophyll concentration}$$

Within this thesis chlorophyll content is expressed as content per unit area, specifically mg m^{-2} , rather than mass per pixel. Adopting this approach allows direct comparison of the relationship between MTCI and chlorophyll independent of the spatial resolution of the sensor used, i.e., GER 1500 Spectrometer (88.2 cm^2), CASI-2 (2-300 m) and MERIS (300 m).



Figure 3.3. Illustration of the flow line that is used in ArcGIS to derive LAI. The centre of the field of view of the GER 1500 was identified using the prepositioned markers; the FOV was then superimposed on the digital imagery. Each green leaf area was digitised in ArcGIS, allowing for leaf overlap. LAI was calculated as the ratio of total one sided leaf area divided by the area of the GER 1500 FOV.

3.3.3 Spectral indices

Several optical indices have been reported in the literature to be strongly correlated with various vegetation parameters such as LAI, biomass, chlorophyll content, and photosynthetic activity. The sensitivity of vegetation indices to variations in observing geometry and soil properties has important bearings upon the performance and the suitability of a particular index to estimate the canopy variable of interest.

Together with the MTCI, four spectral indices and a REP technique were selected to evaluate the relationship between chlorophyll content and the effect of view angle and soil background. Normalised Difference Vegetation Index (NDVI) (3.6) (Rouse *et al.*, 1973), Enhanced Vegetation index (EVI) (3.6), (Huete and Justice, 1999), optimized soil-adjusted vegetation index (OSAVI) (3.8) (Rondeaux *et al.*, 1996), Red edge derived from MERIS data (MERIS REP) (3.9) (Clevers *et al.*, 2002), Red edge position by linear interpolation (REP) (3.10) (Danson and Plummer, 1995; Guyot *et al.*, 1988), Modified chlorophyll absorption ratio (MCARI) (3.11) (Daughtry *et al.*, 2000) and MERIS Terrestrial Chlorophyll Index (MTCI) (2.1) (Dash and Curran, 2004).

$$\text{NDVI} \quad (R_{\text{NIR}} - R_{\text{red}}) / (R_{\text{NIR}} + R_{\text{red}}) \quad (3.6)$$

$$\text{EVI} \quad ((R_{\text{NIR}} - R_{\text{red}}) / ((R_{\text{NIR}} + C_1 * R_{\text{red}}) - (L * R_{\text{blue}} + C_2))) * G \quad (3.7)$$

Where, L = soil adjustment factor (7), C₁ and C₂ are aerosol scattering coefficients of 6 and 1 respectively, G = gain factor of 2.5 (Matsushita *et al.*, 2007). Bandwidth used in NDVI and EVI correspond to the band positioning of the MODIS sensor, where R_{NIR} = 841-876nm, R_{red} = 620-670nm, and R_{blue} = 459 – 479nm (Justice and Huete 1999).

$$\text{OSAVI} \quad (1+0.16)*(R_{800} - R_{670}) / (R_{800} + R_{670} + 0.16) \quad (3.8)$$

$$\text{MERIS REP} \quad (R_{705} = (48.77 * (((R_{665} + R_{775}) / 2 - R_{705} / (R_{537} - R_{705}))) \quad (3.9)$$

Where, R_x is the reflectance corresponding to the central positions of the MERIS spectral bands.

REP (linear interpolation)

$$700+40*((R_{670}/R_{780})/2 - R_{700}) / (R_{740} - R_{700}) \quad (3.10)$$

MCARI

$$2*[(R_{800}-R_{670}) - 0.2*(R_{800}-R_{550})] \quad (3.11)$$

The continuous GER 1500 spectra data were re-sampled through (mean) aggregation to simulated broad spectral bands. Such a method permitted the formulation of the aforementioned vegetation indices (equations 3.6 – 3.9).

3.3.4 Statistical analysis

Bi-variant correlation analysis was used to describe the strength and direction of the relationship between chlorophyll content and spectral indices. Coefficient of determination (R^2) was calculated to determine shared variance between the two variables, with, statistical significance where $p = < 0.05$ was satisfied.

Spectral reflectance indices were analysed and experimental effects on them were assessed using analysis of variance (ANOVA). Mean value of the spectral reflectance indices were compared using Duncan's multiple range test at $p \sim 0.05$. The coefficients of determination were used to study the relationship between the spectral reflectance indices, calculated for different soil backgrounds and viewing geometry. All statistical analyses were conducted using standard SPSS procedures (Pallent, 2007).

3.4 Results and discussion

Spinach plants exhibited the same growth characteristics for each soil medium. Chlorophyll concentration reached a maximum during the second week of measurement, after which it declined to levels that were equivalent to those recorded during the first week. LAI reached maxima during the third week, which can be clearly seen in Figure 3.4, accounting for the increase in reflectance shown in Figure 3.5, where partial canopy closure reduced the effect of soil further and corresponds to increased reflectance principally in the green and NIR wavelengths. After the third week, LAI decreased as the plants started to bud and produce flowers. This also coincided with an observed decrease in foliar chlorophyll concentration and degradation in leaf tissue. Total chlorophyll content, a function of LAI and chlorophyll concentration, increased rapidly after the first week's measurements, reaching a maximum during weeks 2-3, after which it decreased rapidly.

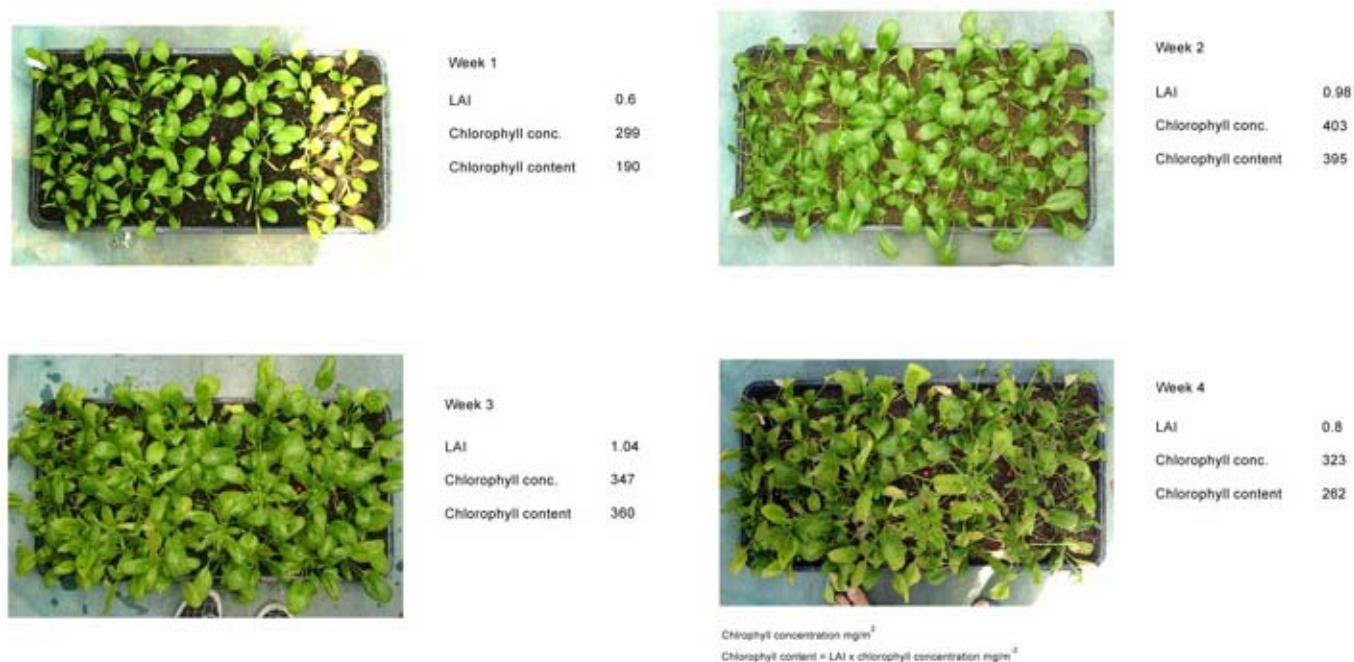


Figure 3.4. The growth of spinach grown in non-fertilised soil. Chlorophyll concentration reaches a maxima at week two, whilst LAI during the third week. Leaf tissue degradation is evident during week 4, with an associated decrease in both LAI and chlorophyll concentration.

Chapter 3. Evaluation of the canopy chlorophyll content and MTCI relationship

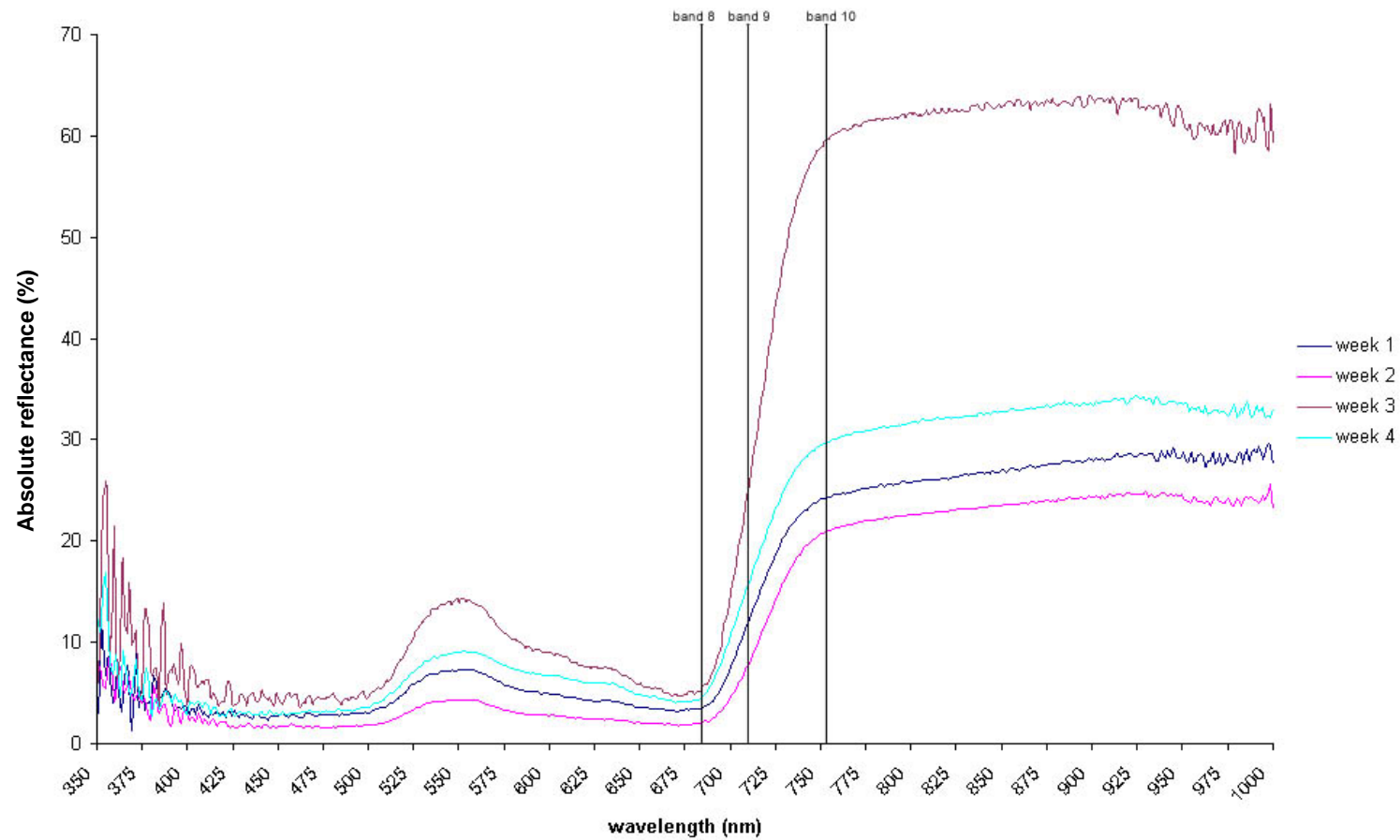


Figure 3.5. Mean spectral reflectance profiles for spinach grown on non-fertilised soils (NF), weeks 1-4. The spectral location of the MERIS bands used in the calculation of the MTCI superimposed on the reflectance spectra (N.B. MERIS band widths are not proportional to line width).

3.4.1 Relationship between chlorophyll content and the MTCI

The MTCI mirrors the change in chlorophyll content well for spinach canopies grown on most soils (Figure 3.6); the most notable exception is for the spinach grown on white soil, where the MTCI is greater than expected at low LAI during the early stages of the experiment and lower than expected during week 3. Spinach grown in medium and non-fertilised soil also exhibited lower than expected MTCI in week 3, which did not reflect changes in measured chlorophyll content. Spinach grown on grey soil (sand) exhibited a marginally higher MTCI than expected for week 3 compared to the incremental increase in chlorophyll content. Aggregating chlorophyll content for all spinach showed that the MTCI and chlorophyll content exhibited the same temporal trend. These findings demonstrated that an increase in LAI (Figure 3.7) from weeks two to three did not result in an increase in MTCI (Figure 3.6). This suggests that for a given chlorophyll content, the MTCI is insensitive to variation in LAI across the range of LAI observed in this series of experiments.

Correlation was used to examine the relationship between MTCI and chlorophyll content, LAI and chlorophyll concentration. Coefficient of determination shows that MTCI has a stronger relationship with chlorophyll content, compared to LAI and chlorophyll concentration (Figure 3.8). This result was expected as MTCI is a function of $LAI \times \text{chlorophyll concentration}$. This relationship shows that the MTCI is coupled with a canopy variable, and can be used to infer such a variable even at low LAI where the influence of background reflectance on measured canopy reflectance is high.

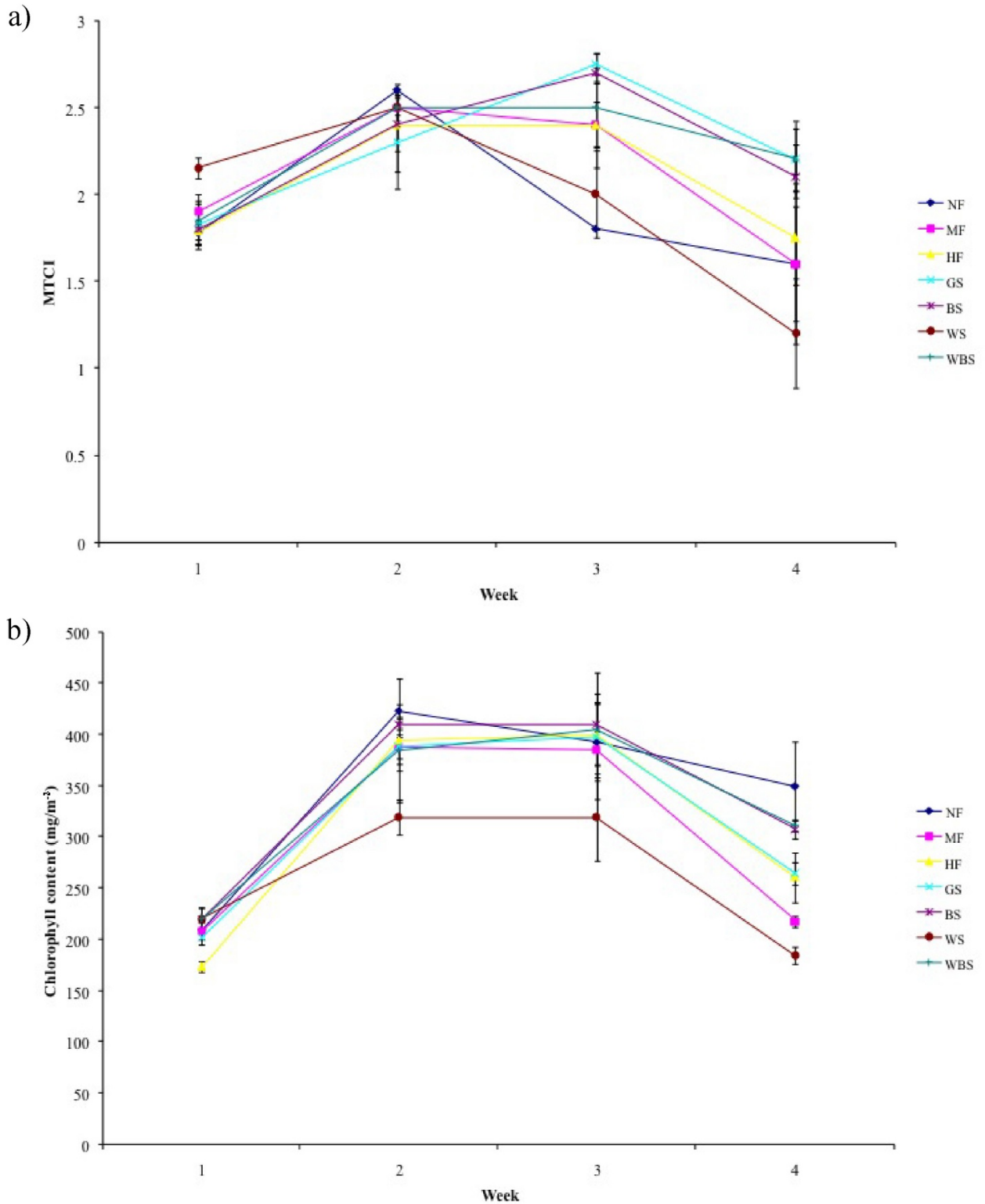


Figure 3.6. Variation in MTCI (a), and chlorophyll content (b) for spinach grown in various soils as derived from GER 1500 reflectance. Points on graph represent mean values per tray (n=3).

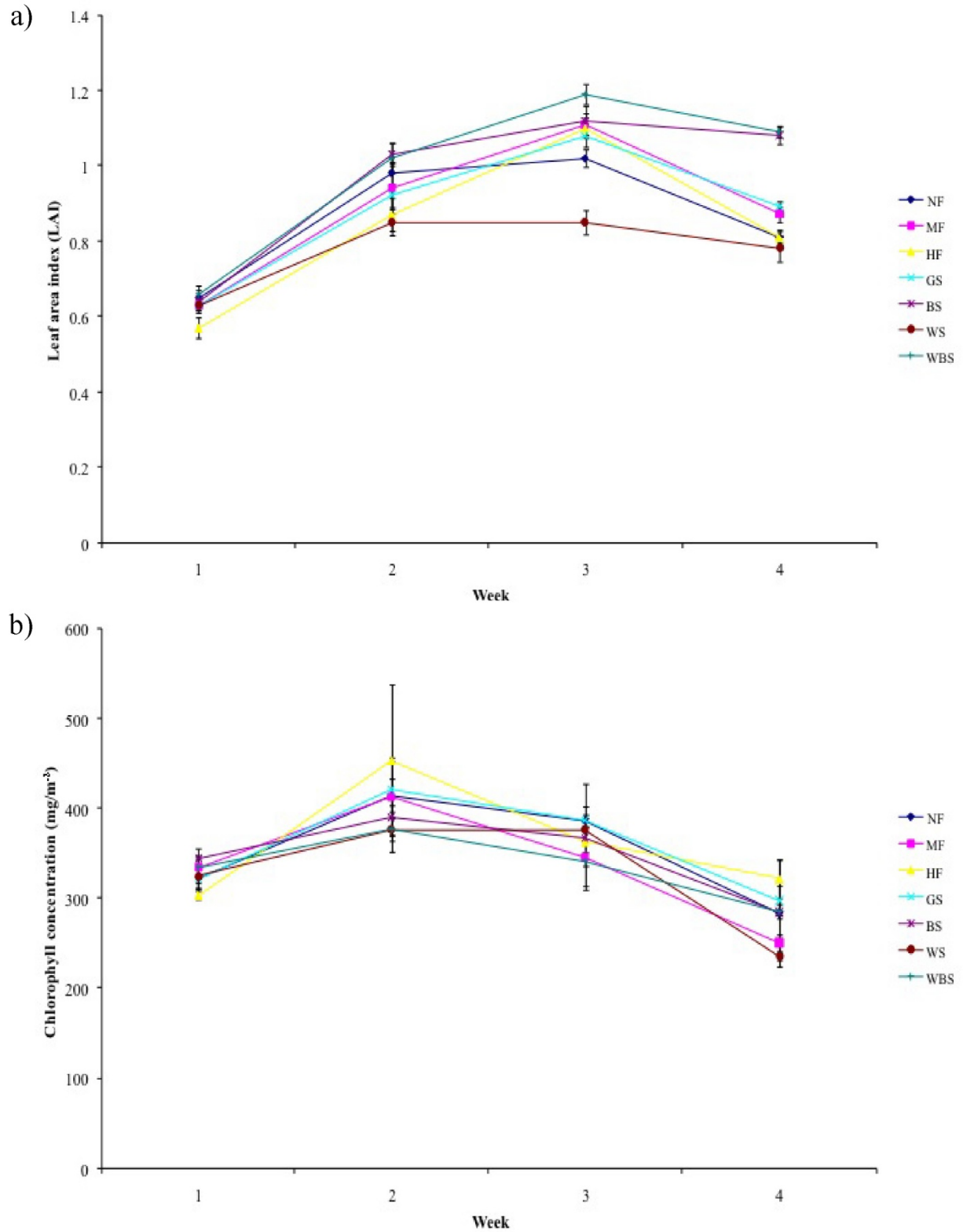


Figure 3.7. Change in LAI (a) chlorophyll concentration (b) over the duration of the laboratory experiment for spinach plants. Points on graph represent mean values per tray (n=3).

Chapter 3. Evaluation of the canopy chlorophyll content and MTCI relationship

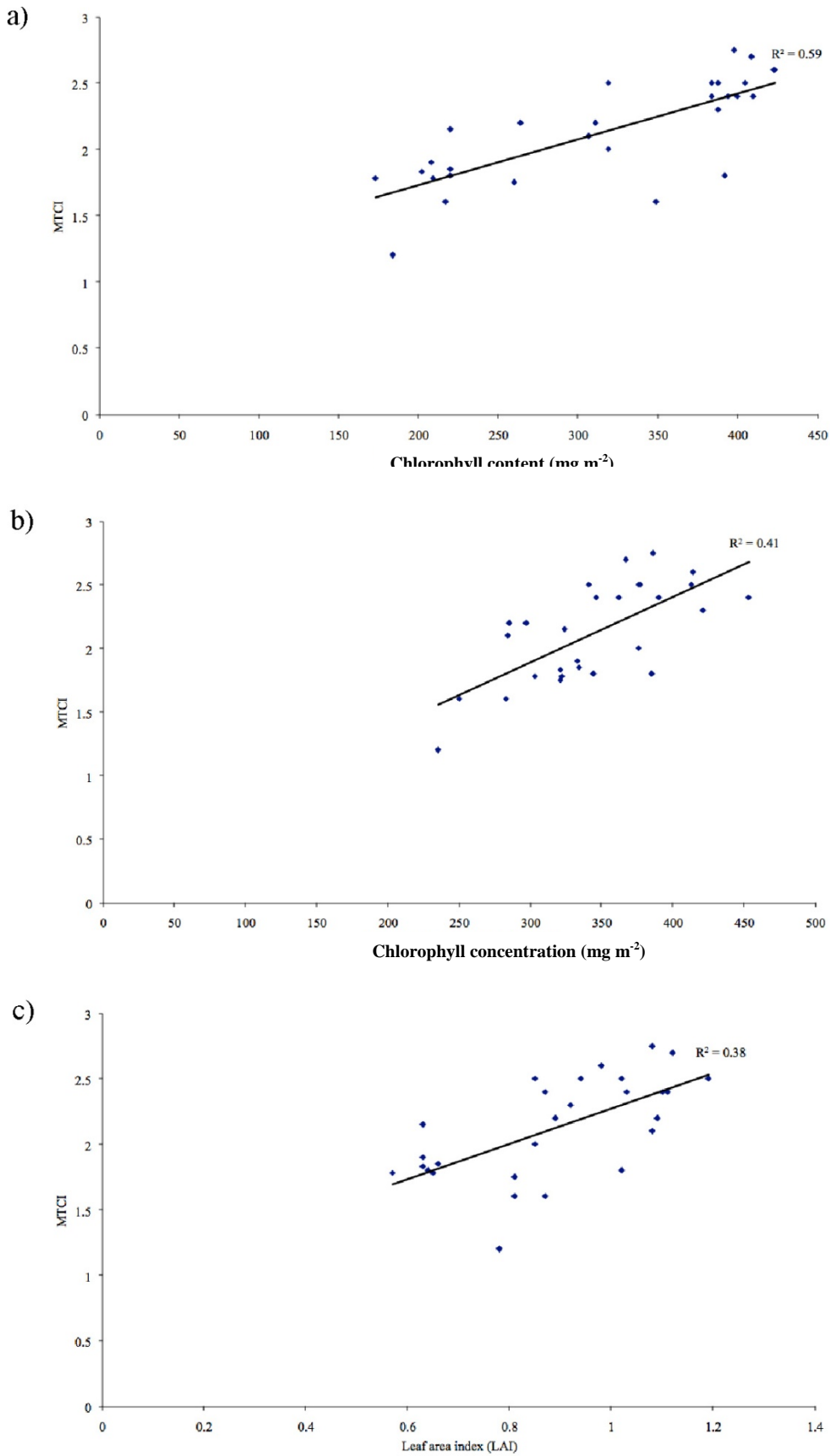


Figure 3.8. The relationship between MTCI and chlorophyll content (a), chlorophyll concentration (b) and LAI for all soil backgrounds.

Chapter 3. Evaluation of the canopy chlorophyll content and MTCI relationship

Regression analysis was used to determine whether soil background affected the relationship between chlorophyll content and the MTCI (Figure 3.9). The four soil backgrounds, standard bare soil (NF, MF, HF and BS), wet standard bare soil (WBS), grey soil (GS) and white soil (WS). The relationship between MTCI and chlorophyll content is weak where spinach is grown in a white soil, $R^2=0.14$, where 14% of the variance in MTCI can be accounted for by chlorophyll content. The relationship is strengthened when considering those cases where $LAI > 1$, R^2 increased from 0.14 to 0.48 ($R^2=0.22$ where $LAI < 1$). Although the sample size was small it suggests that LAI is an important factor when establishing the relationship between MTCI and chlorophyll content in reflective soils. A previous study using modelled spectra (Curran and Dash, 2005) has shown that at an LAI greater than 2 the effect of soil background is minimal. The results show that highly reflective soils have a greater impact at a low LAI but suggest that soil moisture and other soil conditions have a limited effect on reflectance at a low LAI.

The relationship between canopy chlorophyll content and MTCI was shown to be strong for all soil types, except white. The overall correlation between MTCI and chlorophyll content on all experimental soil types was $R^2=0.56$, indicating a relatively strong relationship. When those results relating to white soils were omitted from the analysis, the relationship between MTCI and chlorophyll content was strengthened ($R^2=0.66$) (Figure 3.10).

ANOVA analysis examined whether there was more variability between the MTCI from the different soil backgrounds than the MTCI week on week (a function of chlorophyll content). At the 0.05 level of confidence, F values indicated that there was no difference in variability ($F=0.652$), suggesting that background does not have a significant effect on the MTCI.

Chapter 3. Evaluation of the canopy chlorophyll content and MTCI relationship

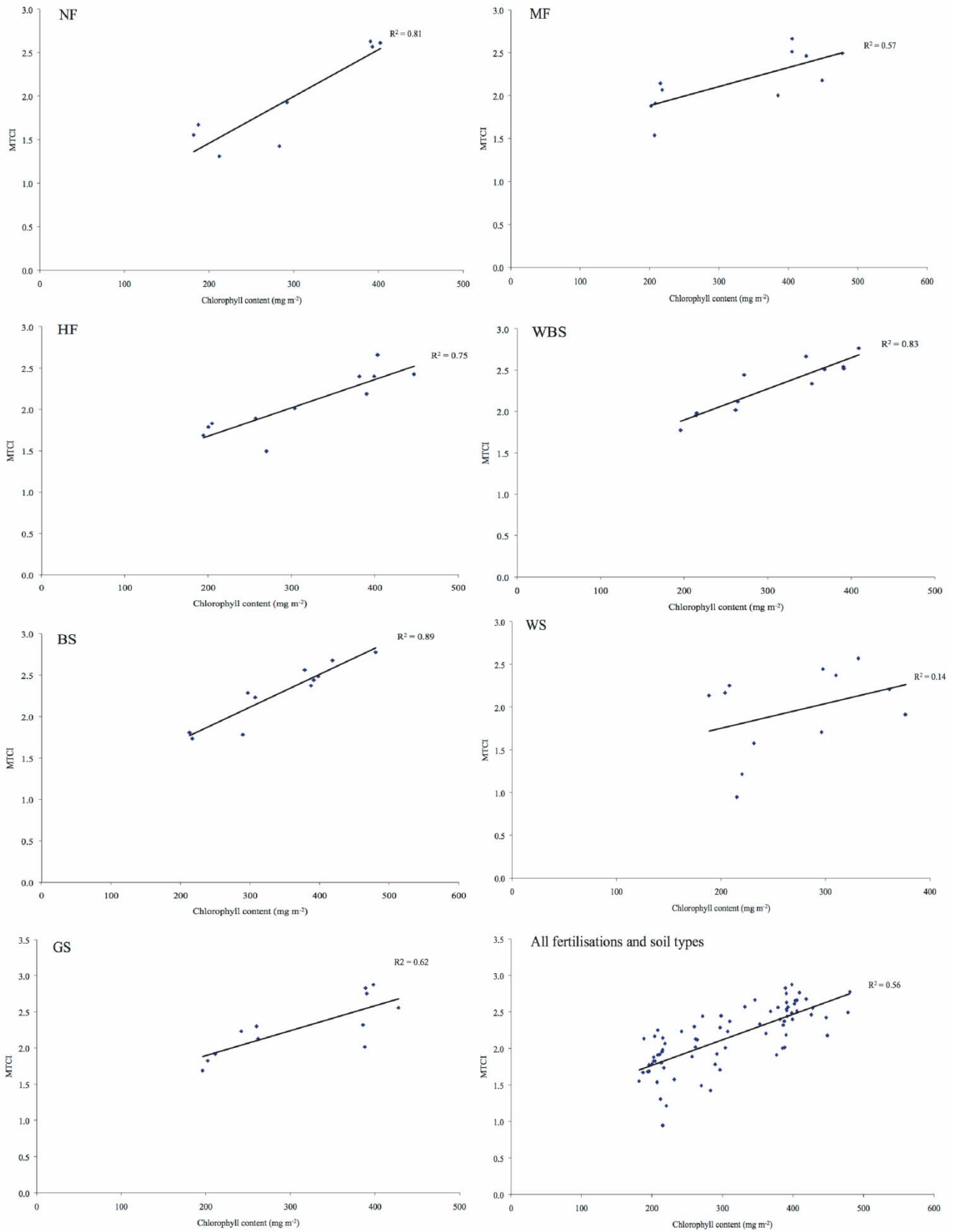


Figure 3.9. The relationship between MTCI and total chlorophyll content for spinach grown on various soil backgrounds.

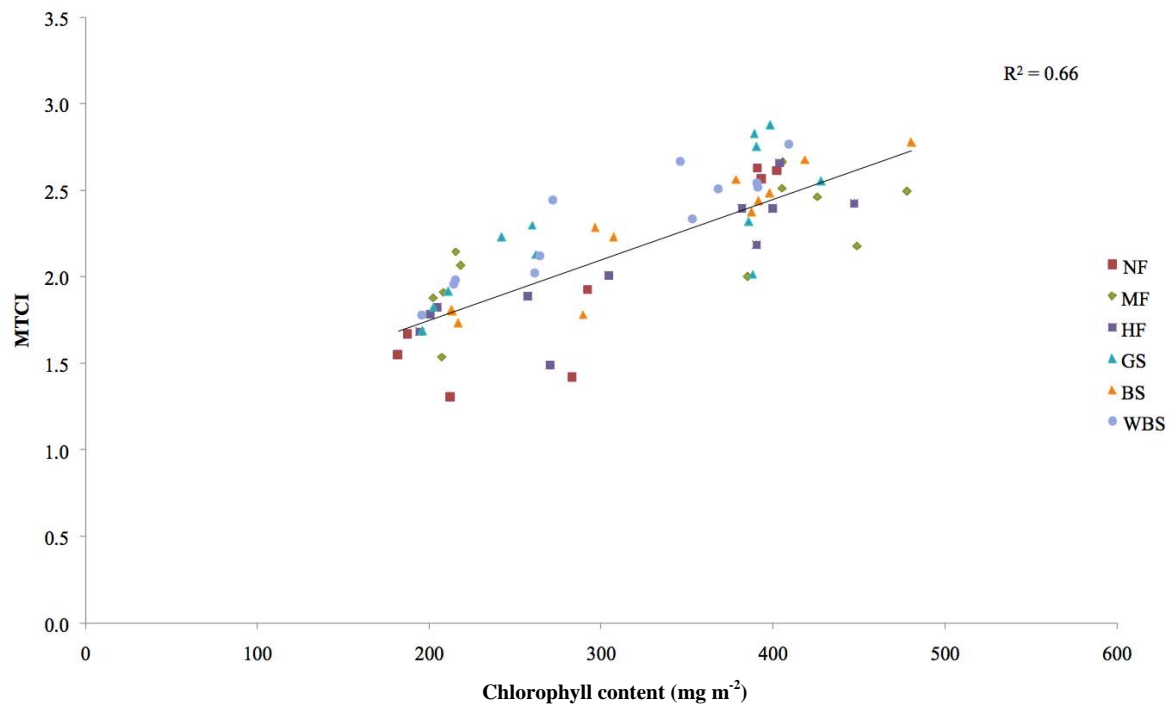


Figure 3.10. Relationship between total chlorophyll content and MTCI was increased when removing measurements from spinach grown on white soils.

3.4.2 The effects of soil reflectance on the MTCI

Four different soils were used to investigate the effect of soil background on the MTCI. Spectra taken from bare soils (prior to planting seeds) demonstrate that soil reflectance characteristics have an effect upon the MTCI. Figure 3.11 shows the reflectance in the MERIS spectral bands used in the MTCI from the four soils. The reflectance spectra from all the soils (except white) have a gentle positive slope in the red – NIR region, exhibiting higher reflectance in the NIR than red. Therefore the smaller difference in reflectance between MERIS bands 8 and 9, compared to 9 and 10 result in a positive MTCI.

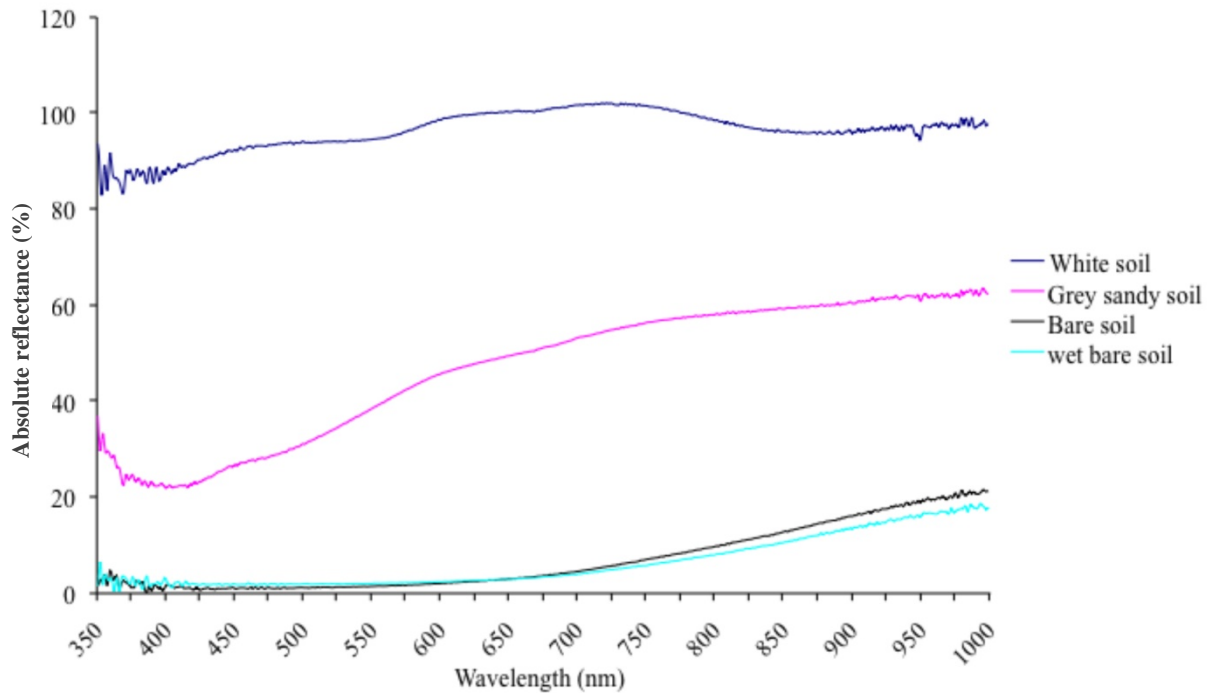


Figure 3.11. The spectral reflectance profiles of a variety of bare soil sample used in this investigation.

The reflectance characteristics of the bare and wet bare soils result in MTCI values comparable to spinach canopies with a chlorophyll content of approximately 300 mg m^{-2} . There is a marked variation between the MTCI values for different soils due to their varying spectral characteristics (Table 3.2). The effect of soil background alone on the MTCI is apparent, where bare bright soils (MTCI -0.8) have a low MTCI compared to bare and wet bare soils.

The effect of bare soil reflectance on the MTCI therefore suggests it will be difficult to interpret vegetation chlorophyll content where LAI is low. However, the reflectance from the white soil was less in MERIS bands 8 and 10 (red and NIR respectively) compared to MERIS band 9 (the red edge) (Figure 3.11), which resulted in a negative MTCI. Table 3.2, shows the effect of soil reflectance on the MTCI.

| MERIS band | Absolute reflectance (%) | | | |
|------------|--------------------------|-----------|--------------------|------------------------|
| | White soil | grey soil | Standard bare soil | wet standard bare soil |
| band 8 | 101.1 | 51.7 | 4.1 | 3.6 |
| band 9 | 101.9 | 53.9 | 5.2 | 4.4 |
| band 10 | 101.2 | 56.6 | 7.5 | 6.2 |
| MTCI | -0.8 | 1.3 | 2.1 | 2.1 |

Table 3.2. Soil reflectance properties as measured in MERIS bands 8, 9 and 10 and the MTCI of bare soil as used in this experiment.

3.4.3 Effect of view angle on the MTCI

The MTCI for spinach plants from the GER 1500 spectra measured over four dates and seven sensor view angles are plotted in Figure 3.12. There was limited variability in MTCI over the viewing angle. ANOVA analysis examined whether there was more variability between the MTCI from week to week (i.e., a function of chlorophyll content) than MTCI across the viewing angles range. At the 0.05 level of confidence, F values indicated ($F=196.3$) that there was a difference in variability showing that the influence of sensor view angle at nadir $\pm 30^\circ$ was less than that of chlorophyll content. The MTCI compounds the effects of viewing and illumination geometry. Dash (2005) also concluded a limited sensitivity of the MTCI to view angle within the nadir $\pm 30^\circ$ range but sensitivity at angles beyond this.

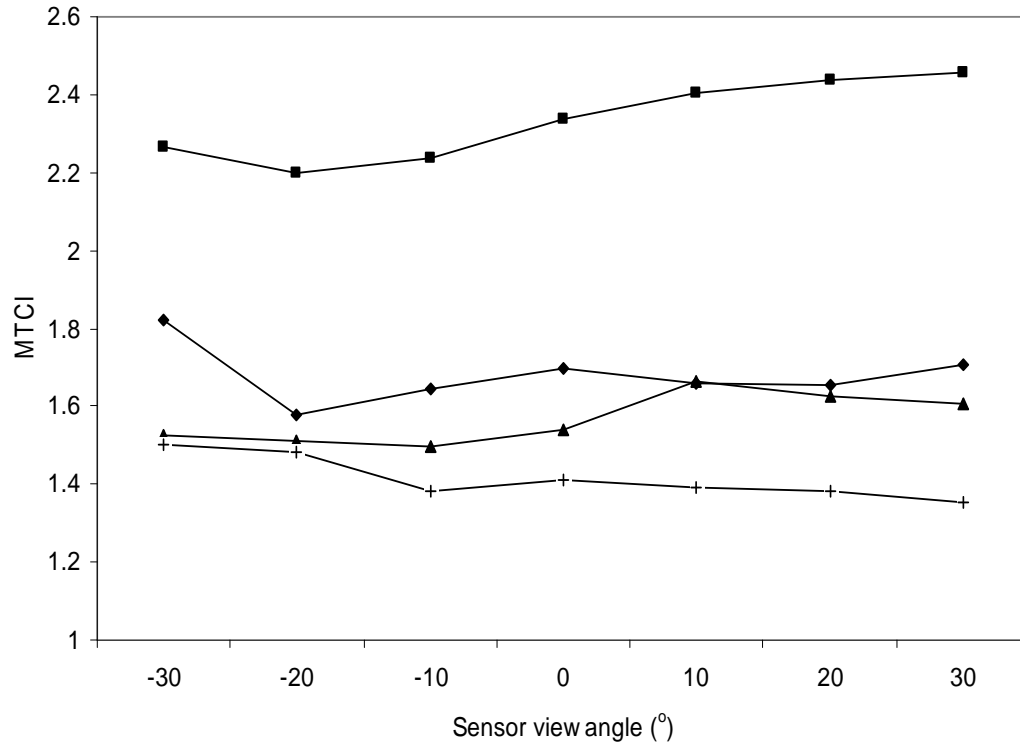


Figure 3.12. MTCI at seven different sensor view angles for spinach: week 1 (▲); week 2 (◆); week 3 (■) and week 4 (+)

3.4.4 Evaluating the performance of spectral indices to infer chlorophyll content

The relationship between chlorophyll content and various spectral indices that are commonly used to estimate green biomass or chlorophyll were investigated. The MCARI proved insensitivity to variation in chlorophyll content (typical $R^2 = 0.1 - 0.3$), whilst responsive to variations in LAI (Haboudane *et al.*, 2004). The MCARI was most resistant to chlorophyll and variation appeared independent of chlorophyll content changes, this may be in part due to the fact that MCARI is insensitive to low chlorophyll contents (Haboudane *et al.*, 2002). Therefore, the MCARI was omitted from further investigation.

Figure 3.13 shows the relationship between spectral indices and chlorophyll content. MTCI and MERIS REP had the strongest relationship with chlorophyll content (coefficient of determination $R^2 = 0.7$) whilst NDVI and EVI had the weakest. This may be because both NDVI and EVI are more sensitive to green biomass and variation in LAI than chlorophyll content. The results of this investigation support the findings of

Chapter 3. Evaluation of the canopy chlorophyll content and MTCI relationship

Oppelt and Mauser (2004) who concluded that NDVI and OSAVI were insensitive at chlorophyll contents below 300 mg m^{-2} . Results suggest that the NDVI and OSAVI were insensitive across the range of chlorophyll contents in this series of experiments. These findings will have important bearings on studies that use these indices to monitor vegetated canopies with a low LAI. Similarly, consideration must be given to the use of such indices to monitor vegetation phenology, particularly at the start and end of the growing seasons when chlorophyll contents and LAI are typically low.

These results suggest that methods that utilise narrow reflectance bands in the REP region of the spectrum, such as MTCI and MERIS REP are the most sensitive to changes in canopy chlorophyll content.

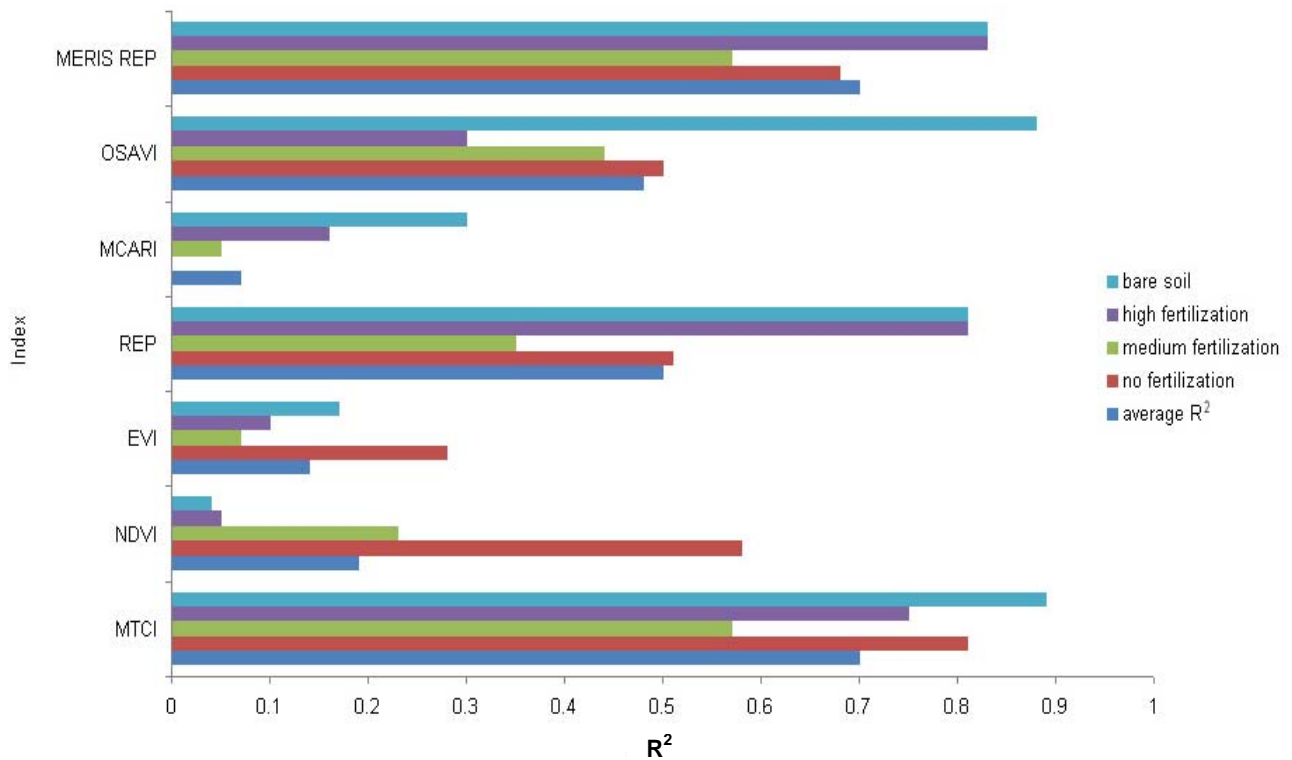


Figure 3.13. Comparison of the performance of vegetation indices for the estimation of chlorophyll content.

3.4.5 The effect of soil background upon the relationship between chlorophyll and vegetation indices

LAI values were low; typically 0.6 in week 1 to 1.2 in the week 3, therefore soil reflectance was a contribution to canopy spectral reflectance throughout the period when reflectance measurements were recorded. The relationship between spectral indices and soil background was explored further. Correlation analysis was used to determine the ability of the indices to estimate chlorophyll content when spinach was grown on varying soil backgrounds. Generally, the increase in reflectance from the soil, corresponding to increased soil brightness weakened the relationship between chlorophyll and the spectral indices. No indices performed well when spectral measurements were taken on a highly reflective white soil background, particularly when LAI were low.

The observed relationship between VI and chlorophyll content did appear to vary as a function of soil reflectance (Figure 3.14). MTCI, MERIS REP, OSAVI and linear REP were robust maintaining a strong relationship with chlorophyll content on bare soil and wet bare soils, indicating that the observed spectral response is a result of vegetation change rather than soil moisture variation. For sandy soils the MTCI and MERIS REP still exhibited a relatively strong correlation with chlorophyll content (R^2 of 0.62 and 0.61 respectively) (weeks 1-4).

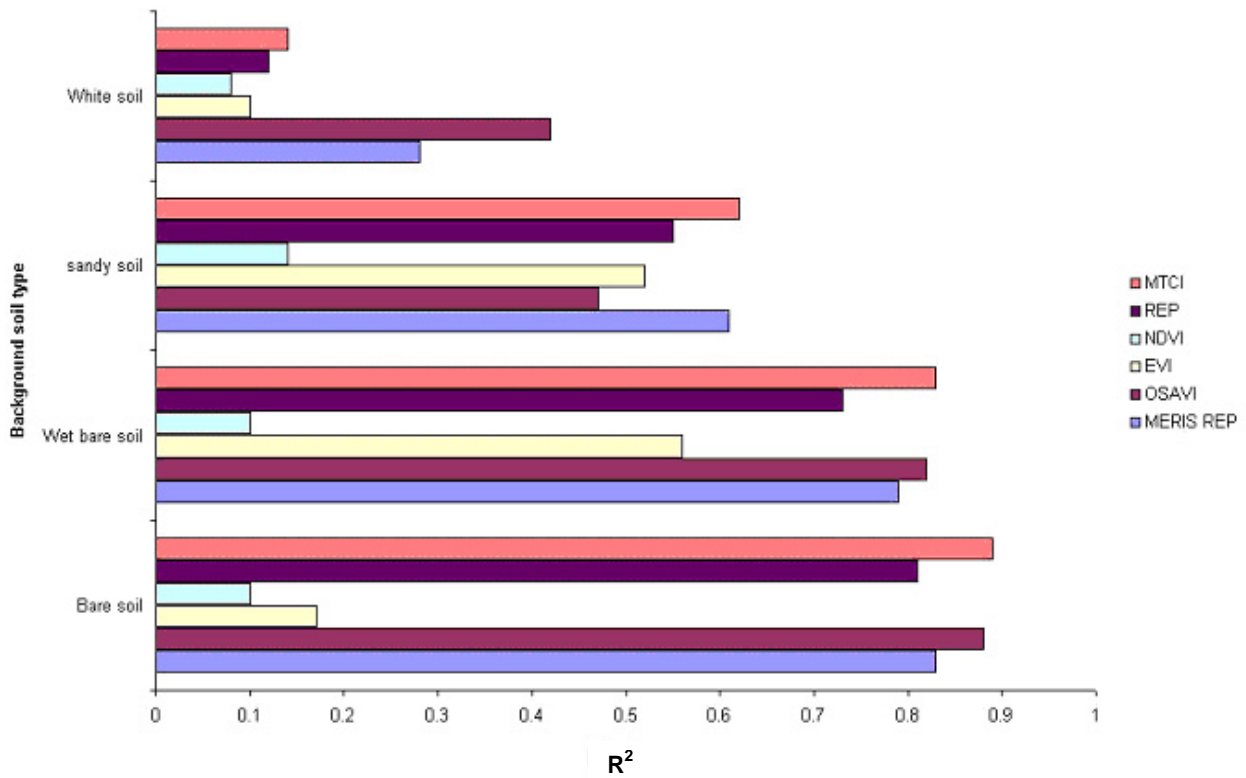


Figure 3.14. The effect of soil background upon the relationship between chlorophyll content and spectral indices.

3.4.6 The influence of view angle on the relationship between chlorophyll content and vegetation indices

Canopy reflectance is determined by a combination of vegetation reflectance, soil background, and illumination and viewing geometry (e.g. the position of the Sun or angle of view) (Aparicio *et al.*, 2004). The spectra in Figure 3.5 show a typical pattern of canopy reflectance, with reflectance being relatively low throughout the visible wavelengths (400–700 nm) and increasing sharply up to the NIR plateau (750–1100 nm). However, with the sensor at +30 degrees more reflected radiation is recorded throughout the range of wavelengths (400–1100 nm) than when placed at nadir (Figure 3.15).

The observed change in canopy reflectance will therefore lead to an increase in VI values towards the ‘hot spot’. This can be explained by the bidirectional properties of the canopy. Towards the ‘hot spot’, an increase in canopy forward scattering is coupled with a decreasing amount of background in view away from nadir, reducing the contribution of soil on reflectance. However, in the back scattering direction, shadowing

effects will increase with view angles away from nadir, leading to a reduction in visible and NIR reflectance, explaining the decrease in MTCI and EVI (Figure 3.15).

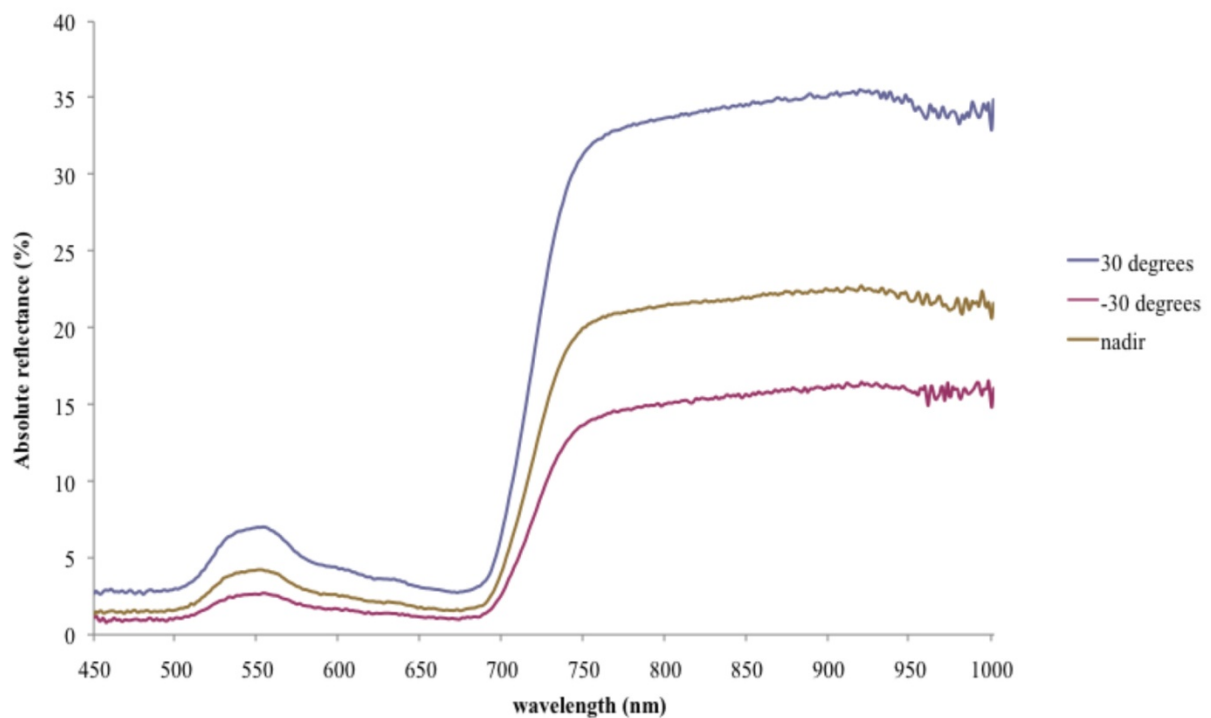


Figure 3.15. The change in observed canopy reflectance in visible and NIR wavelengths due to changing viewing geometry from ± 30 degrees of nadir in the principle plane.

Figure 3.16 represents the percentage change in the spectral indices from nadir to $\pm 30^\circ$ for weeks 2 and week 3, periods where LAI was highest. As can be seen there was little change in the value of the spectral indices values within the viewing range. However, the MTCI shows most variation as a function in viewing geometry. There is a systematic decrease in MTCI values away from the sensor and a systematic increase in MTCI values away from nadir.

Chapter 3. Evaluation of the canopy chlorophyll content and MTCI relationship

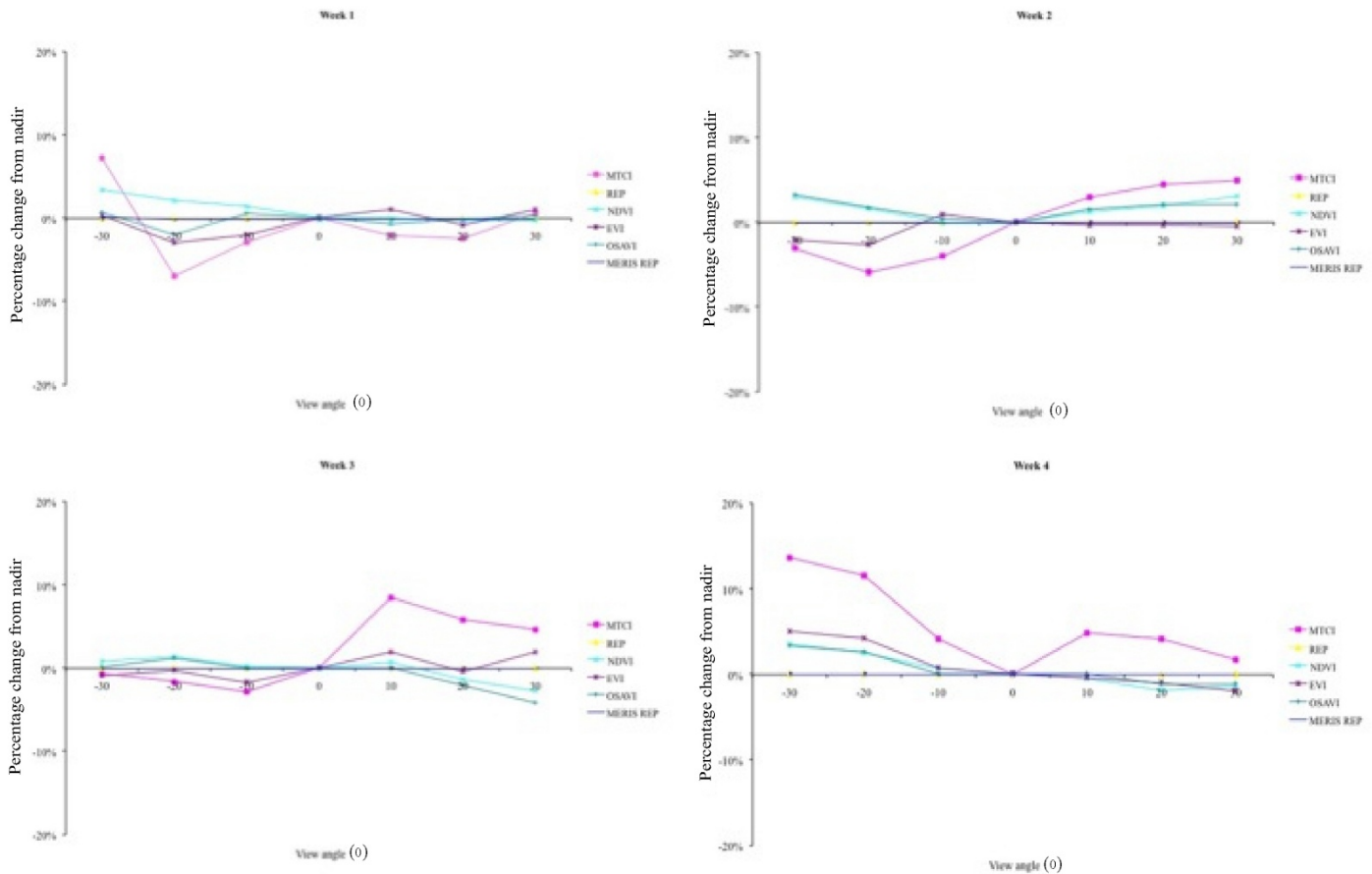


Figure 3.16. Change in spectral vegetation index values as a function of view angle

Analysis of variance (one-way ANOVA) was used to determine if there was a statistically significant variation in each of the six indices across the viewing range. Removing the variation of soil background on canopy was necessary to examine the influence of view angle on the indices. Therefore angular measurements were taken from a single soil type. At the 0.05 level of confidence, there was no significant change in indices, indicating that the influence of sensor view angle at nadir to $\pm 30^\circ$ did not significantly influence index values (Table 3.3). The small F ratio indicates the small variance between groups caused by variation in view angle. Appendix 5 shows the full results from the one-way ANOVA test.

Although the investigation into the effects of view angle on the MTCI did not show any significant statistical effects, it was shown that the MTCI was influenced by view angle to a greater extent than the other vegetation indices were. View angle has been shown to effect the NDVI at the canopy scale. Airborne Hyperspectral Mapper (HYMAP) data

Chapter 3. Evaluation of the canopy chlorophyll content and MTCI relationship

was used to examine the influence of view angle ($\pm 30^\circ$ from nadir) on NDVI from various land cover types in the Amazonian basin. Normalised surface reflectance was shown to increase in both red and NIR bands, from negative to positive view angles up to $+40^\circ$ (Galvao *et al.*, 2004). Such variation in measured reflectance will lead to consequent variation in NDVI values (Walter-Shea *et al.*, 1997). Therefore, further research is required to assess the influence of view angle variation on MTCI at the canopy scale.

| Vegetation index | Levene's test | F ratio | Significance |
|------------------|---------------|---------|--------------|
| MTCI | 0.994 | 0.035 | 1.0* |
| REP | 0.989 | 0.062 | 0.999* |
| NDVI | 0.990 | 0.170 | 0.982* |
| EVI | 0.999 | 0.006 | 1.0* |
| OSAVI | 0.995 | 0.138 | 0.989* |
| MERIS REP | 0.996 | 0.38 | 1.0* |

*not significant > 0.05 , df between groups = 6, within groups = 21

Table 3.3. Results from one-way ANOVA assessing the significant of the influence of variation in view angle on the MTCI – chlorophyll content relationship. Levenes significance was included to show the data did not violate the assumption of heterogeneity of variance.

3.5 Conclusions

Curran and Dash (2005) pinpointed a number of potential limitations with the operational use of the MTCI. One of the aims of this series of experiments was to examine the effect of changing LAI on the relationship between chlorophyll content and MTCI. Fertilisation was designed to influence foliar chlorophyll concentration, without effecting LAI. However, in practice this was hard to control as both LAI and chlorophyll concentration was influenced by fertilisation. Further modelling work needs to be conducted to determine the significance of LAI variation upon the MTCI - chlorophyll content relationship as the range of data derived from these experiments is insufficient to achieve meaningful conclusions. However, these experiments suggest that the MTCI will have limited sensitivity to an increase in LAI. The associated increase in LAI between measurements taken in weeks 2 and 3 shows a decrease in chlorophyll concentration resulted in a marginal decrease in MTCI, which was observed in measured chlorophyll content.

In the MTCI Algorithmic Theoretic Basis Document (ATBD), the potential limiting effects of soil background and viewing geometry were stated. Leaf area throughout the series of experiments was typically low, therefore permitting the effects of soil background on the MTCI to be investigated. Results from this spectroscopy based investigation support the modelled (LIBSAIL) finding stated in the ATBD document (Curran and Dash 2004) indicating that soil background has little effect on the relationship between MTCI and chlorophyll content at the LAI observed in this series of experiments. For spinach grown on differing soil backgrounds, a strong correlation between MTCI and chlorophyll content was observed for all soils backgrounds except white.

Results suggest that bare soils have MTCI values that are comparable to those observed in vegetated canopies. Bare soil reflectance from a mixture of topsoil and compost did have a positive MTCI, whilst white soils revealed a negative MTCI (typically -1.0). The experiments suggest that the presence of vegetation compounds the effects of soil reflectance even at low LAI (as were observed in week 1 of the series of experiments).

Chapter 3. Evaluation of the canopy chlorophyll content and MTCI relationship

However, the effect of the bright background had a significant effect on the MTCI - chlorophyll content relationship across the observed range in LAI.

From this study the major conclusions can be stated as:

- (i) The effect of soil on the MTCI was limited. The observed relationship between chlorophyll content and MTCI was found to be strong on all soil backgrounds, except white.
- (ii) View angle within $\pm 30^\circ$ of nadir had no significant statistical effect on the MTCI. However, as view angle is known to influence NDVI values at the canopy scale, further research is required to assess the potential effects on MTCI
- (iii) Among the six spectral indices, MTCI and MERIS REP had the strongest relationship with chlorophyll content.
- (iv) Soil backgrounds appeared to influence the relationships between chlorophyll content and a number of spectral indices much greater than the MTCI, however this influence was not statistically significant.
- (v) Bare soil has been shown to correspond to positive MTCI values, except white soil, which reflects higher in the visible than NIR regions and therefore has a negative MTCI.

**CHAPTER 4: MULTI-SCALE ANALYSIS AND
VALIDATION OF THE MERIS TERRESTRIAL
CHLOROPHYLL INDEX IN WOODLAND AND ARABLE
STUDY SITES**

Chapter 4

4.1 Introduction

The MTCI has started to be embraced by the user community and has been used in many applications, across numerous cover types (España-Boquera *et al.*, 2006; Dash and Curran, 2006; Zurita-Milla *et al.*, 2007; Foody and Dash, 2007; Rossini *et al.*, 2007, Haboudane *et al.*, 2008). Therefore in understanding the performance of the index and its utility in the provision of robust measures of canopy chlorophyll content there is a need to assess the index across a range of vegetative types and environmental conditions through validation.

Validation is the process of assessing the accuracy of data products through independent means (Justice *et al.*, 2000; Morisette *et al.*, 2006). The process of validation is driven by the need to deliver accurate products to the user community (Cohen and Justice 1999). Validation procedures and frameworks have been largely co-ordinated in accordance with the Committee on Earth Observation Satellites (CEOS) by the Working group on Calibration and Validation (WGCV), sub-group on Land Product Validation (LPV). This provides the user community with consistent approaches to biophysical product validation (Baret *et al.*, in press).

The validation process of moderate resolution satellite products is a challenge (Morisette *et al.*, 2006), as accurate field measurements are typically point based, and therefore are not directly comparable to the resolution of the sensor (Tian *et al.*, 2002). At the pixel level, the (often) heterogeneous land cover will also make the validation procedure challenging. However, careful consideration must be given to account for surface heterogeneity in the validation design. Therefore, there is a requirement to define and refine an appropriate method to account for surface heterogeneity that aggregates point measurements to coarser scales and allows assessment of the performance of satellite sensor products.

A major logistical difficulty associated with validation is scaling spatially variable canopy variables measured at points on the ground to a spatial resolution of the satellite sensor, (i.e., 300m for ‘full resolution’ or 1km for ‘reduced resolution’ of the MERIS

sensor). A proposed method is to scale-up from the ground to the sensor pixel using data acquired at an intermediate scale(s). This approach has been employed in the VALERI network of validation sites, where high resolution satellite or aerial imagery (e.g. SPOT-HRV) is used to generate the high spatial resolution biophysical variable maps based on point based field measurements of a particular set of biophysical variables (Baret *et al.*, in press). This is achieved through the use of a transfer function, which models the numerical relationship between the biophysical variable and high resolution imagery. For example, for the extensive validation of moderate resolution LAI products, the MODIS Land Discipline Team (MODLAND) utilises the relationship between LAI and the spectral values of high resolution imagery (e.g. NDVI, *f*PAR) (Morisette *et al.*, 2006b).

4.2. Chapter aims

In understanding the performance of MTCI and its utility in the provision of scientifically robust estimates of canopy chlorophyll content there is a need to validate the index across a range of vegetative types and environmental conditions. Validation at ‘full resolution’ of 300m is necessary to provide a quantifiable relationship between MTCI and ground chlorophyll content for a range of vegetation types, including woodland and agricultural crops.

This chapter will address the validation procedure carried out at both a woodland site in the New Forest, New Forest and an arable farming site at Brooms Barn, Higham, Suffolk, and assess the procedure and then gives feedback on the performance of the MTCI as a tool for estimating chlorophyll content within the two contrasting study sites.

Several important issues will be addressed in this investigation:

1. Examine the methodological issues with averaging chlorophyll contents acquired at one spatial resolution to coarser spatial resolutions (i.e., scaling-up);
2. Determine the sensitivity of the MTCI to a greater range in chlorophyll content;
3. Assess the transferability of the MTCI from one place to another (Foody *et al.*, 2003), specifically assessing both the relationship with canopy chlorophyll

content and use of the index to predict canopy chlorophyll content at other locations and cover types;

4. Determine the operational influence of soil background on the relationship between MTCI and chlorophyll content.

4.3 Study Areas

4.3.1 New Forest

The New Forest in southern England (0° 56' N, 01° 5' W) comprises of ancient semi-natural and ornamental woodlands and managed coniferous plantations and adjacent open heath and grassland covered in heather and low scrub. The deciduous woodlands were dominated by white birch (*Betula pubescens*), oak (*Quercus robur*) and beech (*Fagus sylvatica*), whilst coniferous areas were dominated by scots pine (*Pinus sylvestri*) corsican pine (*Pinus nigra* var. *Maritima*), weymouth pine (*Pinis strobus*), sitka spruce (*Picea sitchensis*) and Douglas fir (*Pseudotsuga menziesii*). New Forest management practices have resulted in several defined woodland types, varying in species composition and vegetation density. The forest is largely unenclosed and permits the grazing of livestock across the National Park. This practice permits the formation open glades and mature forest with dense bracken and holly (*Ilex aquifolium*) under story. However, there are numerous inclosures within the New Forest. These timber plantations make up approximately one third of the total forested area. Both broadleaf and conifer species are grown in the inclosures, ranging from new plantations to those established in the early 17th Century (Forestry Commission 2006).

The woodland study area, Frame Wood covers approximately 9 km² of open woodland, which is composed of ancient semi-natural and ornamental woodlands and managed coniferous plantations and adjacent open heathland covered in heather and low scrub (Figure 4.1). The range of canopy structures and vegetation types provide a broad range and variability in chlorophyll content (Figure 4.2). In addition, the site was chosen for its topography. The site was essentially flat, minimising the effects of terrain in the remotely sensed data.

4.3.2 Brooms Barn

The Brooms Barn study area is located in western Suffolk, England (52° 16'4 N, 0°34'55 E)(Figure 4.2). The 9km² area is dominated by arable agriculture, although some pig farming occurs on site. The arable crops grown on the site include grains; wheat (*Triticum spp.*), barley (*Hordeum vulgare*), vegetables; potatoes (*Solanum tuberosum*), parsnips (*Pastinaca sativa*), onions (*Allium cepa*), and sugar beet (*Beta vulgaris*). No single crop dominates, and the distribution of each crop is largely equal. The area is relatively flat, minimising the effects of topography upon the remotely sensed imagery.

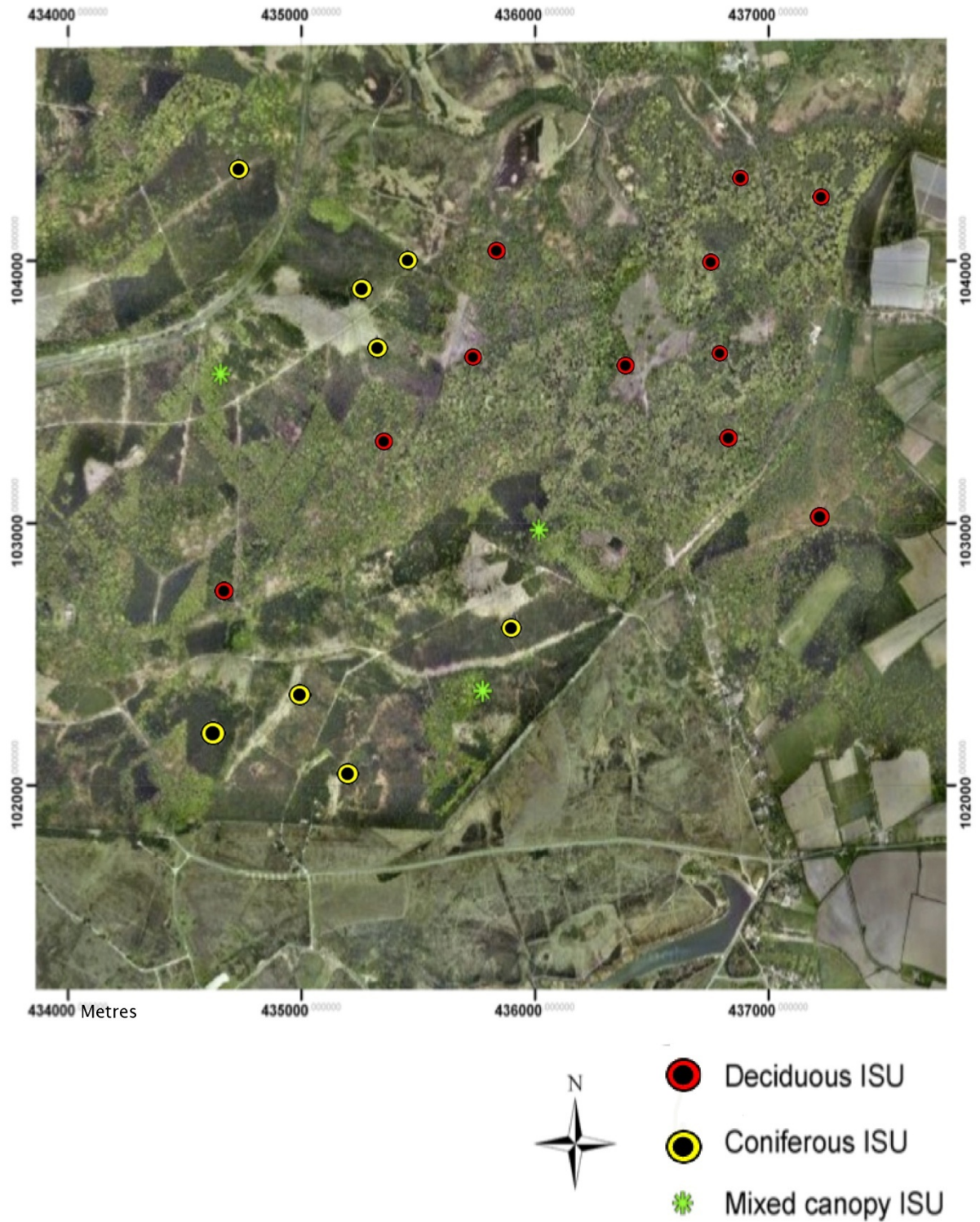


Figure 4.1. Frame Wood, New Forest, MTCI validation study area in southern England showing the location of individual sampling units (ISU) used to derive ground chlorophyll content. The image backdrop is a true colour aerial image re-sampled to a nominal spatial resolution of 0.5m.



Figure 4.2. Brooms Barn study area, Suffolk England showing the location of the individual sampling units (ISU) used to derive ground chlorophyll content.

4.4 Methods

4.4.1 Sampling design

To date, no sampling strategy has been proposed to sample chlorophyll content for MTCI validation at a spatial resolution of 300m. This is because the size of the validation site is directly comparable with the spatial resolution of the satellite product being validated (Morisette *et al.*, 2006). The geolocation accuracy of MERIS and the point-spread function will result in a larger validation site being required, which would be approx 1km². A 3 x 3 km site in each instance was chosen, which allowed for variability in cover type to be introduced, and allow for the analysis of statistical relationships. The main objective of the sampling scheme was to account for the variability in chlorophyll content across the validation site. Measurements at each individual sampling unit (ISU) within the validation site ensured that local variability was considered.

The sampling protocol for ground data collection was driven by the need to:

- (i) Represent the spatial variability in canopy chlorophyll content across the spatial resolution of a MERIS pixel; and
- (ii) Use ground data in conjunction with CASI-2 imagery, with a nominal spatial resolution of 2 meters, to produce a chlorophyll content map of the site.

The semivariogram based sampling method uses prior knowledge of the site to determine the spatial structure of the environment used to derive a sampling scheme (Curran, 1988). However, the rate at which chlorophyll content changed over time meant that the use of the direct semivariogram approach to sampling design was not feasible.

Both the New Forest and Brooms Barn validation sites were visited prior to the field campaigns. These pre-liminary visits, together with OS maps and aerial photography permitted the creation of land cover maps that outlined the main deciduous, coniferous and mixed tree stands, in the case of the New Forest, and crop type at Brooms Barn. At New Forest the location of heath and grasslands were also noted. In light of the preliminary field visit, the distribution and locations of the ISUs across the 9 x 9km

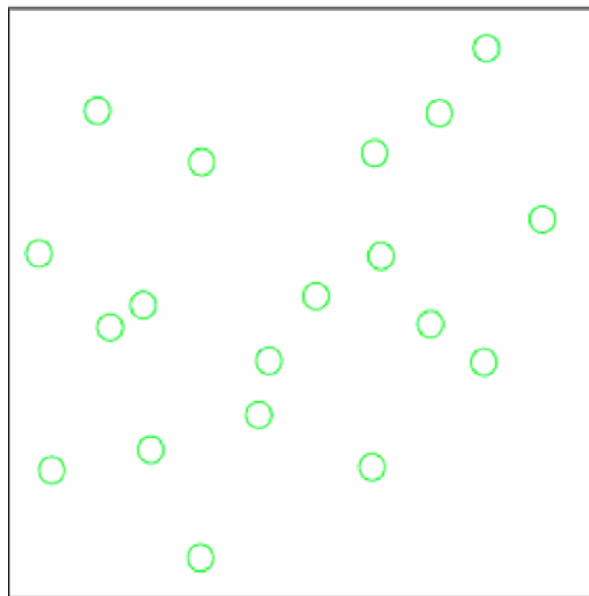
Chapter 4. Multi-scale analysis and validation of the MTCI

validation sites was carefully determined in order to account for heterogeneity in chlorophyll content between and within cover types. However, in reality, practical access considerations, including proximity to paths and roaming restriction had to be considered in the method design.

A dedicated methodology was developed for the validation exercises. This method is based on clusters of local measurements that aim to represent an area of equivalent size to a small group of pixels of the high resolution aerial imagery. To achieve this the 9 km² study area was divided into nine 1 km by 1 km grids and within each grid 3 to 5 individual sampling units (ISUs) (approximately 20 m x 20 m) were identified where practicable. This scheme lead to a total of 27 ISU within the 9 km² study areas, equating to a total sampling rate of 0.12%.

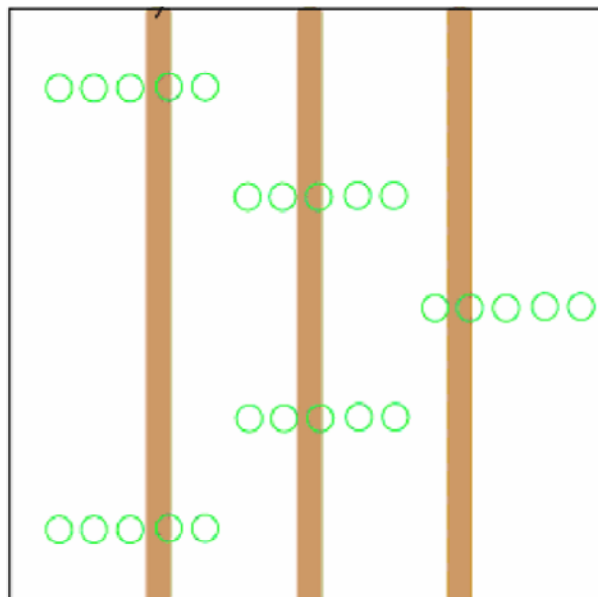
Depending on the features of the canopies at each ISU, two types of sampling methods were used to measure LAI and chlorophyll concentration. If the vegetation canopy was considered locally heterogeneous (at the ISU scale), the measurements followed an alternative sampling method. An alternative sampling protocol was employed to account for species composition and stand structure variation within each ISU (Figure 4.3a), such a technique relied on field measurements being taken at strategic locations that reflected the local species distribution, canopy closure and vegetation density within the ISU.

A stratified sampling scheme was chosen to represent LAI and chlorophyll concentration variation in ISU's with homogeneous canopies. This sampling strategy represented the variability within each ISU due to the systematic planting of the crops (both agricultural and coniferous plantations) and the presence of tractor lines (approx 2.5 meters apart, and 0.8m in diameter) at the Brooms Barn validation site. Individual sampling points were systematically located along 3m (Figure 4.3b). Within ISU with homogeneous canopies four or five transects were defined.



a) Alternative sampling strategy

○ LAI and SPAD measurements taken at each position



b) Stratified sampling strategy

Figure 4.3. Sampling procedures used to account for variation in LAI and chlorophyll concentration within each ISU according to canopy characteristics. The above are an illustration of the location at which measurements were taken following either an alternative (a) or stratified sampling scheme within a single ISU.

4.4.2 Remote sensing data

Two sources of remotely sensed data were used in the New Forest validation project: Compact Airborne Spectrographic Imager (CASI-2) and full resolution MERIS imagery. The high resolution imagery used in this study were acquired with the Itres Research of Canada CASI-2. In spatial mode, this two-dimensional CCD array based pushbroom sensor records a swath width of 512 pixels over a 54.4° Field of View. CASI-2 spatial mode data have 18 programmable bands in the visible to NIR region of the electromagnetic spectrum (405nm – 950nm). The NERC ARSF collected CASI-2 data, on 20th July 2007 at a nominal spatial resolution of 2 metres. Image acquisition occurred around 13.00hrs (solar noon) and the study area was almost cloud free. Seven CASI-2 scan lines recorded in a north- south direction covered the study area, with allowance for overlap between each flight line. The data were re-sampled and Binned to replicate the width and location corresponding to the 15 MERIS spectral bands (Table 2.4, Chapter 2) prior to receipt of the data by the NERC Remote Sensing Group based at Plymouth Marine Laboratory. Such a process employed spectral binning techniques that simulated the spectral response curves of the MERIS instrument.

The New Forest validation used a MERIS Level 2 image acquired on the 4th August 2007 at ‘full resolution’ (300m). This image was the least cloud-contaminated image closest to the time of the field sampling campaign (see table 4.1). Within the image, the study area was located close to nadir, minimising the effects of illumination and sensor geometry on scene properties.

The Brooms Barn validation project used ‘full resolution’ Level 2 MERIS image acquired on 13th May 2008 as this was the least cloud-contaminated image closest to the field sampling campaign. Eagle hyperspectral aerial imagery acquired on the 13th May 2008 by NERC ARSF was deemed unsuitable due to the effects of cloud shadow distributed across the imagery that affected an estimated area greater than a third of the scene.

4.4.3 Ground data collection

For both study sites, ground data collection was completed within 8 days of the satellite overpass. This strict time frame was employed to minimise variation in canopy

Chapter 4. Multi-scale analysis and validation of the MTCI

chlorophyll and vegetation foliage that would reduce the strength of the MTCI chlorophyll content relationship.

LAI can be determined directly using destructive methods. Although accurate, due to the scale of the New Forest and Brooms Barn validation exercises it was not logistically feasible to employ destructive methods or deploy foliar litter traps to estimate LAI. Time consuming wet chemistry assay procedures to determine chlorophyll concentration for all samples at each site was also unfeasible. Therefore chlorophyll concentration was estimated using the Minolta-SPAD chlorophyll meter, whilst Leaf Area Index (LAI) was estimated using a Delta-T Devices Sunscan Plant Canopy Analyser.

For deciduous tree and crop species a set of leaf samples were collected for SPAD calibration. The leaf samples were stored and transferred to the laboratory in cool dark conditions to minimise chlorophyll degradation. The method outlined in chapter 3, was used in the calibration of the Minolta SPAD to estimate foliar chlorophyll. SPAD calibration regression equations for each of the deciduous tree and crop species found at the New Forest and Brooms Barn validation sites can be found in Appendix 1.

Coniferous species needles were collected for each ISU and stored in dark cool conditions (black bags within a cool box) for later analysis. However, due to the relatively small size and narrow structure of the pine needles the SPAD 502 was not used to estimate chlorophyll concentration. Instead a wet chemistry assay procedure was employed to extract chlorophyll from coniferous species using the solvent Acetone. Sample preparation and measurement was undertaken in a dim room, to minimise chlorophyll degradation. The procedure required 0.1 g of fresh needle, along with 5.0ml of 90% aqueous acetone to be ground with a pestle. The leaf sample was ground until a colourless homogenate was produced. Using Whatman (number 1) filter paper, the homogenate suspension was filtered and fibrous material removed. 3.0 ml of the filtrate was then extracted and used to fill a curvette, whilst another curvette filled with 90% aqueous acetone was used as a reference.

Absorption at the wavelengths 664nm and 647nm was used to determine both chlorophyll *a* and *b* concentrations (mg/l) using the following specific extinction coefficients:

Chapter 4. Multi-scale analysis and validation of the MTCI

$$\text{Chlorophyll } a = 12.25 * \text{absorption } 664\text{nm} - 2.55 * \text{absorption } 647\text{nm} \quad (4.1)$$

$$\text{Chlorophyll } b = 20.31 * \text{absorption } 647\text{nm} - 4.91 * \text{absorption } 664\text{nm} \quad (4.2)$$

$$\text{Chlorophyll } a + b = \text{Chlorophyll } a + \text{Chlorophyll } b \quad (4.3)$$

Chlorophyll concentrations were converted into mass as the method required 0.1g of fresh needle; therefore, a simple calculation converted mg l^{-1} into mg g^{-1} . For each coniferous species, 20 x 0.1g of fresh needle samples were digitally imaged using a measuring rule as reference. These images were magnified allowing accurate sample area to be determined. Chlorophyll concentration was then expressed as a function of area (mg m^{-2}).

For deciduous tree and crop species, at both validation sites, within each ISU, 20 LAI readings and SPAD measurements were taken (each SPAD measurement was an average of 10 readings to reduce variability and account for variation in chlorophyll concentrations within leaves and canopy). Permission from the Forestry Commission permitted the use of limited destructive sampling to acquire leaves from the mid-canopy using portable ladder and secateurs although this approach was dependent on canopy structure and height. Where practicable, SPAD measurements were a combination of a twomid / upper canopy measurements with at least eight below canopy measurements to demonstrate chlorophyll concentration heterogeneity. Such an approach was used support the findings of O'Neil et al. (2002) who reported that limited variation in canopy biochemical concentrations throughout the tree canopy.

Chapter 4. Multi-scale analysis and validation of the MTCI

| Validation site | Validation method | High resolution data and acquisition date | MERIS data and acquisition date | Fieldwork date and duration |
|------------------------|---|---|---|---|
| New Forest | VALERI type method using transfer equation derived from high resolution imagery | CASI-2 imagery 20 th July 2007 | Full resolution Level 2 data Acquired 4th August 2007 | 26 th – 30 th July 2007 |
| Brooms Barn | Direct MTCI – ground chlorophyll relationship evaluation | Eagle – unused due to extent of cloud shadow within scene | Full resolution Level 2 data Acquired 13 th July 2008 | 15 th – 18 th May 2008 |

Table 4.1. Summary of the data and method used in the MTCI validation at the New Forest and Brooms Barn sites

4.4.4 Data processing at the New Forest

Data processing was undertaken in four distinct steps:

1. CASI-2 data processing,
2. Ground data processing
3. Chlorophyll map production from CASI-2 data and
4. Derivation of the relationship between MTCI and chlorophyll content at MERIS spatial resolution.

4.4.4.1 CASI-2 data processing

New Forest validation site was covered by seven overlapping flight lines of CASI-2 data. These were processed to create a single image, with a spatial resolution of 2 metres and spectral values calibrated to top of canopy reflectance ($\mu\text{Wcm}^{-2}\text{sr}^{-1}\text{nm}^{-1}$). This was achieved in a number of steps applied to individual flightlines; (i) atmospheric correction, (ii) radiometric normalisation for limb brightening, (iii) geometric correction, (iv) mosaicking and (v) CASI MTCI production.

(i) Atmospheric correction

The CASI-2 data provided by the ARSF had been partially radiometrically and geometrically corrected prior to receipt. Further data pre-processing was necessary to ensure the influence of the atmosphere was minimised, particularly the minor oxygen and water absorption features at 700nm and 800nm. Due to the absence of a ‘dark object’ in the field at the time of data acquisition, atmospheric correction was undertaken using the physical based FLAASH (Fast Line-of-sight Atmospheric Analysis of Spectral Hypercubes) software incorporated in ENVI (Research Systems Inc.) FLAASH is based on the MODTRAN (MODerate resolution atmospheric TRANsmittance) model (Le Maire *et al.*, 2008). Atmospheric correction reduces the effect of atmospheric aerosol scattering and absorption prior to the calculation of surface reflectance. Atmospheric correction was applied using the atmospheric observations contained in the ARSF flight log and the pre-defined atmospheric models within the FLAASH module.

(ii) Across-track normalisation of CASI-2 sensor data

Visual examination of the individual flight lines highlighted limb-brightening effects. This was due to variations caused by viewing and solar geometry within and between flight lines. The CASI-2 data were acquired near to solar noon, to maximise solar irradiance and signal strength, whilst minimising canopy shadow caused by low solar angles (Beisl, 2001). All CASI-2 data were acquired in a north – south orientation. Limb brightening was asymmetrical about the nadir line of flight as a result of the changing viewing geometry across the sensor view angle ($\pm 54.4^\circ$).

The CASI-2 flight lines were independently corrected to normalize cross track illumination that resulted in a general upward trend in the spectral response towards the edge of each flight line. Using ENVI, column averages were created for each band in the flight line. A second order polynomial function was fitted to the column average data. This method captured the overall limb brightening for each flight line. The second order polynomial curves were then used to normalise each band of the individual flight lines to their nadir values. This method minimised the limb brightening effect whilst retaining local scene variability (Figure 4.4).

(iii) Geometric correction

The Azimuth Systems program (AZGCORR) was used to apply the aircraft navigation data to each line of the normalised image and project those onto a geoid-based projection to determine the exact intersection of each pixel's view angle with a 5 metre resolution NEXTMAP DEM (accessed through NEODC). This produced a flight line that was geo-corrected to the British National Grid, using transform coefficients and algorithms provided by the Ordnance Survey of Great Britain (OSGB). The CASI-2 data were resampled to 2m pixel spatial resolution using a bicubic spline interpolation algorithm in AZGCORR (AZGCORR processing code found in Appendix 2).

Each of the flight lines were overlaid on an OSGB 1:10 000 map to visually assess the accuracy the geo-correction. Using the road network in the study area as a reference, visual interpretation suggested all images were geo-corrected to sub-pixel accuracy.

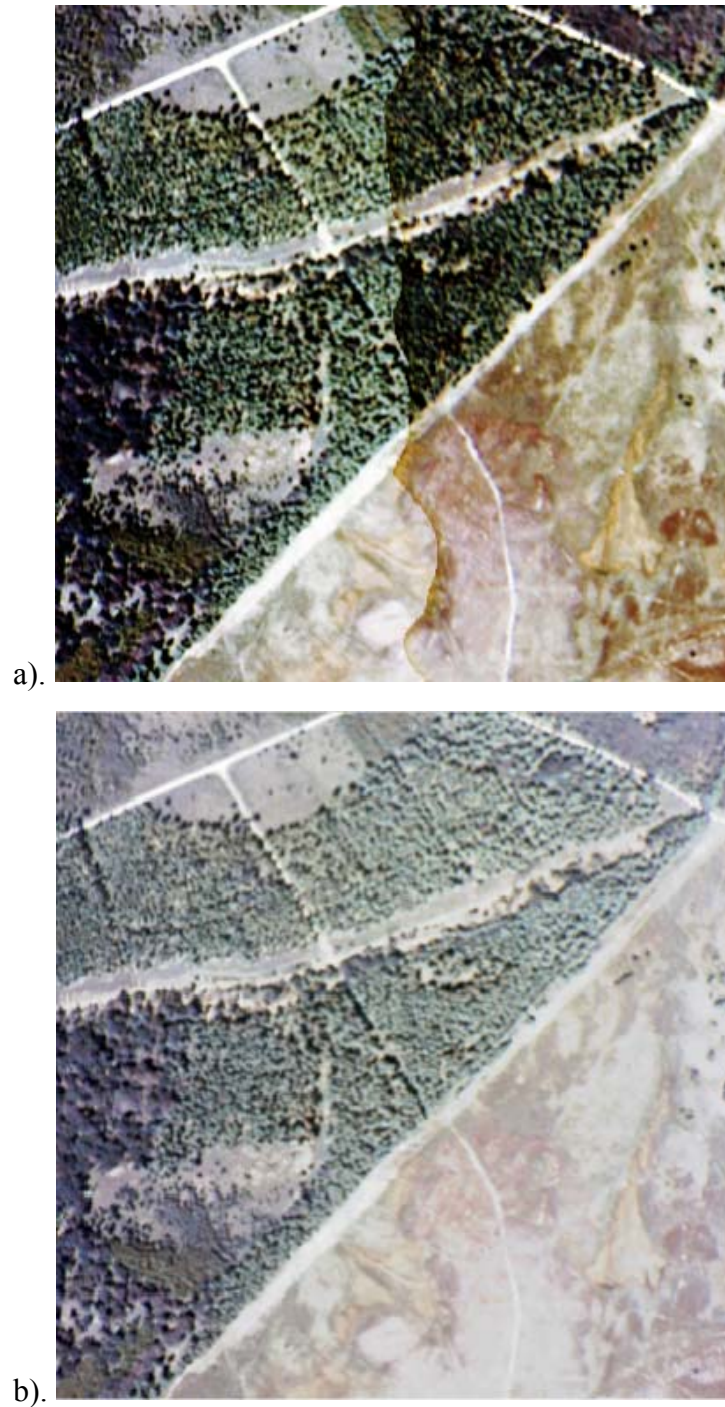


Figure 4.4. Variation in top of canopy reflectance between adjacent CASI-2 flight lines prior to normalising reflectance gradient in the cross track direction (a), (b) after correction.

(vi) Flight line mosaicking

Individual flight lines were mosaicked together to form a single image for the entire validation area (Figure 4.5). Mosaicking was completed using ENVI image processing software.

(v) CASI MTCI image production

Following this preprocessing, the mosaicked CASI-2 image, was used to produce a 2 metre MTCI image. Band math function in the ENVI image processing software was used to derive an MTCI with a floating-point integer from the following band ratio:

$$\text{CASI MTCI} = R_{\text{band } 10} - R_{\text{band } 9} / R_{\text{band } 9} - R_{\text{band } 8}$$



Figure 4.5. CASI-2 RGB mosaic comprised of seven geo-referenced flight scans that have been corrected for the effects of the atmosphere and radiometric variation.

4.4.4.2 Ground data processing

For each ISU, chlorophyll content (mg m^{-2}) was derived from LAI and SPAD derived chlorophyll concentration measurements. For each deciduous tree and crop species present within the ISU, leaf samples (covering the observed low to high SPAD range) were taken for the calibration of the Minolta SPAD instrument. The calibration equations produced for each species were then used to derive chlorophyll concentration for each SPAD measurement taken at each ISU (refer to Appendix 3). For coniferous species, chlorophyll concentration was determined using the wet chemistry assay method outlined in section 4.4.3. Chlorophyll content was derived as a function of chlorophyll concentration \times LAI. Using weighted averaging, based on species percentage cover in the 20 x 20 metre ISU, a single chlorophyll content value was derived for each ISU.

4.4.4.3 Chlorophyll map production

The production of a biophysical variable map that incorporates the high spatial variance of a variable across the validation site allows for spatial aggregation up to the spatial resolution of satellite sensor data. This approach is widely adopted by the Terra MODIS (Yang *et al.*, 2006) and the VALERI validation teams.

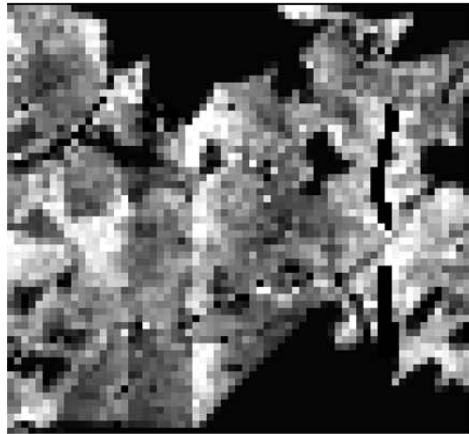
In this case, chlorophyll map production was achieved using the CASI MTCI imagery and average chlorophyll content from the field measurements at each 20 x 20 metre ISU. The Global Positioning System (GPS) locations of the ISUs were used to identify the 100 CASI-2 pixels that corresponded to the 20 x 20 ISU location. Within each ISU, the CASI-2 pixels were aggregated allowing the relationship between CASI MTCI and average chlorophyll content of each ISU to be determined. Regression analysis was used to determine the relationship between CASI MTCI and chlorophyll content for all ISUs in the study area (Equation 4.1, section 4.5.1).

Within the chlorophyll map, pixels with cloud cover, non-vegetated areas and those covered by grass, heathland gorse and heather were identified and removed from further analysis using a binary mask. The 2m CASI-2 chlorophyll map was re-projected to match the projection of the MERIS data, after which, pixels in the CASI-2 chlorophyll map were up-scaled to map chlorophyll content at the spatial resolution of MERIS data. The process of up-scaling needs to preserve the integrity of the information contained in

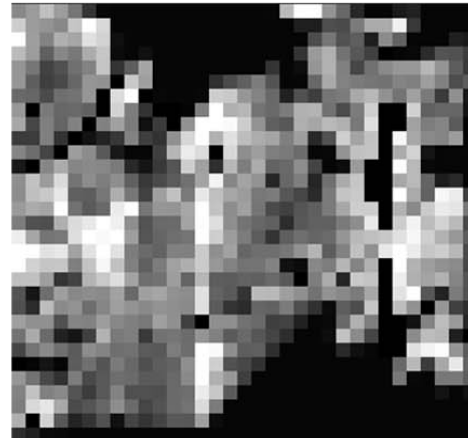
the higher resolution image. To achieve this a mean up-scaling method was used. Gupta *et al.*, (1998) showed that for forests, a mean up-scaling method achieved comparable results to more complex procedures, such as employing local fractal dimensions, for preserving information content to coarser resolutions.

4.4.4.4 Assessing the relationship between chlorophyll content and MTCI

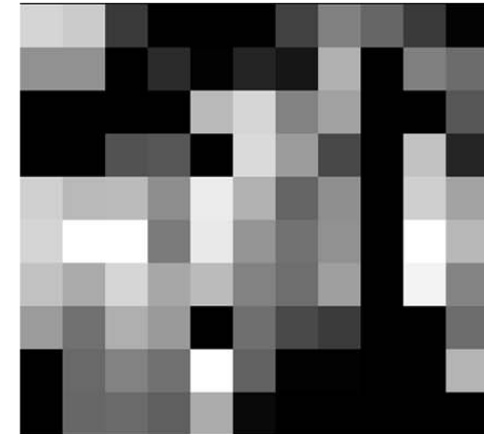
The area of interest, corresponding to the 3 x 3 km study area as derived from CASI-2 imagery was overlain on the level 2 MERIS imagery. MTCI for pixels within the area of interest were extracted. The relationship between per-pixel MTCI and CASI-2 chlorophyll content was then derived. Similarly, the 2 metre CASI MTCI was up-scaled, using the mean method outline previously, to match the spatial resolution of MERIS (Figure 4.6). This permitted sensor spatial resolution to be investigated and the results from MERIS and CASI MTCI to be compared.



a). Resampled 50 meter chlorophyll map



b). Resampled 100 meter chlorophyll map



c). Resampled 300 meter chlorophyll map

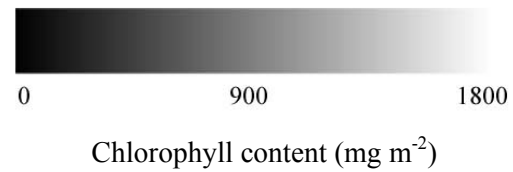


Figure 4.6. Up-scaling process used in this study aggregated the original 2m CASI-2 chlorophyll map to derive the 300 m chlorophyll map. This process permitted direct pixel-to-pixel comparison with ‘full resolution’ MTCI to be made.

4.4.5 Data processing at Brooms Barn

Due to the effects of cloud shadow, the Eagle aerial imagery of the Brooms Barn validation site was not used. The absence of high-resolution imagery to support the May field campaign, meant it was not feasible to adopt the same validation method as was used in the New Forest validation exercise.

The Brooms Barn validation followed the ground data processing method outlined in 4.4.4.2, deriving chlorophyll content for each ISU. Field boundaries were identified from 1:10,000 OS raster maps that were overlaid with the (cloud contaminated) Eagle aerial imagery. Fields containing an ISU, or those that grew a crop that showed small statistical variation in chlorophyll content were digitised in ArcGIS. The vector layers produced were extracted and re-projected to overlay the ‘full resolution’ MTCI.

Landscape heterogeneity at the 300m spatial resolution meant direct MTCI – ground chlorophyll content evaluation was only carried out on those MTCI pixels that fell within the boundary of a vector. Where a ‘full resolution’ MTCI pixel corresponded to an area covered by two or more adjacent vector layers, the chlorophyll content was determined by area of the vector within the MTCI pixel, and a weighting was given accordingly. This approach permitted the inclusion of more ISUs and therefore a larger sample size to assess the chlorophyll – MTCI relationship (Figure 4.7).

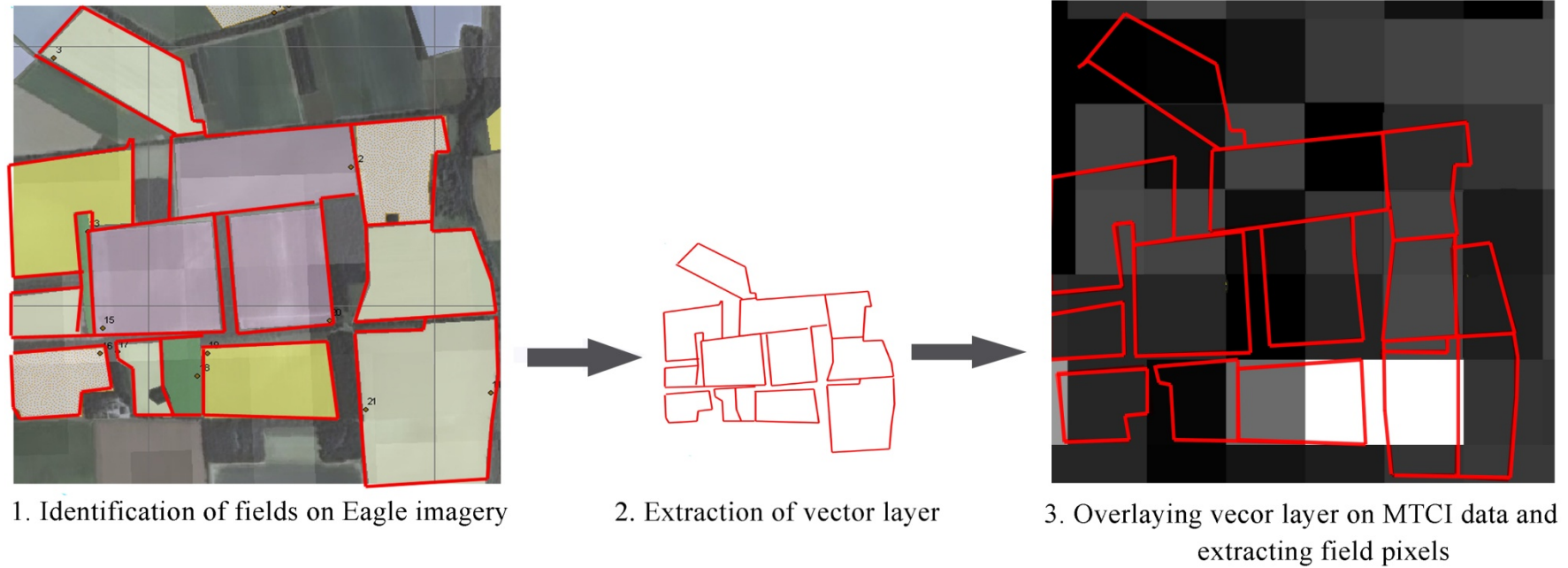


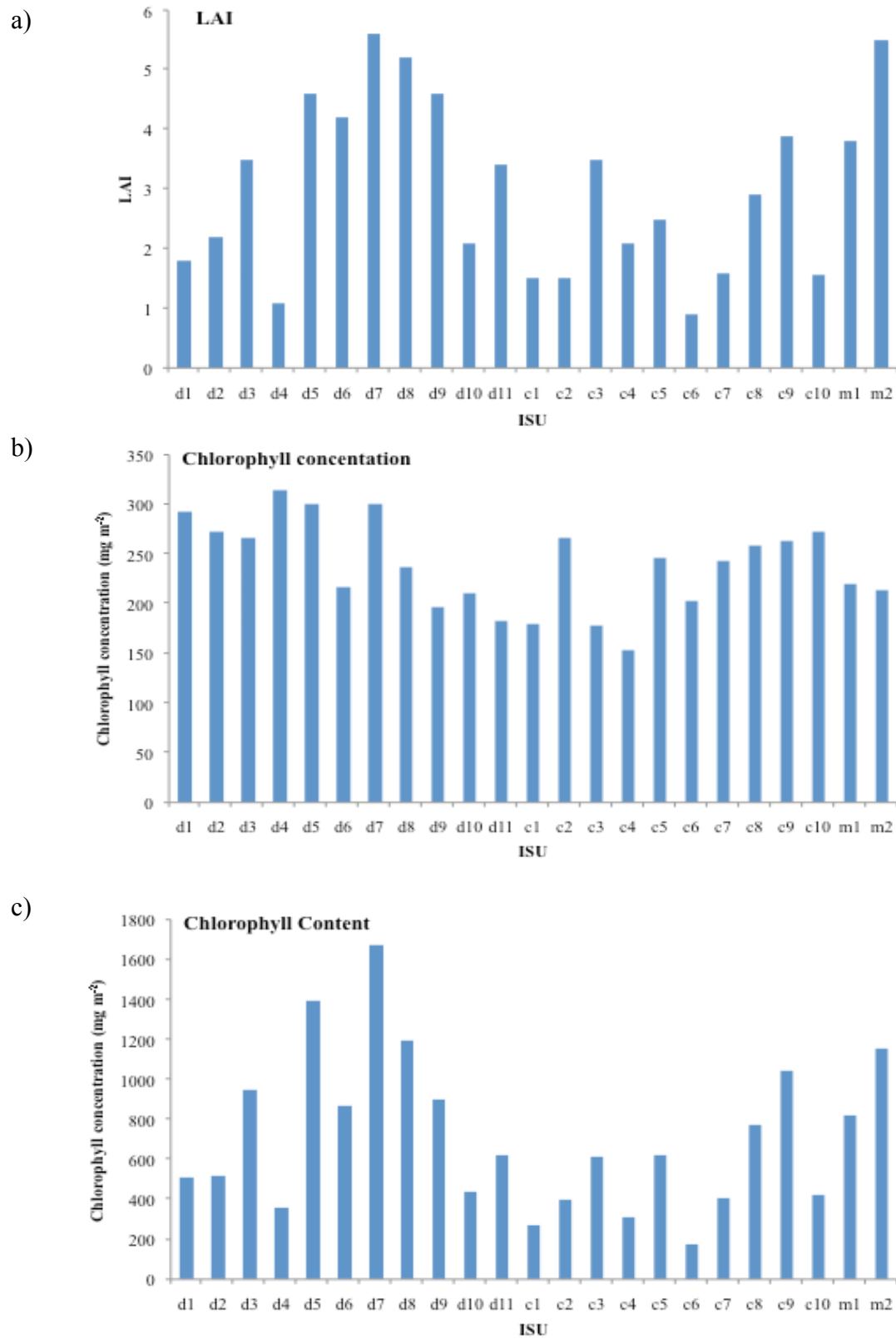
Figure 4.7. The method used to identify and extract MTCI field pixels in the Brooms Barn validation exercise

4.5 Results and discussion

4.5.1 New Forest

Variation in chlorophyll content between ISUs was principally due to variation in LAI rather than differences in chlorophyll concentration (Figure 4.8a and b). LAI was shown to vary between species and was also influenced by forest management practices leading to variation in tree planting densities, arrangement and felling practices. The heterogeneity in LAI at the New Forest validation site resulted in a wide range of chlorophyll contents (Figure 4.8c).

The New forest validation site showed local variability in canopy structure, with closed mature forested areas and open immature coniferous inclosures. At the 20m ISU resolution, understory reflectance and shadowing will be dependent on local canopy closure. Figure 4.9 shows the local variability in canopy closure and therefore influence of understory reflectance and shadowing present in the high resolution CASI-2 imagery. Depending on canopy closure, the aggregated MTCI at the scale of the 20 x 20 m ISU will be influenced by factors other than canopy chlorophyll content (Figure 4.10).



Figures 4.8. The variation in LAI (a), chlorophyll concentration (b) and chlorophyll content (c) between individual sampling units in New Forest study area. Sites with prefix D refer to deciduous, C = coniferous and M = mixed.



Figure 4.9. The local variability in canopy closure, which is representative of the New Forest study site and shown on CASI-2 2 metre RGB mosaic.

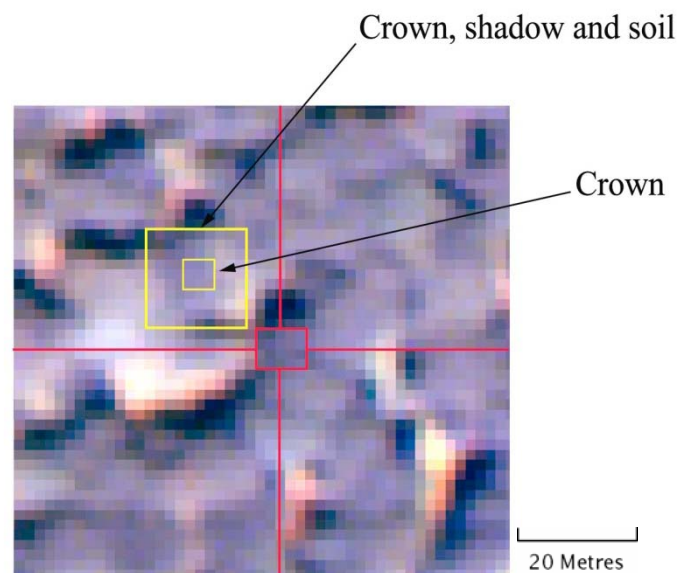


Figure 4.10. The effect of scene component aggregation as a function of spatial resolution. In an open canopy, at 20 metre resolution, pixels are composed of crown, understory and soil.

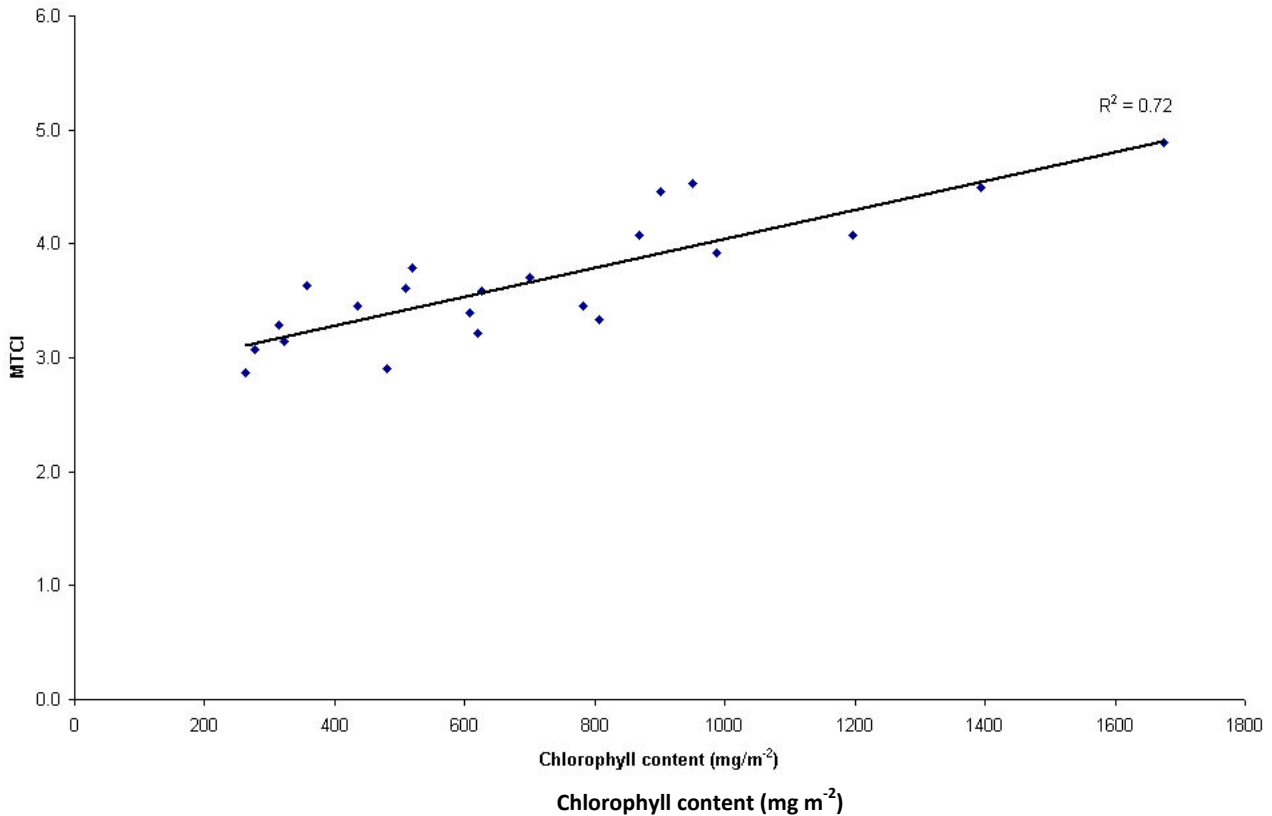


Figure 4.11. Relationship between CASI MTCI and chlorophyll content derived from ground measurement for each ISU in the study area.

The relationship between mean CASI MTCI and chlorophyll content derived from each ISU had a coefficient of determination (R^2) of 0.72, which was statistically significant at the 95% confidence level (Figure 4.11). The strong relationship between ISU chlorophyll content and aggregated CASI MTCI for the same area suggests that local variability in background reflectance and canopy shadow were minimal.

Using a linear regression model which defined the relationship between ISU chlorophyll content and average MTCI (Figure 4.11), a chlorophyll map (Figure 4.12) was produced at the 2 metre spatial resolution of the CASI-2 imagery using the transform equation:

$$\text{Chlorophyll content (mg m}^{-2}\text{)} = 568.68 \cdot \text{MTCI} - 1382.1 \quad (4.1)$$

In open canopies, the increasing spatial resolution of the MTCI will aggregate the effects of canopy shadow and background reflectance. To explore this, the 2 m CASI MTCI and chlorophyll maps were up-scaled using pixel aggregation to a spatial resolution of 300

metres. The relationship between 300metre CASI MTCI and chlorophyll content was strengthened as the effects of background had been aggregated as a function of pixel size. The strong relationship between CASI MTCI and chlorophyll at the both high resolution (20 metres) (R^2 0.72) (Figure 4.11) and 300m scales (R^2 0.87) (Figure 4.13) confirms that the MTCI is a useful tool is estimating chlorophyll content in open woodlands.

The observed relationship between CASI MTCI and chlorophyll content, at both the full resolution and 300 m scales, suggests that the sampling strategy adopted in this study successfully accounted for the heterogeneity in cover type and variation of chlorophyll content in the study area. However, the relationship between ‘full resolution’ MERIS MTCI and the chlorophyll content resampled to 300 m was weaker than the CASI MTCI – ground derived chlorophyll content relationship, with an R^2 of 0.57 (significant at the 95% confidence level) (Figure 4.14). This relationship was not as strong as reported in previous studies (Zhang *et al.* 2008; Curran and Dash, 2007). Although the relationship is significant, the relationship between 300m chlorophyll map and ‘full resolution’ MERIS MTCI will need further investigation to assess why it is not as strong as chlorophyll - CASIMTCI. A concern with MERIS data is the geolocation accuracy. Subpixel geolocation accuracy is necessary in order to accurately retrieve biophysical variables of the land surface (Townshend *et al.* 1992). Studies have suggested the MERIS sensor has inherent geolocation accuracy of $\pm 150\text{m}$ and within scene accuracy of $\pm 50.1\text{m}$ (Dewart *et al.*, 2007). The aggregated CASI-2 imagery has much greater geolocation accuracy than the MERIS imagery. Therefore, given the geolocation uncertainty of MERIS, a MERIS pixel covers (potentially) 0-100% of the ground area compared to a correspondingresampled 300m CASI-2 pixel. Therefore the potential overlap caused by the geolocation accuracy of MERIS will lead to variation between ground and MTCI scene chlorophyll content.

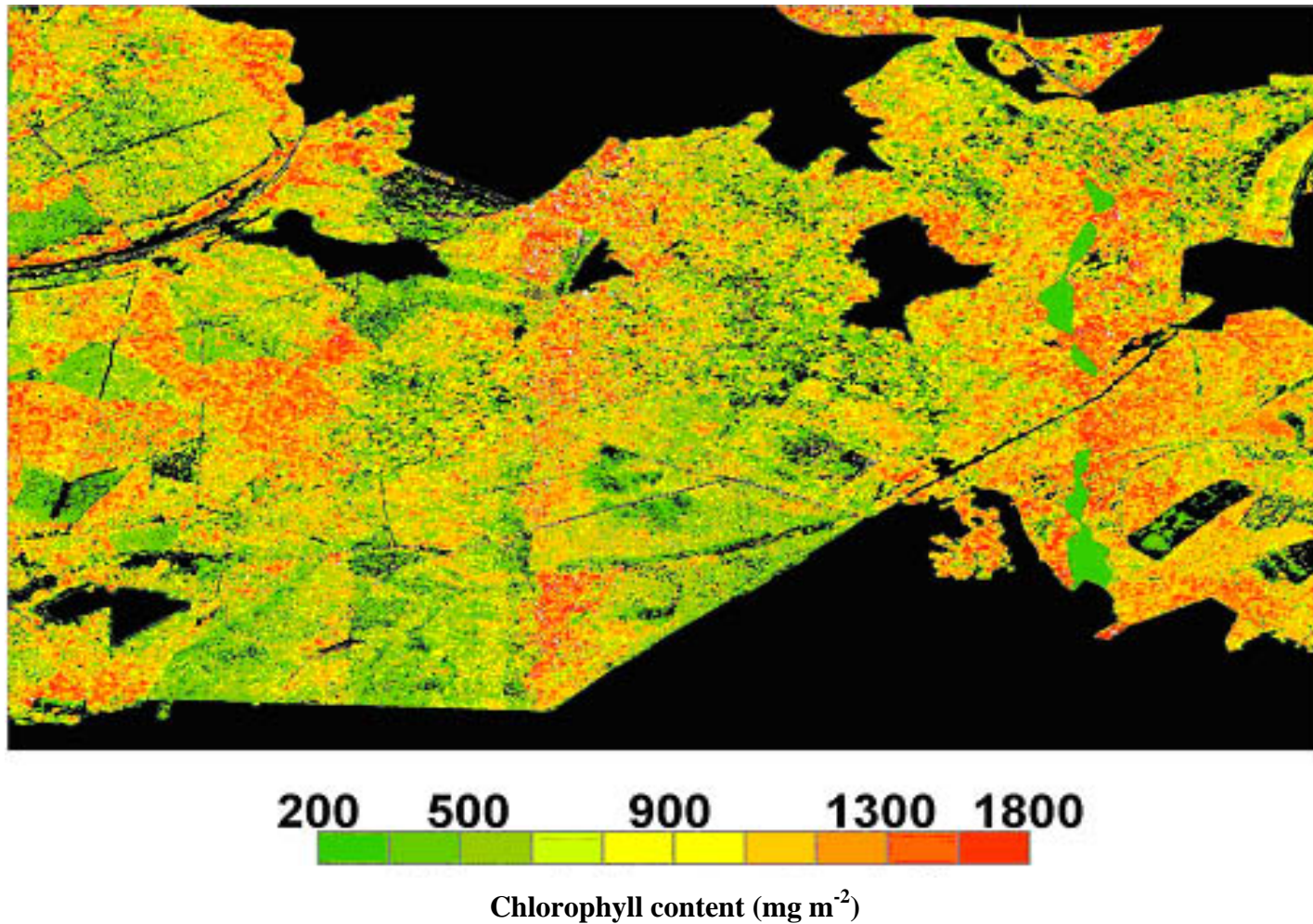


Figure 4.12. Chlorophyll content map of the study area derived from the modelled relationship between CASI MTCI data and chlorophyll. Black areas represent no data, where a binary mask was applied to remove missing data or areas covered by heathland or non-vegetated areas

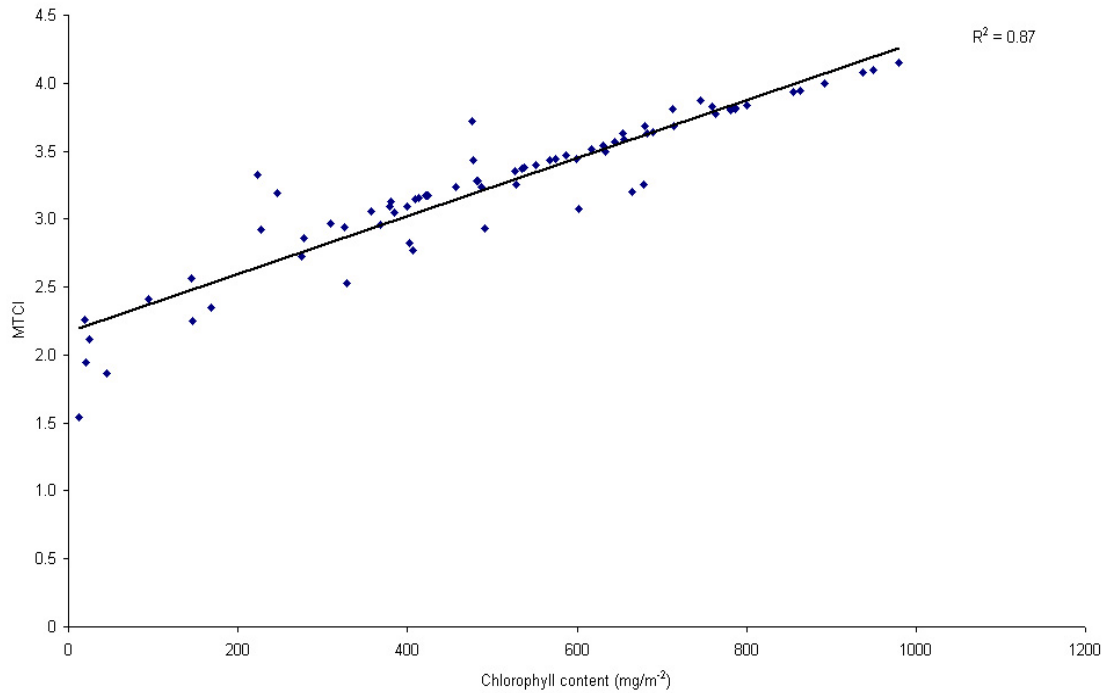


Figure 4.13. The relationship between CASI MTCI and the chlorophyll content map derived from CASI-2 imagery and field based chlorophyll measurements (refer to Figure 4.12). Both datasets were resampled to a spatial resolution of 300m.

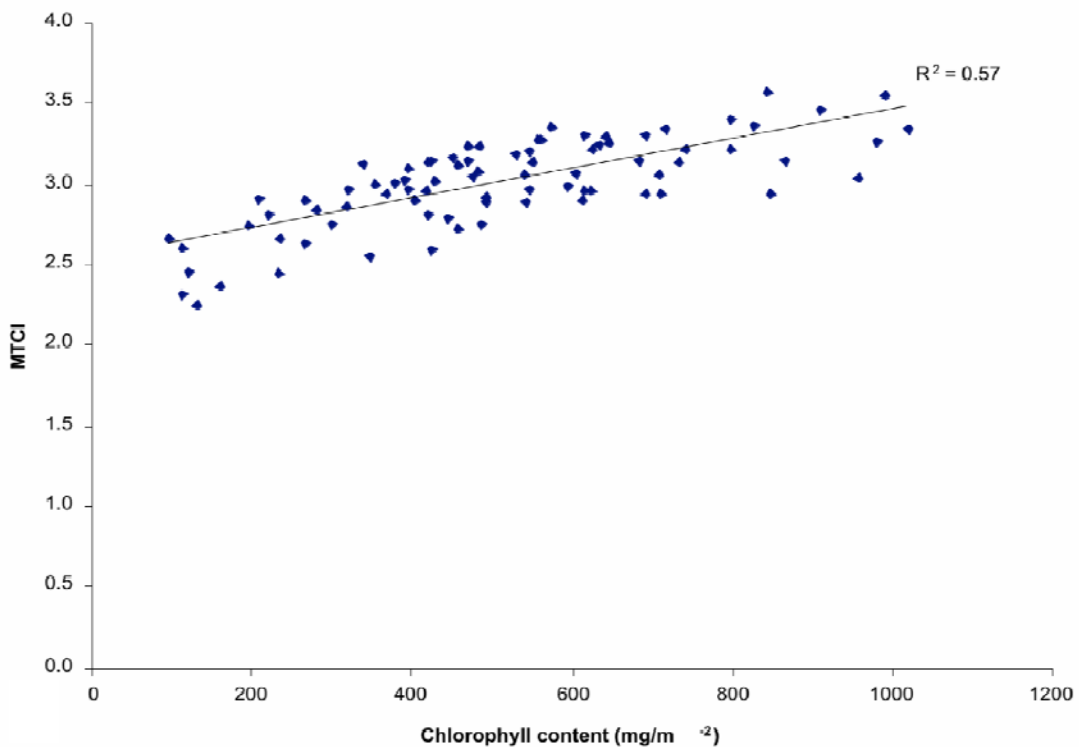


Figure 4.14. The relationship between MERIS 'full resolution' MTCI imagery and the chlorophyll content map derived from CASI-2 imagery and field based chlorophyll measurements resampled to a spatial resolution of 300 m.

4.5.2 Brooms Barn

The variability in chlorophyll content between ISUs of the same crop type was established. Table 4.2 shows the standard deviation in canopy chlorophyll for various crop types found in the Brooms Barn study area. Determining the variation in chlorophyll content for each crop type allowed an increase in the number of MERIS MTCI pixels to be included in evaluating the MTCI - chlorophyll content relationship.

| Crop | Number of ISU | Standard deviation (chlorophyll content mg m ⁻²) |
|-------------|---------------|--|
| Wheat | 5 | 153.1 |
| Barley | 3 | 385.5 |
| Sugar beet | 3 | 9.9 |
| Onions | 2 | 3.3 |
| Wooded area | 5 | 87.6 |
| Potatoes | 6 | 42.0 |

Table 4.2 The variability in chlorophyll content according to crop type in the Brooms Barn study site.

The direct ground chlorophyll content – MTCI relationship for all cover types showed a weak correlation, with an R^2 of 0.33 (Figure 4.15). This relationship was significantly weaker than shown in the New Forest study. Investigation into the likely cause of the weak relationship suggests that the presence of bare fields and those fields that grew sugar beet, onion and pixels that have very low LAI (Figure 4.16) had larger MTCI values than expected. The reflectance of those fields with low LAI and bare soil as measured in MERIS bands 8, 9, and 10 are summarised in Table 4.3. The high MTCI values are a result of the optical properties of the soil rather than chlorophyll content. It was found that removing those pixels with an $LAI \leq 0.3$ (highlighted with an ellipse on Figure 4.15) from further analysis greatly improved the relationship between MTCI and chlorophyll content from $R^2 = 0.33$ to $R^2 = 0.71$ (Figure 4.17).

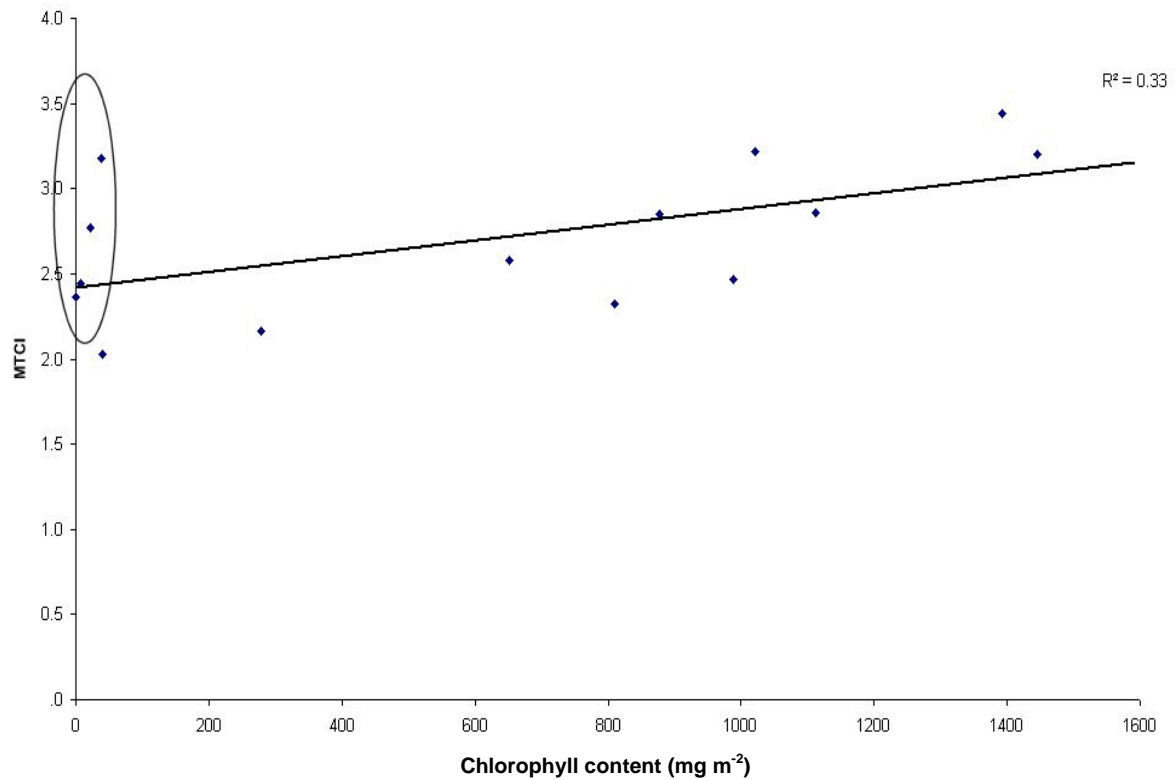


Figure 4.15. The relationship between chlorophyll content and MTCI for all cover types. Highlighted points refer to measurements where LAI \leq 0.3.

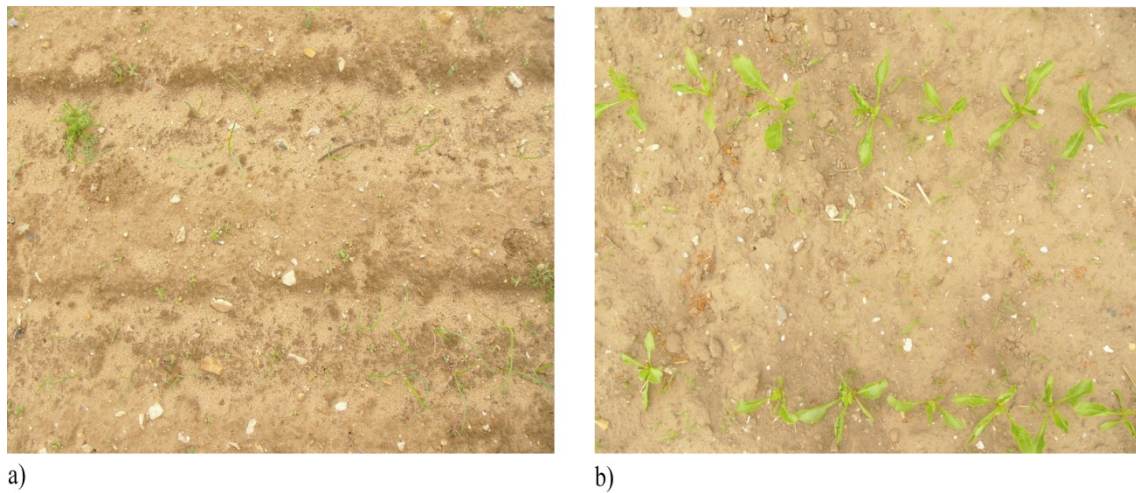


Figure 4.16. Photographs showing the stage of crop development of a typical onion (a) and sugar beet crop (b). Images were taken during the Brooms Barn validation campaign during May 2008.

| MERIS band | Onion field LAI = 0.03 | Bare soil LAI = 0 | Beet field LAI = 0.1 |
|------------|---------------------------|----------------------|-------------------------|
| Band 8 | 14.9 | 16 | 11 |
| Band 9 | 19.7 | 20.2 | 15.6 |
| Band 10 | 29.4 | 28.9 | 30.2 |
| MTCI | 2.0 | 2.1 | 3.2 |

Table 4.3. Surface reflectance from onion, sugar beet and bare soil as measured in MERIS bands 8, 9 and 10 that are used to derive the MTCI.

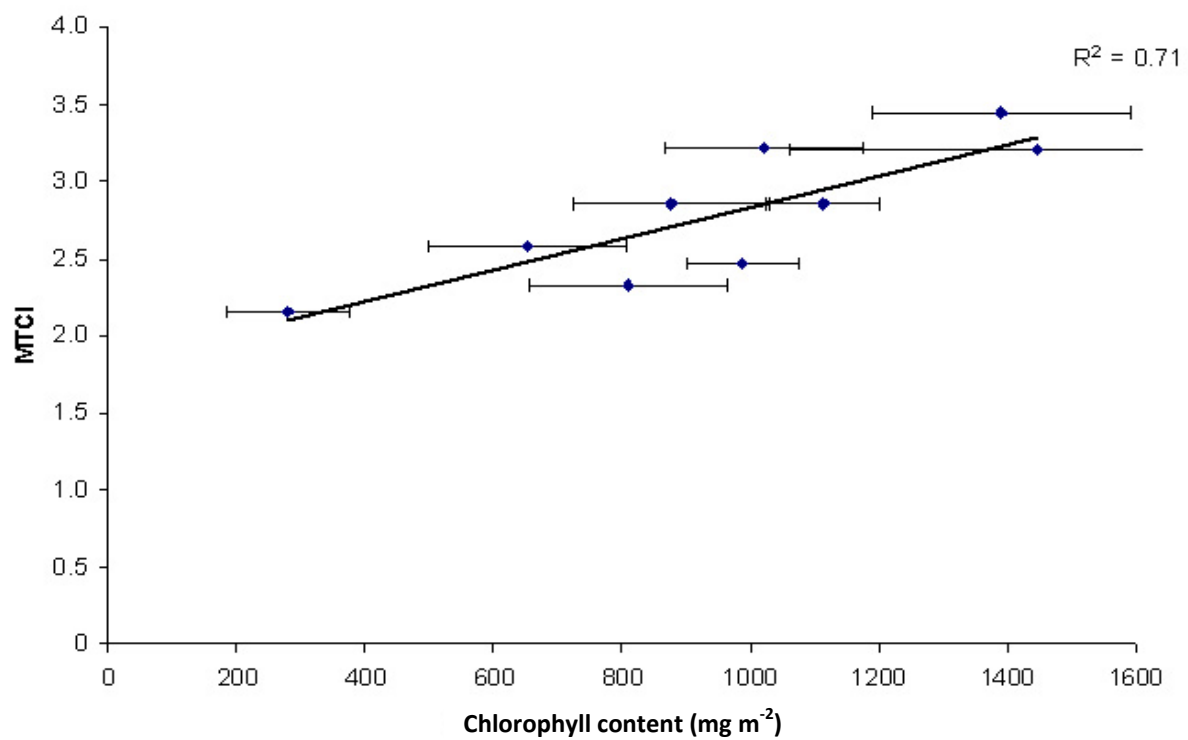


Figure 4.17. The relationship between chlorophyll content for agricultural crops and MTCI where LAI => 0.3. Error bars indicate the standard deviation for a particular cover type to which that pixel relates.

4.6 Discussion of chapter aims

The aims of this chapter were to:

1. Examine the methodological issues with averaging chlorophyll contents acquired at one spatial resolution to coarser spatial resolutions (i.e., scaling-up);
2. Determine the sensitivity of the MTCI to a greater range in chlorophyll content;
3. Assess the transferability of the MTCI from one place to another (Foody *et al.*, 2003), specifically assessing both the relationship with canopy chlorophyll content and use of the index to predict canopy chlorophyll content at other locations and cover types;
4. Determine the operational influence of soil background on the relationship between MTCI and chlorophyll content.

A global product will be required to estimate biophysical variables across a range of contrasting vegetation cover types throughout the growing season. Therefore, in this instance, the MTCI must demonstrate sensitivity to a range of chlorophyll contents and transferability between locations permitting the spatial comparison between sites. The relationship between MTCI and chlorophyll content observed at Brooms Barn supports the MTCI evaluation carried out at a study site near Dorchester by Dash and Curran (2005). The Dorchester evaluation site involved different crops to the Brooms Barn site (including grasses, beans, oats and maize). Although in this study chlorophyll content was expressed as g per MERIS pixel, comparisons can be drawn from the strong positive correlation between MTCI and chlorophyll content, as shown in Figure 4.18, at the Dorchester evaluation site (a) and the Brooms Barn validation site (b) suggesting that there is a consistent and strong relationship between MTCI and chlorophyll content for a variety of agricultural crops. Wu *et al.* (2009) examined the relationship between canopy chlorophyll content and MTCI for six varieties of wheat. Species showed variation in canopy structure, with differences in leaf orientation (including planophile, erectophile and spherical). Regression models explaining the relationship between chlorophyll content and MTCI suggested that the influence of vegetation structure between the variants was limited. Such relationships suggest that variation in canopy structure between crop species has a limited effect on MTCI.

The chlorophyll content map of the New Forest validation site was derived using one MTCI - chlorophyll content relationship for the entire study area without considering the effect of land cover type or variation in canopy structure. It had been assumed that the relationship between MTCI and chlorophyll content is independent of land cover type. If the relationship does vary with canopy structure then this will have decreased the accuracy of the chlorophyll map derived from CASI-2 data. The distinct clustering in Figure 4.19 between vegetation types suggests that canopy structure may influence the relationship between MTCI and chlorophyll content where there is a distinct variation in canopy structure (i.e., between deciduous and coniferous trees species and crops) (Figure 4.18). The relationship between MTCI and cover type suggests that the MTCI may be sensitive to cover type, therefore effecting the transferability of the index as the relationship between MTCI and chlorophyll content will be a function of cover type. The self-shadowing of conifer canopies results from the size and arrangement of trees, Canopy self-shadowing on flat terrain strongly correlates with the canopy's geometric complexity (Kane *et al.*, 2008). Because stands with trees of different sizes, shapes, and arrangements cast different amounts of shadow, self-shadowing as a fraction of the image correlates with the complexity of the canopy structure. Although topographic shade was minimised in the CASI-2 imagery (solar noon acquisition, topographical effects minimised with site selection), the effects of tree shade is a function of the shape and spacing of trees. Reflectance in both the red and NIR regions has been shown to vary according to vegetation type (Soundani *et al.*, 2006). Using PROSAIL, combining leaf optical properties and canopy level bi-directional models, for a given chlorophyll content and LAI there was shown to be variation in red and NIR reflectance between coniferous (Scots pine) and deciduous species (beech and oak) for three different sensors. However, caution should be shown with such findings as such sensors acquired reflectance in broad wavebands compared to the narrow MERIS bands. It should be noted that further work is required to understand the influence of canopy structure on the relationships between chlorophyll content and MTCI between various cover types.

The experimental design adopted in this chapter suggests that canopy architecture does have an influence on the MTCI. However, results suggest that the effects are limited and only apparent where comparisons are made between vegetation types that have significant differences in canopy structure. Caution should be taken when making direct comparisons between the MTCI – chlorophyll content relationship between trees and

crops (as seen in Figure 4.19) as these may be influenced by the radiometric properties of CASI-2 and MERIS. The comparison between trees and crops may be affected by the increased reflectance in MERIS band 8 (red), giving higher values for MTCI derived from CASI-2 data. However, both deciduous and coniferous MTCI were derived from the same sensor, permitting direct comparisons. The method used to derive LAI (using Sunscan) might incorporate systematic positive bias for forested areas as a result woody biomass. This may lead to overestimation in chlorophyll content that contributes to the trends shown in Figure 4.19.

Variation in LAI on the MTCI – chlorophyll content relationship was highlighted in the MTCI Algorithm Theoretical Basis Document (Curran and Dash, 2005) as an area of operational uncertainty. The effect of variation in LAI for given chlorophyll content on the MTCI was unknown. Figure 4.20 shows MTCI – chlorophyll content for each of the types of vegetation investigated in this study as a function of LAI. Figure 4.19 shows no distinct clustering in LAI, suggesting that the differences in Figure 4.18 are a function of canopy structure rather than LAI. Such results support the results from the laboratory-based spectroscopy experiments (Chapter 3) suggesting that for a given chlorophyll content, variation in LAI has no evident effect on the MTCI. Further research is required to assess the effects of canopy structure and LAI on the MTCI. Physically-based models describing the transfer and interactions of radiation inside the canopy based on physical laws (Houborg *et al.*, 2009) provide an opportunity to determine the influence that structural variables have on canopy reflectance and the MTCI.

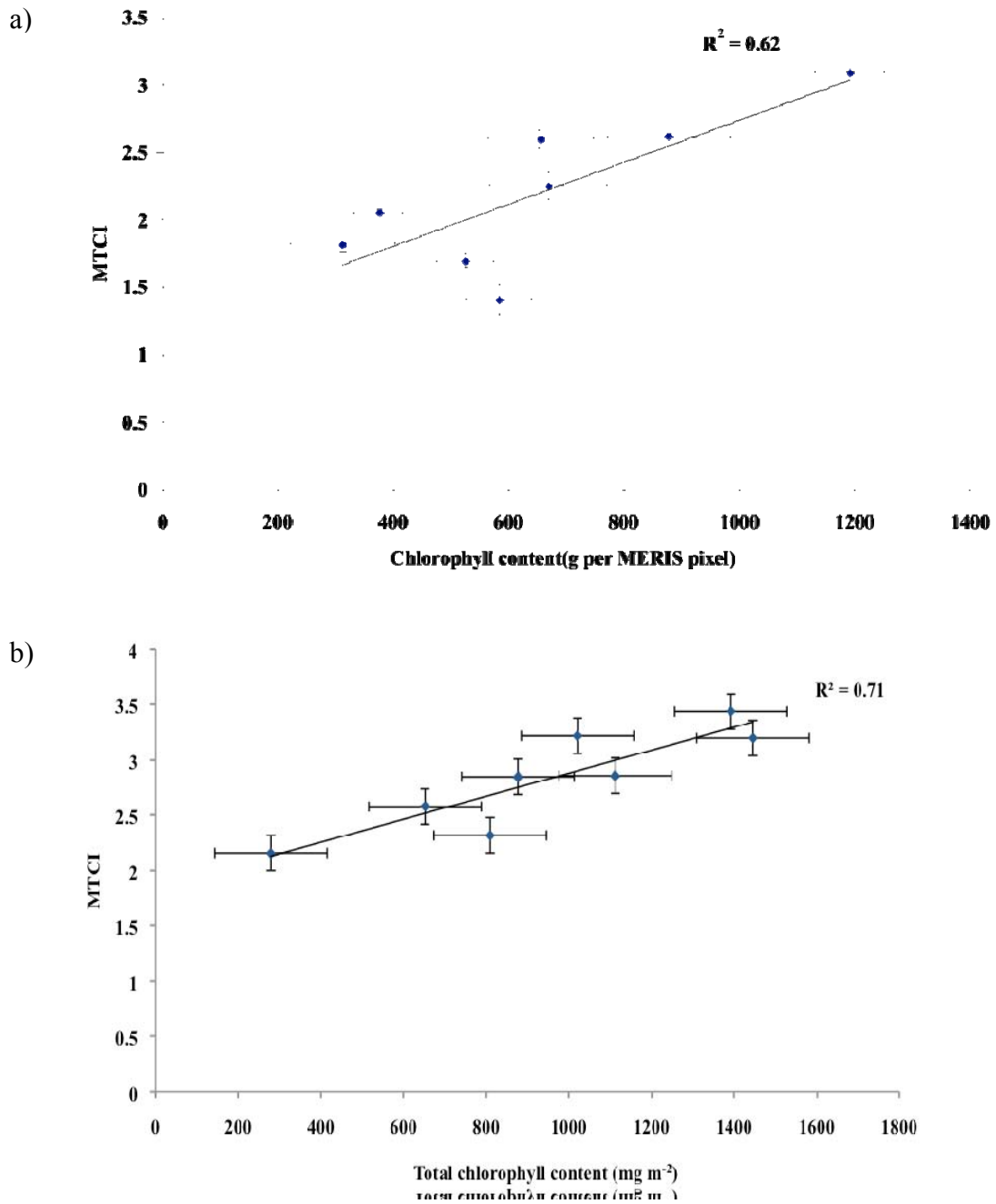


Figure 4.18. The relationship between MTCI and chlorophyll content in agricultural crops as determined at the Dorchester study site (a) from Dash and Curran (2007), and (b) Brooms Barn validation.

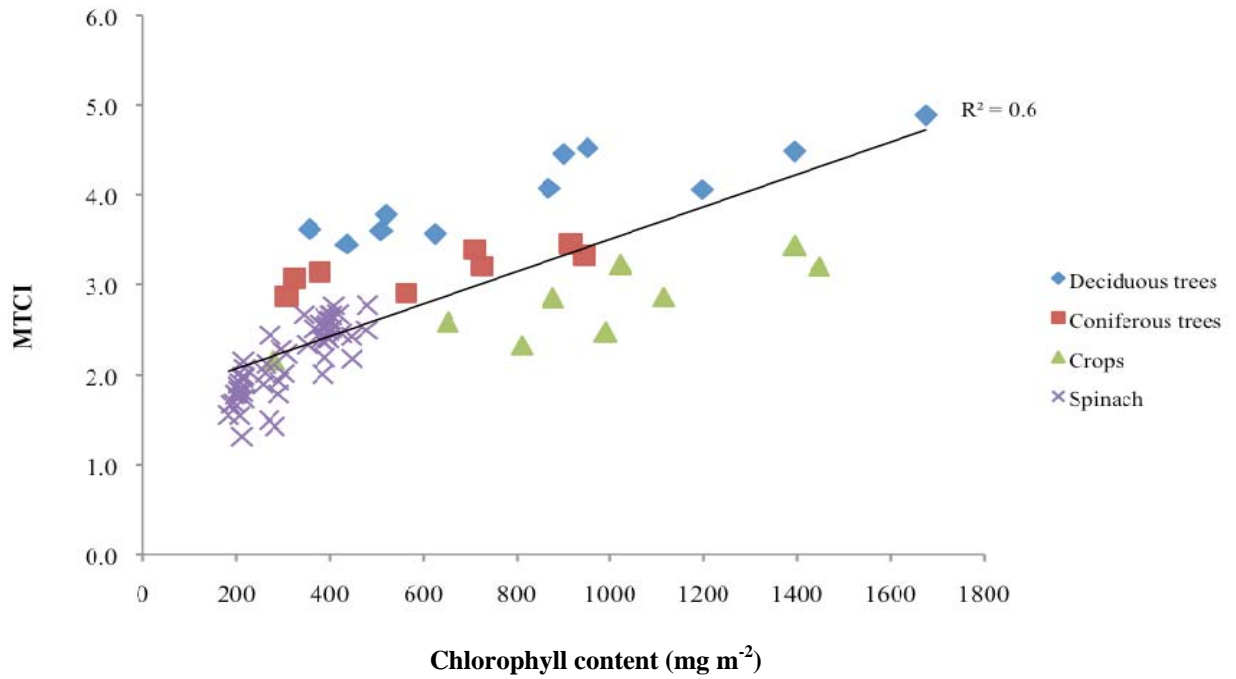


Figure 4.19. The relationship between chlorophyll content and MTCI for various cover types.

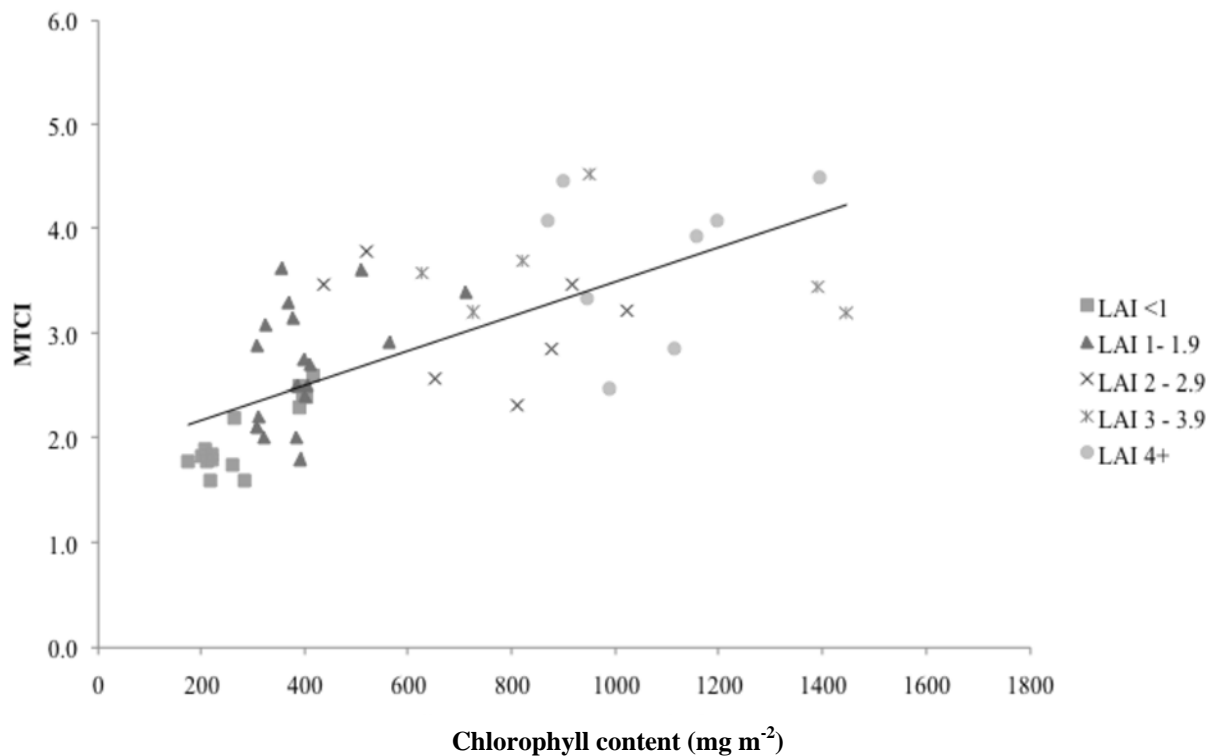


Figure 4.20. The relationship between MTCI and chlorophyll content as a function of LAI.

The effects of background reflectance on the MTCI needs to be understood in if MTCI is to be used to capture the spatial and temporal dynamics of terrestrial vegetation. The

Chapter 4. Multi-scale analysis and validation of the MTCI

fundamental objective of the MTCI is to isolate the chlorophyll content from the spatially and temporally variable 'mixed' pixels, to allow meaningful spatial and temporal comparisons of vegetation activity. The results from Brooms Barn suggest that where LAI is low, the soil background reflectance was a significant contributor to the canopy reflectance signal (Houborg *et al.*, 2009) and therefore MTCI value. Due to the effects of bare soil on the MTCI Bannari *et al.* (2008) suggested it would be very difficult to interpret the MTCI at very low LAI and sparse vegetation cover. However, results from both Chapter 3 and the Brooms Barn study have shown that the effect of soil reflectance on the MTCI are compounded at relatively low LAI. The Brooms Barn study suggests that vegetation cover with an LAI ≥ 0.3 were able to compound the effects of soil reflectance.

4.7 Limitations of the study

The geolocation accuracy associated with the MERIS sensor meant that it was not possible to obtain a 100% pixel match between the aggregated CASI-2 re-sampled chlorophyll content map and the MERIS pixels. Therefore, the MTCI estimated from MERIS data did not represent the exact ground over which chlorophyll content was estimated. Also the point-spread-function for MERIS was not considered in the degradation, or up-scaling of CASI-2 data, nor were adjacency effects from neighbouring pixels considered. This might have introduced some further uncertainty in the ‘full resolution’ MERIS MTCI - chlorophyll content relationship.

The radiometric sensitivity of MERIS and CASI-2 has been assumed to be similar, and any differences between them ignored. A similar approach was adopted by Clevers *et al.*, (2001) who simulated MERIS imagery from high resolution AVIRIS imagery. Further investigation is necessary to determine whether differences in radiometric sensitivity between sensors contributed toward the relationship between MERIS MTCI and CASI MTCI, where a greater range in MTCI values were observed in CASI-2 data (Figure 4.21). However, scatter plots between the bands 8 – 10 and the MTCI show that there was greater reflectance in the red band of CASI-2 compared with MERIS, whilst bands 10 and 9 showed a similar spread in points (Appendix 3). Therefore, results suggest that the increase in red reflectance in CASI-2 band 8 resulted in a smaller difference between band 9 and 8, which consequently resulted in higher CASI MTCI at higher chlorophyll contents. The increase in reflectance in CASI-2 band 8 could be related to the radiometric differences between sensors, or an artefact of adjacency effects that can be observed in high spatial resolution imagery (Richter and Schläpfer, 2002) from which the CASI MTCI was derived.

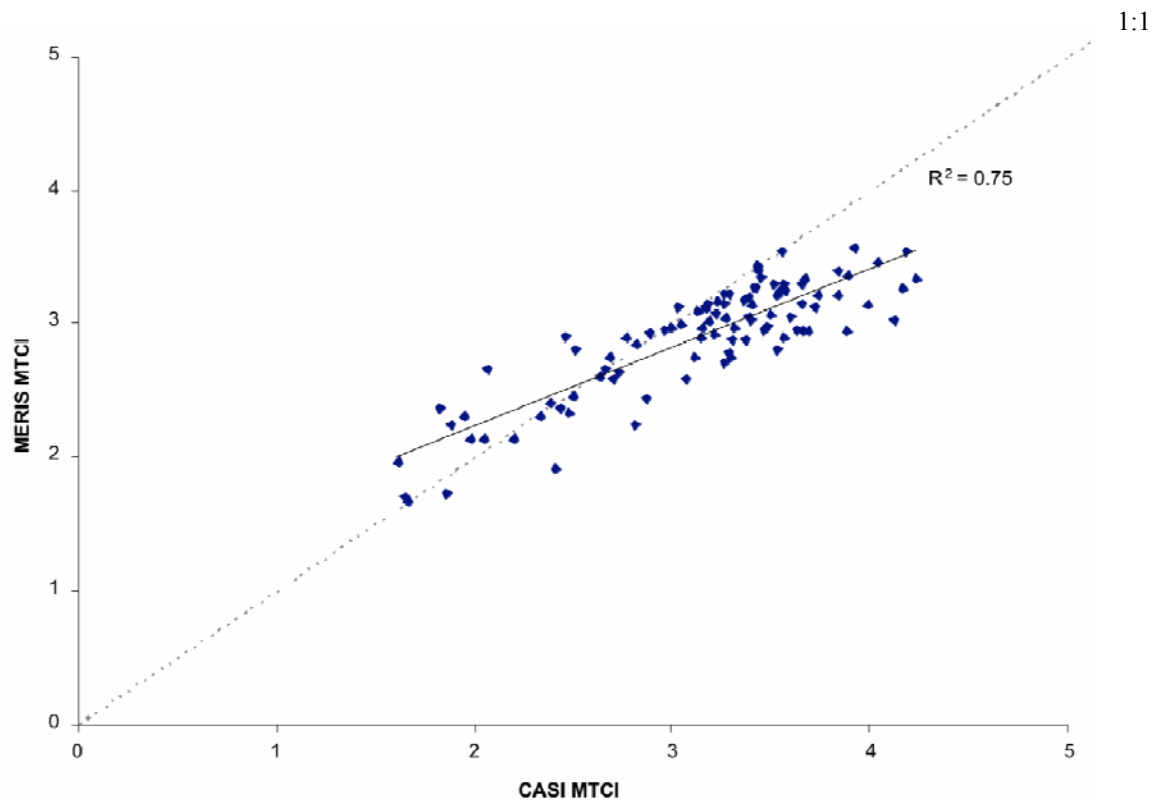


Figure 4.21. Relationship between MERIS MTCI and that derived from CASI-2 imagery

The process of validation requires the assessment of the accuracy of data products through independent means (Justice *et al.*, 2000; Morisette *et al.*, 2006). However, in this investigation, the MTCI was evaluated through direct comparison with ground-based chlorophyll measurements without employing independent estimates. The method used to validate the MTCI was used as opposed to canopy modelling as estimates of leaf chlorophyll derived using inverse modelling techniques have been associated with reasonably large uncertainties (Houborg *et al.*, 2009). Jacquemoud *et al.* (2000) reported inaccuracies when four canopy reflectance models were inverted with airborne CASI-2 reflectance spectra over corn and soybean fields. Similarly vegetation indices that have been used to estimate chlorophyll content successfully have generally been based upon the reflectance in the red edge. Due to the high correlation between REP techniques and MTCI (Haboudane *et al.*, 2008) direct, chlorophyll content to CASI-MTCI evaluation was adopted in this investigation. Moreover, REP methods have been shown to be sensitive to variations in LAI, particularly at low LAI (Clevers *et al.*, 2001).

There are potential limitations associated with the use of the SunScan instrument that was used to derive LAI. Although the apparatus has been used to estimate LAI in croplands with success (95% agreement with destructive LAI measurements in cereals and sugar cane) the estimation of LAI in woodlands is limited in the literature (Oguntunde *et al.*, 2007). The SunScan requires an above canopy reference signal to derive accurately LAI, however the height of the woodland canopy may introduce practical difficulties for acquiring above canopy reference. Although attention was paid to locate the PAR sensor in clearing, the potential limitation associated with LAI retrieval in woodlands may introduce systematic bias / error into the results. The Sunscan apparatus (and the LAI-2000) does not distinguish between photosynthetic material and structural or non-photosynthetic biomass. This would be particularly relevant to the New Forest study, and would have consistently over-estimated LAI. The inclusion of woody biomass into the LAI estimates will therefore be a systematic error in the calculation of chlorophyll content, and therefore not effect the relationship between chlorophyll content and MTCI for a homogenous cover type. Such a factor would need to be considered when assessing the transferability of the MTCI. (Numerous Sunscan measurements were taken of dead pine trees to examine the effect of woody biomass on chlorophyll content estimations). To overcome the potential limitation of estimating LAI from the SunScan future consideration should be given to alternative methods of LAI retrieval in woodlands. Hemispherical photography has been demonstrated to provide good estimates of LAI regardless of illumination conditions and provides the opportunity to remove the influence of woody biomass (using image processing techniques).

4.8 Conclusions

MTCI was validated with ground chlorophyll content for a woodland area in Southern England, adopting the validation method similar to that employed in the ESA VALERI campaign; employing high resolution imagery to produce a transfer function between MTCI and canopy chlorophyll content. Ground chlorophyll concentration and LAI data were obtained for 31 ISU (20 m x 20 m) and these, in conjunction with CASI-2 data were used to derive a high spatial resolution chlorophyll content map. There was a strong correlation between CASI MTCI and chlorophyll content for each sampling plot; with an overall R^2 of 0.72 (0.78 for deciduous plots and 0.68 for coniferous). The MTCI

Chapter 4. Multi-scale analysis and validation of the MTCI

was therefore proved successful in estimating total chlorophyll content for woodland environments.

At both the New Forest and Brooms Barn validation sites, the main variability in chlorophyll content between ISUs was due to the variations in LAI, as chlorophyll concentration between species was found to be relatively consistent. The strong correlation between MTCI and chlorophyll content suggests that the change in canopy reflectance due to variation in LAI had little effect on the MTCI.

The chlorophyll map was aggregated to the spatial resolution of MERIS and then related to MERIS MTCI. The positive relationship between chlorophyll content and MTCI was weakened to R^2 0.57. Although results were promising and align with earlier studies, the effect of land cover type was not considered. LAI was potentially over-estimated by the use of the Delta-T Sunscan instrument in some areas and these alone introduced a large degree of variability into the MTCI – chlorophyll content relationship.

Direct chlorophyll content – ‘full resolution’ MTCI relationship was investigated at the Brooms Barn study site, Suffolk. The Brooms Barn site is an agricultural area in Eastern England, growing a variety of crops. The field collection of chlorophyll content was timed to permit a wide range of LAI, so that the effects of surface reflectance could be assessed. The presence of immature crop canopies, with very low LAI, significantly weakened the MTCI – chlorophyll content relationship. In such cases MTCI values were related to the optical properties of bare soils, and, therefore, it was very difficult to interpret this index at low LAI. Removing those areas with an $LAI \leq 0.3$ greatly improved the MTCI - chlorophyll relationship ($R^2=0.71$). A linear relationship was observed, indicating that variations in canopy structure between crop types was not a significant factor in estimating chlorophyll content in crops using the MTCI.

**CHAPTER 5: MTCI AS A TOOL TO MONITOR
PHENOLOGICAL CHANGE**

Chapter 5

5.1 Introduction

5.1.1 Vegetation phenology and productivity

Natural vegetation is finely tuned to the seasonality of the environment; therefore variations in seasonal temperature are likely to influence activity. There is mounting evidence to suggest that climate change will have many impacts on terrestrial ecosystems (Nigh, 2006); including changes in ecosystem productivity, shifts in the distribution of species (including migration of the tree line towards the polar regions) and variation in the natural timing of phenological phases.

Interest in terrestrial ecosystem phenology has been driven, in part, by the focus upon ecosystem productivity and atmospheric modelling of carbon dioxide (CO₂) concentration and the role vegetation plays on the timing and magnitude of carbon uptake through photosynthesis. It is widely accepted that global climate change could alter plant phenology significantly because temperature influences the timing of leaf development, both alone and through interaction with other climate variables, such as photoperiod (Cleland *et al.*, 2007). In temperate and higher latitudes, temperature is a limiting factor to vegetation growth, and precipitation and photoperiod have a less pronounced effect on phenology (Chen *et al.*, 2005). The effects of temperature alone on phenology are difficult to isolate, as both leaf development and senescence occur during seasons where air temperature, day length and rainfall, often change at the same time (Rosenthal and Camm, 1997). Therefore, an ability to couple vegetation phenology with climatic variation over large areas is vitally important to predict and manage the impact of climatic change on ecosystems. Higher spring temperatures have been shown to trigger both growth and early leafing in deciduous trees (Sparks *et al.*, 2005; Fisher *et al.*, 2006) and growth in grasslands (Piao *et al.*, 2006), whilst autumnal temperature decrease is one of the triggers for the onset of senescence (Fisher *et al.*, 2007).

Changes in global climate will influence not only the timing of leaf development and senescence but the length of the growing season (Rosenzweig *et al.*, 2008). Analysis of long term phenological trends and meteorological data suggest that enhanced plant growth and the duration of the growing season in northern high latitudes since the

1980s increased as a result of elevated global temperatures (Denman *et al.*, 2007). Therefore, the forecast change in climate is likely to have consequences for ecosystem productivity (Myneni *et al.*, 1997).

Remote sensing studies have indicated that forest primary productivity in the Northern Hemisphere has increased substantially as a direct response to increased growing season temperatures (Myneni *et al.*, 1997; Coa and Woodward, 1998). Likewise, phenological modelling has demonstrated the positive relationship between extended growing season and net carbon fixation in northern latitude deciduous forests.

Phenology remains one of the most difficult processes to parameterise in the terrestrial ecosystem component of climate and biochemical process models due to a relatively poor understanding of the physical processes that initiate leaf growth and senescence (Arora and Boer, 2005). In the light of this, coupling phenological observations with those climatic factors that are believed to play an important role in vegetation growth and seasonal development can help to develop our understanding of vegetation phenology and provide important inputs to climate models.

5.1.2 Remote sensing and phenology

Traditionally, phenological networks rely on volunteers collecting *in situ* observations related to vegetation growth, such as first leaf and leaf fall, to determine change in the physiological development of vegetation. Most of these networks are located in populous regions in Europe and North America and therefore are focused on temperate ecosystems (Cleland *et al.*, 2007). For example long-term point-based observations, by the UK Phenology Network (UKPN), are crucial in developing an understanding of the factors that influence vegetation phenology.

Numerous methods have been used to estimate the onset of spring growth, including modelling and field observation. The most accurate models for the prediction of spring growth accumulate temperatures (after a trigger date) by species and geographical location. However, such models often fail to capture the spring growth detected by satellite sensors, as the underlying mechanisms triggering vegetation

growth are not well understood (Fisher *et al.*, 2007). Research utilising remote sensing shifts the emphasis from point observations, to regional and global scales and provides an opportunity to couple climate variables with the mechanics of vegetation phenology (Zhang *et al.*, 2003). Such a perspective is crucial in analysing, interpreting and predicting the effects of climate variation on vegetated ecosystems.

Satellite sensor observations have been used study of seasonal vegetation dynamics for over thirty years (Reed *et al.*, 1994; Reed and Bradley, 2006). Due to the temporal sampling and synoptic coverage, remote sensing has become increasingly important in studies of phenological change, the forcing effect of climate on ecosystems (Petorelli *et al.*, 2005) and vegetation dynamics at regional to global scales (Cleland *et al.*, 2007). Vegetation indices (e.g., NDVI) that are correlated with green leaf area and total green biomass have been the most popular method for inferring vegetation phenology from remote sensing platforms (Asrar *et al.*, 1989). Until the turn of the millennium, AVHRR provided the only source of global data for this purpose (due to temporal coverage and spatial resolution). However, because AVHRR was not designed for land applications, these data are not well suited for vegetation monitoring purposes. Because of the lack of precise calibration, poor geometric registration, and difficulties involved in cloud screening, AVHRR NDVI data contain high levels of noise (Zhang *et al.*, 2006). Saturation at relatively low levels of biomass will also mean that the NDVI is limited as a tool to monitor phenology (Zarco – Tajada *et al.*, 2001). In recent years a new generation of remote sensing data sources have become available that greatly improve the potential to identify changes in ecosystem phenology (Zhang *et al.*, 2003). In particular, MODIS, at spatial resolutions of 250 m, 500 m and 1 km globally, has provided data for the study of ecosystem dynamics due to greatly improved geometric, radiometric properties and atmospheric correction when compared with AVHRR. Similarly, MERIS, with spatial resolutions of 300 m and 1 km globally, offers great potential to monitor global vegetation dynamics.

Satellite sensor records of phenology provide an important opportunity to develop and test ground-based phenological models. Despite active research in satellite sensor based phenological studies and the availability of data, there have been few studies to parameterise simple models using remotely sensed phenological time series and surface meteorological data (Fisher *et al.*, 2007).

5.1.3 Vegetation phenology

Field-based ecological studies have demonstrated that vegetation phenology tends to follow relatively well-defined temporal patterns. The annual growth cycle of vegetation is characterised by phenological transition phases, where vegetation growth enters a distinct stage (Figure 5.1). For example, in deciduous vegetation and many crops, leaf emergence tends to be followed by a period of rapid growth, followed by a relatively stable period of maximum leaf area. The transition to senescence and dormancy follows a similar pattern in reverse.

Such transition phases are (adapted from Reed *et al.*, 2003):

1. Greenup, the beginning of measurable photosynthetic activity.
2. Maturity, where photosynthetic potential is maximised.
3. Senescence, where photosynthetic activity rapidly decreases.
4. Dormancy, or end of growing season, where photosynthetic activity is minimised.

Length of growing season is the period when photosynthetic activity occurs.

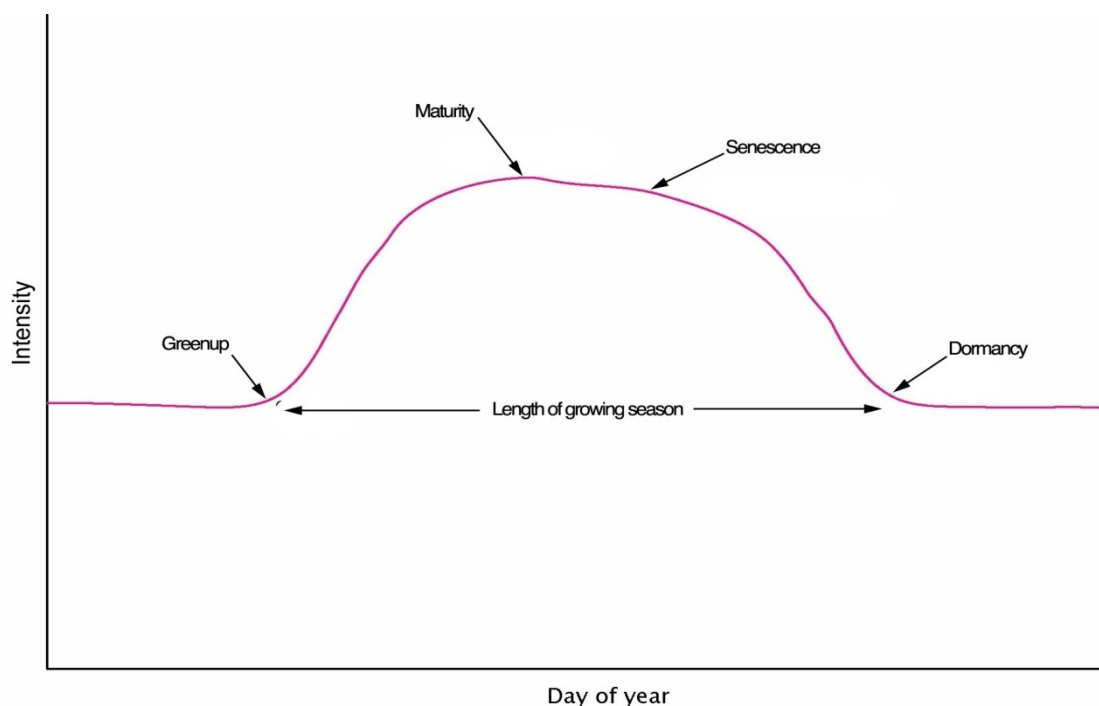


Figure 5.1. Field and satellite sensor studies have demonstrated that vegetation growth exhibits distinct temporal trends. For illustrative purposes, intensity has been labelled on the Y-axis. However, as the phenological profile is related to leaf development and associated chlorophyll content, MTCI can be substituted for intensity.

5.1.4 Determining phenological phases using remote sensing

The potential of remote sensing to estimate phenological transition phases and, using time series data, identify the dates when phenological change occurred will provide information on the effect of climate change on vegetation (Zhang *et al.*, 2003). There is a need to remove noise from the remotely sensed time series while preserving the phenological content. Research into the smoothing of temporal data has used numerous statistical approaches, including amongst others Gaussian filtering, Median filters, splines and inverse Discrete Fourier Transformation. However, inter-comparison between smoothing techniques has shown that the smoothing method does not lead to significant variation in the day of year estimates in phenological transition dates (White *et al.*, 2009). Much of the variability is therefore associated with the method employed to estimate those transition dates.

Various analytical methods have been employed on smoothed temporal data to determine phenological transition dates. The identification of thresholds identifies a pre-defined reference value for extracting information relating to phenological transition dates, e.g., the start or end of the growing season. White *et al.* (1997) used an NDVI threshold of 0.5 of seasonal amplitude as measured from the start of year minima, which defines the period between canopy dormancy and maturity. Although suitable for determining inter-annual variability for a single location, such approaches are not transferable to other locations with differing vegetation types, as the position of the threshold does not relate to an observable ground based phenomena and lacks physical meaning (Fisher *et al.*, 2006).

The inflection point method detects the points (dates) with maximum curvature in a time series dataset (Zhang *et al.*, 2003). The point where the rate of curvature is maximal indicates the occurrence of phenological phases. For example, the start of the growing season is defined as the point in the time series where the rate of change becomes positive from local null values (Zhang *et al.*, 2006). This method has the advantage of being transferable, as well as identifying multiple or complex growing seasons (e.g., in mixed arable agricultural areas) (Zhang *et al.*, 2003). However, the inflection point method is sensitive to the addition of noise in sparse time series.

5.1.5 The relationship between MTCI and phenology

Vegetation growth cycles can be characterised through changes in chlorophyll concentration and leaf area index, which determine chlorophyll content (Curran *et al.*, 2007). The start of vegetation growth (i.e., greenup) will lead to a rapid increase in either or both chlorophyll concentration and LAI (species dependant), therefore increasing foliar chlorophyll content. Similarly, autumnal senescence, and the associated breakdown in photosynthetic pigments, reduces leaf chlorophyll content. The ability of a vegetation index to monitor phenological change is reliant on its sensitivity to changes in LAI and chlorophyll concentration alike.

Spectroscopy on fresh deciduous leaves during the transition from late summer to autumn senescence has shown a significant shift in REP to shorter wavelengths (Cipour *et al.*, 2008), whilst numerous vegetation indices, including NDVI, only exhibit a slight decrease. As discussed in previous chapters, the REP is correlated strongly to the content of foliar photosynthetic pigments (Carter and Spiering, 2002) and can be used to indicate the onset of senescence before structural changes (e.g., in LAI) are evident (Miller *et al.*, 1991; Davids and Tyler, 2003). As the MTCI is designed to exploit the spectral reflectance in red edge wavelengths, the MTCI should be sensitive to the early decrease in chlorophyll content at senescence. Therefore, it is expected that estimating growing season length using the MTCI will yield different results to EVI or NDVI, which are primarily sensitive to variation in LAI.

5.2 Chapter aims

A goal of global change research is to quantify the influence of a changing climate (i.e., elevated temperature) on vegetation phenology (Cleland *et al.*, 2007). The aim of this research is to examine inter-annual in variability woodland phenology and investigate the abiotic factors that drive this variability. This research will develop our understanding of woodland phenological variability through coupling the MTCI time-series to meteorological observations of temperature and precipitation. This in turn will develop our understanding of the link between estimated foliar chlorophyll content and climatic variation.

The MERIS archive allows continual phenological observations to be made from the start of the 2003 growing season to date. The analysis of the temporal variability of

MTCI to date will provide an insight into the possible effects of predicted climate variation on phenology in terrestrial ecosystems located in mid latitudes, where temperature can be a limiting factor to vegetation growth.

5.3 The study areas

5.3.1 The New Forest

This chapter focuses on the phenological variability of study areas within the New Forest National Park. A full description of the study area can be found in Chapter 4, section 4.2.

Land use practices and vegetation heterogeneity at the pixel level (1 km² ‘reduced resolution’ of the MERIS sensor) meant that study areas were composed of a number of species, therefore study areas were selected according to landcover type. Woodland study areas consisted of both deciduous and coniferous species and their understory vegetation. The distribution of grasses and heath vegetation was also variable at the MERIS ‘reduced resolution’ pixelscale and so defined another class (Figure 5.3).

The phenological profile from the study areas will be an aggregated response of the species present within a given area. Field surveys were used to determine the species in each study area and their percentage cover (Figure 5.2); Table 5.1a for woodland study areas, and table 5.1b for grass and heathland study areas.

Field surveys revealed four woodland inclosures were sufficiently large and covered an area greater than one reduced resolution MERIS pixel (Figure 5.4). Such inclosures were dominated by either coniferous or deciduous species, whilst the presence of other cover types was minimal (below 15% threshold). These largely homogeneous inclosures were used to estimate the contribution that coniferous and deciduous species made to the aggregated phenological profiles of individual study areas in the New Forest.



Figure 5.2. Photographs illustrating the species composition at four of study areas in the New forest. Deciduous tree species and understory vegetation typical of the Deny Wood inclosure (a), coniferous inclosure at Bolderwood (b). The mixed grass and heathland study area of Ridley Plain (c). The local distribution of grasses and heather at Picket plain study area (d) is typical of the species composition and distribution found in the grass and heathland study sites in the New Forest.

Chapter 5. MTCI as a tool to monitor phenological change

| Woodland study areas | | | | | | | |
|----------------------|---|----------------------|------------------------|-------------------------------------|---|--|---|
| Area | Area name | Area km ² | Number of MERIS pixels | Co-ordinates (WGS) | Dominant cover type | Approximated species composition (% cover) | Presence of homogenous cover type within study area (>1km ²) |
| 1 | Island Thorns and Amberwood Inclosures | 3.1 | 1 | 1° 43' 43.85" W 50° 52' 37.83" N | Mixed deciduous and coniferous woodland | Oak, birch, beech, sweet chestnut 50% Coniferous sp. Scots pine, Corsican pine, Douglas fir 50% | No |
| 2 | Red Shoot Wood and Roe Inclosure | 2.7 | 1 | 1° 41' 47.71" W 50° 55' 34.05" N | Mixed deciduous and coniferous woodland | Oak, birch, beech, sweet chestnut 60% Coniferous sp. Scots pine, Corsican pine, Douglas fir 40% | No |
| 3 | Church place and Longdown Inclosure | 3.28 | 2 | 1° 30' 16.78" W 50° 52' 48.09" N | Coniferous woodland | Corsican pine, scots pine, sitka spruce 90% Deciduous sp. Birch 10% | Yes - Coniferous area |
| 4 | Denny wood, Park Ground Inclosure and Kings Hat | 9.1 | 7 | 1° 33' 13.05" W 50° 50' 44.1" N | Mixed deciduous and coniferous woodland | Oak, birch, beech, sweet chestnut 60% Coniferous sp. scots pine, Corsican pine, Douglas fir 40% | Yes – 2 deciduous areas Oak, birch, beech, sweet chestnut 80% Coniferous sp. Scots pine, Corsican pine, Douglas fir 20% |
| 5 | Shave Green Inclosure | 2.3 | 1 | 1° 35' 19.21" W 50° 54' 38.3" N | Mixed deciduous and coniferous woodland | Oak, birch, beech, 40% Coniferous sp. Scots pine, Corsican pine 60% | No |
| 6 | Bolderwood | 5.1 | 3 | 1° 38' 19.15" W 50° 52' 46.3" N | Mixed deciduous and coniferous woodland | Oak, birch, beech, 30% Coniferous sp. Scots pine, Corsican pine 70% | Yes – Coniferous area Scots pine, Corsican pine, Douglas fir, sitka spruce 90% Deciduous sp. Birch, oak 10% |

Table 5.1a. Location and composition of woodland study areas within the New Forest

| Grass and heathland study areas | | | | | | | |
|---------------------------------|---------------------------------|----------------------|------------------------|---|---------------------|--|--|
| Area | Area name | Area km ² | Number of MERIS pixels | Co-ordinates (WGS) | Dominant cover type | Approximated species composition (% cover) | Presence of homogenous cover type within study area (>1km ²) |
| 7 | Yew Tree Heath and Black Down | 4.7 | 4 | 1 ⁰ 28' 48.35" W 50 ⁰ 51' 33.81" N | Grass and heathland | Heathers 60%, grasses 35% and bracken 5% | No |
| 8 | White Moor | 2.6 | 2 | 1 ⁰ 32' 52.4" W 50 ⁰ 52' 14.5" N | Grass and heathland | Heathers 40%, grasses and bracken 60% | No |
| 9 | Chibden Bottom and Great Bottom | 3.7 | 2 | 1 ⁰ 44' 42.2" W 50 ⁰ 53' 44.3" N | Grass and heathland | Heathers 60%, grasses and bracken 40% | No |
| 10 | Ridley Plain | 2.2 | 1 | 1 ⁰ 41' 59.5" W 50 ⁰ 51' 42.95" N | Grass and heathland | Heathers 40%, grasses 50%, bracken and gorse 10% | No |
| 11 | Picket Plain | 2.8 | 2 | 1 ⁰ 43' 27.4" W 50 ⁰ 50' 43.4" N | Grass and heathland | Heathers 40%, grasses 55% and bracken 5% | No |

Table 5.1b. Locations and estimated composition of grass and heathland study areas within the New Forest.

5.3.2 Ancillary study areas

Ancillary study areas were located in Cornwall and Kent in Southern England (Table 5.2). Sites were selected according to three criteria; relatively flat (to minimise topographical effects), near homogeneous vegetation cover and close (within 25km) to a meteorological weather station.

The Kings Wood study area (0° 54'52.0" E, 51° 13'11.4" N) was selected due to the similarities in species composition with the woodland areas in the New Forest. Kings Wood comprises both ancient deciduous woodland and mixed deciduous and coniferous woodland and covers 7.2km². The main species of tree species include oak, sweet chestnut, corsican pine and Douglas fir. The low-lying heathland found within the boundary of Bodmin Moor (4° 36'72.3" W, 50° 34'14.1" N) is similar to the heath and grassland study areas in the New Forest. This study area comprises open moorland with of coarse grassland, distinct areas of bracken, gorse and wet heathland.

The Kings Wood and Bodmin study areas were used to compare and support those findings made at the New Forest. Coupling the phenology of each study area to local meteorological observations made it possible to determine the extent to which phenology is driven by changes in local climatic variation.

| Study areas | Vegetation type | Area | Co-ordinates (WGS 84) | Number of Full MERIS pixels |
|--------------------------|--------------------------------------|---------------------|-------------------------------|--------------------------------|
| Bodmin Moor, Cornwall | Low lying grass and heathland | 14.0km ² | 4° 36'72.3 W 50° 34'14.1 N | 7 |
| Kings Wood, Kent | Mixed forest and ancient woodland | 7.2km ² | 0° 54'52.02E 51° 13'11.37N | 4 |

Table 5.2. Location, area and vegetation type of the auxiliary study areas.

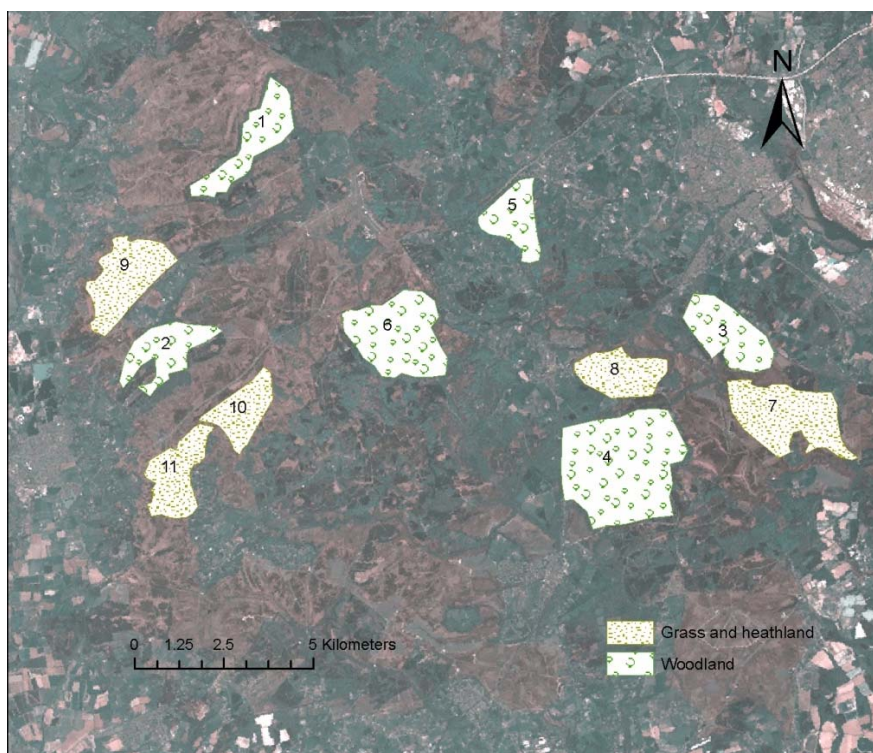


Figure 5.3. Woodland and heath and grassland study areas used in the phenology study in the New Forest, Hampshire, UK. For illustrative purposes, these are superimposed upon a Landsat TM image. Numbers 1-11 relate to area descriptions in tables 2a and 2b.

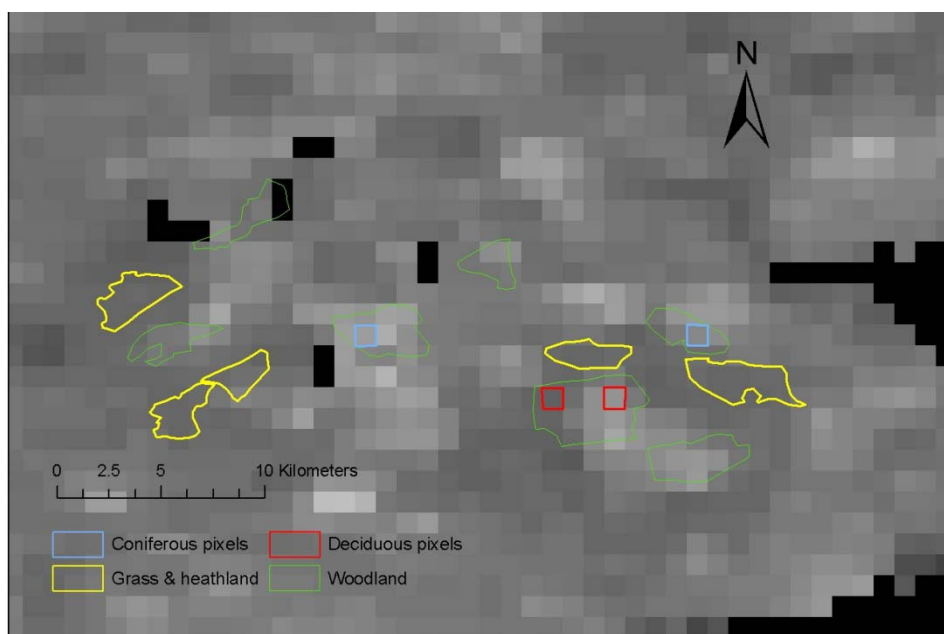


Figure 5.4. Vector layers used to select MTCI pixels located within the boundary of each study area in the New Forest. Also shown are the locations of the homogenous coniferous and deciduous woodland pixels.

5.4 Methods

5.4.1 Study area selection

Study areas had to cover an area greater than one 'reduced resolution' MERIS pixel (consideration was also given to the geolocation accuracy of the MERIS sensor). True colour aerial photographic imagery of the New Forest, acquired during July 2005 and re-sampled to a spatial resolution of 5 metres was used to find representative study areas. These were located on an OS Outdoor Leisure 22 map of the New Forest (1:25,000 scales). This permitted co-ordination of site visits to validate study area size and the vegetation type present at each study area. GPS co-ordinates were taken in the field at the boundaries of homogenous vegetation types (i.e., woodland or grass and heathland areas). GPS co-ordinates from the field visits and high resolution imagery were used to refine study area boundaries in ArcGIS and produce area datasets for both woodland and grass and heathlands.

The locations of ancillary study areas were derived using an alternative method. Digital boundary vector layers produced by English Nature were initially used to determine both cover type and study area size (<http://www.gis.naturalengland.org.uk/>). The shapefile boundary datasets that corresponded to the location of indicator species indicative of given land cover type were used to identify potential study areas. After suitable areas had been identified, Landat TM data were used to verify the location, extent and heterogeneity of the study areas. Only study areas with an area greater than 2x1 km were selected as this corresponded to the ground area covered by two reduced resolution MERIS pixels.

5.4.2 Remotely sensed data

MERIS data

Envisat MERIS 'reduced resolution' (1 km) data were used. Level 2 MERIS imagery was used to produce 8-day MTCI composites for the growing season of 2005 and for January – May 2006. An arithmetic mean composite was produced for each 8-day period during January – December 2005 and January – May 2006 from cloud free MTCI imagery. Flux conserving re-sampling level 3 binning was used to create a composite Level 3 product. The accumulation of EO data samples into geocoded 'bins' is a commonly used method for creating Level 3 weekly and monthly composite products (Lankester *et al.*, 2003). Binning refers to the process of distributing the radiance within Level 2 pixels to a fixed Level 3 grid using a geographic reference system.

These data were complemented with pre-processed 8-day composites for the growing seasons of 2003, 2004, and for May – December 2006, 2007 and 2008 generated by the UK Multi-Mission Product Archive Facility (UK-MM-PAF) at Infoterra Ltd., accessed through NEODC, that has been batch processed using the same method. Infoterra Ltd. minimised cloud contamination through omission of cloud-flagged MERIS data. Together, both sources of MTCI composites provided a complete time series from February 2003 to December 2008. Within ENVI the MTCI composites were stacked chronologically to produce a time series layer stack for each growing season (Figure 5.5).

The vector shapefiles defining the boundaries of the study sites were imported into ENVI software to identify those MTCI pixels located within each chosen study area. Pixels corresponding to each study area were extracted for growing seasons 2003 - 2008. For both woodland and grass and heathland sites at the New Forest, Bodmin and Kings Wood sites pixels values were aggregated (to reduce noise in the phenological profile), producing a single value for each 8-day composite within the growing season.

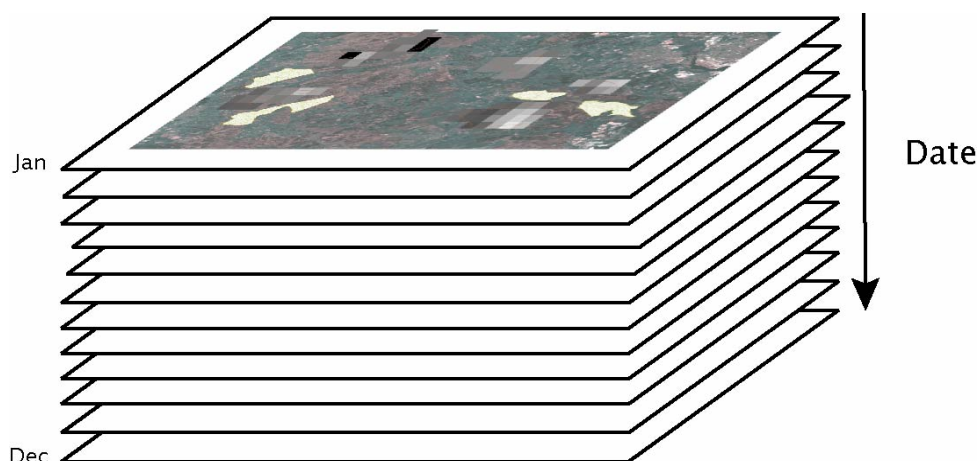


Figure 5.5. Diagrammatic representation of the layer stacked MTCI 8-day composites.

MODIS data

MODIS vegetation (MOD13A2) 16-day product, including both MODIS EVI and NDVI vegetation at 1km spatial resolution, was accessed through the NASA Warehouse Inventory Search Tool (WIST) (accessed at <https://wist.echo.nasa.gov/api/>). MODIS-VI products are made from the level 2 daily MODIS surface reflectance (MOD09), corrected for molecular scattering, ozone absorption, and aerosols. The maximum value composite (MVC) algorithm operates on a per-pixel basis and relies on multiple observations over a 16-day period to generate a composited value (Van Leeuwen *et al.*, 1999; Cheng 2006). This method was suitable for AVHRR NDVI that had not been atmospherically corrected. In the MODIS case, surface anisotropy effects are more pronounced since reflectance values are atmospherically corrected prior to compositing and VI computation. The MVC method, in this case, will dramatically increase the selection of off-nadir pixels, particularly over open canopies, which exhibit higher NDVI values when viewed obliquely. To address this, the MODIS-VI compositing algorithm utilizes the constrained view angle (CV-MVC) criterion, with the VI value at the view zenith angle from the two highest filtered VI values that is closer to the nadir being selected (Huete *et al.*, 2002).

Layer stacks were produced from the 16-day composites for both EVI and NDVI to span the 2006 and 2007 growing seasons. Therefore a direct comparison between the MODIS VI and MTCI can be made.

5.4.3 Auxiliary data

Climate data, local to each study area, were obtained from the Meteorological Office UK weather station network. Weather station observations within 25 km of each study area (Table 5.3), together with the Central England Temperature (CET) series were provided by the Meteorological Office (UK). Average daily temperature (T_{mean}) was calculated as a mean of the daily maximum (T_{max}) and the daily minimum (T_{min}) (Perry and Hollice 2005). Eight day average temperatures were derived from the daily temperature dataset for each weather station to correspond with the temporal format of the MTCI composites.

The long-running CET (<http://badc.nerc.ac.uk/data/cet/>) was used to describe national weather, rather than averaging data from each site. The CET is strongly correlated (with a strong statistical significance where $p < 0.001$) with local station observations throughout England (Croxtton *et al.*, 2006; Sparks, 2006).

| <i>Weather Station</i> | <i>Study area</i> | <i>Proximity</i> |
|------------------------|-------------------|------------------|
| Hurn | New Forest | 12 km |
| St Mawgan | Bodmin Moor | 7 km |
| Manston | Kings Wood | 25 km |

Table 5.3. Location of weather stations in relation to the study areas.

The UK Phenology Network (UKPN), run jointly by the Woodland Trust and the Centre for Ecology and Hydrology (CEH), provides point based phenological ground observations from sites around the UK (<http://www.naturescalendar.org.uk/>). The UKPN records first leaf and leaf fall dates of several indicator species, including the oak, birch and beech that were abundant in the woodland sites in the New Forest study area. For the purpose of this investigation, mean first leaf and leaf fall dates have been calculated for the pre-mentioned species. Data were used to compare and support the phenological trends inferred from the MTCI time series.

5.4.4 Estimating phenological phases from MTCI time series data

Although cloud contamination was minimised by compositing noise was added as a result of both compositing and re-sampling. Data smoothing was used to remove noise in time series data whilst maintaining phenological information.

Harmonic analysis (specifically using Fourier series) has been shown to produce an accurate representation of a single year phenology across a range of land cover (Bradley *et al.*, 2006). In this study, the MTCI phenological profiles were smoothed using Discrete Fourier Transformation (DFT). The DFT method decomposes the complex waveform into individual sinusoids, and omits noise introduced in the compositing procedure (Jakubauskas *et al.*, 2001). Amalgamating the sinusoids inversely using the first five harmonics removes noise from the phenological profile and produces a smoothed MTCI time series (Figure 5.6) (Geerken *et al.*, 2005). This approach has been used successfully to remove noise in the composite data whilst preserving phenological information (Jakubauskas *et al.*, 2001; Dash personal communication). Inverse Fourier Transformation was employed on the MTCI time series data using a MATLAB script.

The inflection point method was used to derive the phenological transition dates. Dates were identified using the rate of change in the curvature of the cumulative curve derived from the DFT smoothed data (Figure 5.7). Transition dates correspond to the location in time where the rate of change in the MTCI phenology profile exhibits local maxima or minima (Zhang *et al.*, 2003).

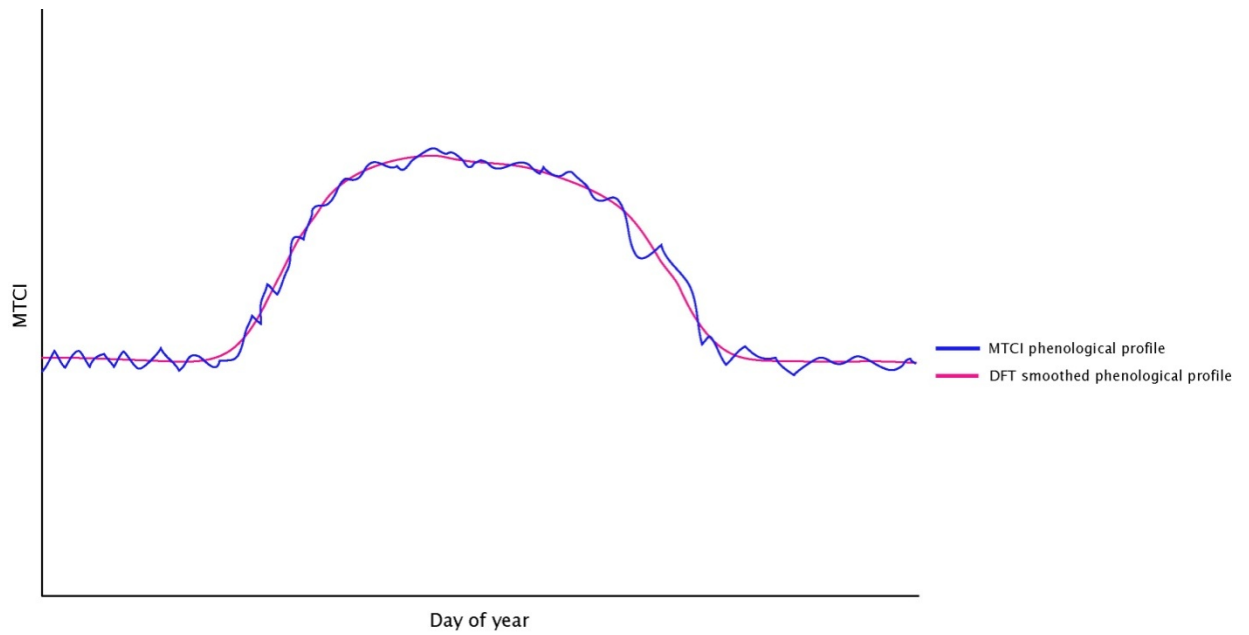


Figure 5.6. Discrete Fourier Transformation (DFT) was used to remove noise (smooth) from the MTCI phenological profile.

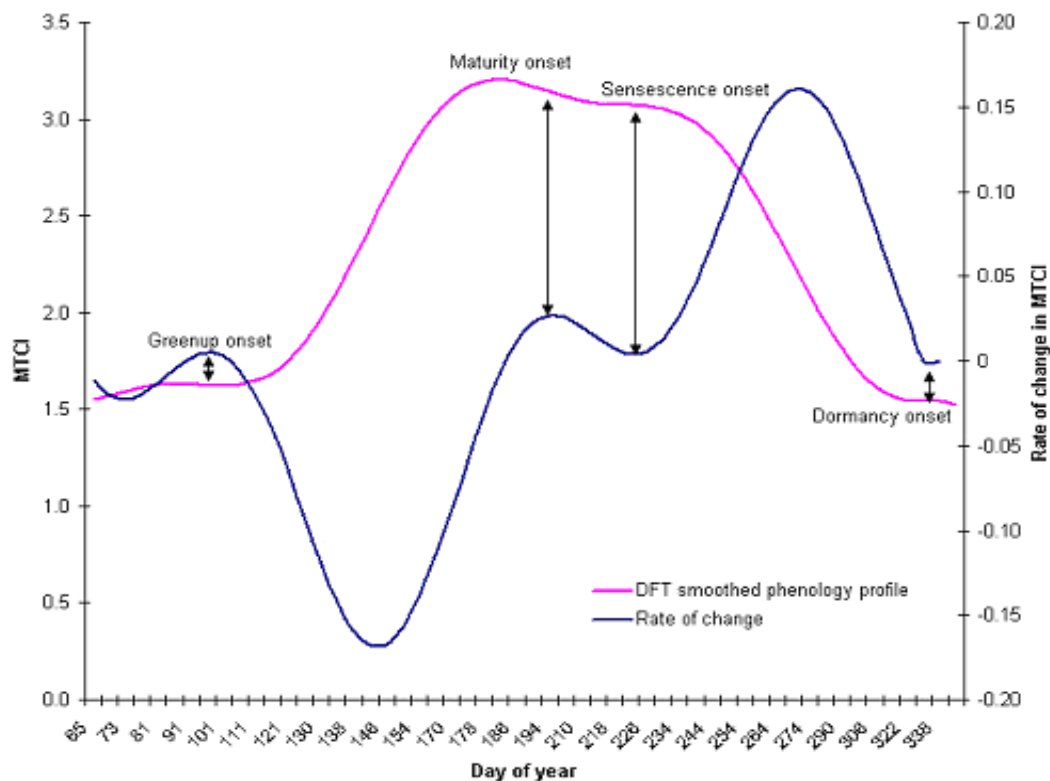


Figure 5.7. Phenology transition dates were determined using maximum and minimum values in the rate of change of the (DFT smoothed) MTCI phenology profile.

5.4.5 Predicting MTCI using mean temperature observations

Understanding the physiological response of vegetation to predicted climatic change would aid in our knowledge of potential changes in ecosystem productivity and terrestrial carbon budgets.

Prediction of MTCI values for the 2008 growing season used a regression model based on the relationship between MTCI and 8 day mean local temperature for each study area for the growing seasons 2003 – 2007. Estimates made using this regression model were compared with the 8-day MTCI composites for the 2008 growing season. This approach offers an insight into the potential changes that could arise in ecosystem phenology (and productivity) as a result of climate-induced changes in canopy chlorophyll content.

5.5 Results and Discussion

5.5.1 Woodlands

The presence of large (greater than one ‘reduced resolution’ MERIS pixel) woodland inclosures enabled phenological investigation of the estimated chlorophyll content of deciduous and coniferous canopies. Figure 5.8 shows the phenological profiles of deciduous and coniferous canopies for the 2003 – 2007 growing season. Coniferous species maintained a minimum greenness during the winter and did not shed all of their needles each year as deciduous species did (Fisher *et al.*, 2006) accounting for the higher MTCI values during the early and later growing seasons. Coniferous species have been shown not to exhibit large seasonal variation in photosynthetic biomass (Kimball *et al.*, 2004), so observed changes in estimated coniferous chlorophyll content was due to changes in chlorophyll concentration rather than LAI. The phenological profiles show that the timing and rate of greenup was consistent between coniferous and deciduous species. This suggests that leaf development in deciduous species and bud burst, a period where new needles emerge in some coniferous species (Cannell and Smith, 1983), and the associated increase in foliar chlorophyll content in both deciduous and coniferous species is triggered by similar environmental variables. Similarly, the timing of senescence between deciduous and coniferous species is similar, although during the 2004 and 2006 growing seasons the rate of chlorophyll content decrease was less in coniferous stands. At maturity, the deciduous woodland had a greater MTCI compared to coniferous woodland, which

was maintained throughout the peak of the growing season. Generally, coniferous species became dormant later in the growing season in comparison with the deciduous woodland (Figure 5.9).

Satellite sensor phenological studies of woodland stands at moderate to coarse spatial resolution are likely to include both deciduous and coniferous species. Site visits confirm a mixed species assemblage in the New Forest study areas. In this study, canopy dormancy is defined as the date at which coniferous species exhibit minimum estimated chlorophyll content and this date is likely to be after deciduous species have become dormant. In mixed coniferous and deciduous study areas, the presence of coniferous species limits the minimum MTCI value during the winter months as observed in the temporal MTCI profiles, where MTCI values fluctuated between 1.3 – 1.7. The aggregated woodland MTCI temporal profiles revealed a clear seasonal pattern, which was characterised by a trapezoid phenology curve. This general pattern is evident for all six years of data, indicating that the MTCI was a reliable tool for determining the phenological development of the woodland study areas (Figure 5.8). In general terms, the MTCI increased rapidly from mid April, this rapid greenup corresponded to an inferred period of increased foliar chlorophyll content. The curve stabilised during June, followed by a decrease in MTCI from the end of August, marking the onset of the senescence. The MTCI reached a minimum during early winter, denoting canopy dormancy.

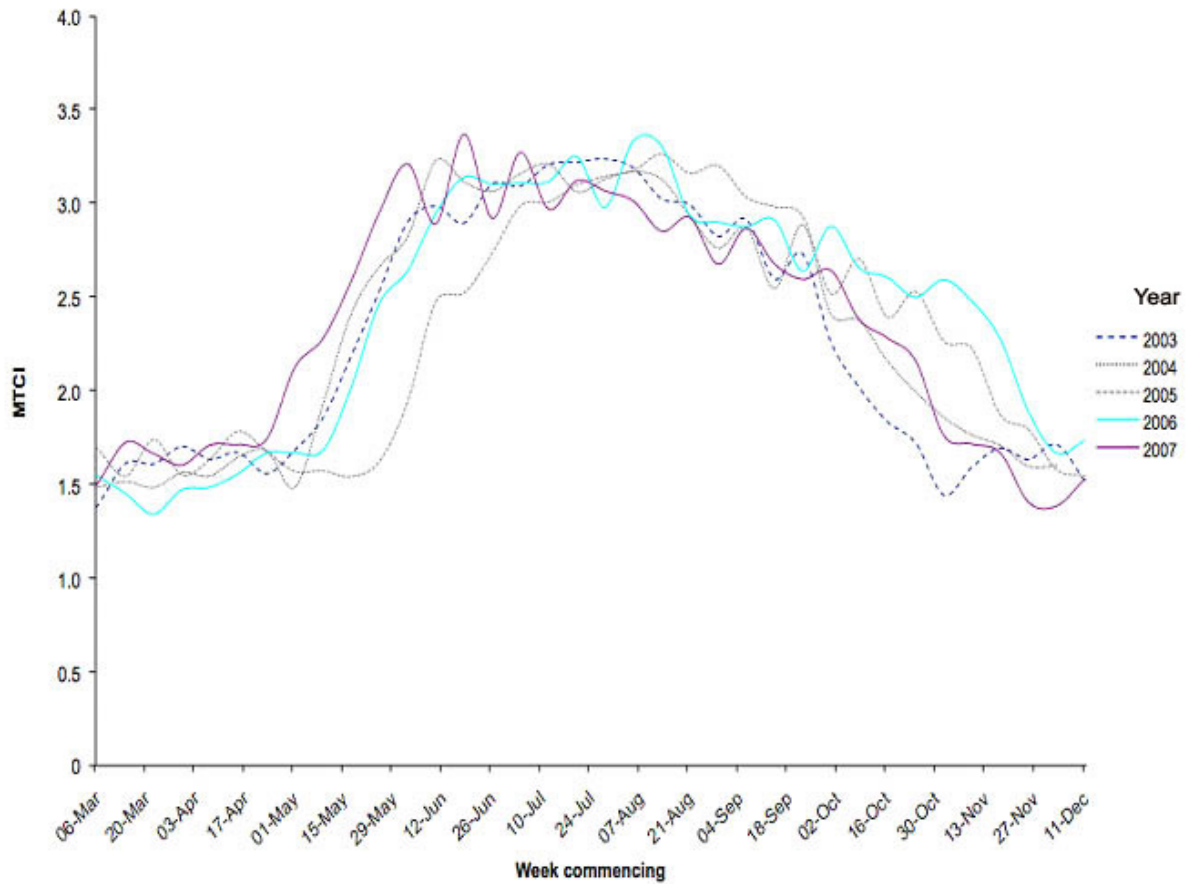


Figure 5.8. Seasonal MTCI phenological profiles for woodland study areas in the New Forest National Park; 2003 - 2007.

Chapter 5. MTCI as a tool to monitor phenological change

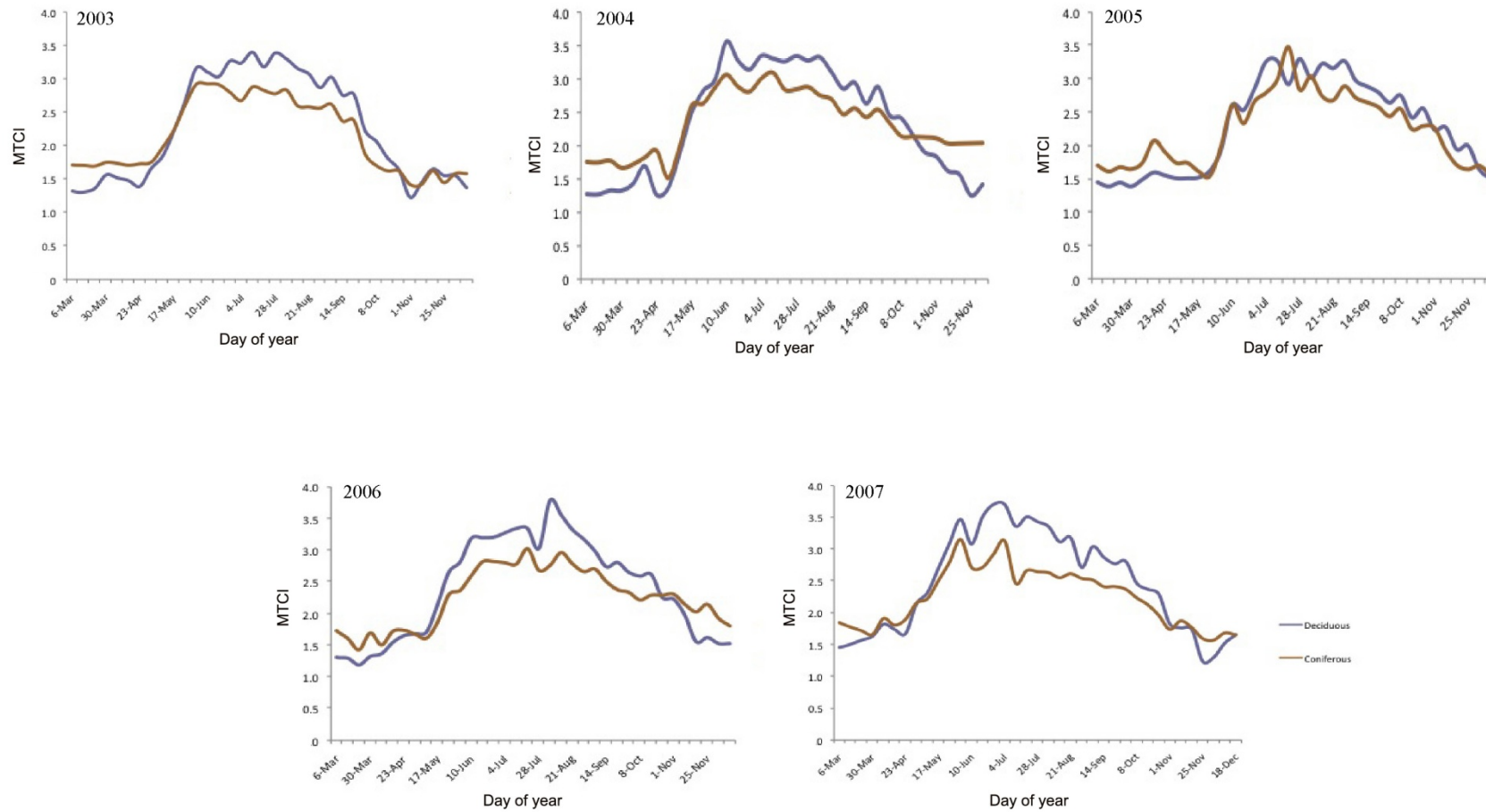


Figure 5.9. Comparison between deciduous and coniferous woodland MTCI profiles in the New Forest study site for growing seasons 2003 - 2007.

5.5.2 Grass and heathlands

MTCI derived grassland phenology exhibited a different phenological profile to that of the woodland sites. Ground based observations made by Kodani *et al.* (2002) support the shape of the convex MTCI phenology profile. The MTCI gradually increased (at a much slower rate than woodland MTCI), stabilised, and then gradually decreased in the autumn (Figure 5.10).

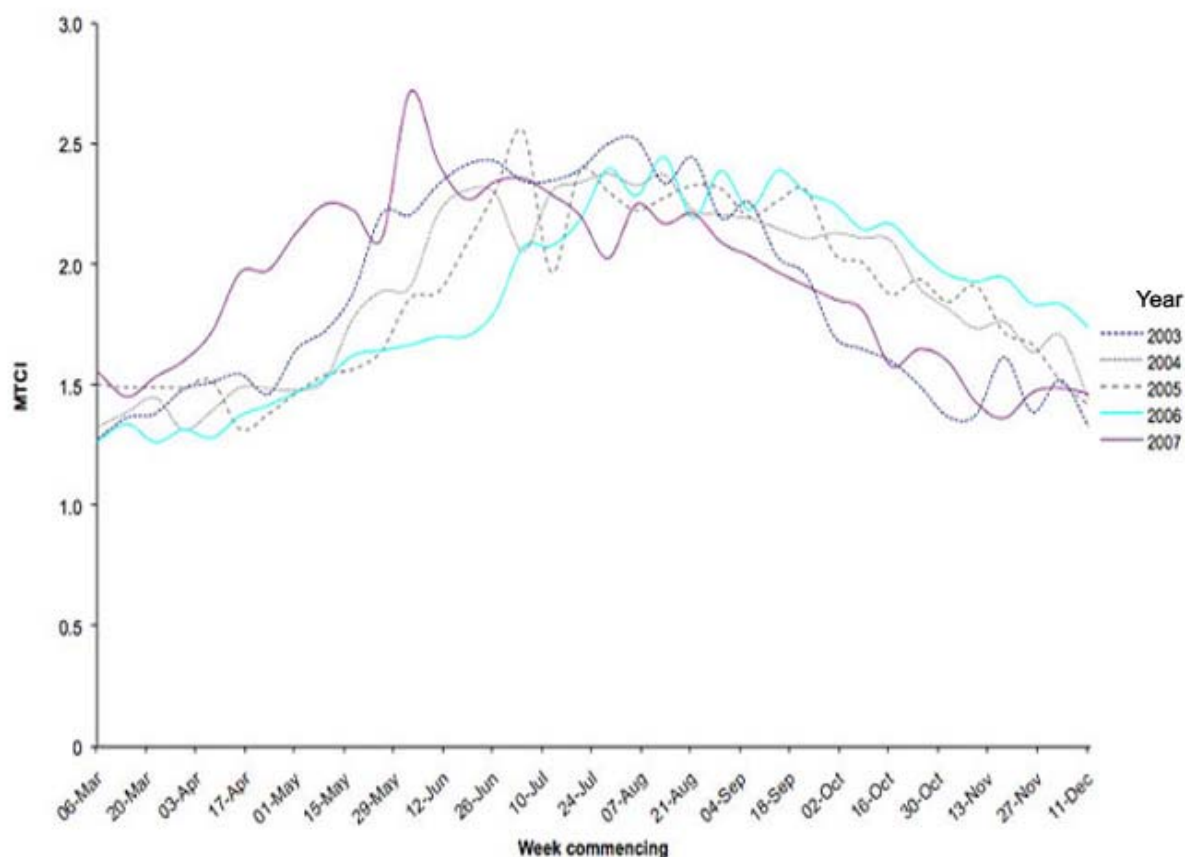


Figure 5.10. Seasonal MTCI phenological profile for heath and grassland sites in the New Forest National Park; 2003 - 2007.

The shape of the phenological profile can be attributed to the growing characteristics of heath and grassland vegetation, where foliar construction and shedding in distinct events at the start and end of the growing season is largely absent. The major phenological trends observed in heath and grassland areas were a gradual greenup, where chlorophyll content increased until maturity. In the absence of leaf fall, chlorophyll concentrations decreased in the grass and heath species during senescence. Therefore, heath and grassland phenology curves exhibited a gradual start and end to the growing seasons.

5.5.3 Accounting for inter-annual variation

This research will couple phenological observations derived utilising the MTCI with temperature observations made by Meteorological Office weather stations. Meteorological data revealed a clear warming trend in the long running CET average, e.g., years 2003 to 2008 (Figure 5.11). During the period 2003 – 2008 there were documented variations from the average expected climate that resulted in changes to vegetation phenology. For example, elevated autumnal temperatures were observed across Northern and Western Europe during the 2006 growing season. The Meteorological Office and the Royal Netherlands Meteorological Institute recorded May to October 2006 as the warmest on record in the UK since 1659. These observed temperatures led to reports of an extended growing season (and thus delayed senescence) (www.eumetsat.int/Home/Main/Media/News, accessed 6th March 2007; BBC News accessed 30th October 2006; Van Oldenborgh, 2006).

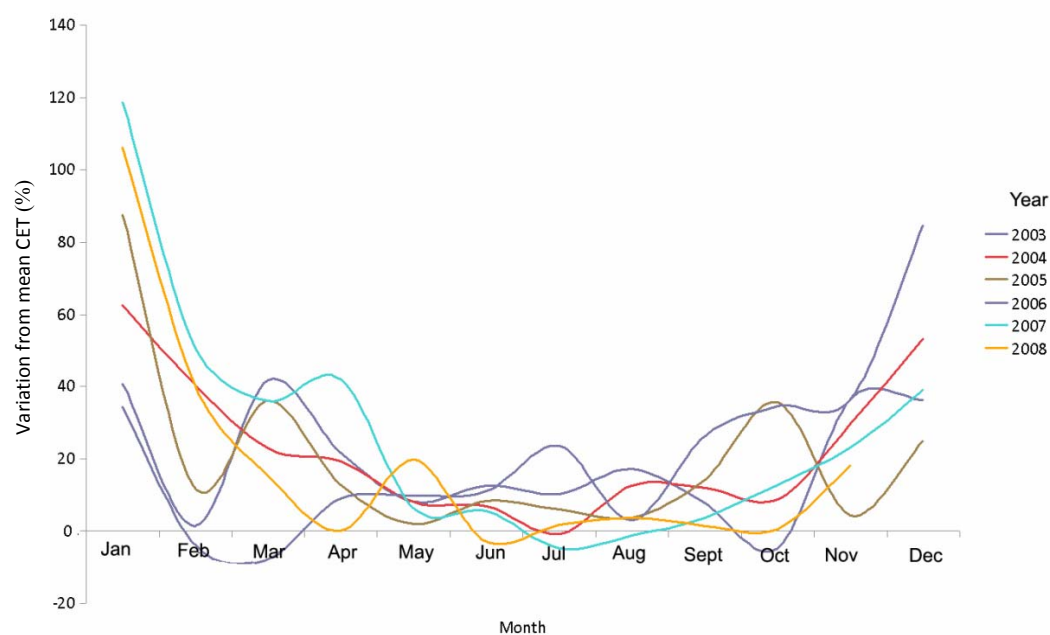


Figure 5.11. Variation between the long term CET (1669-2002) monthly mean temperature and the years 2003-2008. A clear trend of milder winters is apparent as is elevated spring and autumnal temperatures for all years 2003 –2008.

The temporal phenology profile for all sites indicated an increase in MTCI (and thus inferred chlorophyll content) for the autumnal period of 2006 compared to the same period for each of the earlier three years. Late October 2006 MTCI values were comparable with mid September values for the years 2003 and 2004, indicating a delay in vegetation canopy senescence

Both the local T_{mean} and CET T_{mean} data were correlated with MTCI for each study area. A strong positive correlation between local T_{mean} and MTCI was observed for both woodland (Figure 5.12 a) and heath and grassland (Figure 5.12 b) in the New Forest. Coefficient of determination shows a strong positive relationship between T_{mean} local and MTCI for all three woodland study areas (mean R^2 for period 2003 – 2007; Bodmin moor $R^2 = 0.92$, and Kings Wood $R^2 = 0.88$), indicating that the inferred chlorophyll canopy content is correlated strongly with mean temperature. Such a relationship suggests that changes in observed MTCI are a response to temperature rather than the availability of nutrients or water table height. Results indicate that T_{mean} is potentially a limiting factor to chlorophyll content development and therefore productivity, suggesting that water, nutrients, carbon dioxide and light were not limiting the development of foliar chlorophyll content of woodland or heath and grassland species for the years 2003 - 2007.

The relationship between MTCI and CET $_{\text{mean}}$ for the 2006 growing season and also the growing seasons of 2003 - 2005 revealed a marked increase in temperature and MTCI for all study areas. From July – November 2006 the high MTCI values were maintained, indicating a delay in autumnal senescence. During mid-October the mean inferred chlorophyll content for all sites was approximately 54% greater than the average of the previous three years. Figure 5.13 shows a response lag of approximately two weeks between T_{mean} and MTCI response, suggesting that foliar chlorophyll content adjusts, albeit with a time lag, to local climate conditions. The 2006 MTCI profile also reveals a delay in reaching canopy maturity as MTCI values were below average until early July, as a result of lower mean temperatures throughout the early growing season (February – May).

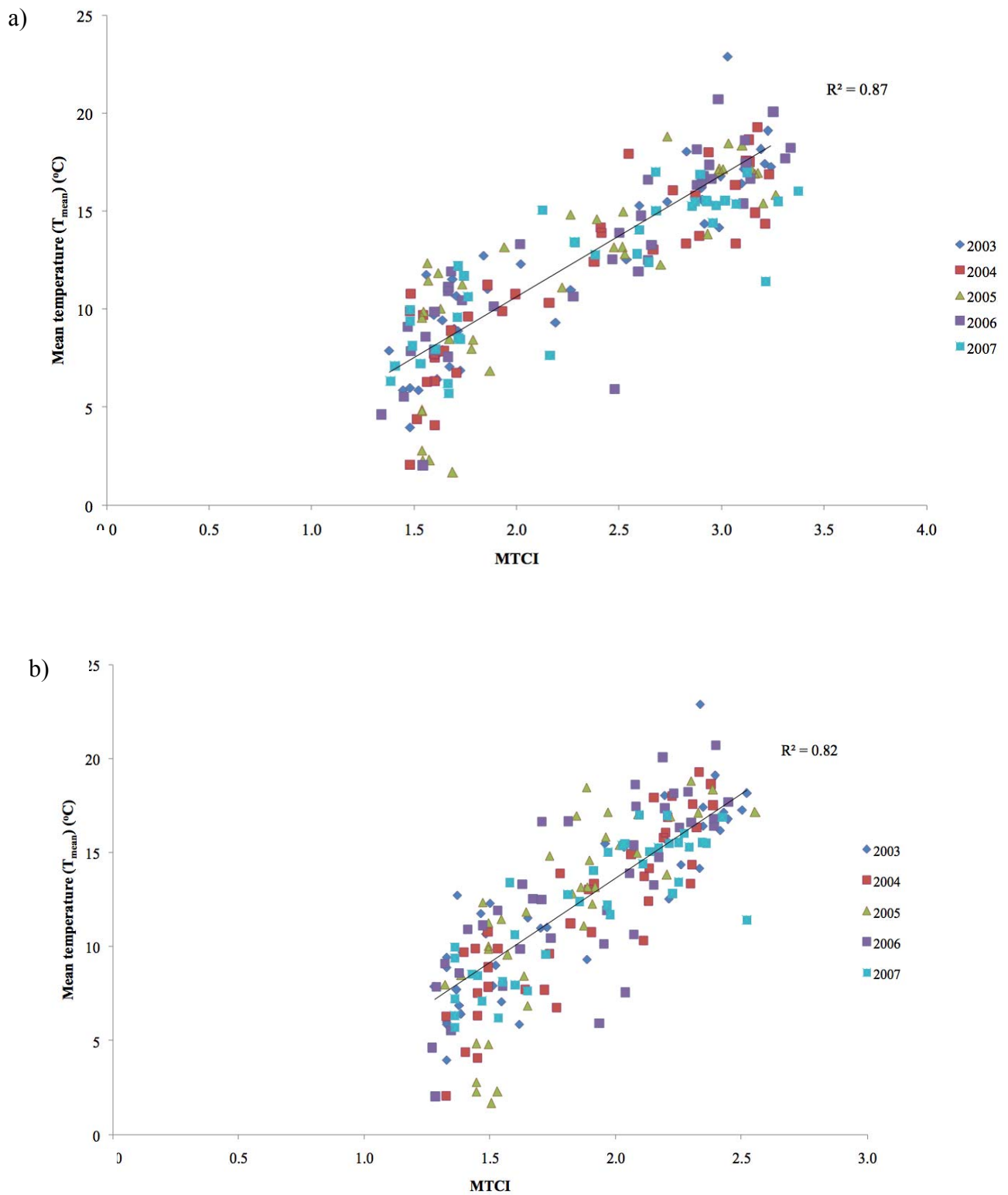


Figure 5.12. Relationship between MTCI and local T_{mean} for woodland and heath and grassland sites, New Forest, using 2003 - 2007 data; woodland sites (a) 2003-2007; grass and heathland sites (b).

Change in temperature has been shown to affect the phenology of woodland species (Deng *et al.*, 2007), leading to earlier spring greenup in woodlands in the mid- and higher latitudes (Menzel *et al.*, 2006). Findings in this chapter support the notion of delayed senescence due to favourable growing conditions; this was particularly evident in the MTCI growing season temporal profile for 2006.

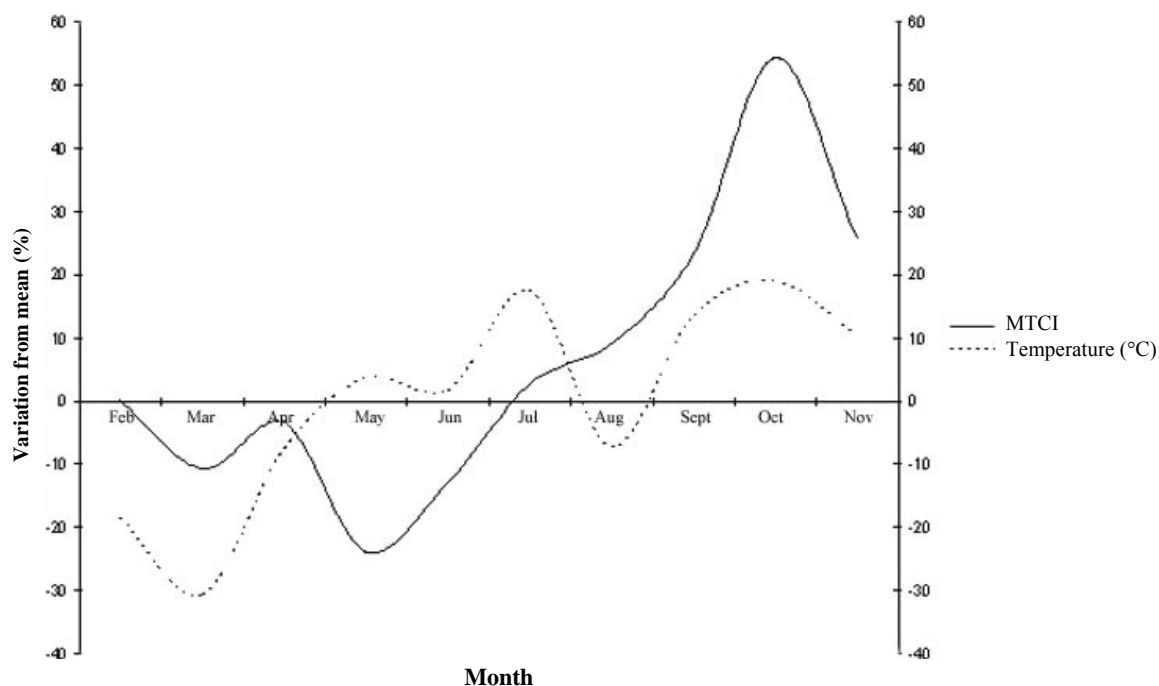


Figure 5.13. Variation in MTCI and mean monthly temperature (CET_{mean}) in 2006 compared to the running average 2003 –2005 and 2007 for both woodland and heath and grassland study areas at all three study areas.

An early greenup was observed in 2007 for both woodland and heath and grassland areas. This coincided with elevated mean temperatures (in relation to 2003 – 2006) at the local weather stations and CET. These findings support the findings of Fisher *et al.* (2006) and Sparks *et al.* (2005) who related increased cumulative temperatures to leaf development of deciduous woodland in temperate latitudes. Bassow and Bazzaz (1998) linked an increase in seasonal temperature with increased photosynthetic rates, as ecosystems modify their photosynthetic capacity in relation to a change in limiting factors through changes in foliar chlorophyll content (Dawson *et al.*, 2003). The MTCI values would suggest that foliar chlorophyll content was higher in early 2007

in comparison with previous years, indicating that higher seasonal temperatures can, indirectly, increase the photosynthetic potential of the vegetation canopy.

Heath and grasslands exhibit a distinct phenological profile and clear responses to a change in seasonal temperatures. Such change has been observed in temperate grasslands and linked to variations in annual weather patterns (Kammer, 2002). The results suggest early spring growth, as inferred by increased MTCI, supporting the findings of Yang *et al.* (1998) who suggested that early spring warming leads to enhanced photosynthetic activity and growth rates.

5.5.4 Variation in phenological transition dates

Changes in temperature corresponded to change in the derived phenological transition dates in the New Forest study areas. Figure 5.14 shows the inter-annual variability in estimated phenological transition dates derived from the inflection point methodology using MTCI temporal data from woodland study areas. Delayed senescence is shown during the 2006 growing season as a result of climatic variability. Whilst the early spring growth associated with elevated spring 2007 temperatures is indicated by an earlier estimated greenup and maturity date.

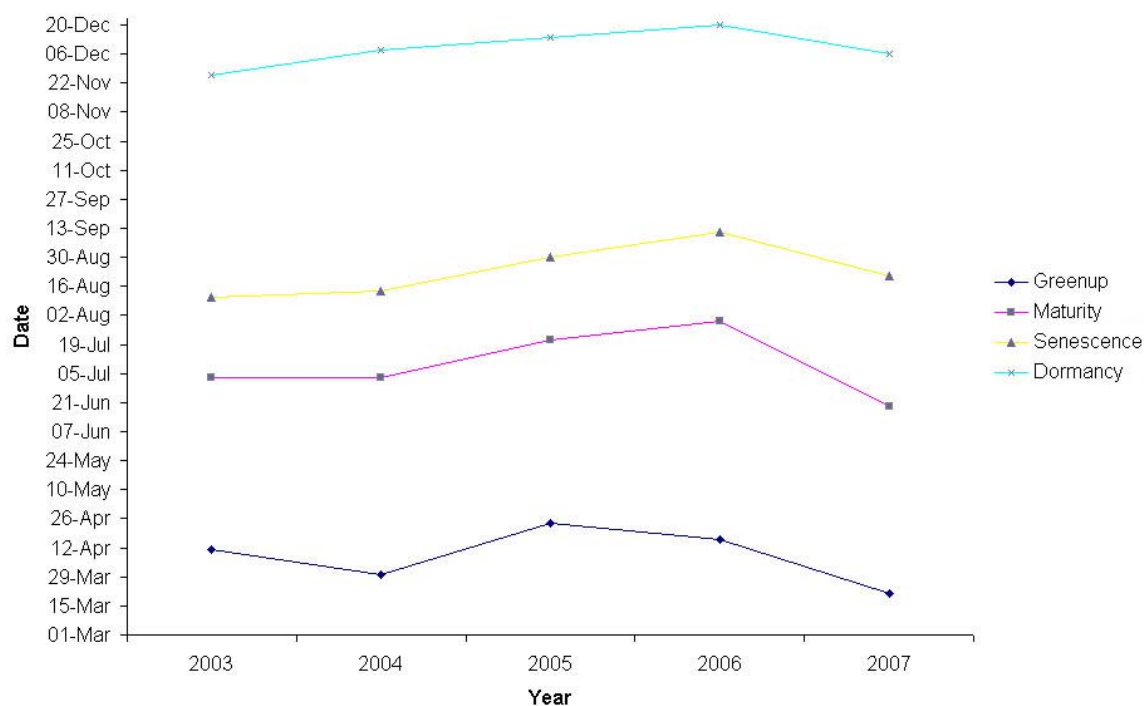


Figure 5.14. Variation in key phenological transition dates through the growing season as determined by the rate of change in curvature in the MTCI profile for the New Forest woodland study areas.

| Phenology markers | Year | | | | |
|----------------------|---------------------------|--------------------------|--------------------------|--------------------------|---------------------------|
| | 2003 | 2004 | 2005 | 2006 | 2007 |
| Greenup | 11 th April | 12 th April | 12 th April | 23 rd April | 11 th April |
| Dormancy | 23 rd November | 2 nd December | 8 th December | 3 rd December | 26 th November |
| Season length (days) | 226 | 234 | 240 | 224 | 229 |

Table 5.4. Phenological transition dates derived from the UK Phenology Network.

UKPN observations use a network of point-based ground observations around the UK to record the first leaf and leaf fall date of several indicator species, including oak, birch and beech. These species are abundant in the woodland sites in the New Forest study area. For the purpose of this investigation, greenup corresponds to the date the first leaf appeared for any of the species listed above. Dormancy relates to latest recorded leaf fall (of any species). Observations by the UKPN (Table 5.4) support the early onset of spring growth as inferred by the 2007 MTCI time series in woodland study areas (Table 5.5). Although such results cannot be used as a direct comparison, due to differences in geographical scale and the presence of coniferous species in the New Forest study area, trends in phenology are apparent and can be linked to seasonal temperature.

Similar trends in phenological transition dates were observed between woodland and grass and heathland study areas (Table 5.6) in the New Forest. Growing season length showed similar trends between years, except the growing season of 2004 for the grass and heathland study area that was shorter than expected. The delay in senescence during the 2006 growing season and the early greenup of 2007 were observed in the phenological transition dates for the grassland study areas.

Chapter 5. MTCI as a tool to monitor phenological change

| Phenology Markers | Year | | | | |
|-------------------------------------|---------------------------|--------------------------|---------------------------|----------------------------|--------------------------|
| | 2003 | 2004 | 2005 | 2006 | 2007 |
| Greenup onset | 11 th April | 30 th March | 24 th April | 16 th April | 21 st March |
| Maturity onset | 3 rd July | 3 rd July | 21 st July | 30 th July | 19 th June |
| Senescence onset | 11 th August | 14 th August | 30 th August | 11 th September | 21 st August |
| Dormancy onset | 26 th November | 8 th December | 14 th December | 20 th December | 6 th December |
| Greenup duration (days) | 83 | 95 | 88 | 105 | 90 |
| Peak growing season duration (days) | 39 | 42 | 40 | 43 | 63 |
| Season length (days) | 229 | 253 | 234 | 248 | 260 |

Table 5.5. Inter-annual variability in phenological transition dates as derived from the MTCI time series for woodland study areas in the New Forest.

Chapter 5. MTCI as a tool to monitor phenological change

| Phenology Markers | Year | | | | |
|-------------------------------------|----------------------------|----------------------------|---------------------------|--------------------------|---------------------------|
| | 2003 | 2004 | 2005 | 2006 | 2007 |
| Greenup onset | 31 st March | 8 th April | 16 th April | 16 th April | 7 th March |
| Maturity onset | 7 th August | 29 th July | 6 th August | 22 nd July | 11 th June |
| Senescence onset | 18 th September | 11 th September | 7 th September | 17 th October | 6 th August |
| Dormancy onset | 10 th November | 10 th November | 4 th December | 4 th December | 18 th November |
| Greenup duration (days) | 129 | 112 | 112 | 97 | 96 |
| Peak growing season duration (days) | 42 | 44 | 32 | 87 | 56 |
| Season length (days) | 224 | 216 | 232 | 232 | 256 |

Table 5.6. Inter-annual variability in phenological transition dates as derived from the MTCI time series for grass and heathland study areas in the New Forest.

5.5.5 Comparison of MTCI and MOD13 phenological profiles

The Aqua and Terra satellites, hosting the MODIS sensor, provide daily observations of the land surface at moderate spatial resolution (250m–1000m). MODIS has been used to monitor vegetation phenology using both the MOD13 validated vegetation indices, i.e., the NDVI and EVI (Xiao *et al.*, 2004, 2005; Zhang *et al.*, 2003, 2006). The majority of satellite sensor phenological investigations utilise the NDVI vegetation index. However, the EVI has been widely used to monitor vegetation phenology due to its insensitivity to background effects. This section will evaluate the MTCI as a tool to estimate phenology in relation to the MOD13 vegetation indices.

MTCI is sensitive to variation in chlorophyll content, whereas the NDVI is principally sensitive to green biomass (LAI), therefore explaining the shape of the phenology curve. NDVI has an operational range of -1 to 1, where values which approach the upper limits correspond to dense vegetation, whereas low values indicate low vegetation densities or non vegetated surfaces (Wulder, 1998). However, in this study the NDVI demonstrates a small amplitude between summer maxima and winter minima compared to the MTCI temporal profile (Figure 5.15 a). Due to mixed species stands in the New Forest, pixels will contain coniferous and deciduous species. Therefore, the small seasonal variation in photosynthetic biomass demonstrated by coniferous areas results in a small change in LAI throughout the growing season (Kimball *et al.*, 2004) compared to deciduous areas. Compared to the NDVI, the MTCI is more suited to determine phenological change in mixed tree pixels as total chlorophyll content will be more variable between seasons than LAI. The NDVI will therefore respond to the aggregated change in seasonal LAI between coniferous and deciduous species. The effect of background reflectance will be a function of vegetation phenology and linked directly to foliar development of deciduous species. Therefore, during the period, late autumn – early spring, which coincides with ‘leaf off’ of deciduous tree species, the positive NDVI values are the result of background reflectance (including leaf litter, understory vegetation and soil) as well as the presence of coniferous species within the study area.

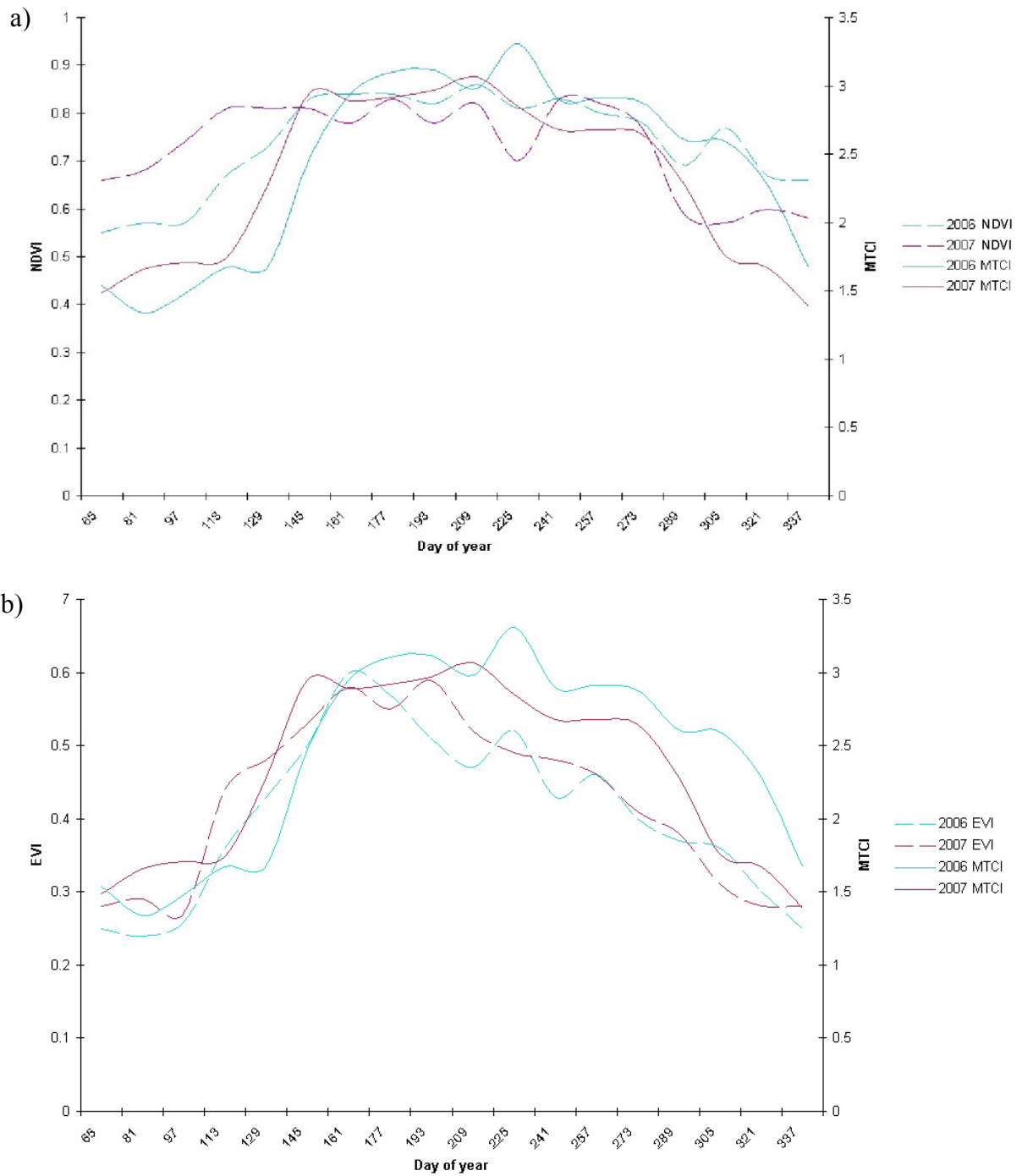


Figure 5.15. Comparison between MTCI and the phenological profiles derived from MODIS NDVI (a), and MODIS EVI (b).

| Growing season | Greenup | Maturity onset | Senescence | End of growing season | VI |
|----------------|------------------------|-----------------------|----------------------------|---------------------------|------|
| 2006 | 22 nd March | 18 th June | 16 th October | 19 th December | NDVI |
| | 7 th April | 18 th June | 29 th August | 19 th December | EVI |
| | 7 th April | 12 th July | 14 th September | 21 st December | MTCI |
| 2007 | 6 th March | 8 th June | 30 th September | 19 th November | NDVI |
| | 14 th March | 10 th June | 29 th August | 3 rd December | EVI |
| | 6 th March | 2 nd June | 13 th August | 3 rd December | MTCI |

Table 5.7. Comparison between estimated transition dates derived from NDVI, EVI and MTCI time series.

Saturation in high biomass ecosystems and during the peak of the growing season where saturation occurs below typical LAI (Zarco-Tajada *et al.*, 2001) limits the use of the NDVI as a tool for phenological monitoring. A number of studies have shown that the NDVI saturates at LAI of 3-4 (Ustin *et al.*, 2001), whilst LAI during peak growing season exceeds this for the study areas (this is confirmed from validation fieldwork of the same study areas completed during July 2007). The MTCI is based upon the relationship between chlorophyll content and REP, both of which have a strong correlation with green biomass (Eitel *et al.*, 2007).

The associated decrease in MTCI from late August 2007 was considerably earlier than the observed senescence observed by the MODIS NDVI time series (Table 5.7). This supports the assumption that chlorophyll content declines prior to a decrease in leaf area, during autumnal senescence (Millar *et al.*, 1991).

Whereas the NDVI is chlorophyll sensitive and responds mostly to the visible or red band variations, the EVI is more sensitive to variation in near-infrared reflectance and therefore responsive to canopy structural variations, including LAI, canopy type, and canopy architecture (Gao *et al.*, 2000).

The EVI temporal profiles reveal earlier senescence when compared with MTCI results, but does not capture the extended 2006 growing season (Figure 5.15b). This opposes the expected trend, which is related to earlier canopy chlorophyll decrease. Similarly, the greenup in the 2007 growing season revealed by the MTCI temporal profile, and supported by UKPN field observations, was also delayed in the EVI temporal profile. The EVI profiles of 2006 and 2007 reveal similar greenup and canopy maturation dates, a trend that was unsupported by the UKPN and MTCI phenology profiles.

EVI and NDVI data from MODIS utilize Maximum Value Composite (MVC) data. The MVC filter (Holben, 1986) is designed to find the highest VI value (and therefore lowest noise) in a fixed time period. The MVC introduces temporal uncertainty when the acquisition period falls within a week- to month-long window (in this instance the compositing period is 16 days). Such uncertainty therefore means that MVC data cannot be used to determine phenological events with an accuracy of a week or two (Fisher *et al.*, 2006).

5.5.6 Predicting MTCI using temperature data

The linear relationship between season mean temperature and MTCI enables the use of a simple regression model to predict MTCI for a given future seasonal temperature. A regression model was used to predict MTCI values for the 2008 growing season from aggregated 8-day mean surface temperatures observations recorded at the Hurn weather station (Figure 5.16). The regression model was derived for both grassland and woodland sites in the New Forest. The fit of this model was tested using actual MTCI data for the 2008 growing season (Figure 5.17a, woodland study area, and Figure 5.17b, grass and heathland).

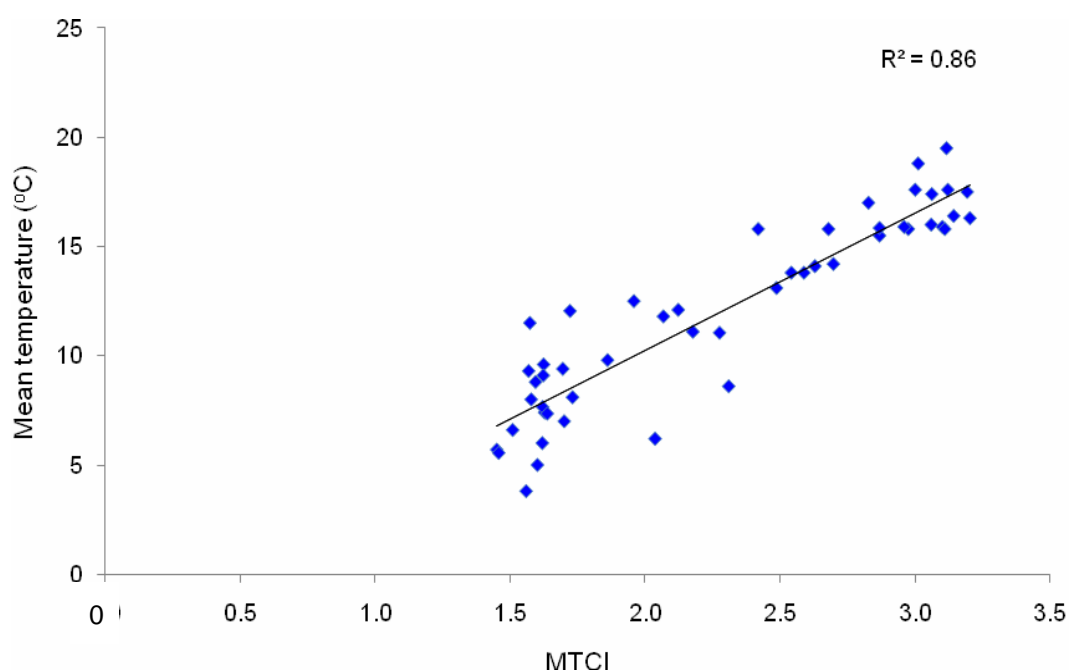


Figure 5.16. The relationship between temperature ($T_{\text{mean local}}$) and MTCI at the New Forest woodland sites, 2003-2007.

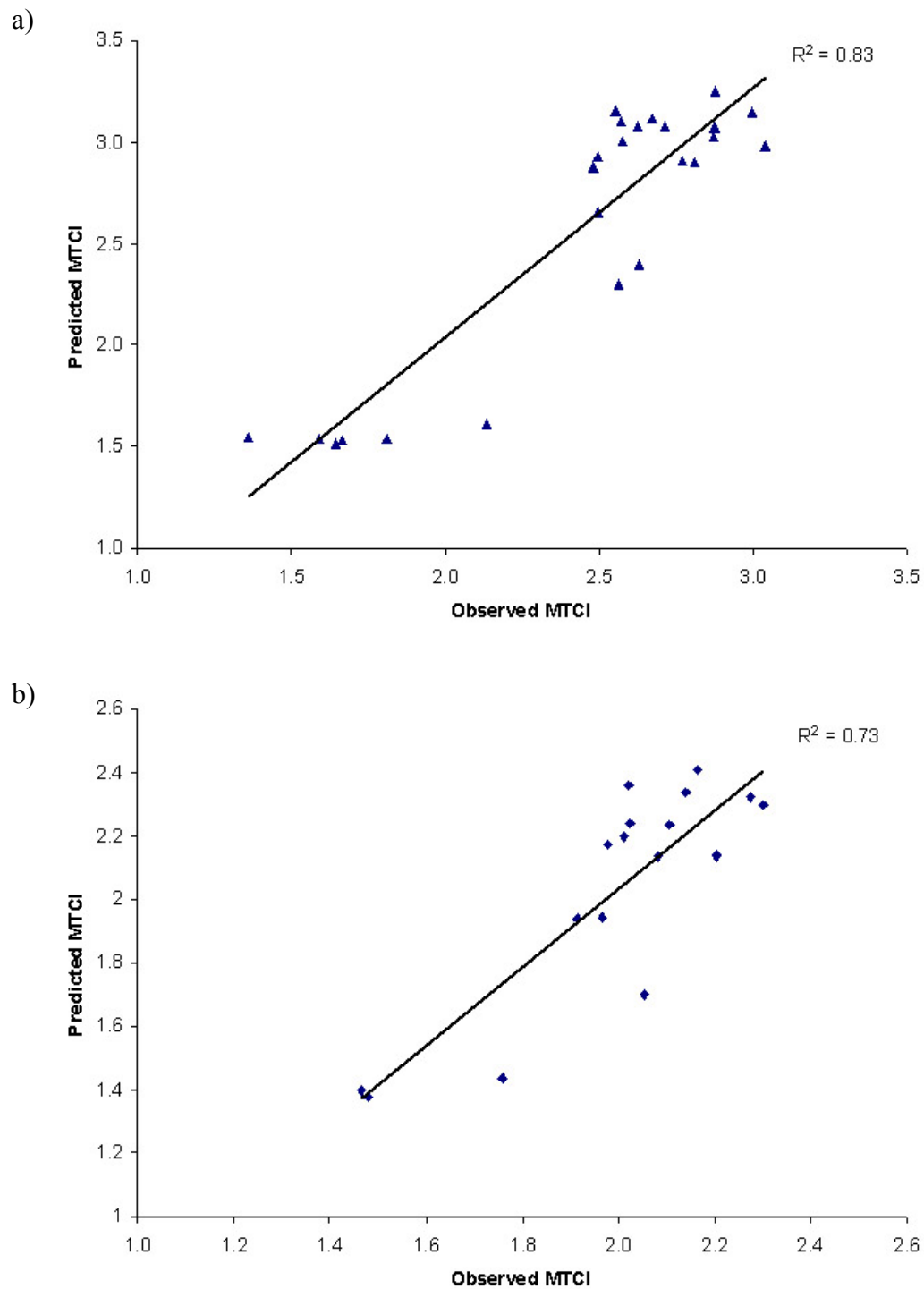


Figure 5.17. Employing the linear relationship observed between MTCI and temperature ($T_{\text{mean local}}$) 2003 – 2007 for all study areas a simple regression was used to predict MTCI based upon observed mean season temperature for the New Forest woodland sites (a) and heath and grassland sites (b).

The New Forest validation campaign established an important quantifiable relationship between MTCI and ground based chlorophyll content. Such findings will have an important bearing upon the observed relationship between MTCI and mean seasonal temperature. They will also enable estimates of canopy chlorophyll content to be made based upon observed and predicted seasonal temperature. The sensitivity of the MTCI to inferred changes in canopy chlorophyll content is an important step in understanding carbon capture and sequestration by foliar chlorophyll as a function of observed temperature in future climate scenarios. However, the linear relationship only holds true for temperature observed in this study. Higher temperatures may result in physiological stress and a subsequent decrease in foliar chlorophyll content and therefore MTCI.

5.6 Conclusions

The MTCI is sensitive to chlorophyll content, which allows first leafing as well as pigment breakdown associated with autumnal senescence to be identified. The MTCI has proven useful for estimating seasonal variation in chlorophyll content of both woodland canopies and heath and grassland. The sensitivity of the MTCI in estimating change in foliar chlorophyll during late summer, earlier than the onset of senescence as observed by changes in plant structure and physiology as determined through field observations (phenology networks) suggests that the MTCI would be useful for assessing canopy productivity and therefore changes in ecosystem productivity as a function of climatic variability.

The observed relationship between MTCI and mean temperature enables the effect of climate variability upon vegetation dynamics to be established. The influence of higher than average autumnal temperatures of 2006 and the early spring of 2007 were clearly evident in the seasonal MTCI profiles (whilst delayed senescence was not evident in the MODIS EVI phenological profile).

A relationship between seasonal mean temperature variability and phenological changes suggest that long-term observations in canopy chlorophyll content can serve as a proxy for mean temperature over time and space. Establishing the relationship between MTCI and mean seasonal temperature permits the modelling of chlorophyll

content based upon future temperature estimates. Although in reality this relationship is complex due to other factors such as photoperiod, or the availability of water and nutrients. At the study areas, the most significant limiting factor is temperature. Determining the relationship between temperature and canopy chlorophyll content, for a given vegetation type or geographical area, provides an insight into the effects of future climatic regimes on phenology, vegetation productivity and vegetation health.

**CHAPTER 6: EXAMINATION OF THE RELATIONSHIP
BETWEEN GROSS PRIMARY PRODUCTIVITY AND
MTCI IN VARIOUS ECOSYSTEMS**

Chapter 6

6.1 Introduction

As was stated in the previous section, global climate change is a topic of vital importance to the scientific community. Atmospheric carbon dioxide concentration has risen by 31% since 1750 (Heinsch *et al.*, 2006), mainly due to the burning of fossil fuels and changing land use practices, including the burning of biomass in tropical forests associated with deforestation (IPCC 2007). The observed increase in atmospheric carbon dioxide concentration has not been as great as predicted once all the identified sources and sinks have been considered. The difference between the observed and expected concentration of atmospheric CO₂ can be partially explained through a process of sequestration by terrestrial vegetation. Terrestrial vegetation is an important sink of carbon dioxide, especially in the mid-latitudes (Turner *et al.*, 2004), driving the research community to investigate the use of terrestrial carbon sinks to offset industrial CO₂ emissions. However, predictions of the ability of terrestrial vegetation to sequester carbon are uncertain and related to global climate variations. The ability to quantify net carbon uptake by terrestrial vegetation is of vital importance. However, such understanding will only be possible at the global scale if we are able to monitor terrestrial vegetation productivity.

Gross primary productivity (GPP) is a measure of photosynthetic activity of terrestrial vegetation and is an important variable in the global carbon cycle as it defines the rate at which an ecosystem will accumulate biomass (Wu *et al.*, 2009). Estimates of gross primary productivity at the regional to global scale are important indicators of ecosystem response to elevated atmospheric carbon dioxide levels and the associated increase in global temperatures. Additionally, GPP is a useful measure of ecosystem health and is relevant in understanding the impact of human activity on ecosystems.

Eddy covariance techniques, employing flux tower measurements, provide the best method of estimating ecosystem GPP. Extensive flux tower networks have been established in North America (Ameriflux and FLUXNET) and Europe (Euroflux). However, this method of deriving GPP only provides CO₂ flux estimates over an area that varies in size and shape according to the physical height of the tower, canopy

physical characteristics and wind velocity. Eddy covariance techniques also have the inherent problem of partitioning autotrophic respiration and heterotrophic respiration as well as being expensive to establish and maintain (Gilmanov *et al.*, 2005).

Remote sensing allows systematic and consistent observations of vegetated ecosystems, providing the opportunity to overcome the problems of limited measurement of GPP at flux tower sites; thus permitting the monitoring of ecosystem productivity across the Earth's land surface.

Estimating terrestrial vegetation GPP using remote sensing is a major challenge in global change research. Satellite sensors measuring in the visible and NIR wavelengths have the ability to provide quantitative estimates of GPP, providing the opportunity to monitor the spatial and temporal variability of vegetation productivity. The Moderate Resolution Imaging Spectrometer (MODIS) is mounted on both the Aqua and Terra satellites and was designed, in part, to address the need for global estimates of vegetation productivity. Together, the MODIS sensors provide repeat temporal coverage of the Earth's surface at 1km spatial resolution. Many products have been developed to exploit the sensor's radiometric resolution to infer vegetation productivity. The MOD17 product is based on the theories of Monteith (1972) that relate gross photosynthetic potential to the amount of absorbed photosynthetically active radiation (APAR). The ability of vegetation to utilise radiation for photosynthesis is termed its light use efficiency (LUE). Daily GPP estimates are easily computed in the MODIS productivity algorithm from this logic using:

$$GPP = e * PAR * fPAR \quad (6.1)$$

Where GPP equals daily gross primary productivity (kg cm^{-2}), e is the LUE, PAR is photosynthetically active radiation in the visible region between 400 nm – 700 nm and $fPAR$ is the fraction of PAR absorbed by the canopy. However, to derive e , the MOD17 product uses a regionally assigned LUE using a look-up table (LUT) based on biome type classification, which is modified if additional inputs of temperature and high pressure vapour deficit are suboptimal (Nightingale *et al.*, 2007). Such additional inputs are obtained from coarse spatial resolution datasets from the NASA Data Assimilation Office (DAO). Although the MOD17 algorithm includes variables to

account for short-term inhibition of photosynthetic rates, the accuracy of the MOD17 product is limited by the coarse spatial resolution of the meteorological inputs and the accuracy of the land classifications that are used to define biome type. Studies have suggested that significant errors in the estimated carbon fluxes are a result of coarse resolution data or estimations of LUE. Variations in LUE have been shown to exist within heterogeneous landscapes, whereby significant variation between species was observed (Ahl *et al.*, 2004). This species specific variation in LUE would therefore not be represented at the biome level, and may potentially effect GPP estimates.

Due to such shortcomings, it is important to explore methods that estimate GPP which do not require as many additional input variables (Wu *et al.*, 2009). Many recent studies have focused on the empirical relationship between spectral reflectance and GPP through the use of vegetation indices. Such approaches will have the spatial resolution of the sensor and are not reliant upon additional inputs such as meteorological data and land cover classification to determine LUE. The simplicity of vegetation indices will consequentially mean that short-term variations in photosynthetic activity will be untracked, as rapid changes in PAR, temperature and the availability of moisture are likely to have an effect on vegetation productivity. However, studies have demonstrated that vegetation indices are able to infer carbon flux over a period of several days as vegetation is able to respond and adapt to changing environmental conditions (Harris and Dash, 2009). Vegetation indices that are related to vegetation greenness, such as the NDVI, have been correlated with GPP to varying degrees of success in grasslands (Harris and Dash, 2009; Wylie *et al.*, 2003). The simplicity of NDVI and its inherent link to photosynthetic activity, make NDVI a popular tool for monitoring crop activity (Reeves *et al.*, 2005).

The photochemical reflectance index (PRI) was developed as a proxy for LUE. The PRI was developed to estimate LUE without the use of LUT and therefore increase the spatial performance of GPP models. The PRI is defined as:

$$\text{PRI} = (\text{R}_{531} - \text{R}_{570}) / (\text{R}_{570} + \text{R}_{531}) \quad (6.2)$$

Reflectance changes at R_{531} are theoretically linked to irradiance associated with foliar pigment energisation that is closely related to photochemical efficiency (Gamon

et al., 1992). Reflectance measured at R_{570} reduces the reflectance produced by the movement of chloroplasts (Gitelson *et al.*, 2006). The relationship between LUE and PRI has been mixed. Whilst a linear relationship has been observed for a number of species, the PRI is mostly sensitive to variation in LAI (Barton and North, 2001).

6.2 Chapter aims

A growing body of interest into the role that foliar chlorophyll may play in the estimation of GPP is emerging in the scientific literature. According to the logic of Monteith (1972), vegetation GPP is linearly related to the amount of absorbed photosynthetically active radiation and the ability of the vegetation to utilise the light in photosynthesis (LUE). In this investigation, it will be hypothesised that foliar chlorophyll content is a surrogate for LUE given the fact that plant physiological status is related closely to chlorophyll content (Sellers *et al.*, 1992). As chlorophyll content is one of the main requirements for photosynthesis (Dash *et al.*, 2009), vegetation productivity will be related to the foliar chlorophyll content. Laboratory studies have shown that variation in canopy total chlorophyll content of miniature Douglas fir canopies was significantly correlated with photosynthetic rates (Yoder and Waring, 1994). Given that vegetation responds to changes in the availability of nutrients and favourable environmental conditions through its photosynthetic capacity, the productivity of vegetation will be related to foliar chlorophyll content (Dawson *et al.*, 2003). Similarly, vegetation stress caused by unfavourable conditions, leading to physiological stress, corresponds to negative change in foliar chlorophyll content, which will subsequently affect photosynthetic rates and productivity. Waring *et al.*, (1995) found a strong correlation between canopy leaf chlorophyll concentration of deciduous species and maximum LUE at the primarily deciduous Harvard Forest flux site. Their findings support the link between chlorophyll content and LUE in deciduous forests.

Gitelson *et al.* (2006) demonstrated that remotely sensed estimates of foliar chlorophyll content, measured in the NIR and either the red or green regions has, a strong correlation with the day to day variation in GPP. Therefore, with reflectance measured in narrow bands in the red and NIR region, the MTCI as a tool to estimate GPP will be explored.

Using field spectroradiometers, Gitelson *et al.* (2006) demonstrated that remote sensing techniques used to estimate canopy chlorophyll content could be used to drive models that estimate GPP in both Soya bean and maize fields employing the rationale that LUE is proportional to GPP/PAR. Wu *et al.* (2009) assessed the suitability of various vegetation indices to estimate chlorophyll content and GPP in six wheat species. Both investigations provided accurate assessment of GPP in crops using chlorophyll indices and have indicated the potential of using such techniques to derive estimates of GPP. To date, the approach adopted by Gitelson *et al.* (2006) and later adopted by Wu *et al.* (2009) has not been applied to estimate GPP in other vegetation types nor has the suitability of such a technique been assessed using satellite sensor data. This investigation explored the potential of the MTCI to estimate GPP in four vegetation types, including temperate deciduous forest, coniferous boreal forest, mixed temperate forest and grass rangelands.

6.3 Study sites

Study sites were selected to explore the relationship between GPP and MTCI for a range of vegetation types (Figure 6.1). Sites consisted of a single dominant vegetation type and were required to be at least 3x3 km to allow for potential geolocation errors in imagery, reducing any errors associated with mixed pixels. Careful consideration was given to minimise the effects of topography, therefore only small scale topographic variations were permitted in selecting the sites.

6.3.1 Grassland site

Grasslands make up 40% of the Earth's terrestrial surface within which temperate grasslands contain about 18% of global carbon reserves (Wylie *et al.*, 2007). Given the expansive areas of rangelands, how rangelands respond to climatic variation is of great importance to global carbon budgets (Gilmanovet *al.*, 2005). Fort Peck (48° 30'77" N and 105° 10'19" W) is located in Montana, USA, forming part of the Great Northern Plains (Zhang *et al.*, 2008). The Fort Peck flux towers lie within the heart of the Northern Plain eco-region. The site is characterised by grassland species. The Northern Plain grass species include wheatgrass (*Agropyron* sp.), green needlegrass

(*Stipa spartea*), grama grass (*Bouteloua* sp.), and buffalo grass (*Buchloe dactylides*) with a canopy height of 20-30 cm (Zhang *et al.*, 2007).

6.3.2 Coniferous boreal site

Boreal forests constitute over 10% of the Earth's terrestrial surface occupying the circumpolar region between 50° and 70° North (Sanchez *et al.*, 2009). The extent and biophysical properties of Boreal forests mean that these ecosystems have great potential to impact on the Earth's climate. The University of California, Irvine (UCI) 1850 site (55° 87' N and 98° 48' W) is located in a continental boreal forest, dominated by black spruce (*Picea mariana*) with an open understorey composed of alders (*Rosa* sp.), Labrador tea (*L. groenlandicum*), and willow (*V. oxycoccus*). The mature spruce forest was last cleared by fire in 1850, and is located within the Boreal Ecosystem-Atmosphere Study (BOREAS) northern study area in central Manitoba, Canada (Goulden *et al.*, 2006).

6.3.3 Deciduous study site

The Harvard Forest Environmental Monitoring Station (EMS) hosts one of the longest operational eddy flux towers, providing turbulent flux estimates since 1991. The site (42° 54' N and 72° 18' W, 180–490 m elevation) is located in western Massachusetts, USA. The deciduous broadleaf forest is 50–70 years old and is dominated by oak (*Quercus rubra*), red maple (*Acer rubrum*), birch (*Betula lenta*) and Hemlock (Li *et al.*, 2009). There was approximately 12% coniferous cover within the forest. The canopy height is approximately 20–24 m (Zhang *et al.*, 2005).

6.3.4 Mixed woodland site

The Fort Dix flux tower is located (39° 97' N and 74° 43' W) in New Jersey, USA. The New Jersey Pinelands encompass 1.1 million acres of pine, oak and wetland forests, covering 23% of New Jersey (Skowronski *et al.*, 2007). The Fort Dix study site is dominated by white pine (*Pinus strobus*) with oaks (*Quercus rubra*) in the canopy, and relatively dense understorey vegetation. Canopy height is approximately 13m.

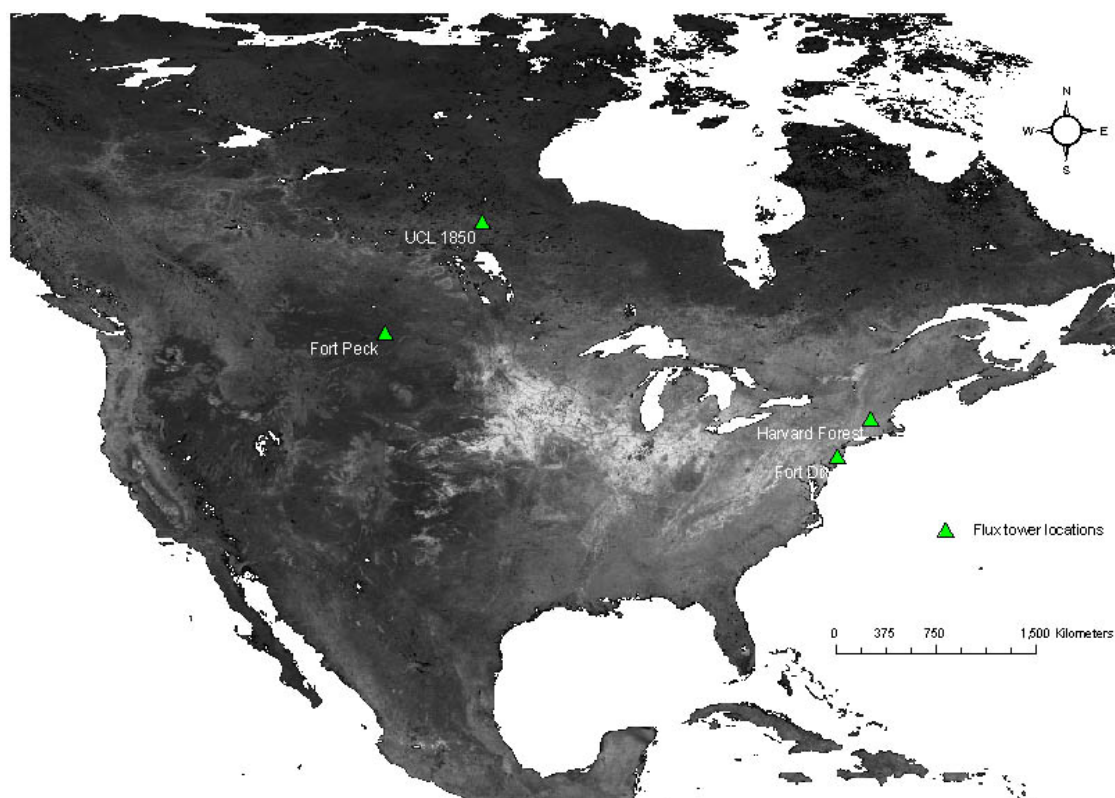


Figure 6.1. The location of the flux tower sites that were used in this study.

Map derived from ESRI maps.

6.4 Method

6.4.1 Flux and site data

This study uses GPP data, which were obtained from the Ameriflux network (<http://public.ornl.gov/ameriflux/>), providing continuous observations of ecosystem level exchanges of CO₂ between a vegetated canopy and the atmosphere. Ameriflux is part of FLUXNET (<http://www.fluxnet.ornl.gov/fluxnet/index.cfm>) that coordinates regional and global analysis of observations from micrometeorological tower sites across the USA and Canada (Wylie *et al.*, 2007). There are about 53 Ameriflux sites with data available through FLUXNET. The U.S. Department of Energy (DOE) runs the Ameriflux network with support from the National Aeronautics and Space Administration (NASA), National Oceanic and Atmospheric Administration (NOAA), National Science Foundation (NSF), US Department of Agriculture (USDA) and U.S. Geological Survey (USGS).

Ameriflux Level 4, gap filled data includes estimates of GPP based upon Net Ecosystem Exchange, LAI and local metrological measurements according to the

partitioning algorithm used. 30 minute GPP time series data for each site were used from January 2004 to December 2005, except for the Fort Dix location, where only 2005 data were available. 8 day GPP aggregates were produced to calculate mean daily GPP rates for the compositing period. This approach was adopted as this corresponded with the MTCI and MODIS compositing time period, allowing direct comparison between MTCI, flux tower GPP measurements and MOD17 GPP estimates. The flux tower data collection differs from optical remote sensing as data are collected regardless of cloud cover. To make a direct comparison only GPP for active photosynthesis was used, which represents a positive flux and CO₂ uptake from the atmosphere by the vegetation.

Flux towers also housed point quantum sensors (LI-190, LI-COR Inc.) to measure incoming PAR ($\mu\text{mol photons m}^{-2} \text{ s}^{-1}$). Diurnal PAR data was measured at 30-minute intervals, however only data recorded during 10.00 and 15.00 hrs were used in this investigation, which corresponded to positive photon flux. PAR was aggregated to correspond with the MTCI, MOD17 GPP and MOD15 *f*PAR 8-day compositing period. Gaps in the PAR time series were filled using interpolation.

6.4.2 Remotely sensed data

MERIS data

MTCI 1km 'reduced resolution' 8 day composites of central and northern North America were accessed through the NEODC server and made into layer stacks in ENVI that covered the growing seasons of 2004 and 2005. Details of the compositing period are found in chapter 5, page 136.

MODIS data

All 1km spatial resolution MODIS Data were accessed through the NASA WIST (Warehouse Inventory Search Tool (<https://wist.echo.nasa.gov>)).

MOD17 is computed using the LUE type model as proposed by Monteith (1972). The MOD17 product is an eight-day summation of GPP, a period that is the result of the orbiting characteristics of the Terra and Aqua platforms that carry the MODIS instrument (Reeves *et al.*, 2005). The summation is computed by adding all eight days

of productivity estimates (kg C m^{-2}), therefore it was necessary to derive a mean daily GPP rate ($\text{g C m}^{-2} \text{ d}^{-1}$) to allow comparison between flux tower observations.

The MOD15 $f\text{PAR}$ product is derived from the Surface Reflectance Product (MOD09), Land Cover Product (MOD12) and ancillary information on surface characteristics such as land cover type and background. MOD15 $f\text{PAR}$ is derived from a three-dimensional formulation of the radiative transfer, describing the propagation of light within a vegetation canopy (Nemani *et al.*, 2003) to derive spectral and angular biome specific signatures of vegetation canopies. The RTM estimates $f\text{PAR}$ as a function of NDVI, and is therefore related to canopy LAI (Running *et al.*, 2004). Should the main $f\text{PAR}$ algorithm fail, a back-up algorithm is triggered to estimate LAI and $f\text{PAR}$ using NDVI. The NDVI has been shown to be sensitive to both increases in the amount of chlorophyll visible to the sensor, either through an increase in foliar or understorey chlorophyll content (Dawson *et al.*, 2003). Due to the linear relationship between NDVI - $f\text{PAR}$, such sensitivity has been shown to account for significant errors in remotely sensed estimates of $f\text{PAR}$ and therefore estimations of GPP.

All MODIS land products have quality assurance data associated with each pixel for each composite period. The quality assurance layer provides a means for screening all pixels that are not suitable for analysis as a result of sensor or algorithm performance or atmospheric conditions. In this study, only the best quality MOD17 and 15 pixels were retained for further analysis. This procedure meant that $f\text{PAR}$ estimated using the back-up algorithm based on NDVI were not used.

Temporal layer stacks were produced for each MOD15 $f\text{PAR}$ and MOD17 scene relating to each study area to cover the growing seasons 2004 and 2005.

6.4.3 Calculation of site specific light use efficiency

LUE is derived to determine the relationship between remotely sensed and flux tower estimates of GPP and will indicate the role that factors other than PAR and foliar chlorophyll (such as metrological factors) have in defining ecosystem GPP. LUE was estimated from flux tower PAR ($\mu\text{mol m}^2 \text{ s}^{-1}$), aggregated to mean daily PAR to match the 8-day compositing of MOD17 and MTCI and MOD15 $f\text{PAR}$ product. Only

MOD15 $fPAR$ flagged as excellent were used in the calculation of LUE. Two methods were used to estimate LUE following the methods of Monteith (1972) and Gitelson *et al.* (2006).

$$LUE = GPP / PAR \text{ (Gitelson } et al., 2006) \tag{6.3}$$

$$LUE = GPP / APAR \text{ (Monteith, 1972)} \tag{6.4}$$

$$\text{Where } APAR = fPAR * PAR \tag{6.5}$$

6.5 Results and discussion

6.5.1 Inter-annual variability in the relationship between flux tower GPP and MTCI

The first step to establishing whether the method proposed by Gitelson *et al.* (2006), where GPP can be estimated through canopy chlorophyll content and incident radiation in the 400 – 700nm region, can be applied to other vegetated ecosystems is to determine the relationship between flux tower GPP and MTCI. The observed GPP in 2004 and 2005 had similar seasonal dynamics with MTCI in the plant growing season (Figure 6.2), with a peak value in an 8-day period of late June for the Harvard Forest and Fort Dix, whilst a peak in GPP was slightly later (July) at UCI 1850 and Fort Peck due to latitude. The temporal variability in carbon flux as measured at the flux tower sites is matched closely by MTCI for all four sites. This trend was expected as canopy chlorophyll content has been shown to relate to day-to-day variations in GPP in cereal crops (Gitelson *et al.*, 2006), and Canadian boreal peatland sites (Harris and Dash, 2009). The close relationship between GPP and MTCI was shown at all four sites and for both years where data were available.

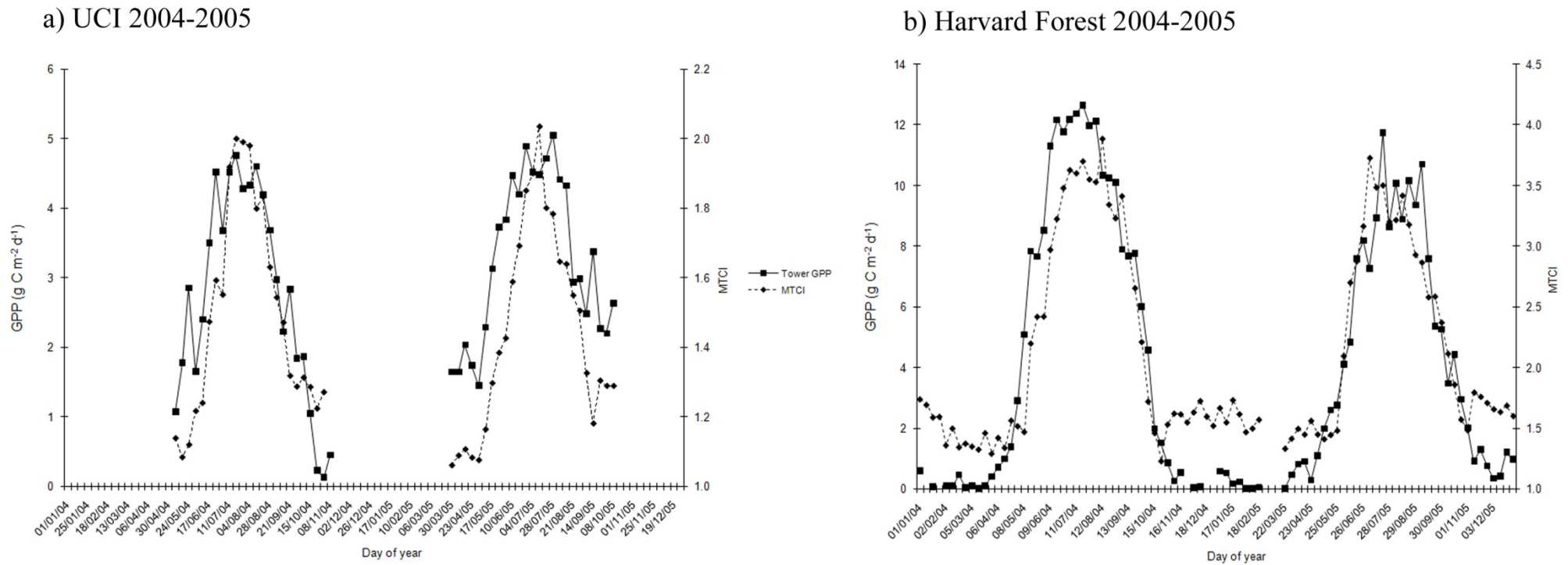
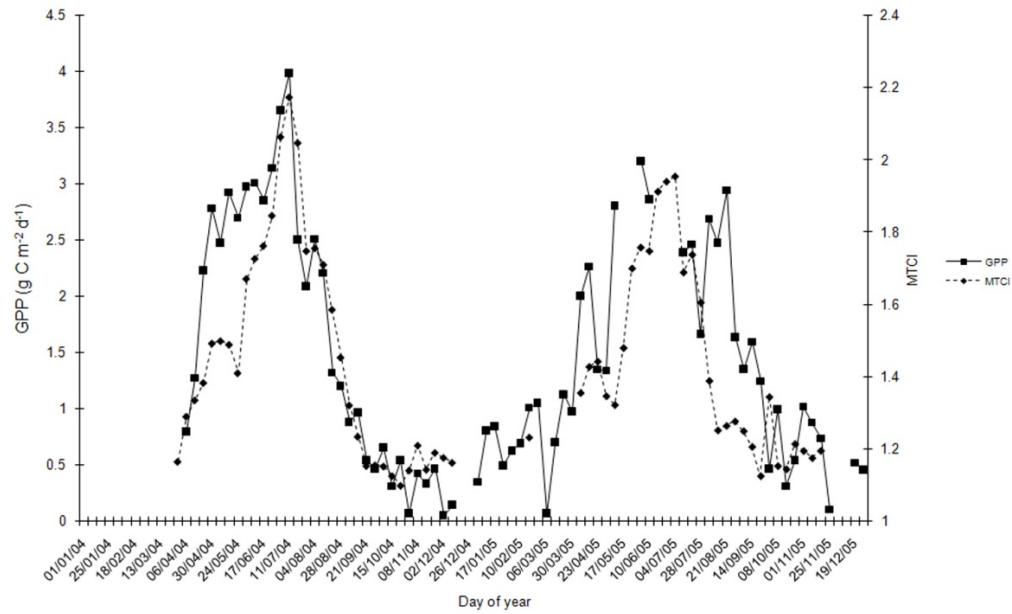


Figure 6.2 (a and b). The temporal variation in flux tower GPP as measured using eddy covariance techniques for UCI 1850 (a) and Harvard Forest (b) sites and corresponding MTCI values.

c) Fort Peck 2004-2005



d) Fort Dix 2005

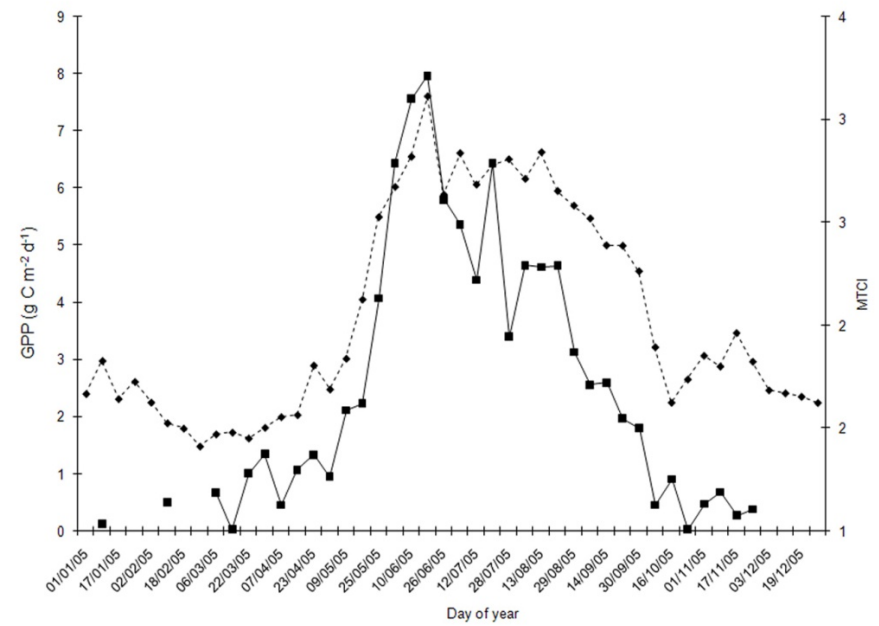
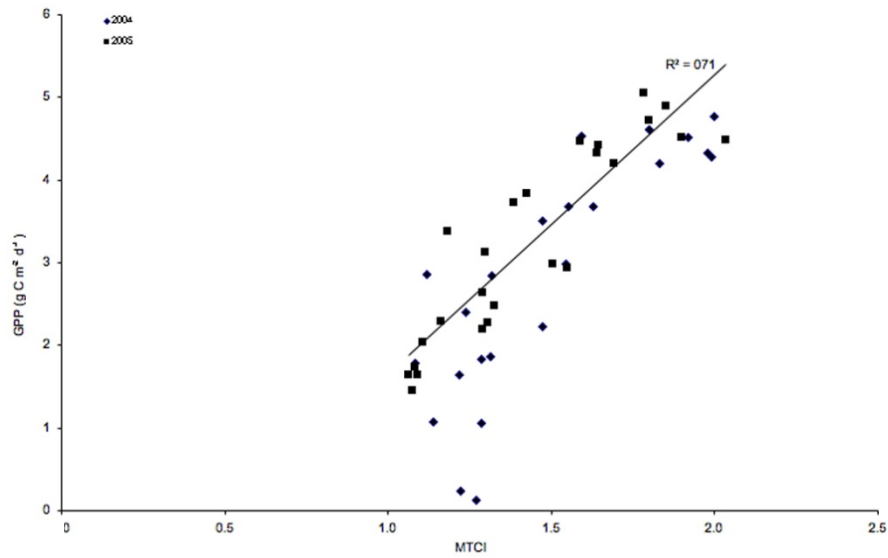


Figure 6.2 (c and d). The temporal variation in flux tower GPP as measured using eddy covariance techniques for Fort Peck (c) and Fort Dix (d) sites and corresponding MTCI values.

Correlation coefficients were derived to determine the strength of the relationship between MTCI and GPP for each site (Figure 6.3). Generally, the MTCI – GPP relationship was strong enough to enable MTCI to be, in turn, used as a robust proxy to infer GPP in a range of cover types. The relationship between MTCI and GPP was particularly strong for the deciduous Harvard Forest site (Figure 6.3 (b)), where MTCI accounted for 89% and 84% of the variation in GPP (for 2004 and 2005 respectively). The correlation between GPP and MTCI for Fort Peck (grassland site) (Figure 6.3 c) varied markedly from 2004 – 2005, as indicated by the slope of the regression, which showed a degree of divergence at low rates of GPP. The slope of regression between sites and years were similar, therefore permitting the regression model to be applied to all sites, for both years (except Fort Dix, 2005 only). The MTCI showed a strong correlation with tower GPP, with a coefficient of determination (R^2) of 0.73. The strong relationship has shown that the MTCI can be used to estimate GPP across a range of vegetation cover types. These results indicate that the MTCI is a useful tool in estimating ecosystem productivity.

a) UCI 1850 2004 - 2005



b) Harvard Forest 2004 - 2005

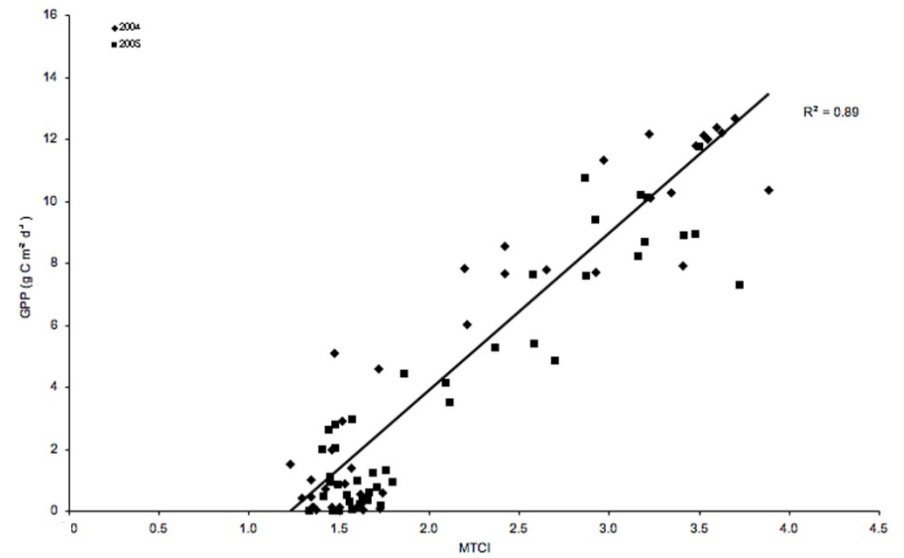
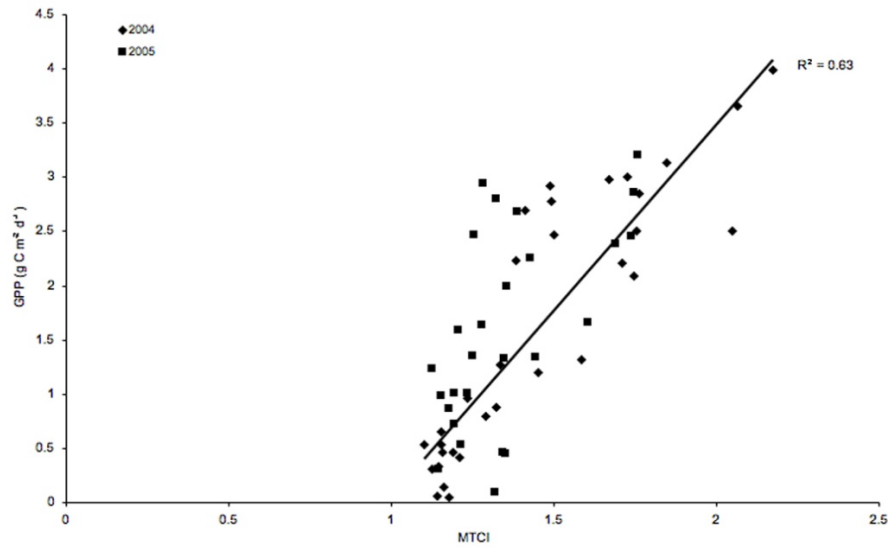


Figure 6.3 (a and b). The relationship between tower GPP and MTCI for UCI 1850 (a) and Harvard Forest (b). The relationships are based on data from both years.

c) Fort Peck 2004 - 2005



d) Fort Dix 2005

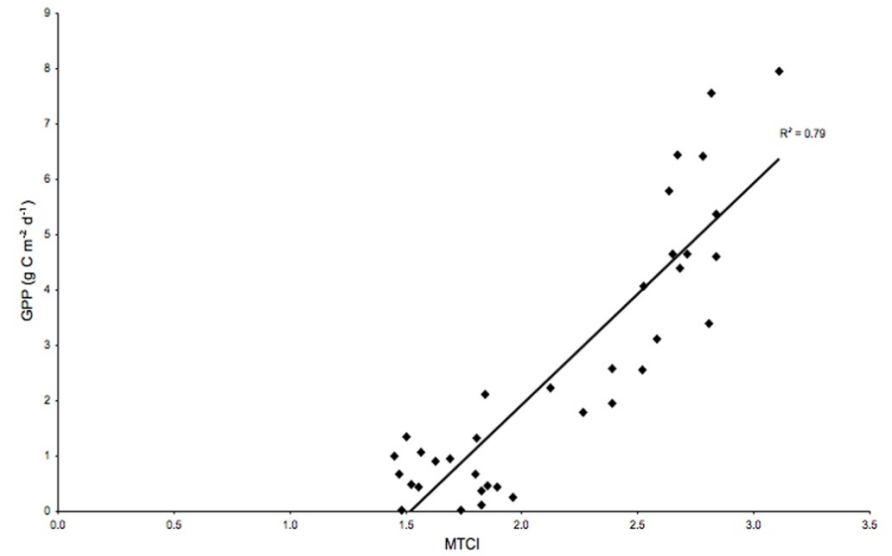


Figure 6.3 (c and d). The relationship between tower GPP and MTCI for Fort Peck (a) and Fort Dix (b). The relationships are based on data from both years, where available.

6.5.2 The relationship between flux tower GPP estimates, MTCI and PAR

The method proposed by Gitelson *et al.*, (2006) and later adopted by Wu *et al.*, (2009) estimates GPP based on the remote estimation of chlorophyll content. This approach is based on the underlying hypothesis that total chlorophyll content is related closely to the low frequency, i.e. day-to-day, variation of GPP that is associated with vegetation phenological stage and physiological status (Gitelson *et al.*, 2006). Figure 6.4 Shows a relatively strong correlation between flux tower GPP and MTCI*PAR, with an overall R^2 of 0.67. This result can be compared to that of Wu *et al.*, (2009), who showed a coefficient of determination R^2 of 0.66 for canopies of various species of corn. The similarities between the results given the contrasting cover types, suggests that chlorophyll content, and more specifically MTCI, is able to provide robust estimates of GPP for various vegetation cover types. The spread of points from the line of best fit suggest that the MTCI*PAR model only has limited species-specific sensitivity (Figure 6.4 below). However, it should be noted, that the model incorporating variation in incident light use as MTCI*PAR did not correlate as closely with flux tower measurements of GPP compared to MTCI alone.

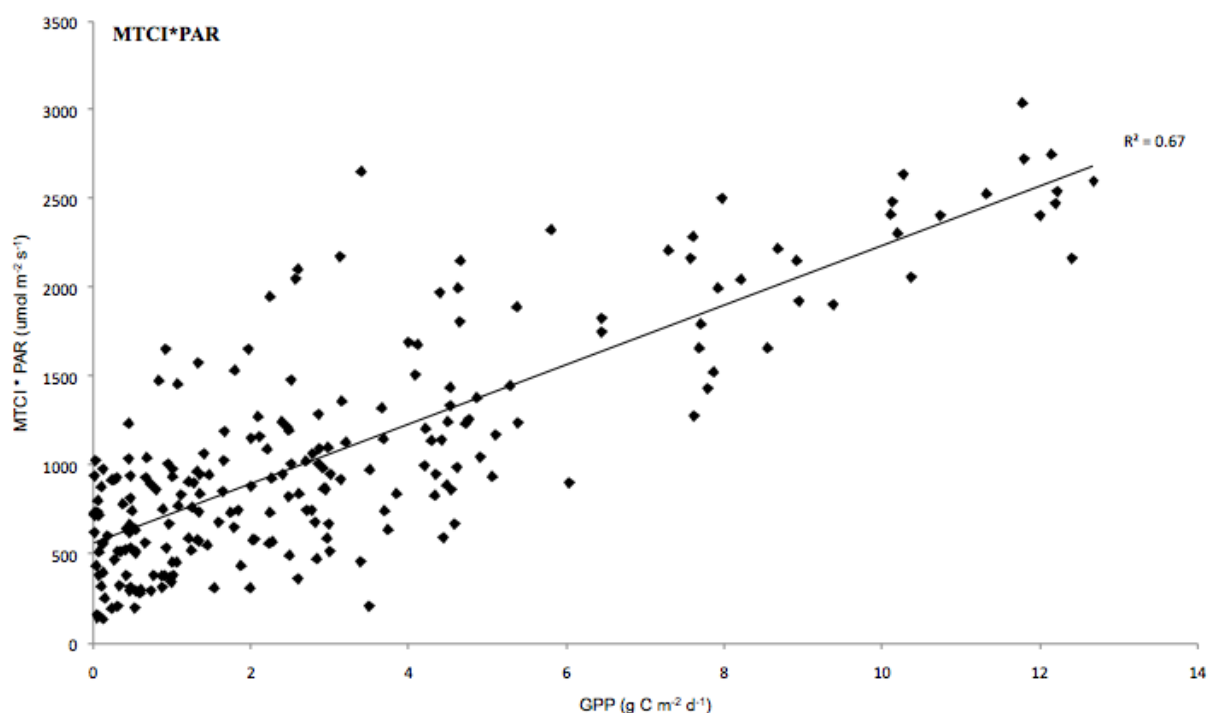


Figure 6.4. Relationship between flux tower GPP and MTCI*PAR for all sites and both years where data were available.

6.5.3 The relationship between GPP and MTCI and APAR

Chapter 6. Relationship between GPP and MTCI in various ecosystems

Given that vegetation canopies change throughout the growing season according to their phenological development, the incorporation of PAR alone will not explain the amount of radiation made available for use in photosynthesis. For example, during the ‘leaf off’ stage in deciduous vegetation the canopy absorbs no PAR. Whilst at canopy maturity, maximum PAR is absorbed. The fraction in the amount of absorbed PAR is not accounted for in the model developed by Gitelson *et al.* (2006) and therefore will be unsuitable for estimating GPP throughout the growing season given that variation in PAR absorbed by vegetation will be a function of leaf area. Given that only absorbed PAR (APAR) is used for photosynthesis, it could be argued that APAR would be more suitable than PAR to provide remote estimations of GPP. With this considered, MOD15 *f*PAR was used to assess the amount of PAR absorbed throughout the growing season from flux tower PAR measurements for all study sites.

$GPP = MTCI*(PAR*fPAR)$ model was developed for each of the four sites and each year (where data were available) (Figure 6.5 a – d). Coefficient of determination R^2 values for the $MTCI*APAR - GPP$ relations were calculated for all sites and years; results are shown in table 6.1. Results show that there was consistency in the relationship between flux tower measured GPP and the $MTCI*APAR$ models between 2004 and 2005 growing seasons for all sites except UCI 1850, which showed a relatively strong relationship between $MTCI*APAR$ and flux tower GPP for 2005. Excluding UCI 1850 2005, such consistencies suggest that the models successfully account for variation in GPP between years. The similar regression slopes between years and study sites suggest that the approach to estimate GPP using $MTCI*APAR$ is independent of cover type. This permitted a regression model to be applied to all the available data, where the relationship between flux tower GPP measurements and $MTCI*APAR$ could be assessed. The $MTCI*APAR$ regression model took the form;

$$GPP = 0.004*(MTCI*(PAR*fPAR) + 0.057 \quad (6.4)$$

The above regression model successfully accounted for 82% of the variation in flux tower GPP (Figure 6.6). The scatter of points from the regression line was reduced compared to the $MTCI*PAR$ model, suggesting that $MTCI*APAR$ successfully accounts for small variation in GPP attributed to environmental stress.

Chapter 6. Relationship between GPP and MTCI in various ecosystems

The model performance was evaluated through the relationship between predicted and flux tower GPP measurements. Generally there is good agreement between predicted and actual GPP, as was indicated Figure 6.6. The MTCI*APAR model underestimates GPP in deciduous species during the peak growing season as measured at the Harvard Forest flux tower. The spread of the points around the 1:1 line indicate the generally satisfactory performance of the model in estimating GPP (Figure 6.7). However, the model underestimates GPP for both coniferous and grassland species as measured at the UCI 1850 and Fort Peck flux towers.

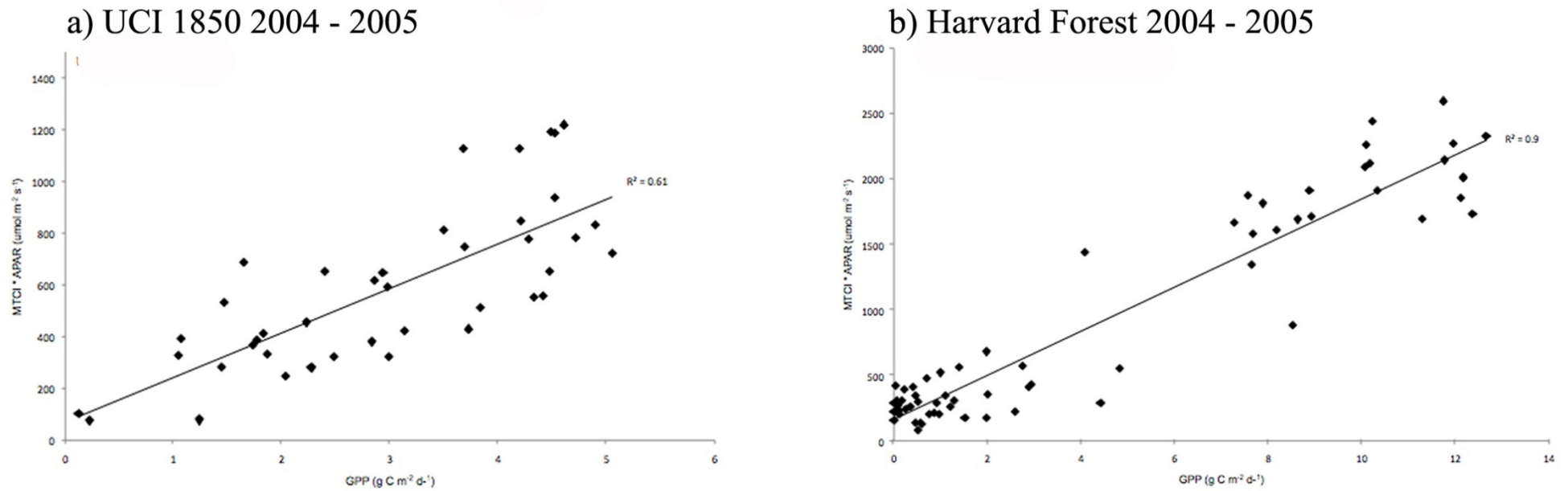
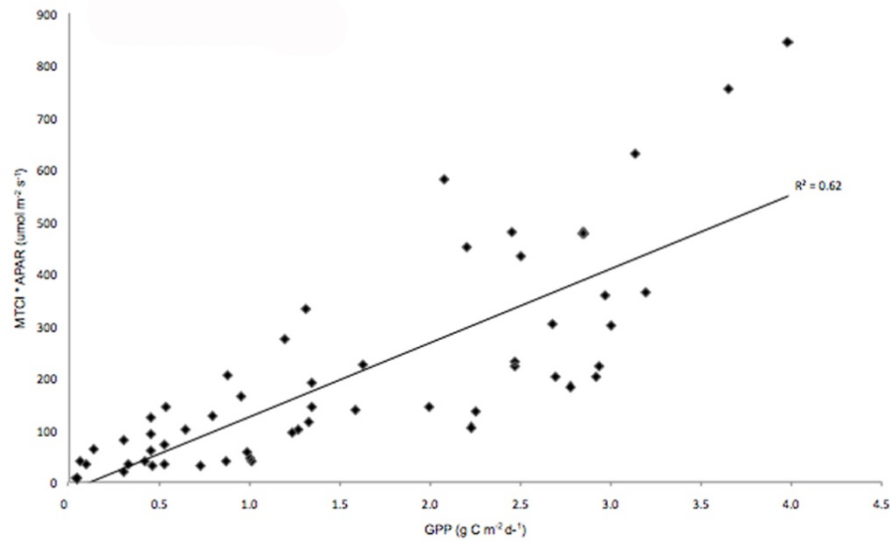


Figure 6.5 (a and b). The relationship between flux tower GPP measurements and MTCI*APAR at UCI 1850 (a) and Harvard Forest (b). Except (d) 2005 only. The relationship MTCI*APAR using all data (e).

c) Fort Peck 2004 - 2005



d) Fort Dix 2005

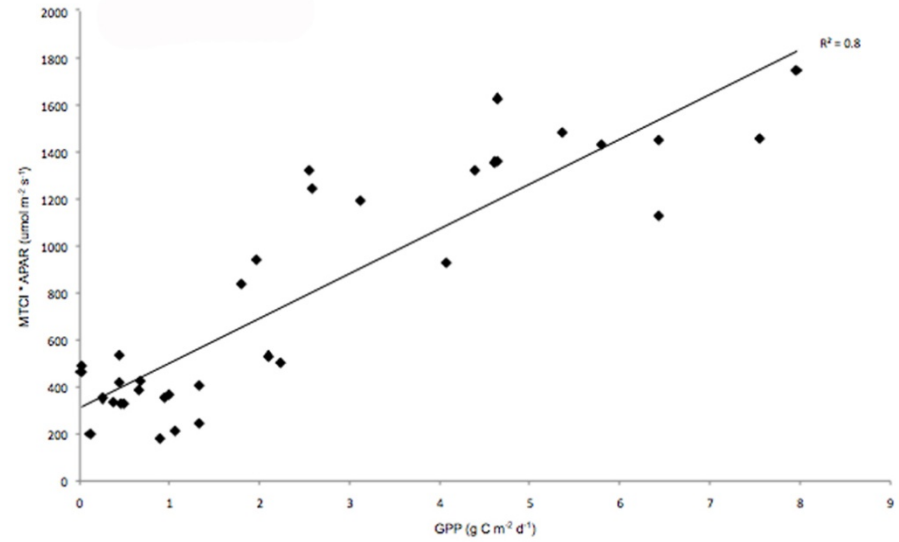


Figure 6.5 (c and d). The relationship between flux tower GPP measurements and MTCI*APAR at Fort Peck (c) and Fort Dix (d) (2005 only).

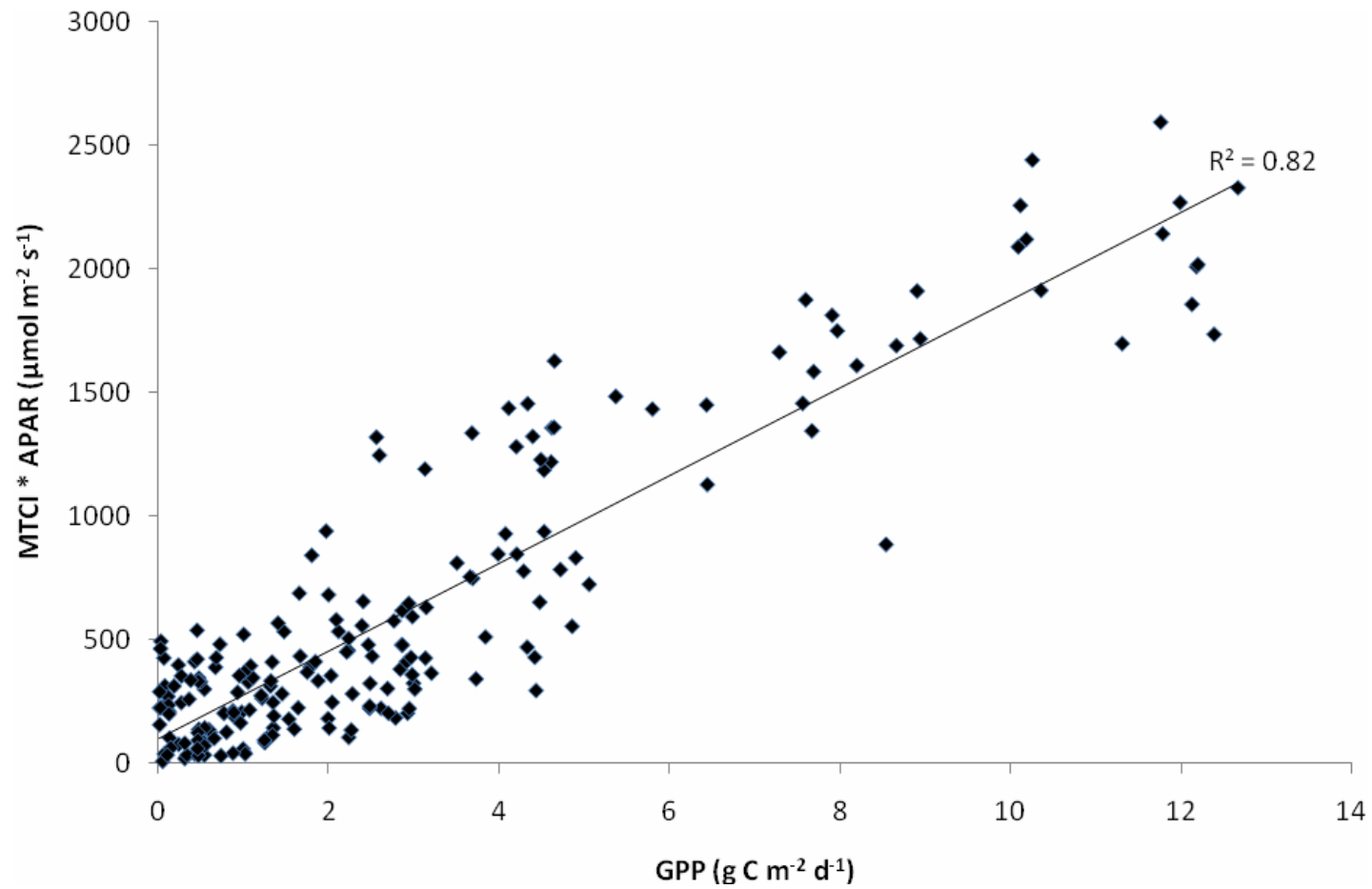


Figure 6.6. The relationship MTCI*APAR using all data from 2004 and 2005 (except Fort Dix, 2005 only).

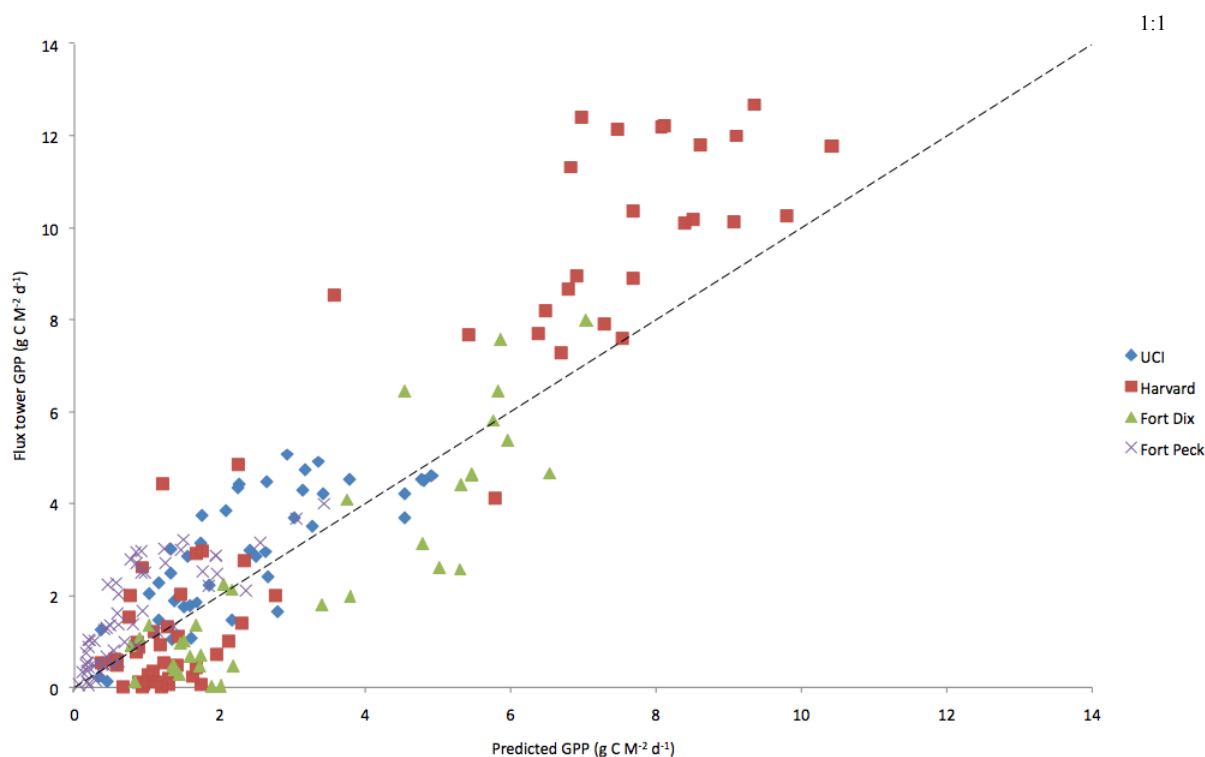


Figure 6.7. Relationship between predicted GPP based on the MTCI*APAR model and flux tower GPP for all four sites.

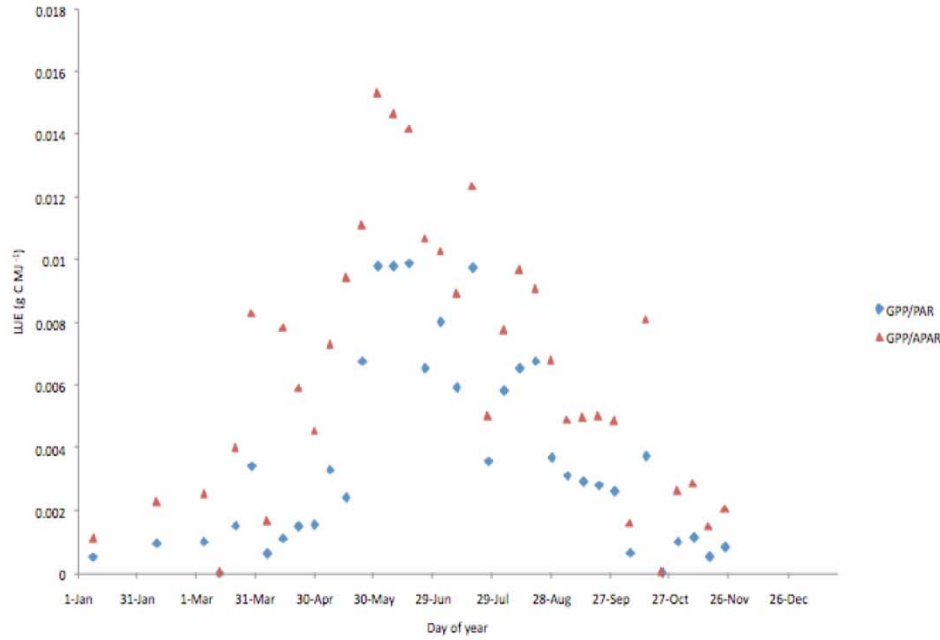
6.5.4 Accounting for the relationship between expected and actual GPP using LUE

The photosynthetic efficiency (LUE) of the contrasting cover types shows temporal profiles that correspond with canopy phenological development (as inferred through temporal profile in MTCI) reaching a maximum during early summer and decreasing toward the winter months (Figure 6.8 a). The temporal trends observed in LUE were matched by APAR and MTCI (Figure 6.8 b). Showing that chlorophyll content (inferred through MTCI) increases in line with APAR ($PAR \cdot fPAR$). Similar trends were observed for all sites for both years of data used in this study. However, the UCI 1850 data revealed differences in LUE within the growing seasons and marked differences between years.

The temporal variation in LUE at the coniferous UCI 1850 study site is shown in Figure 6.9 (a). The variation within and between years is clearly visible; LUE for much of the 2005 growing season is greater than observed during the growing season of 2004. Variation in LUE throughout the 2005 growing season is not accounted for

by the MTCI*APAR model and offers an explanation to the underestimation of GPP at the UCI 1850 study site. This can be demonstrated in Figure 6.9 (b), where predicted GPP accounts for 41% of the observed variation in LUE. Further investigation into the causes of such variation is required. However, the results suggest that LUE is an important factor in determining GPP and will reduce error in estimating GPP where vegetation may be stressed. Further work will need to assess whether stress was specific to the UCI 1850 site, where environmental stress was evident only during 2005. If stress conditions were apparent at other location the model described it well, through short-term variation in canopy chlorophyll content. If this is the case, then the MTCI*APAR model will be unable to account for GPP variation brought on by short-term environmental stress in coniferous species. This may suggest that variation in LUE rather than chlorophyll content is more important in estimating GPP in coniferous vegetation. Assessing the relationship between environmental factors known to affect LUE, e.g., temperature, available soil moisture, at each site will help determine the importance of LUE in GPP models driven by chlorophyll content. Including LUE estimates into the MTCI*APAR model will therefore improve the model performance to provide increasingly accurate estimates of GPP.

a) LUE Fort Dix 2005



b) APAR and MTCI Fort Dix 2005

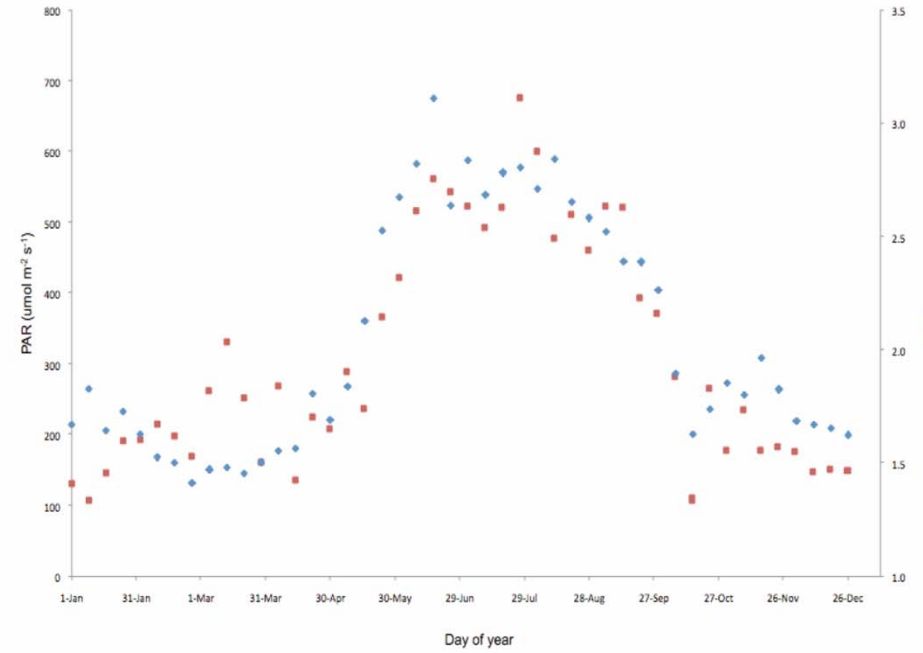


Figure 6.8. Variation in LUE as defined by Monteith (1972) and Gitelson *et al* (2006) across the 2005 growing season at Fort Dix (a). Variation in APAR and MTCI throughout the growing season of 2005 for the Fort Dix study site (b).

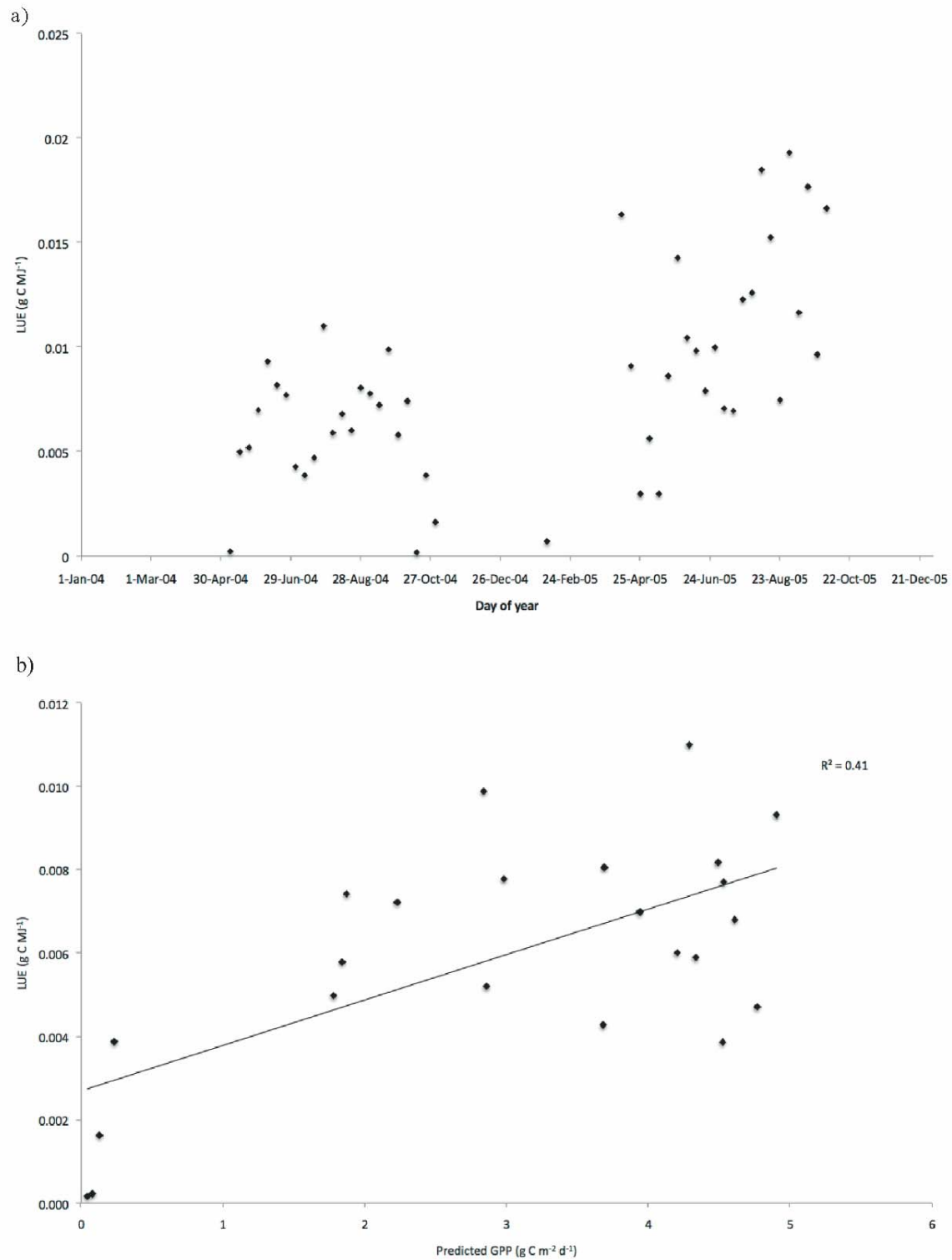


Figure 6.9. Variation in photosynthetic LUE for UCI 1850 site for 2004 and 2005 growing seasons (a). The relationship between predicted GPP (MTCI*APAR) and LUE (b).

6.5.5 Comparison of developed models with MODIS GPP product

The results from the various models used in this study suggested that chlorophyll content, as estimated using MTCI, was able to successfully drive simple models to estimate GPP in contrasting cover types. The MODIS sensor provided near real-time estimates of gross primary production (GPP) since March 2000 (Heinsch *et al.*, 2006). However, the ability to derive accurate estimates of GPP is necessary across a range of cover types. For each study site MOD17 GPP was able to follow the temporal trend in productivity throughout the growing seasons. However, the data displayed more temporal variability than was measured *in-situ* at the flux tower sites. Scatter plots between flux tower GPP and MOD17 show consistent discrepancies at each site, where for both UCI 1850 (coniferous site) and Harvard Forest (deciduous) peak growing season GPP was either under or overestimated (Figure 6.10 a and b respectively). However, both the Fort Peck (grassland) and Fort Dix (mixed temperature woodland) study sites were systematically over and underestimated throughout the growing seasons of 2004 and 2005 (Figure 6.10 c and d). Large discrepancies between predicted GPP from the MOD17 algorithm and observed GPP from the Harvard flux tower were observed by Xiao *et al.* (2004). Supporting the findings that MOD17 underestimates GPP during the peak growing season. Further work has demonstrated bias associated with GPP estimates using MOD17. Heinsch *et al.* (2006) stated that the bias is dependent upon the productivity of the ecosystem, whereby MOD17 tends to overestimate tower GPP for most sites. However, for the most productive sites MOD17 underestimates GPP (Turner *et al.*, 2006).

Overall, the correlation between flux tower and MOD17 GPP estimates were not as strong as those methods used to derive GPP using MTCI. Table 6.1 shows the R^2 values for the relationship between each contrasting cover type, for both the growing seasons of 2004 and 2005. The results suggest that GPP estimates made using MTCI and MTCI*APAR model describe flux tower GPP better than MOD17 which is dependent on additional meteorological data and land cover LUT to define site specific LUE.

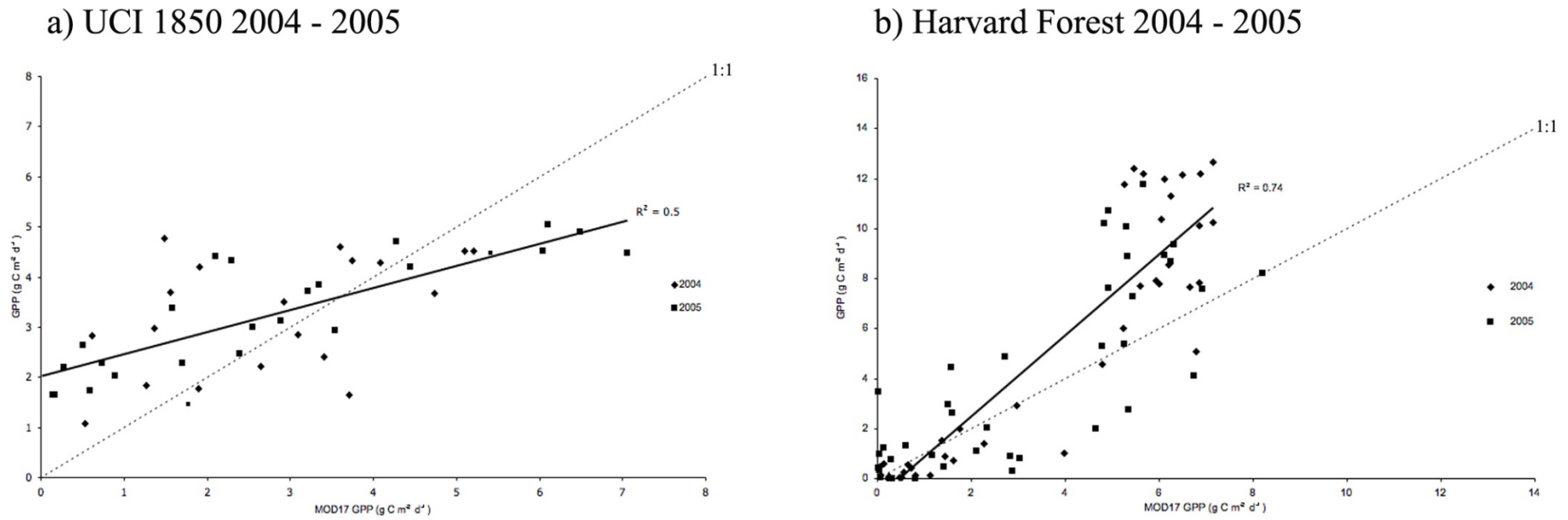
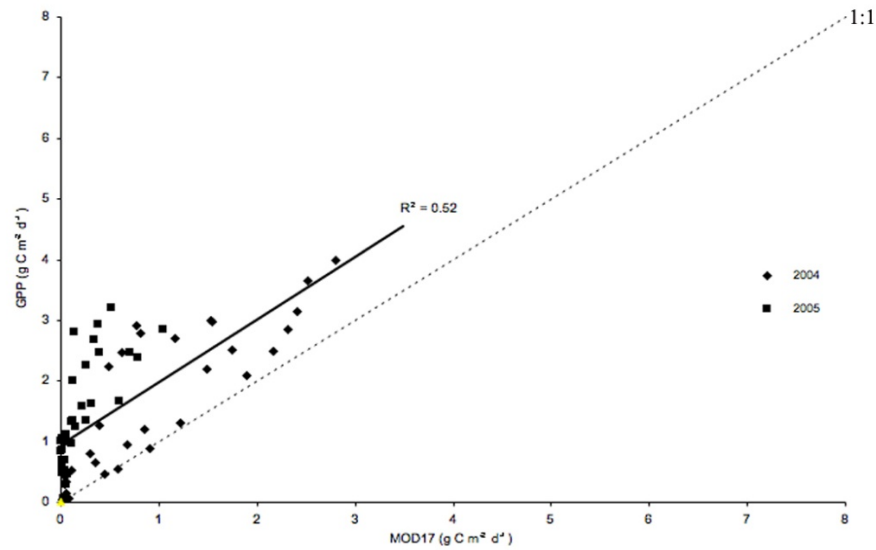


Figure 6.10 (a and b). The relationship between flux tower GPP and MOD17 estimates at UCI 1850 (a) and Harvard Forest (b).

c) Fort Peck 2004 - 2005



d) Fort Dix 2005

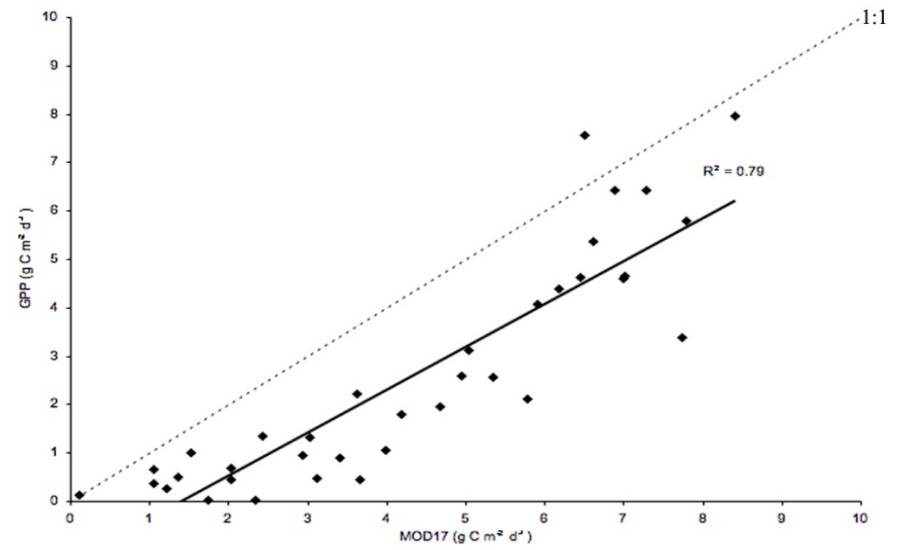


Figure 6.10 (c and d). The relationship between flux tower GPP and MOD17 estimates for Fort Peck (c) and Fort Dix (d).

| GPP model | UCI 1850 (n) | | Harvard (n) | | Fort Peck (n) | | Fort Dix (n) | All data (n) |
|-----------|--------------|--------------|--------------|--------------|---------------|--------------|-----------------|-----------------|
| | 2004 (24) | 2005 (22) | 2004 (36) | 2005 (39) | 2004 (33) | 2005 (28) | 2005 (35) | (217) |
| MTCI | 0.7* | 0.81* | 0.89* | 0.84* | 0.78* | 0.55* | 0.79* | 0.74* |
| MTCI*PAR | 0.61* | 0.52* | 0.89* | 0.75* | 0.75* | 0.6* | 0.61* | 0.66* |
| MTCI*APAR | 0.74* | 0.55* | 0.92* | 0.90* | 0.65* | 0.67* | 0.81* | 0.82* |
| MOD17 GPP | 0.50* | 0.69* | 0.82* | 0.63* | 0.51* | 0.56* | 0.74* | 0.64* |

* = p < 0.05

Table 6.1 Comparison of the coefficients of determination between modelled and *in-situ* flux tower GPP measurements for UCI 1850, Harvard, Fort Peck and Fort Dix study sites. The table shows the R^2 values of the various methods used to estimate GPP in this investigation.

6.5.6 Potential limitations and further work

Almost all terrestrial ecosystem models require incident PAR. However, the current PAR products developed for climate studies have much coarser spatial resolution and are therefore not suitable for estimating terrestrial GPP (Liang *et al.*, 2007). At present, there is no high resolution PAR (1km) satellite sensor product and PAR inputs in to the MOD17 algorithm have a $1^\circ - 1.5^\circ$ degree resolution (Running *et al.*, 2004). Therefore, there is a requirement to fulfil the needs of the user community and develop a 1km global PAR product with a suitable temporal resolution to complement the 8-day compositing of the MTCI and MODIS *f*PAR (MOD15) and GPP (MOD17) products. The potential shown through the utilisation of MTCI to estimate GPP will be unrealised without a fine spatial resolution source of incident PAR. Further work will be required to address the suitability and variation in GPP estimates introduced through the use of MODIS high-level land products that can be used for calculating incident PAR at $1^\circ - 1.5^\circ$ degrees.

The MOD15A2 algorithm provides essential inputs to the $GPP = MTCI * (PAR * fPAR)$ model. The *f*PAR is used to directly calculate the APAR of a pixel. In this study, the

calculation of APAR was dependent upon the use of MOD15 $fPAR$ product. Following the rationale of Monteith (1972), $fPAR$ is an important biophysical variable in defining LUE, and GPP. Errors in $fPAR$ will lead to errors in the estimate of GPP. However, few tower sites measure site-specific $fPAR$ over the areas necessary for comparison with MODIS data; therefore it was not possible to assess the accuracy of the MOD15 $fPAR$ product. However, it is beyond the remit of this research to diagnose potential errors in MOD15 $fPAR$ algorithm.

Chlorophyll driven GPP models, where chlorophyll content is a surrogate for LUE, will not account for limitations due to short-term environmental extremes so variation in LUE attributed to environmental stress may still need to be considered. Furthermore, photosynthesis of evergreen conifer forests are less sensitive to changes in chlorophyll content than are broadleaf forests as evidenced by the continuous green colour of conifer forests even during the coldest periods of winter. Results from UCI 1850 2005 growing season suggest that LUE in coniferous species is an important factor to consider in order to minimise error in GPP estimates. Further investigation utilising local meteorological data is required to address this issue.

One such climate variable that potentially can be attributed to vegetation stress could be addressed in the future with data from the new ESA Soil Moisture and Ocean Salinity (SMOS) Living Planet mission as this provides global estimates of soil moisture. The potential to include data related to soil moisture may prove to be a better indicator of vegetation stress than precipitation data due to issues associated with local soil moisture deficit and the availability of water for vegetation. However, it could be argued that chlorophyll-based estimates of GPP have the potential to indirectly account for environmentally-induced stress and associated decrease in productivity via temporal variations in chlorophyll content. This direct approach reduces uncertainty in estimating temperature, vapour pressure deficit, and soil moisture for specific pixels, which limits the accuracy of MOD17 GPP estimations.

Only PAR absorbed by chlorophyll is used for photosynthesis (Zhang *et al.*, 2005). Therefore, the presence of non-photosynthetic biomass, including leaf tissue, in the canopy has been shown to significantly overestimate the value of $fPAR$. Therefore, developing the research of Zhang *et al.* (2005, 2009), who using an RTM partitioned

$fPAR_{\text{chlorophyll}}$ from $fPAR$, will permit the possibility of deriving $fPAR_{\text{chlorophyll}}$ based on canopy chlorophyll content as estimated using MTCI. Such theoretical applications are the first step in defining an integrated approach to estimate GPP using chlorophyll content data.

6.6 Conclusions

This investigation has trialled a number of approaches to the use of MTCI data for the estimation of GPP over a number of contrasting cover types. Ameriflux data were used to provide ground eddy flux covariance methods to estimate GPP, thus allowing the relationship between MTCI and flux tower GPP to be established. Utilising flux tower measurements of PAR (day time only) and MOD15 estimates of $fPAR$, different approaches were used to establish a robust estimation of GPP across four contrasting cover types. The MTCI*PAR method to estimate GPP as used by Gitelson *et al.* (2006) and Wu *et al.* (2009) demonstrated a relatively strong correlation with flux tower GPP. The results were in line with Wu *et al.* (2009) where they successfully estimated GPP in a variety of corn canopies. This approach therefore allows the potential to estimate GPP for a number of contrasting cover types. However, the relationship between MTCI and flux tower GPP is stronger than that derived using the MTCI*PAR model; simple linear regression analysis showed an R^2 of 0.73 compared to 0.63 when data from all sites and both years were included. The accuracy of the MTCI*PAR model was increased when only PAR absorbed by the canopy was incorporated into the model. MTCI*APAR (where $APAR = (PAR * fPAR)$) proved to be the best model to estimate GPP in most of the study sites, and provided the best predictions of GPP when considering all data.

The simple model, $GPP = 0.004 * (MTCI * (PAR * fPAR)) + 0.057$, is based on the hypothesis that chlorophyll content is a proxy for LUE. The relationship between MTCI*APAR and GPP indicates that the method is not cover type specific. Further work will need to be carried out to determine whether variation in canopy chlorophyll content can successfully account for vegetation stress and therefore limit the need for additional inputs that characterise environmental conditions. The $GPP = MTCI * (fPAR * PAR)$ model accounts successfully for short-term variation in PAR that can effect photosynthetic rates that limit the use of VI alone in GPP estimations.

Chapter 6. Relationship between GPP and MTCI in various ecosystems

The benefit of the model is that it is based on minimal inputs and easy to derive compared to MOD17, which is dependent on several meteorological datasets to estimate GPP. For the study sites used, our model showed an increased accuracy of GPP estimation across all four contrasting cover types when compared to MOD17 product. Such results demonstrate the potential of GPP estimates using MTCI data and APAR. Further work is required to develop a suitable method to estimate GPP using the MTCI*APAR model given there is no current high resolution PAR product.

CHAPTER 7: THESIS SUMMARY

Chapter 7

The focus of the first half of this thesis has been to assess the effects of canopy and non-canopy variables on the MTCI and examine the relationship between canopy chlorophyll content and MTCI through laboratory based spectroscopy and field based validation. Such findings have been applied to provide an insight into the potential of the MTCI to monitor vegetation dynamics at the local – global scales; specifically vegetation phenology and ecosystem gross primary productivity; which is the focus of the second half of the thesis. This chapter draws the main conclusions from the work presented in Chapters 3 – 6, with a specific view of assessing the objectives of the research stated in Chapter 1.

7.1 Summary of work

Chapter 2 has provided a review of the methods traditionally applied to the estimation of chlorophyll content from remote sensing data. The limitations of these are discussed and the requirements for a novel approach for the estimation of chlorophyll content introduced. As a result of the limitations of existing techniques to estimate chlorophyll content at the regional to global scales the MTCI was developed (Curran and Dash, 2005). Optimising the unique spectral resolution of the MERIS sensor, with reflectance measured in narrow wavebands positioned in the red / NIR regions, the MTCI is positively related to canopy chlorophyll content, a function of foliar chlorophyll concentration and canopy LAI. Initial validation and application of the MTCI has demonstrated a strong correlation with canopy chlorophyll content and has proved sensitive to variation in chlorophyll content. The MTCI has also been shown to provide estimates of canopy chlorophyll content in areas of high biomass that REP and other VIs, such as the NDVI often saturate (Curran and Dash, 2005). The potential of the MTCI to monitor regional – global vegetation dynamics (vegetation condition, stress and productivity) is currently in its infancy, partly due to the lack of validation across a variety of land cover types and operational conditions. Such a point was addressed in Chapters 3 and 4; which explored the relationship between MTCI and foliar / canopy chlorophyll content and the effects of canopy and non-canopy variables on this relationship. Laboratory spectroscopy was used to investigate the relationship between MTCI and chlorophyll content whilst assessing the effect of

view angle geometry and background reflectance on the MTCI.

Validation of the MTCI was necessary to determine the accuracy of data products, in so allowing the delivery of accurate products to the user community. Chapter 4 outlined procedures that permitted the validation of the MTCI in heterogeneous woodland and agricultural study areas.

Chapter 5 focused on the potential of the MTCI to monitor vegetation phenology for contrasting land cover types in the New Forest National Park. The sensitivity of the MTCI to seasonal variations in estimated chlorophyll content meant that variations in vegetation phenology could be identified between growing seasons for both woodland and grass and heathland study areas. The influence of seasonal climate variability on vegetation phenology was assessed through the comparison of temporal MTCI profiles. It was established that mean seasonal temperature was strongly correlated with MTCI, suggesting that vegetation adapts to climate variability through adjusting foliar chlorophyll content and the timing of key phenological transitions, i.e. greenup, maturity, senescence and dormancy. The MTCI proved a robust tool for estimating phenological variation between growing seasons, inferring that growing season length increased as a result of elevated autumnal mean temperature observed during 2006. Similarly, an early greenup was inferred in the temporal MTCI profile, supporting meteorological records and point-based ground observations of tree phenology made by the UK Phenology Network.

Canopy chlorophyll content is closely related to vegetation productivity (Gitelson *et al.*, 2006), therefore the relationship between MTCI – chlorophyll content provided an opportunity to investigate temporal variation in GPP. Flux tower estimates of GPP were highly correlated with MTCI for a number of vegetation types, suggesting that estimating chlorophyll content over the growing season provided accurate estimates of ecosystem productivity. Only PAR absorbed by chlorophyll is used for photosynthesis, and chlorophyll is the key ingredient in photosynthesis, the temporal variability in canopy chlorophyll content can be used to estimate vegetation productivity. Coupling the temporal variation in both MTCI with fluctuation in APAR provided an opportunity to produce a simple model that will account for both variations in both canopy chlorophyll content and incident radiation. Such a model

provided better correlation with ecosystem GPP compared to MTCI, MTCI*PAR and the standard MOD17 GPP product.

7.2 Objectives of the thesis

The principal objectives of the research were stated in Chapter 1 as:

1. Assessing the MTCI – chlorophyll content relationship and the effects of illumination geometry and soil background reflectance on this relationship.
2. Development and application of validation procedure to assess the relationship between MTCI and chlorophyll content in woodland and agricultural regions.
3. The characterization and analysis of vegetation dynamics using MTCI over a number of growing seasons for a variety of contrasting vegetation types.

The following sections assess the accomplishment of these objectives in this thesis. A discussion of the key issues associated with each is provided, and conclusions are drawn.

Objective 1: Explaining the relationship between MTCI and chlorophyll content and the effect of viewing geometry and background reflectance on this relationship.

The relationship between MTCI and chlorophyll content was thoroughly investigated in Chapters 3 and 4. In these chapters the effects of vegetation type as well as a number of canopy and viewing variables were investigated. The linear response of the MTCI to canopy chlorophyll content was demonstrated, supporting initial findings of Curran and Dash (2005). The research investigated spinach, woodland and agricultural crops, demonstrating the sensitivity of the MTCI to estimate chlorophyll content across a wide range in chlorophyll contents.

Bringing together the results from the laboratory and validation exercises, it was demonstrated that the relationship between chlorophyll content and MTCI is affected by vegetation structure, although analysis of results as detailed in Chapter 4 suggest

the effect is limited. When considering the relationship between MTCI and chlorophyll content for all vegetation types investigated in those chapters, the correlation between MTCI and chlorophyll content was still strong ($R^2=0.60$). Such findings suggest that the MTCI is a valuable tool in estimating chlorophyll content for a range of vegetation types. Such a characteristic allows temporal and spatial comparisons in vegetation health and status to be made.

Laboratory experiments were designed to assess the influence of both variation in viewing geometry and background reflectance on the relationship between MTCI and chlorophyll content. Statistically, it was shown that variation in viewing geometry did not significantly influence the MTCI – chlorophyll content relationship. Similarly, for a spinach canopy, it was shown soil reflectance properties did not significantly affect the ability of the MTCI to estimate canopy chlorophyll content. However, bare soil reflectance was shown to influence MTCI, whereby all soils except white, resulted in positive MTCI values. The Booms Barn site included a number of fields without significant vegetation cover. It was shown that bare soil resulted in MTCI values that were higher than expected. However, the effects of background reflectance were readily compounded as vegetation cover increased. Objective 1 can be fulfilled with the findings of Chapters 3 and 4.

Objective 2: Development and application of procedure to validate MTCI in woodland and agricultural study areas.

The robust relationship between MTCI and chlorophyll content has been established, coupling the MTCI to a measurable canopy variable permits the evaluation and quality control of the index through validation. Validation is necessary to assess the accuracy of satellite products and deliver accurate products to the user community. The MTCI was validated using two approaches:

New Forest validation used high-resolution aerial imagery to derive a transfer function to produce a chlorophyll map of the woodland study area. A very strong relationship between high resolution CASI MTCI, 300m CASI MTCI and chlorophyll content was observed. The scaling up of the chlorophyll map allowed the relationship between canopy chlorophyll content and ‘full resolution’ MTCI to be investigated.

Chapter 7. Thesis summary

The coefficient of determination between ‘full resolution’ MTCI and the 300m chlorophyll map was weaker than those derived from CASI-2 imagery. The geolocation of the MERIS imagery and radiometric characteristics between MERIS and CASI-2 may help explain the variability in the relationships.

Direct MTCI validation, employed at the Brooms Barn site as a result of cloud shadow in the high resolution aerial imagery, established the relationship between MTCI and chlorophyll content in crops a range of crop types. Results highlighted the ability of the MTCI to successfully estimate chlorophyll content for a range of chlorophyll content in both woodland and agricultural study areas.

The validation methods employed were successful in scaling up field chlorophyll content measurements, accounting for heterogeneity in chlorophyll content across the 3 x 3 km study sites, allowing the assessment of the accuracy of the MTCI. The findings from Chapter 4 fulfil research Objective 2.

Objective 3: Characterisation and analysis of vegetation dynamics using the MTCI

The conclusions drawn from Chapters 3 and 4 suggest that the MTCI is sensitive to a range of chlorophyll content for different vegetation types, whereby canopy structure exerts a limited influence. The experiments show that the effect of view angle and background reflectance has no significant statistical effects on the MTCI. Such conclusions suggest that the MTCI demonstrates the required properties to be a robust global product, allowing precise and consistent, spatial and temporal comparisons of vegetation conditions. Such properties coupled with the orbiting characteristics of MERIS provide the potential to monitor vegetation dynamics with a high temporal resolution.

The strong relationship with a biophysical canopy permits the use of the MTCI to monitor temporal vegetation dynamics providing information on vegetation condition, health and status throughout the growing season. Such conclusions demonstrate the suitability of the MTCI as a tool to infer the phenological characteristics of both mixed woodland and grass and heathland study sites over the duration of a growing season. Changes in chlorophyll content throughout the growing season can be

estimated from temporal MTCI composites, chronologically stacked to cover the growing season.

The MTCI is sensitive to a range of chlorophyll contents, allowing the identification of canopy greenup as well as pigment breakdown associated with autumnal senescence. The MTCI has proven useful for estimating seasonal variation in chlorophyll content of both woodland canopies and heath and grassland. Due to the lack of ground based validation data the MTCI temporal profiles for the growing seasons 2003 – 2007 were compared against the three independent data sources commonly used to infer vegetation phenology; these were (i) MODIS NDVI (ii), MODIS EVI and (iii) phenological observations made by the UK Phenology Network. The results demonstrate the sensitivity of the MTCI in estimating change in foliar chlorophyll during late summer, earlier than the onset of senescence as observed by changes in plant structure and physiology as determined through field observations (phenology networks). However, the MTCI mirrors the results of the UK Phenology Network, which showed both the extended growing season of 2006 and the early greenup of 2007, which were a result of variation in seasonal temperature. Such results suggest that the MTCI would be useful for assessing canopy productivity and therefore changes in ecosystem productivity as a function of climatic variability. Such findings provided the opportunity to estimate ecosystem gross primary productivity for a range of vegetation types. Chapters 5 and 6 have demonstrated the potential of the MTCI to estimate vegetation dynamics, characterising the temporal characteristics in both phenology and GPP through estimation of canopy chlorophyll content, therefore fulfilling Objective 3.

7.3 Limitations and uncertainties introduced by experimental design

Limitations have been addressed in previous sections, and therefore will not be thoroughly discussed at this point. However, it is worth noting that the experimental approach employed in this study (rather than modeling techniques) does have limitations. The approach used in this thesis to understand the relationship between MTCI and chlorophyll content was limited in addressing the influence of both canopy and non-canopy variables that may influence such a relationship. The laboratory experiments (chapter three) employed variable application of fertilizer to explore LAI variation and the extent to which MTCI - chlorophyll content is affected. Further research will be necessary to understand the effect of increase LAI on MTCI due to the limited influence the fertilizer had on spinach LAI. Furthermore, due to the experimental approach employed, it was not possible to control LAI whilst maintaining total canopy chlorophyll content. Therefore, although results suggest LAI does not influence MTCI (where chlorophyll content is constant), the results are inconclusive. MTCI was shown to have limited sensitivity to variation in viewing geometry ($\pm 30^\circ$ in the principal plane). Although statistical analysis suggested such sensitivity was insignificant, the MTCI did show more sensitivity to viewing geometry than other VI to which it was compared. A number of studies have shown that viewing geometry leads to significant variation in NDVI, especially in open canopies, therefore field experiments utilizing aerial imagery will go some way to understand the operational effects of viewing geometry on the MTCI.

Limitations to the approach used in chapter four have already been addressed, however, the SunScan instrument used to estimate LAI at the woodland validation site could influence error that may subsequently influence the MTCI – chlorophyll content relationship. Alternative methods that have been proved to be robust in estimating LAI in woodland environments would have added extra confidence to results. Similarly the sampling strategy used in heterogeneous canopies as part of the field validation of the MTCI was dependent on personal judgment regarding the location of measurements within each ISU. Such a method may not be the most suitable approach to represent the variation in both LAI and chlorophyll concentration within each ISU.

7.4 Principal contributions

This thesis has made contributions to the fields of estimating canopy chlorophyll content utilising the MTCI, validation methodology of standard products at the scale of ‘moderate resolution’ satellites and study of ecosystem dynamics. Such contributions have been the basis for research presented in conference proceedings and journal papers (Appendix 4).

Multi-scale MTCI validation is an important step in understanding the relationship between MTCI and canopy variables. The finding in this thesis relating to the influence of background reflectance on the MTCI will have implication for the estimation of chlorophyll content using not only the current MERIS sensor, but also the future ESA Sentinel missions. Sentinel 2 data will have the MTCI as a standard Level 2 product, providing the opportunity to estimate chlorophyll content at the spatial resolution of 30 meters. An understanding of the influence of soil reflectance will be relevant to the interpretation of MTCI at higher spatial resolution in open canopies, where the likelihood of soil / background composing a significant proportion of the pixel is greater. Within open canopies, the contribution of background reflectance at the 30 metre pixel resolution will be a greater consideration than at the 300 metre pixel resolution of MERIS. The finding in this thesis relating to the MTCI value of bare soil will also be important when studying vegetation dynamics in an agricultural context using MTCI, where bare soil will be present prior to crop growth at the start of the growing season.

This research has contributed to the field of understanding vegetation dynamics through the estimation of chlorophyll content. The sensitivity of the MTCI to variation in canopy chlorophyll content permits key phenological transition phases to be monitored. Comparing the MTCI with other VI used to estimate vegetation phenology, it was shown that the MTCI was able to successfully monitor the changes in growing season length that were a result of variation in seasonal mean temperature. The MTCI, being coupled to key biochemical variables, provides the ability to monitor vegetation dynamics with spatial and temporal consistency and is vitally important to the field of global change research. Chapter 6 introduced novel approaches to estimate GPP using the MTCI. The ability to estimate vegetation productivity is of vital importance to

understand changes in carbon budgets due to changes in global climate. The models utilizing the MTCI and PAR have been shown to provide more reliable estimates of GPP compared to MOD17 GPP product. The relationship between $MTCI \cdot APAR$ and GPP indicates that the method is not cover type specific, permitting the temporal and spatial monitoring of vegetation productivity. The benefit of the model is that it is based on minimal inputs and is easy to derive compared to MOD17, which is dependent on a number of meteorological datasets to estimate GPP.

7.5 Further Research

The work documented in this thesis has show the provision of the MTCI to estimate chlorophyll content for a range of chlorophyll contents from a number of contrasting vegetation types. This research has shown the MTCI as a useful and sensitive tool for the estimation of chlorophyll content throughout the growing season and demonstrated the potential to use the MTCI to monitor vegetation phenology and drive GPP ecosystem models. The research has identified exciting new avenues of research that would provide an opportunity to develop our understanding of vegetation dynamics at the local to global scales.

The experimental approach to investigate the effect of canopy variables on the MTCI did not provide the complete understanding of the effects of canopy LAI on the MTCI. Although laboratory results suggest the influence is limited, further research is required to thoroughly explore the effects of increasing canopy LAI whilst maintaining constant canopy chlorophyll content. Canopy modelling provides an opportunity to identify the effects of variation in LAI and canopy structure on the MTCI.

The ability to estimate ecosystem GPP from MTCI is an exciting opportunity. Further research is required to assess whether the model developed in Chapter 6 can be transferred to estimate GPP at other sites. This 'validation' is possible using the other flux sites to provide GPP measurements with which to correlate $MTCI \cdot APAR$ estimates. However, a major limiting factor in the further development of such a model would be the remotely sensed estimates of PAR. Top of atmosphere radiance and surface incident PAR based on an atmospheric radiative transfer model provides

one avenue to explore to derive a PAR product with suitable spatial resolution. This method was adopted by Liang *et al.* (2006) to estimate PAR at 1 km using MODIS data. The adoption of such a technique to estimate PAR for the inclusion in the MTCI*APAR model is the necessary step to develop the model further.

Developing the research of Zhang *et al.*, (2005, 2009), who using RTM partitioned $fPAR_{\text{chlorophyll}}$ from $fPAR$, will permit the possibility of deriving $fPAR_{\text{chlorophyll}}$ based on canopy chlorophyll content as estimated using MTCI. Research identifying the relationship between APAR and chlorophyll content could eliminate the effect of non-photosynthetic biomass, including leaf tissue, in the canopy that has been shown to significantly overestimate the value of $fPAR$. Such theoretical applications are an important step in defining an approach to estimate GPP using chlorophyll content data.

7.6 Concluding comments

This thesis has demonstrated the MTCI to be a valuable tool in estimating vegetation dynamics across multiple cover types, independent of variations in view geometry and soil background. The robust relationship between MTCI and chlorophyll content provides the opportunity to monitor variations in both vegetation phenology and gross primary productivity. The MTCI offers a macroscopic view of temporal vegetation dynamics, offering the opportunity to understand the effect that climate change is having on the health of our planet.

REFERENCES

References

AHL, D. E., GOWER, S. T., *et al.* (2006). Monitoring spring canopy phenology of a deciduous broadleaf forest using MODIS. *Remote Sensing of Environment***104**, 88-95.

APARICIO N., VILLEGAS, D., ROYO C., *et al.* (2004). Effect of sensor view angle on the assessment of agronomic traits by ground level hyperspectral reflectance measurements in durum wheat under contrasting Mediterranean conditions. *International Journal of Remote Sensing*, **25**, 1131 – 1152.

ARORA, V. K. and BOER, G. J. (2005). A parametrization of leaf phenology for the terrestrial ecosystem component of climate models. *Global Change Biology***11**, 39-59.

ASNER, G. P., BRASWELL, B. H., *et al.* (1998). Ecological research needs from multiangle remote sensing data. *Remote Sensing of Environment*,**63**, 155-165.

ASNER, G. P. (1998). Biophysical and biochemical sources of variability in canopy reflectance. *Remote Sensing of Environment*, **64**, 234-253.

ASNER, G.P. (2000), Contributions of multi-view angle remote sensing to land-surface and biogeochemical research. *Remote Sensing Reviews*, **18**, 137–162.

ASNER, G. P., WESSMAN, C. A. *et al.* (1998). Variability in leaf and litter optical properties: Implications for BRDF model inversions using AVHRR, MODIS, and MISR. *Remote Sensing of Environment*,**63**, 243-257.

ASRAR, G. (1998). Biophysical and biochemical sources of variability in canopy reflectance. *Remote Sensing of Environment*, **64**, 234-253.

ASRAR, G., MYNENI, R. B. *et al.* (1997). Enhanced plant growth in the northern high latitudes from 1981-91. *Physical Measurements and Signatures in Remote Sensing*, **2**, 623-627.

ASRAR, G., MYNENI, R. B., *et al.* (1992). Spatial heterogeneity in vegetation canopies and remote-sensing of absorbed photosynthetically active radiation - a modeling study. *Remote Sensing of Environment*,**41**, 85-103.

References

ASRAR, G., MYNENI, R. M., and KANEMASU, E. T. (1989), Estimation of plant canopy attributes from spectral reflectance measurements. In *Theory and Applications of Optical Remote Sensing*, 252–296, Wiley, New York.

BACOUR, C., BREON, F. M., *et al.* (2006). Normalization of the directional effects in NOAA-AVHRR reflectance measurements for an improved monitoring of vegetation cycles. *Remote Sensing of Environment*, **102**, 402-413.

BACOUR, C., BARET, F., *et al.* (2006a). Neural network estimation of LAI, faPAR, fcover and LAI x C (ab), from top of canopy MERIS reflectance data: Principles and validation. *Remote Sensing of Environment* **105**, 313-325.

BADECK, F. W., BONDEAU, A., *et al.* (2004). Responses of spring phenology to climate change. *New Phytologist*, **162**, 295-309.

BANNARI, A., STAENZ, K., *et al.* (2006). Sensitivity analysis of chlorophyll indices to soil optical properties using ground-reflectance data. 2006 *IEEE International Geoscience and Remote Sensing Symposium*, **1**, 120-123.

BANNARI, A., KHURSHID, K. S., *et al.* (2007). A comparison of hyperspectral chlorophyll indices for wheat crop chlorophyll content estimation using laboratory reflectance measurements. *IEEE Transactions on Geoscience and Remote Sensing* **45**, 3063-3074.

BANNARI, A., KHURSHID, K.S., STAENZ, K., and SCHWARZ, J. (2008) Potential of Hyperion EO-1 hyperspectral data for wheat crop chlorophyll content estimation. *Canadian Journal of Remote Sensing*, **34**, 139-157.

BARET, F., and FOURTY, T. (1997). Radiometric estimates of nitrogen status of leaves and canopies. In G. Lemaire (Ed.), *Diagnosis of Nitrogen Status in Crops*, 201–227, SpringerVerlag, Berlin.

References

BARET, F., and GUYOT, G. (1991). Potentials and limits of vegetation indexes for LAI and APAR assessment. *Remote Sensing of Environment*, **35**, 161–173.

BARET, F., JACQUEMOUD, S., GUYOT, G., and LEPRIEUR, C. (1992), Modeled analysis of the biophysical nature of spectral shifts and comparison with information content of broad bands. *Remote Sensing of Environment*, **41**, 133–142.

BARET, F., MORISSETTE, J.T., FERNANDES, R.A., CHAMPEAUX, J.L., MYNENI, R.B., CHEN, J., PLUMMER, S., WEISS, M., BACOUR, C., GARRIGUES, S., and NICKESON, J.E. (2006). Evaluation of the representativeness of networks of sites for the global validation and intercomparison of land biophysical products: Proposition of the CEOS-BELMANIP. *IEEE Transactions on Geoscience and Remote Sensing*, **44**, 1794-1802.

BARET, F., WEISS, M., ALLARD, D., GARRIGUES, S., LEROY, M., JEANJEAN, H., *et al.* (in press) VALERI: a network of sites and a methodology for the validation of medium spatial resolution land satellite products. *Remote Sensing of Environment*.

BARTON, C. V. M. and NORTH, P. R. J. (2001). Remote sensing of canopy light use efficiency using the photochemical reflectance index. Model and sensitivity analysis. *Remote Sensing of Environment*. **78**, 264-273.

BASSOW, S. L. and BAZZAZ, F. A. (1998). How environmental conditions affect canopy leaf-level photosynthesis in four deciduous tree species. *Ecology* **79**, 2660-2675.

BEISL, U. (2001). A new method for correction of bidirectional effects in hyperspectral imagery. *Proceedings: International Workshop on Spectroscopy Application in Precision Farming*, Freising-Weihenstephan.

BINDI, M., HACOUR, A., *et al.* (2002). Chlorophyll concentration of potatoes grown under elevated carbon dioxide and/or ozone concentrations. *European Journal of Agronomy*, **17**, 319-335.

References

BLACKBURN, G. A. (1999). Relationships between spectral reflectance and pigment concentrations in stacks of deciduous broadleaves. *Remote Sensing of Environment*, **70**, 224-237.

BLACKBURN, G. A. and MILTON, E. J. (1995). Seasonal-variations in the spectral reflectance of deciduous tree canopies. *International Journal of Remote Sensing*, **16**, 709-720.

BLACKBURN, G. A. and PITMAN, J. I. (1999). Biophysical controls on the directional spectral reflectance properties of bracken (*Pteridium aquilinum*) canopies: results of a field experiment. *International Journal of Remote Sensing*, **20**, (11) 2265-2282.

BOISVENUE, C. and RUNNING, S. W. (2006). Impacts of climate change on natural forest productivity - evidence since the middle of the 20th century. *Global Change Biology*, **12**, 862-882.

BONHAM-CARTER, G. F. (1988). Numerical procedures and computer program for fitting an inverted Gaussian model to vegetation reflectance data. *Computers and Geosciences*, **14**, 339-356.

BOYD, D. S. and DANSON, F. M. (2005). Satellite remote sensing of forest resources: three decades of research development. *Progress in Physical Geography*, **29**, 1-26.

BRADLEY, B.A., JACOB, R.W., HERMANCE, J.F., *et al.* (2006). A curve fitting procedure to derive inter-annual phenologies from time series of noisy satellite NDVI data. *Remote Sensing of Environment*, **106**, **2**, 137-145.

CROXTON, P.J., HUBER, K., COLLINSON, N. and SPARKS, T. (2006). How well do the Central England temperature and the England and Wales precipitation series represent the climate of the UK? *International Journal of Climatology*, **26**, 2287-2292.

References

CANNELL, M. G. R. and SMITH, R. I. (1983). Thermal time, chill days and prediction of budburst in *Picea-sitchensis*. *Journal of Applied Ecology***20**, 951-963.

CARTER, G. A. (1994). Ratios of leaf reflectances in narrow wavebands as indicators of plant stress. *International Journal of Remote Sensing*, **15**, 697– 704.

CARTER, G. A. and SPIERING, B. A. (2002). Optical properties of intact leaves for estimating chlorophyll concentration. *Journal of Environmental Quality*,**31**, 1424-1432.

CHO, M. A. and SKIDMORE, A. K. (2006). A new technique for extracting the red edge position from hyperspectral data: The linear extrapolation method. *Remote Sensing of Environment*,**101**, 181-193.

CHEN, X. Q., HU, B., *et al.* (2005). Spatial and temporal variation of phenological growing season and climate change impacts in temperate eastern China. *Global Change Biology*,**11**, 1118-1130.

CHENG, Q. (2006). Multisensor comparisons for validation of MODIS vegetation indices. *Pedosphere*,**16**, 362-370.

CHENG, Y. F., GAMON, J. A., *et al.* (2006). A multi-scale analysis of dynamic optical signals in a Southern California chaparral ecosystem: A comparison of field, AVIRIS and MODIS data. *Remote Sensing of Environment*,**103**, 369-378.

CLELAND, E. E., CHUINE, I., *et al.* (2007). Shifting plant phenology in response to global change. *Trends in Ecology and Evolution*,**22**, 357-365.

CLEVERS, J. G. P. W., DE JONG, S. M., *et al.* (2001). MERIS and the red-edge position. *International Journal of Applied Earth Observation and Geoinformation*,**3**, 313-320.

References

CLEVERS, J., DE JONG, S. M., *et al.* (2002). Derivation of the red edge index using the MERIS standard band setting. *International Journal of Remote Sensing*, **23**, 3169-3184.

COA, M.K. and WOODWARD, F. (1998). Dynamic responses of terrestrial ecosystem carbon cycling to global climate change, *Nature*, **393**, 249-252.

COHEN, W. B. and JUSTICE, C. O. (1999). Validating MODIS terrestrial ecology products: Linking in situ and satellite measurements. *Remote Sensing of Environment*, **70**, 1-3.

COHEN, W. B., MAIERSPERGER, T. K., *et al.* (2003). Comparisons of land cover and LAI estimates derived from ETM plus and MODIS for four sites in North America: a quality assessment of 2000/2001 provisional MODIS products, *Remote Sensing of Environment*, **88**, 233-255.

COPPIN, P., NACKAERTS, K., QUEEN, L., and BREWER, K. (2001). Operational monitoring of green biomass change for forest management. *IEEE Transactions on Geoscience and Remote Sensing*, **67**, 603-611.

CURRAN, P. J. (1988). The semivariogram in remote-sensing - an introduction. *Remote Sensing of Environment*, **24**, 493-507.

CURRAN, P. J. (1989). The remote sensing of foliar chemistry, *Remote Sensing of Environment*, **30**, 271-278.

CURRAN, P. J. (1994). Imaging spectrometry. *Progress in Physical Geography*, **18**, 247-266.

CURRAN, P. J. (2001). Imaging spectrometry for ecological applications. *International Journal Applied Earth Observation and Geoinformation*, **3**, 305-312.

CURRAN, P. J., DUNGAN, J. L., *et al.* (1990). Exploring the relationship between reflectance red edge and chlorophyll content in slash pine. *Tree Physiology*, **7**, 33-48.

References

CURRAN, P. J., DUNGAN, J. L., *et al.* (1991). The effect of a red leaf pigment on the relationship between red edge and chlorophyll concentration. *Remote Sensing of Environment*,**35**, 69-76.

CURRAN, P.J. and DASH, J. (2005). Algorithm Theoretical Basis Document (ATBD), chlorophyll index. European Space Agency, Noordwijk, The Netherlands, (Version 2.2).

CURRAN, P. J., DASH, J., *et al.* (2007). Indian Ocean tsunami: The use of MERIS (MTCI) data to infer salt stress in coastal vegetation. *International Journal of Remote Sensing*,**28**, 729-735.

CURRAN, P. J., DUNGAN, J. L., *et al.* (2001). Estimating the foliar biochemical concentration of leaves with reflectance spectrometry testing the Kokaly and Clark methods. *Remote Sensing of Environment*,**76**, 349-359.

CURRAN, P. J. and STEELE, C. M. (2005). MERIS: the re-branding of an ocean sensor. *International Journal of Remote Sensing*,**26**, 1781-1798.

DANGEL, S., VERSTRAETE, M. M., *et al.* (2005). Toward a direct comparison of field and laboratory goniometer measurements. *IEEE Transactions on Geoscience and Remote Sensing*, **43**,2666-2675.

DANSON, F. M. and PLUMMER, S. E.(1995). Red edge response to forest leaf area index. *International Journal of Remote Sensing*,**16**, 183-188.

DASH, J. and CURRAN, P. J. (2004). The MERIS terrestrial chlorophyll index. *International Journal of Remote Sensing*,**25**, 5403-5413.

DASH, J. and CURRAN, P.J. (2006). Validation procedure for the MERIS Terrestrial Chlorophyll Index (MTCI). *Proceedings of the Second Working Meeting on MERIS and AATSR Calibration and Geophysical Validation (MAVT-2006)*, Frascati, Italy (CD-ROM), Noordwijk, The Netherlands.

References

DASH, J. and CURRAN., P.J. (2006). Relationship between herbicide concentration during the 1960s and 1970s and the contemporary MERIS Terrestrial Chlorophyll Index (MTCI) for Southern Vietnam. *International Journal of Geographical Information Science*,**20**, 929-939.

DASH, J. and CURRAN, P.J. (2009). The relationship between MTCI and terrestrial chlorophyll content. *International Journal of Remote Sensing*, **29**, (in press).

DASH, J., MATHUR, A., FOODY, G. M., CURRAN, P. J., CHIPMAN, J. and LILLESAND, T. M.(2007b), Landcover classification using multi-temporal MERIS vegetation indices. *International Journal of Remote Sensing*, **28**, 1137-1159.

DASH, J., CURRAN, P. J., TALLIS, M. J., LLEWELLYN, G. M., TAYLOR, G. and SNOEIJ, P.(2007a), The relationship between the MERIS Terrestrial Chlorophyll Index and chlorophyll content, *Second Envisat Symposium*. European Space Agency, Noordwijk. (ESA SP- 636) (CD ROM).

DASH, J. and CURRAN, P. J.(2007). Relationship between the MERIS vegetation indices and crop yield for the state of South Dakota, USA. *Second Envisat Symposium*. European Space Agency, Noordwijk. (ESA SP- 636) (CD ROM).

DASH, J. and CURRAN, P.J.(2007). Evaluation of the MERISterrestrial chlorophyll index (MTCI). *Advances in Space Research*,**39**, 100-104.

DASH, J., P. J. CURRAN, *et al.* (2009). Remote sensing of terrestrial chlorophyll content. In *Global Climatology and Ecodynamics*, (Cracknell, A., Krapivin, V.F., Varotsos, C.A., eds. Springer Praxis Books, Chichester. 77-105.

DAUGHTRY, C. S. T., WALTHALL, C. L., *et al.* (2000). Estimating corn leaf chlorophyll concentration from leaf and canopy reflectance. *Remote Sensing of Environment*,**74**,229-239.

References

DAVIDS, C. and TYLER, A.N.(2003). Detecting contamination-induced tree stress within the Chernobyl exclusion zone. *Remote Sensing of Environment*, 85, 30-38.

DAWSON, T. P. and CURRAN, P. J.(1998). A new technique for interpolating the reflectance red edge position. *International Journal of Remote Sensing*,**19**, 2133-2139.

DAWSON, T.P., CURRAN, P.J., NORTH, P.R.J. and PLUMMER, S.E. (1999). The propagation of foliar biochemical absorption features in forest canopy reflectance: A theoretical analysis. *Remote Sensing of Environment*, **67**, 147-159.

DAWSON, T. P. (2000). The potential for estimating chlorophyll content from a vegetation canopy using the Medium Resolution Imaging Spectrometer (MERIS). *International Journal of Remote Sensing*,**21**, 2043-2051.

DAWSON, T. P., NORTH, P. R. J. PLUMMER, S. E. and CURRAN,P. J. (2003). Forest ecosystemchlorophyll content: implications for remotely sensed estimates of net primaryproductivity. *International Journal of Remote Sensing*,**24**, 611-617.

DELWARD, S., PREUSKER, R., BOURG, L., SANTER, R., RAMON, D. and FISCHER, J. (2007). MERIS in flight calibration. *International Journal of Remote Sensing*, **28**, 479-496.

DENG, F.P., SU, G.L. and LIU, C.(2007). Seasonal variation ofMODIS vegetation indexes and their statistical relationship withclimate over the subtropic evergreen forest in Zhejiang, China.*IEEE Geoscience and Remote Sensing Letters*, **4**, 236-240.

DENMAN, K.L., G. BRASSEUR, A. CHIDTHAISONG, P. CIAIS, *et al.*(2007). Couplings Between Changes in the Climate System and Biogeochemistry. In: *Climate Change 2007: The Physical Science Basis. Contribution of Working Group I to the Fourth AssessmentReport of the Intergovernmental Panel on Climate Change*. Solomon, S., Qin, D., Manning, M., Chen, Z., Marquis, M., Averyt, K.B., Tignor, M. and Miller, H.L. (eds.). Cambridge University Press, Cambridge, New York.

DIXON, K. R. (1976). Analysis of seasonal leaf fall in north temperate deciduousforests. *Oikos*, **27**, 300-312.

References

DIXON, R.K., S. BROWN, R. A. HOUGHTON, A. M. SOLOMON, M. C. TREXLER and WISNIEWSKI, J. (1994). Carbon pools and flux of global forest ecosystems. *Science*, 263, 185-190.

DEMAREZ, V. and GASTELLU-ETCHEGORRY, J. P. (2000). A modeling approach for studying forest chlorophyll content. *Remote Sensing of Environment*, **71**, 226-238.

DORIGO, W., GERIGHAUSEN, H., and BORG, E. (2008). Automated retrieval of biophysical and biochemical canopy variables: an example based on AHS data from the AGRISAR campaign. *AGRISAR and EAGLE Campaigns Final Workshop*, ESA/ESTEC Noordwijk, The Netherlands, 15-16 October 2007, CD-ROM.

DUCHEMIN, B. and MAISONGRANDE, P. (2002). Normalisation of directional effects in 10-day global syntheses derived from VEGETATION/SPOT: I. Investigation of concepts based on simulation. *Remote Sensing of Environment*, **81**, 90-100.

DUCHEMIN, B. (1999). NOAA/AVHRR bidirectional reflectance: modelling and application for the monitoring of a temperate forest. *Remote Sensing of Environment*, **67**, 51-67.

EITEL, J. U. H., LONG, D. S., *et al.* (2007). Using in-situ measurements to evaluate the new rapideye (TM) satellite series for prediction of wheat nitrogen status. *International Journal of Remote Sensing*, **28**, 4183-4190.

ESPAÑA-BOQUERA, M.L. *et al.* (2006) Estimating the nitrogen concentration of strawberry plants from its spectral response. *Communications in Soil Science and Plant Analysis*, **37**, 2447-2459.

ESRI, (1999), *ESRI data and maps*, ESRI, Redlands, CA.

References

FILELLA, I. A. and PENUELAS, J. (1994). The red edge position and shape as indicator of plant chlorophyll content, biomass and hydric status. *International Journal of Remote Sensing*, **15**, 1459-1470.

FISHER, J. I. and MUSTARD, J. F. (2007). Cross-scalar satellite phenology from ground, Landsat, and MODIS data. *Remote Sensing of Environment*, **109**, 261-273.

FISHER, J. I., RICHARDSON, A. D., *et al.* (2007). Phenology model from surface meteorology does not capture satellite-based greenup estimations. *Global Change Biology*, **13**, 707-721.

FISHER, J. I., MUSTARD, J. F., *et al.* (2006). Green leaf phenology at Landsat resolution: Scaling from the field to the satellite. *Remote Sensing of Environment*, **100**, 265-279.

FOODY, G. M., BOYD, D. S., *et al.* (2003). Predictive relations of tropical forest biomass from Landsat TM data and their transferability between regions. *Remote Sensing of Environment* **85**, 463-474.

FOODY, G.M. and DASH, J. (2007) Discriminating and mapping the C3 and C4 composition of grasslands in the northern Great Plains, USA. *Ecological Informatics*, **2**, 89-93.

FORESTRY COMMISSION (2006) *New Forest Inclosures – New Forest District Inclosure Forest Design Plans Phase B*. British Forestry Commission, Edinburgh.

FORESTRY COMMISSION (2000). *Management Plan for the Crown Lands of the New Forest 2001-2006*. British Forestry Commission, Edinburgh.

GALVAO, L. S., PONZONI, F. J., *et al.* (2004). Sun and view angle effects on NDVI determination of land cover types in the Brazilian Amazon region with hyperspectral data. *International Journal of Remote Sensing*, **25**, 1861-1879.

References

GAMON, J. A., FIELD, C. B., *et al.* (1993). Functional Patterns in an annual grassland during an AVIRIS overflight. *Remote Sensing of Environment***44**, 239-253.

GAMON, J. A. and SURFUS, J. S. (1999). Assessing leaf pigment content and activity with a reflectometer. *New Phytologist* **143**, 105-117.

GAMON, J.A., J. PENUELAS and FIELD, C.B. (1992). A narrow waveband spectral index that tracks diurnal changes in photosynthetic efficiency.**4**, 35-44.

GAO, X., A. R. HUETE, *et al.* (2000). Optical-biophysical relationships of vegetation spectra without background contamination. *Remote Sensing of Environment*,**74**, 609-620.

GAO, F., SCHAAF, C. B., *et al.* (2003). Detecting vegetation structure using a kernel-based BRDF model. *Remote Sensing of Environment***86**, 198-205.

GAO, F., *et al.*(2004). Deriving albedo from coupled MERIS and MODIS surface products. *Proceedings MERIS user workshop*, Frascati, Italy. European Space Agency, Noordwijk, The Netherlands

GAUSMAN, H. W. (1977). Reflectance of Leaf Components. *Remote Sensing of Environment*,**6**, 1-9.

GER, 2000, GER 3700 Specifications, <http://www.ger.com/3700.html>, Accessed: November 2006.

GEERKEN, R., ZAITCHIK, B., *et al.* (2005). Classifying rangeland vegetation type and coverage from NDVI time series using fourier filtered cycle similarity. *International Journal of Remote Sensing***26**, 5535-5554.

GIBSON, P. J. and POWER, C.H. (2000). *Introductory Remote Sensing - Digital Image Processing and Applications*. London: Routledge.

References

GILMANOV, T. G., TIESZEN, L. L. *et al.* (2005) Integration of CO₂ flux and remotely-sensed data for primary production and ecosystem respiration analyses in the Northern Great Plains: potential for quantitative spatial extrapolation. *Global Ecology and Biogeography*, **14**, 271-292.

GITELSON, A. A., and MERZLYAK, M. N. (1996). Signature analysis of leaf reflectance spectra: Algorithm development for remote sensing of chlorophyll. *Journal of Plant Physiology*, **148**, 494– 500.

GITELSON, A. A. and MERZLYAK, M. N. (1997). Remote estimation of chlorophyll content in higher plant leaves. *International Journal of Remote Sensing* **18**, 2691-2697.

GITELSON, A. A., VIÑA, A., VERMA, S. B., RUNDQUIST, D. C., ARKEBAUER, T. J., KEYDAN, G., LEAVITT, B., CIGANDA, V., BURBA, G. G. and SUYKER, A. E. (2006). Relationship between gross primary production and chlorophyll content in crops: Implications for the synoptic monitoring of vegetation productivity. *Journal of Geophysical Research*, **111**, 1248-1261.

GOBRON, N., PINTY, B., *et al.* (1999). The MERIS Global Vegetation Index (MGVI): description and preliminary application. *International Journal of Remote Sensing*, **20**, 1917-1927.

GOETZ, A.F.H., VANE, S. J., and ROCK, B.N. (1985). Imaging spectrometry for Earth remote sensing. *Science*, **218**, 1020 – 1024.

GOND, V., DE PURY, D. G. G., *et al.* (1999). Seasonal variations in leaf area index, leaf chlorophyll, and water content; scaling-up to estimate *f*PAR and carbon balance in a multilayer, multispecies temperate forest. *Tree Physiology*, **19**, 673-679.

GOULDEN, M. L., WINSTON, G. C. *et al.* (2006). An eddy covariance mesonet to measure the effect of forest age on land-atmosphere exchange. *Global Change Biology*, **12**, 2146-2162.

References

GRACE, J., NICHOL, M., *et al.*, (2007). Can we measure terrestrial photosynthesis from space directly, using spectral reflectance and fluorescence? *Global Change Biology*, **13**, 1484-1497.

GRAETZ, D.(1990). Remote sensing of terrestrial ecosystem structure: an ecologist's pragmatic view. *Ecological Studies*, **79**, 5-30.

GUPTA, R. K., PRASAD, S., *et al.* (1998). Evaluation of spatial upscaling algorithms for different land cover types. *Advances in Space Research*. **22**, 625-628.

GUYOT, G., and BARET, F. (1988). Utilisation de la haute résolution spectrale poursuivre l'état des couverts végétaux. *Proceedings of the 4th International Colloquium on Spectral Signatures of Objects in Remote Sensing*. ESA SP-287, Assois, France, 279–286.

HABOUDANE, D., MILLER, J. R., *et al.* (2004). Hyperspectral vegetation indices and novel algorithms for predicting green LAI of crop canopies: Modeling and validation in the context of precision agriculture. *Remote Sensing of Environment*, **90**, 337-352.

HABOUDANE, D., TREMBLAY, N., *et al.* (2008). Remote estimation of crop chlorophyll content using spectral indices derived from hyperspectral data. *IEEE Transactions on Geoscience and Remote Sensing*, **46**, 423-437.

HABOUDANE, D., MILLER, J. R., TREMBLAY, N., ZARCO-TEJADA, P. J., and DEXTRAZE, L.(2002). Integrated narrow-band vegetation indices for prediction of crop chlorophyll content for application to precision agriculture. *Remote Sensing of Environment*, **81**, 416–426.

HANHONG, B.and SICHER, R. (2004). Changes of soluble protein expression and leaf metabolite levels in *Arabidopsis thaliana* grown in elevated atmospheric carbon dioxide. *Field Crops Research*, **90**, 61–73

References

HEINSCH, F. A., ZHAO, M., RUNNING, S. W. *et al.* (2006). Evaluation of remote sensing based terrestrial productivity from MODIS using regional eddy flux network observations. *IEEE Transactions on Geoscience and Remote Sensing*, **44**, 1908-1925.

HEINSCH, F. A., REEVES, M., VOTAVA, P., KANG, S., MILESI, C. *et al.* (2003). *User's Guide: GPP and NPP (MOD17A2/A3) Products*. NASA MODIS Land Algorithm. Version 2.0. NASA Algorithm Theoretical Basis Document (ATBD). Data Assimilation Office, Goddard Space Flight Center, Greenbelt.

HABOUDANE, D., MILLER, J.R., PATTEY, E., ZARCO-TEJADA, P.J., STRACHAN, I. (2004). Hyperspectral vegetation indices and novel algorithms for predicting green LAI of crop canopies: modeling and validation in the context of precision agriculture, *Remote Sensing of Environment*, **90**, 337-352.

HARRIS, A. and DASH, J. (2009). Assessing gross primary productivity in North American ecosystems using a chlorophyll-based vegetation index. *New Dimensions in Earth Observation. Proceedings of the 2009 Annual Conference of the Remote Sensing and Photogrammetry Society (RSPSoc 2009)*. Remote Sensing and Photogrammetry Society, Nottingham (CD ROM).

HILL, M. J., HELD, A. A., *et al.* (2006). MODIS spectral signals at a flux tower site: Relationships with high-resolution data, and CO₂ flux and light use efficiency measurements. *Remote Sensing of Environment*, **103**, 351-368.

HOLBEN, B. N. (1986). Characteristics of maximum-value composite images from temporal AVHRR data. *International Journal of Remote Sensing*, **7**, 1417-1434.

HORLER, D. N. DOCKRAY, H., M., *et al.* (1983). The red edge of plant leaf reflectance. *International Journal of Remote Sensing*, **4**, 273-288.

HOUBORG, R., SOEGAARD, H., *et al.* (2007). Combining vegetation index and model inversion methods for the extraction of key vegetation biophysical parameters using Terra and Aqua MODIS reflectance data. *Remote Sensing of Environment*, **106**, 39-58.

References

HOUBORG, R., ANDERSON, M., *et al.* (2009). Utility of an image-based canopy reflectance modelling tool for remote estimation of LAI and leaf chlorophyll content at the field scale. *Remote Sensing of Environment***113**, 259-274.

HOUGHTON, J.T., DING, Y., GRIGGS, D.J., NOGUER, M., VAN DERLINDEN, P.J., DAI, X., MASKELL, and JOHNSON, K. (eds) (2001). *Intergovernmental Panel on Climate Change, The Scientific Basis. Contribution of Working Group I to the Third assessment Report of the Intergovernmental Panel on Climate Change*, Cambridge University Press, Cambridge UK.

HU, B. X., LUCHT, W., *et al.* (1997). Validation of kernel-driven semi-empirical models for the surface bidirectional reflectance distribution function of land surfaces. *Remote Sensing of Environment*,**62**, 201-214.

HUETE, A. R. (1988). A Soil-Adjusted Vegetation Index (SAVI). *Remote Sensing of Environment*,**25**, 295-309.

HUETE, A., C. JUSTICE, *et al.* (1994). Development of vegetation and soil indexes for MODIS-EOS. *Remote Sensing of Environment*,**49**, 224-234.

HUETE, A., JUSTICE, C., and VAN LEEUWEN, W. (1999). *MODIS vegetation index (MOD13). Algorithm Theoretical Basis Document (ATBD)*. http://modis.gsfc.nasa.gov/data/atbd/atbd_mod13.pdf.

IPCC (2007). *Climate change 2007: The Physical Science Basis*: Cambridge University Press, Cambridge.

JACQUEMOUD, S., BACOUR, C., POILVÉ, H., and FRANGI, J. P. (2000). Comparison of four radiative transfer models to simulate plant canopy reflectance: Direct and inverse mode. *Remote Sensing of Environment*, **74**, 471–481.

JACQUEMOUD, S. and BARET, F. (1990). PROSPECT: A model of leaf optical properties spectra. *Remote Sensing of Environment*, **34**, 75–91.

References

- JACQUEMOUD, S., BARET, F., *et al.* (1995). Extraction of vegetation biophysical parameters by inversion of the PROSPECT plus SAIL models on sugar-beet canopy reflectance data - application to TM and AVIRIS sensors. *Remote Sensing of Environment*, **52**, 163-172.
- JACQUEMOUD, S., USTIN, S. L., *et al.* (1996). Estimating leaf biochemistry using the PROSPECT leaf optical properties model. *Remote Sensing of Environment*, **56**, 194-202.
- JAGO, R. A., CUTLER, M.E. and CURRAN, P.J. (1999). Estimation of canopy chlorophyll concentration from field and airborne spectra. *Remote Sensing of Environment*, **68**, 217-224.
- JAKUBAUSKAS, M. E., LEGATES, D. R., *et al.* (2001). Harmonic analysis of time-series AVHRR NDVI data. *Photogrammetric Engineering and Remote Sensing*, **67**, 461-470.
- JORDAN, C. F. (1969). Derivation of leaf area index from quality of light on the forest floor. *Ecology*, **50**, 663–666.
- JUSTICE, C.O., BELWARD, A., *et al.* (2000). Developments in the ‘validation’ of satellite sensor products for the study of the land surface. *International Journal of Remote Sensing*, **21**, 3383-3390.
- JUSTICE, C. O., TOWNSHEND, J. R. G., *et al.* (1985). Analysis of the phenology of global vegetation using meteorological satellite data. *International Journal of Remote Sensing*, **6**, 1271-1318.
- JUSTICE, C. O. and TUCKER, C. J. (2009). Coarse Spatial Resolution Optical Sensors. In *The SAGE Handbook of Remote Sensing* (ed.) Warner, T., Foody, G.M., Duane, M., SAGE Publications Ltd, London, 139-149.

References

JUSTICE, C. O., VERMOTE, E., *et al.* (1998). The Moderate Resolution Imaging Spectroradiometer (MODIS): Land remote sensing for global change research. *IEEE Transactions on Geoscience and Remote Sensing*, **36**, 1228-1249.

KAMMER, P. M. (2002). Developmental responses of subdominant grassland species to current weather conditions and their relevance for annual vegetation changes. *Folia Geobotanica*, **37**, 185-204.

KANE, V. R., GILLESPIE, A. R., *et al.* (2008). Interpretation and topographic compensation of conifer canopy self-shadowing. *Remote Sensing of Environment*, **112**, 3820-3832.

KAUFMAN, Y. J. and TANRE, D. (1992). Atmospherically Resistant Vegetation Index (ARVI) for EOS-MODIS. *IEEE Transactions on Geoscience and Remote Sensing*, **30**, 261-270.

KIMBALL, J.S., McDONALD, K.C., RUNNING, S.W. *et al.* (2004) Satellite radar remote sensing of seasonal growing seasons for boreal and subalpine evergreen forests. *Remote Sensing of Environment*, **90**, 243–258.

KIMBALL, J. S., McDONALD, K. C., *et al.* (2004). Satellite radar remote sensing of seasonal growing seasons for boreal and subalpine evergreen forests. *Remote Sensing of Environment*, **90**, 243-258.

KODANI, E., AWAYA, Y., TANAKA, K., and MATSUMURA, N. (2002). Seasonal patterns of canopy structure, biochemistry and spectral reflectance in a broad-leaved deciduous *Fagus crenata* canopy. *Forest Ecology and Management*, **167**, 233–249.

KOKALY, R. F. and CLARK, R. N. (1999). Spectroscopic determination of leaf biochemistry using band-depth analysis of absorption features and stepwise multiple linear regression. *Remote Sensing of Environment*, **67**, 267-287.

KUUSK, A. (1996), A computer-efficient plant canopy reflectance model. *Computers and Geoscience*, **22**, 149–163.

References

LANKESTER, T., LOIAL, C., HUBBARD, S., ANDERSSON, K., and PITTELLA, G. (2003). HIPROGEN A system to generate high level products, *Proceedings of the MERIS User Workshop*, ESA-ESRIN, Frascati, Italy. European Space Agency, Noordwijk.

LAWSON, T., CRAIGON, J., *et al.* (2001). Photosynthetic response to elevated CO₂ and O₃ in field grown potato (*Solanum Tuberosum*), *Journal of Plant Physiology*, **158**, 309-323.

LE MAIRE, G., FRANCOIS, C., *et al.* (2008). Calibration and validation of hyperspectral indices for the estimation of broadleaved forest leaf chlorophyll content, leaf mass per area, leaf area index and leaf canopy biomass. *Remote Sensing of Environment*, **112**, 3846-3864.

LEROY, M., and HAUTECOEUR, O. (1999). Anisotropy-corrected vegetation indexes derived from POLDER/ADEOS. *IEEE Transactions on Geoscience and Remote Sensing*, **37**, 1698–1708.

LEROY, M. and BREON F. M. (1996). Angular signatures of surface reflectances from airborne POLDER data. *Remote Sensing of Environment* **57**, 97-107.

LI, R., MIN, Q. *et al.* (2009). Estimation of evapotranspiration in a mid-latitude forest using the microwave emissivity difference vegetation index (EDVI). *Remote Sensing of Environment*, **113**, 2011-2018.

LIANG, S. L., FANG, H. L., *et al.* (2002). Validating MODIS land surface reflectance and albedo products: methods and preliminary results. *Remote Sensing of Environment*, **83**, 149-162.

LIANG, S. L. and STRAHLER, A. H. (1994). Retrieval of surface BRDF from multiangle remotely-sensed data. *Remote Sensing of Environment* **50**, 18-30.

References

LIANG, S., STRAHLER, A. H., BARNESLEY, M., BOREL, C., GERSTL, S., DINER, D., PRATA, A., and WALTHALL, C. (2000). Multiangle remote sensing: Past, present and future. *Remote Sensing Reviews*, **18**, 83–102.

LIANG, S.L., ZHENG, T., WANG, D., *et al.* (2007). Mapping high-resolution incident photosynthetically active radiation over land from polar-orbiting and geostationary satellite data. *Photogrammetric Engineering and Remote Sensing*, **73**, 1085–1089

LUCHT, W. and LEWIS, P. (2000). Theoretical noise sensitivity of BRDF and albedo retrieval from the EOS-MODIS and MISR sensors with respect to angular sampling. *International Journal of Remote Sensing*, **21**, 81-98.

MARKWELL, J., OSTERMAN, J.C., MITCHELL, L. (1995). Calibration of the Minolta SPAD-502 leaf chlorophyll meter. *Photosynthetic Research*, **46**, 467-472.

MARTIN, M. E. and ABER, J. D. (1997). High spectral resolution remote sensing of forest canopy lignin, nitrogen, and ecosystem processes. *Ecological Applications*, **7**, 431-443.

MATTHEWS, D. H. (2007). Implications of CO₂ fertilization for future climate change in a coupled climate–carbon model. *Global Change Biology*, **13**, 1068–1078,

McDONALD, A. J., GEMMELL, F. M., *et al.* (1998). Investigation of the utility of spectral vegetation indices for determining information on coniferous forests. *Remote Sensing of Environment*, **66**, 250-272.

MENZEL, A., SPARKS, T. H., *et al.* (2006). European phenological response to climate change matches the warming pattern. *Global Change Biology*, **12**, 1969-1976.

MENZEL, A., SPARKS, T. H., ESTRELLA, N. and ROY, D.B.(2006). Altered geographic and temporal variability in phenology in response to climate change. *Global Ecology and Biogeography*, **15**, 498-504.

References

MILLER, J. R., WU, J. Y., *et al.* (1991). Seasonal patterns in leaf reflectance red-edge characteristics. *International Journal of Remote Sensing*, **12**, 1509-1523.

MILTON, E. J., SCHAEPMAN, M. E., ANDERSON, K., KNEUBUHLER, M., and FOX, N. (2007). Progress in field spectroscopy. *Remote Sensing of Environment*, **113**, S92–S109.

MONTEITH, J. L. (1972). Solar-radiation and productivity in tropical ecosystems. *Journal of Applied Ecology*, **9**, 747-766.

MOORTHY, I., MILLER, J. R. *et al.* (2003). Needle chlorophyll content estimation: A comparative study of PROSPECT and LIBERTY. *23rd International Geoscience and Remote Sensing Symposium (IGARSS 2003)*, Toulouse, France, IEEE.

MORAN, R. and D. PORATH (1980). Chlorophyll determination in intact tissues using N,N-Dimethylformamide. *Plant Physiology*, **65**, 478-479.

MORISSETTE, J.T., PRIVETTE, J.L., and JUSTICE, C.O. (2002). A framework for the validation of MODIS Land products. *Remote Sensing of Environment*, **83**, 77–96.

MORISSETTE, J. T., BARET, F., *et al.* (2006). Special issue on global land product validation. *IEEE Transactions on Geoscience and Remote Sensing*, **44**, 1695-1697.

MORISSETTE, J.T., BARET, F. and LIANG, S. (2006). Overview of the special issue on global land product validation. *IEEE Transactions on Geoscience and Remote Sensing*, **44**, 1695-1697.

MORISSETTE, J. T., BARET, F., *et al.* (2006a). Validation of global moderate-resolution LAI products: A framework proposed within the CEOS Land Product Validation subgroup. *IEEE Transactions on Geoscience and Remote Sensing*, **44**, 1804-1817.

References

MUNDEN, R., CURRAN, P. J., *et al.* (1994). The relationship between red edge and chlorophyll concentration in the Broadbalk winter-wheat experiment at Rothamsted. *International Journal of Remote Sensing*,**15**, 705-709.

MUTANGA, O. AND SKIDMORE, A. K. (2004). Narrow band vegetation indices overcome the saturation problem in biomass estimation. *International Journal of Remote Sensing*,**25**, 3999-4014.

MYNENI, R. B. and ASRAR, G. (1994). Atmospheric effects and spectral vegetation indexes. *Remote Sensing of Environment*,**47**, 390-402.

MYNENI, R. B., ASRAR, G., *et al.* (1992). A 3-dimensional radiative-transfer method for optical remote-sensing of vegetated land surfaces. *Remote Sensing of Environment*,**41**, 105-121.

MYNENI, R. B., HOFFMAN, S., *et al.* (2002). Global products of vegetation leaf area and fraction absorbed PAR from year one of MODIS data. *Remote Sensing of Environment*,**83**, 214-231.

MYNENI, R. B., KEELING, C. D., *et al.* (1997). Increased plant growth in the northern high latitudes from 1981 to 1991. *Nature*,**386**, 698-702.

MYNENI, R. B. and WILLIAMS, D. L., (1994). On the relationship between FAPAR and NDVI. *Remote Sensing of Environment*,**49**, 200-211.

NEMANI, R. R., KEELING, C. D.,*et al.* (2003). Climate-driven increases in global terrestrial net primary production from 1982 to 1999. *Science*, **300**, 1560-1563

NEWTON, A.C., HILL, R.H., ECHEVERRÍA, C., GOLICHER, D., REYBENAYAS, J.M., *et al.* (2009). Remote sensing and the future of landscape ecology. *Progress in Physical Geography*,**33**, 528–546.

References

NICODEMUS, F., J., RICHMOND, J., HSIA, I. GINSBERG, T. (1977). *Geometrical considerations and nomenclature for reflectance*, NBS, US Department of Commerce, Washington, D.C.

NIGH, G. D. (2006). Impact of climate, moisture regime, and nutrient regime on the productivity of Douglas-fir in coastal British Columbia, Canada. *Climatic Change*, **76**, 321-337.

NIGHTINGALE, J. M., COOPS, N. C. *et al.* (2007). Comparison of MODIS gross primary production estimates for forests across the USA with those generated by a simple process model, 3-PGS. *Remote Sensing of Environment*, **109**, 500-509.

O'Neill, A.L., Kupiec, J.A. and Curran, P.J. (2002) Biochemical and reflectance variation throughout the canopy of a Sitka spruce plantation. *Remote Sensing of Environment*, **80**, 134-142.

OPPELT, N. AND MAUSER, W. (2004). Hyperspectral monitoring of physiological parameters of wheat during a vegetation period using AVIS data. *International Journal Remote Sensing*, **25**, 145–159.

PALLENT, J. (2007). *SPSS Survival Manual: A Step by Step Guide to Data Analysing using SPSS for Windows (Third Edition)*. Open University Press, Maidenhead.

PERRY, M. AND HOLLIS, D. (2005). The development of a new set of long-term climate averages for the United Kingdom. *International Journal of Climatology*, **25**, 1023-1039.

PETTORELLI, N., VIK, J. O. *et al.* (2005). Using the satellite-derived NDVI to assess ecological responses to environmental change. *Trends in Ecology and Evolution*, **20**, 503-510.

PFUFF, A. S. P., KERR, S., *et al.* (2000). The Kyoto protocol and payments for tropical forest: An interdisciplinary method for estimating carbon-offset supply and

References

increasing the feasibility of a carbon market under the CDM. *Ecological Economics*,**35**, 203-221.

PIAO, S. L., FRIEDLINGSTEIN, P., *et al.* (2007). Growing season extension and its impact on terrestrial carbon cycle in the Northern Hemisphere over the past 2 decades. *Global Biogeochemical Cycles*,**21**.

PIAO, S. L., MOHAMMAT, A. *et al.* (2006). NDVI-based increase in growth of temperate grasslands and its responses to climate changes in China. *Global Environmental Change-Human and Policy Dimensions*,**16**, 340-348.

PORRA, R. J. (2002). The chequered history of the development and use of simultaneous equations for the accurate determination of chlorophylls a and b. *Photosynthesis Research*, **733**, 149-156.

PORRA, R. J., THOMPSON, W. A. *et al.* (1989). Determination of accurate extinction coefficients and simultaneous-equations for assaying chlorophyll-a and chlorophyll-b extracted with 4 different solvents - verification of the concentration of chlorophyll standards by atomic-absorption spectroscopy. *Biochimica et Biophysica Acta*, **975**, 384-394.

PRENTICE, C., FARQUHAR, G., FASHAM, M.,*et al.* (2001) The carbon cycle and atmospheric carbon dioxide. In: *Climate Change 2001: The Scientific Basis* (eds Houghton J.,*et al.*), Cambridge University Press, Cambridge, UK, 183–237.

PRICE, J. C. (1990). On the Information-Content of Soil Reflectance Spectra. *Remote Sensing of Environment*,**33**, 113-121.

QI, J., CHEHBOUNI, A., *et al.* (1994). A Modified Soil Adjusted Vegetation Index. *Remote Sensing of Environment*,**48**, 119-126.

REED, B.C., WHITE, M., BROWN, J.F. (2003). Remote sensing. In *Phenology: An Integrative Environmental Science*. Schwartz, S.C. (ed). Kluwer Academic Publishers. Netherlands, 365-381.

References

REED, B. C., BROWN, J. F., VANDERZEE, D., LOVELAND, T. R., MERCHANT, J. W., and OHLEN, D. O. (1994). Measuring phenological variability from satellite imagery. *Journal of Vegetation Science*, **5**, 703–714.

REED, B. C. (2006). Trend analysis of time-series phenology of North America derived from satellite data. *GIScience and Remote Sensing*, **43**, 24-38.

REEVES, M. C., ZHAO, M., *et al.* (2005). Usefulness and limits of MODIS GPP for estimating wheat yield. *International Journal of Remote Sensing*, **26**, 1403-1421.

RICHTER, R. and SCHLAPFER, D. (2002). Geo-atmospheric processing of airborne imaging spectrometry data. Part 2: atmospheric/topographic correction. *International Journal of Remote Sensing*, **23**, 2631–2649.

ROCK, B. N., WILLIAMS, D. L., *et al.* (1994). High-spectral-resolution field and laboratory optical reflectance measurements of red spruce and eastern hemlock needles and branches. *Remote Sensing of Environment*, **47**, 176-189.

RONDEAUX, G., STEVEN, M., *et al.* (1996). Optimization of soil-adjusted vegetation indices. *Remote Sensing of Environment*, **55**, 95-107.

ROSENTHAL, S. I. and CAMM E. L. (1997). Photosynthetic decline and pigment loss during autumn foliar senescence in western larch (*Larix occidentalis*). *Tree Physiology*, **17**, 767-775.

ROSENZWEIG, C., KAROLY, D., *et al.* (2008). Attributing physical and biological impacts to anthropogenic climate change. *Nature*, **453**, 353-U20.

ROSSINI M. *et al.* (2007). Monitoraggio delle condizioni della farnia (*Quercus robur* L.) Nel parco del Ticino mediante tecniche di telerilevamento iperspettrale. *Forest*, **4**, 194-203 (In Italian).

References

ROUSE, J. W., HAAS, R. H., SCHELL, J. A., and DEERING, D. W., (1973). Monitoring vegetation systems in the Great Plains with ERTS. *Third ERTS Symposium*, Washington, DC, NASA, Greenbelt, 309–317.

RUNNING, S., NEMANI, R., HEINSCH, F., ZHAO, M., REEVES, M., and HASHIMOTO, H. (2004). A continuous satellite-derived measure of global terrestrial primary production. *BioScience*, **54**, 547–560.

SANCHEZ, J.M., CASELLES, V., NICLOS, R., *et al.* (2009). Estimating energy balance fluxes above a boreal forest from radiometric temperature observations. *Agricultural and Forest Meteorology*, **149**, 1037-1049

SANDMEIER, S., MULLER, C., *et al.* (1998). Sensitivity analysis and quality assessment of laboratory BRDF data. *Remote Sensing of Environment*, **64**, 176-191.

SCHAAF, C. B. AND STRAHLER, A. H. (1994). Validation of bi-directional and hemispherical reflectances from a geometric-optical model using ASAS imagery and pyranometer measurements of a spruce forest. *Remote Sensing of Environment*, **49**, 138-144.

SCHAAF, C. B., GAO, F., *et al.* (2002). First operational BRDF, albedo nadir reflectance products from MODIS. *Remote Sensing of Environment*, **83**, 135-148.

SCHAEPMAN, M. (2009). Imaging spectrometers. *In The SAGE Handbook of Remote Sensing*. Warner, T., Foody, G.M., Duane, M. (ed.) SAGE Publications Ltd, London, 166-178.

SCHAEPMAN-STRUB, G., SCHAEPMAN, M. E., *et al.* (2006). Reflectance quantities in optical remote sensing-definitions and case studies. *Remote Sensing of Environment*, **103**, 27-42.

SCHLEIP, C., MENZEL, A., *et al.* (2006). The use of Bayesian analysis to detect recent changes in phenological events throughout the year. *Agricultural and Forest Meteorology*, **141**, 179-191.

References

SELLERS, P. J., MEESON, B. W., *et al.* (1995). Remote-sensing of the land-surface for studies of global change - models, algorithms, experiments. *Remote Sensing of Environment*, **51**, 3-26.

SELLERS, P. J., BERRY, J. A., COLLATZ, G. J. FIELD C. B. and HALL. F. G. (1992). Canopyreflectance, photosynthesis and transpiration. III. A reanalysis using improved leafmodels and a new canopy integration scheme. *Remote Sensing of Environment*, **42**, 187-216.

SKOWRONSKI, N., CLARK, K. *et al.* (2005). Remotely sensed measurements of forest structure and fuel loads in the Pinelands of New Jersey. *Remote Sensing of Environment*, **108**, 123-129.

SMITH, K. L., STEVEN, M. D. and COLLS, J. J.(2004). Use of hyperspectral derivative ratios in the red-edge region to identify plant stress responses to gas leaks. *Remote Sensing of Environment*, **92**, 207-217.

SOUDANI, K., FRANCOIS, C., *et al.* (2006). ComPARative analysis of IKONOS, SPOT, and ETM+ data for leaf area index estimation in temperate coniferous and deciduous forest stands. *Remote Sensing of Environment*, **102**, 161-175.

SPARKS, T.H., CROXTON, P.J., COLLINSON, N. and TAYLOR, P.(2005).Example of phenological change, past and present, in UKfarming, *Annals of Applied Biology*, **146**, 531-537.

SPARKS, T. H. (2006). How well do the central England temperature and the England and Wales precipitation series represent the climate of the UK? *International Journal of Climatology* **26**, 2287-2292.

STARKS, P. J., ZHAO, D. L., *et al.* (2006). Development of canopy reflectance algorithms for real-time prediction of Bermuda grass pasture biomass and nutritive values. *Crop Science*, **46**, 927-934.

References

TIAN, Y., WOODCOCK, C.E., *et al.* (2002) Multiscale analysis and validation of the MODIS LAI product II. Sampling strategy. *Remote Sensing of Environment*, **83**, 431–441.

TOWNSHEND, J. R. G. and JUSTICE, C. O. (2002). Towards operational monitoring of terrestrial systems by moderate-resolution remote sensing. *Remote Sensing of Environment*, **83**, 34-42.

TOWNSHEND, J., JUSTICE, C., GURNEY, C., and MCMANUS, J.(1992), The impact of misregistration on change detection. *IEEE Transactions on Geoscience and Remote Sensing*, **30**, 1054–1060.

TREITZ, P. M. and HOWARTH, P. J. (1999). Hyperspectral remote sensing for estimating biophysical parameters of forest ecosystems. *Progress in Physical Geography*, **23**, 359-390.

TUCKER, C. J., and SELLERS, P. J. (1986). Satellite remote sensing of primary production. *International Journal of Remote Sensing*, **7**, 1395–1416.

TURNER, D. P., RITTS, W. D., *et al.* (2006). Evaluation of MODIS NPP and GPP products across multiple biomes. *Remote Sensing of Environment*, **102**, 282-292.

TURNER, D. P., OLLINGER, S., SMITH, M. L., KRANKINA, O., and GREGORY, M. (2004). Scaling net primary production to a MODIS footprint in support of Earth observing system product validation. *International Journal of Remote Sensing*, **25**, 1961–1979.

UDDLING, J., GELANG-ALFREDSSON, J., PIIKKI, K., and PLEIJEL, H. (2007). Evaluating the relationship between leaf chlorophyll concentration and SPAD-502 chlorophyll metre readings. *Photosynthetic Research*, **91**, 37–46.

USTIN, S.L., ZARCO-TEJADA, P.J. and ASNER, G.P. (2001). The role of hyperspectral data in understanding the global carbon cycle, *AVIRIS Workshop*. JPL-NASA, Greenbelt.

References

USTIN, S. L., ROBERTS, D.A., GAMON, J.A., ASNER, G.P. and GREEN, R.O. (2004). Using imaging spectroscopy to study ecosystem processes and properties. *Bioscience*, **54**, 523-534.

USTIN, S. L., *et al.* (2009), Retrieval of foliar information about plant pigment systems from high resolution spectroscopy, *Remote Sensing of Environment*, 103, Supplement 1, S67-S77.

USTIN, S. L., ROBERTS, D.A, *et al.* (2004). Using imaging spectroscopy to study ecosystem processes and properties. *Bioscience*, **54**, 523-534.

VAN DER MEER, F., BAKKER, W., *et al.* (2001). Spatial scale variations in vegetation indices and above-ground biomass estimates: implications for MERIS. *International Journal of Remote Sensing*, **22**, 3381-3396.

VAN LEEUWEN, W. J. D., HUETE, A. R., *et al.* (1999). MODIS vegetation index compositing approach: A prototype with AVHRR data. *Remote Sensing of Environment*, **69**, 264-280.

VAN LEEUWEN, W. J. D., HUETE, A. R., *et al.* (1997). Deconvolution of remotely sensed spectral mixtures for retrieval of LAI, faPAR and soil brightness. *Journal of Hydrology*, **188-189**, 697-724.

VAN OLDENBORGH, G.J. (2006). Extraordinarily mild European autumn 2006 due to global warming. *Global Change Newsletter*, **67**, 18-20.

VAN VILET, A. J. H., DE GROOT, R. S., *et al.* (2003). The European Phenology Network. *International Journal of Biometeorology*, **47**, 202-212.

VERSTRAETE, M. M., GOBRON, N., *et al.* (2008). An automatic procedure to identify key vegetation phenology events using the JRC-FAPAR products. *Advances in Space Research*, **41**, 1773-1783.

References

VERSTRAETE, M. M., PINTY, B., *et al.* (1999). MERIS potential for land applications. *International Journal of Remote Sensing*,**20**, 1747-1756.

WALTERSHEA, E. A., PRIVETTE, J., *et al.* (1997). Relations between directional spectral vegetation indices and leaf area and absorbed radiation in alfalfa. *Remote Sensing of Environment*,**61**, 162-177.

WARING, R.H., LAW, B., GOULDEN, M.L., BASSOW, S.L., MCCREIGHT, R.W., WOFSY, S.C., BAZZAZ, F.A.(1995). Scaling gross ecosystem production at Harvard Forest with remote sensing: a comparison of estimates from a constrained quantum-use efficiency model and eddy correlation. *Plant, Cell and Environment***18**, 1201–1213.

WARING, R.H., MILNER, K.S., JOLLY, W.M., PHILLIPS, L., MCWETHY, D.(2005). A basis for predicting site index and maximum growth potential across the Pacific and Inland Northwest U.S.A with aMODIS satellite-derived vegetation index. *Forest Ecology and Management*,**228**, 285–291.

WARING, R. H., COOPS, N. C., *et al.* (2006). MODIS enhanced vegetation index predicts tree species richness across forested ecoregions in the contiguous USA. *Remote Sensing of Environment*,**103**, 218-226.

WATKISS, P., DOWNING, T., HANDLEY, C., BUTTERFIELD, R.(2005). The Impacts and Costs of Climate Change. AEA Technology and Stockholm Environment Institute, Didcot and Oxford http://europa.eu.int/comm/environment/climat/pdf/final_report2.pdf.

WELLBURN, A. R. (1994). The spectral determination of chlorophyll-a and chlorophyll-a, as well as total carotenoids, using various solvents with spectrophotometers of different resolution. *Journal of Plant Physiology*,**144**, 307-313.

WHITE, M., A., DE BEURS, K., M., INOUE, D., W. *et al.* (2009). Intercomparison, interpretation, and assessment of spring phenology in North

References

America estimated from remote sensing for 1982–2006. *Global change biology*, **15**, 1141-1152.

WHITE, M. A., THORNTON, P. E. *et al.* (1997). A continental phenology model for monitoring vegetation responses to interannual climatic variability. *Global Biogeochemical Cycles*, **11**, 217-234.

WOOLLEY, J. T. (1971). Reflectance and Transmittance of Light by Leaves. *Plant Physiology*, **47**, 656.

WU, C., ZHENG, N., *et al.* (2009). Remote estimation of gross primary production in wheat using chlorophyll-related vegetation indices. *Agricultural and Forest Meteorology*, **149**, 1015-1021.

WULDER, M. (1998). Optical remote-sensing techniques for the assessment of forest inventory and biophysical parameters, *Progress in Physical Geography*, **22**, 449 – 476.

WYLIE, B., FOSNIGHT, E. A., GILMANOV, T.G., *et al.* (2007). Adaptive data-driven models for estimating carbon fluxes in the Northern Great Plains, *Remote Sensing of Environment*, **106**, 399–413.

WYLIE, B. K., JOHNSON, D. A., *et al.* (2003). Calibration of remotely sensed, coarse resolution NDVI to CO₂ fluxes in a sagebrush-steppe ecosystem. *Remote Sensing of Environment*, **85**, 243-255.

XIAO, X. M. (2006). Light absorption by leaf chlorophyll and maximum light use efficiency. *IEEE Transactions on Geoscience and Remote Sensing*, **44**, 1933-1935.

XIAO, X. HOLLINGER, M., D., *et al.* (2004). Satellite-based modeling of gross primary production in an evergreen needleleaf forest. *Remote Sensing of Environment*, **89**, 519-534.

References

XIAO, X. M., ZHANG, Q. Y., *et al.* (2005). Satellite-based modeling of gross primary production in a seasonally moist tropical evergreen forest. *Remote Sensing of Environment*,**94**, 105-122.

YANG, L. M., WYLIE, B. K., *et al.* (1998). An analysis of relationships among climate forcing and time-integrated NDVI of grasslands over the US northern and central Great Plains. *Remote Sensing of Environment*,**65**, 25-37.

YANG, W., SHABANOV, N. V., *et al.* (2006). Analysis of leaf area index products from combination of MODIS Terra and Aqua data. *Remote Sensing of Environment*,**104**, 297-312.

YODER, B. J. and WARING, R. H. (1994). The normalized difference vegetation index of small Douglas-fir canopies with varying chlorophyll concentrations. *Remote Sensing of Environment*.**49**, 81–91.

ZARCO-TEJADA, P. J., MILLER, J. R., *et al.* (2000). Chlorophyll fluorescence on vegetation apparent reflectance: II laboratory and airborne canopy-level measurements with hyperspectral data. *Remote Sensing of Environment*, **74**, 582-595.

ZARCO-TEJADA, P. J., MILLER, J. R., *et al.* (2001). Scaling-up and model inversion methods with narrowband optical indices for chlorophyll content estimation in closed forest canopies with hyperspectral data. *IEEE Transactions on Geoscience and Remote Sensing*,**39**, 1491-1507.

ZARCO-TEJADA, P. J., USTIN, S. L., *et al.* (2005). Temporal and spatial relationships between within-field yield variability in cotton and high-spatial hyperspectral remote sensing imagery. *Agronomy Journal*,**97**, 641-653.

ZARCO-TEJADA, P. J., MILLER, J. R. *et al.* (2004). Hyperspectral indices and model simulation for chlorophyll estimation in open-canopy tree crops. *Remote Sensing of Environment*,**90**, 463-476.

References

ZARCO-TEJADA, P.J., and MILLER, J.R. (1999). Land cover mapping at BOREAS using red edge spectral parameters from CASI imagery. *Journal of Geophysical Research*, **104**, 921-933.

ZURITA-MILLA, R., CLEVERS, J.G.P.W., SCHAEPMAN, M.E. and KNEUBUEHLER, M. (2007) Effects of MERIS L1b radiometric calibration on regional land cover mapping and land products. *International Journal of Remote Sensing*. **28**, 653-673.

ZHANG, Q. Y., MIDDLETON, E. M., *et al.* (2009). Can a satellite-derived estimate of the fraction of PAR absorbed by chlorophyll (FAPAR (chl)) improve predictions of light-use efficiency and ecosystem photosynthesis for a boreal aspen forest? *Remote Sensing of Environment*, **113**, 880-888.

ZHANG, Q. Y., XIAO, X. M., *et al.* (2006). Characterization of seasonal variation of forest canopy in a temperate deciduous broadleaf forest, using daily MODIS data. *Remote Sensing of Environment*, **105**, 189-203.

ZHANG, X. Y., FRIEDL, M. A., *et al.* (2003). Monitoring vegetation phenology using MODIS. *Remote Sensing of Environment*, **84**, 471-475.

ZHANG, Y. J., XU, M., *et al.* (2009). Can Landsat imagery detect tree line dynamics? *International Journal of Remote Sensing*, **30**, 1327-1340.

ZHANG, Y., CHEN, J. M., MILLER, J. R. and NOLAND, T.L. (2008). Leaf chlorophyll content retrieval from airborne hyperspectral remote sensing imagery. *Remote Sensing of Environment*, **112**, 3234-3247.

ZHANG, L., WYLIE, B., LOVELAND, T., *et al.* (2007). Evaluation and comparison of gross primary production estimates on the Northern Great Plains grasslands, *Remote Sensing of Environment*, **106**, 173–189.

ZHANG, Q. Y., XIAO, X. M., BRASWELL, B., LINDER, E., BARET, F., and MOORE, B. (2005). Estimating light absorption by chlorophyll, leaf and canopy in a

References

deciduous broadleaf forest using MODIS data and a radiative transfer model. *Remote Sensing of Environment*, **99**, 357–371.

ZHANG, X., FRIEDL, M.A., SCHAAF, C.B., *et al.* (2004). The footprint of urban climates on vegetation phenology. *Geophysical Research Letters*, **31**, 12209.

ZHANG, X., FRIEDL, M.A., SCHAAF, C.B., *et al.* (2003). Monitoring vegetation phenology using MODIS. *Remote Sensing of Environment*, **84**, 471–475.

References

Websites:

English Nature GIS website <http://www.gis.naturalengland.org.uk> - accessed 21st October 2007.

EUMETSAT news website <http://www.eumetsat.int/Home/Main/Media/News> - accessed 6th March 2007.

Met Office, UK Climate Impacts Programme (UKIP) website www.metoffice.gov.uk/research/hadleycentre/obsdata/ukcip/index.html - accessed 29th January 2009

NASA Warehouse Inventory Search Tool (WIST) website <https://wist.echo.nasa.gov/api/> - accessed 30th March 2009.

NERC Earth Observation Data Centre (NEODC), UK website www.neodc.rl.ac.uk - accessed 15th April 2009.

APPENDICES

Appendices

Appendix 2 – Wet chemistry assay results

| July wet chemistry analysis | | | | | | | | | | | | | | |
|-----------------------------|--------|---------|---------|-----------|-------|-------|-----------|-----------|-----------|--------------------|----------------|-----------|---------------------------------------|--------------|
| | | | | Constants | 12.25 | | | | | Sample Volume 10ml | | | | |
| Batch 24/07 | | | | | 2.55 | | | | | | | | | |
| | | | | | 20.31 | | | | | | | | | |
| | | | | | 4.91 | | | | | | | | | |
| Sample | Sample | Wt (mg) | Abs 664 | Abs 647 | Chl a | Chl b | Total Chl | Ratio a/b | Chla Mg/g | Chl b mg/g | Total Chl mg/g | Chl mg/m2 | | |
| Branch No. | | | | | | | | | | | | | | |
| PG2 | | 102.00 | 2.99 | 2.05 | 31.41 | 26.89 | 58.30 | 1.17 | 3.08 | 2.64 | 5.72 | | Comments: | Date |
| PG3 | | 101.10 | 2.99 | 2.03 | 31.42 | 26.50 | 57.92 | 1.19 | 3.11 | 2.62 | 5.73 | | Frozen pine 3-4 cm needles | 24th July 07 |
| PG4 | | 100.00 | 2.63 | 2.02 | 27.09 | 28.10 | 55.19 | 0.96 | 2.71 | 2.81 | 5.52 | | Frozen pine 3-4 cm needles | 24th July 07 |
| PG5 | | 101.10 | 1.98 | 1.38 | 20.69 | 18.40 | 39.09 | 1.12 | 2.05 | 1.82 | 3.87 | | Fresh pine 3-4cm needles | 24th July 07 |
| PG6 | | 100.00 | 1.97 | 1.35 | 20.73 | 17.81 | 38.54 | 1.16 | 2.07 | 1.78 | 3.85 | | Fresh pine 3-4cm needles | 24th July 07 |
| PG7 | | 100.00 | 2.06 | 1.16 | 22.31 | 13.47 | 35.78 | 1.66 | 2.23 | 1.35 | 3.58 | | Long needle fresh | 24th July 07 |
| PG8 | | 101.00 | 2.06 | 1.16 | 22.31 | 13.47 | 35.78 | 1.66 | 2.21 | 1.33 | 3.54 | | Long needle fresh | 24th July 07 |
| PG9 | | 99.80 | 1.94 | 1.36 | 20.28 | 18.14 | 38.42 | 1.12 | 2.03 | 1.82 | 3.85 | | Heather, location 6, 2 | 24th July 07 |
| PG10 | | 101.00 | 1.94 | 1.36 | 20.28 | 18.14 | 38.42 | 1.12 | 2.01 | 1.80 | 3.80 | | Heather, location 6, 3 | 24th July 07 |
| PG11 | | 102.00 | 1.17 | 0.61 | 12.83 | 6.56 | 19.40 | 1.96 | 1.26 | 0.64 | 1.90 | | Pine 2cm needles, silver tinge | 24th July 07 |
| PG12 | | 101.00 | 1.17 | 0.61 | 12.83 | 6.60 | 19.43 | 1.94 | 1.27 | 0.65 | 1.92 | | Pine 2cm needles, silver tinge | 24th July 07 |
| PG13 | | 100.00 | 2.09 | 1.59 | 21.57 | 22.04 | 43.61 | 0.98 | 2.16 | 2.20 | 4.36 | | Pine needles 4-5 cm | 24th July 07 |
| PG14 | | 101.00 | 2.09 | 1.59 | 21.60 | 22.01 | 43.61 | 0.98 | 2.14 | 2.18 | 4.32 | | Pine needles 4-5 cm | 24th July 07 |
| PG15 | | 101.00 | 1.98 | 1.67 | 20.05 | 24.18 | 44.22 | 0.83 | 1.98 | 2.39 | 4.38 | | Pine needles 2 cm, relately soft, 2 | 24th July 07 |
| PG16 | | 100.00 | 1.99 | 1.67 | 20.09 | 24.20 | 44.29 | 0.83 | 2.01 | 2.42 | 4.43 | | Pine needles 2 cm, relately soft, 2 | 24th July 07 |
| PG17 | | 104.00 | 1.98 | 1.74 | 19.76 | 25.58 | 45.35 | 0.77 | 1.90 | 2.46 | 4.36 | | Pine, similar to above, but thin grey | 24th July 07 |
| PG18 | | 101.00 | 1.98 | 1.74 | 19.76 | 25.62 | 45.38 | 0.77 | 1.96 | 2.54 | 4.49 | | Pine, similar to above, but thin grey | 24th July 07 |
| PG19 | | 102.00 | 1.97 | 1.65 | 19.91 | 23.86 | 43.77 | 0.83 | 1.95 | 2.34 | 4.29 | | Pine long needles, 8-10 cm | 24th July 07 |
| PG20 | | 101.00 | 1.97 | 1.65 | 19.86 | 23.86 | 43.73 | 0.83 | 1.97 | 2.36 | 4.33 | | Pine long needles, 8-10 cm | 24th July 07 |
| PG21 | | 101.00 | 1.96 | 1.41 | 20.46 | 18.92 | 39.38 | 1.08 | 2.03 | 1.87 | 3.90 | | Gorse | 24th July 07 |
| PG22 | | 99.00 | 1.96 | 1.41 | 20.43 | 18.97 | 39.40 | 1.08 | 2.06 | 1.92 | 3.98 | | Gorse | 24th July 07 |
| PG23 | | 100.00 | 2.01 | 1.73 | 20.17 | 25.23 | 45.40 | 0.80 | 2.02 | 2.52 | 4.54 | | Pine, star arrangement | 24th July 07 |
| PG24 | | 101.00 | 2.01 | 1.72 | 20.24 | 25.04 | 45.28 | 0.81 | 2.00 | 2.48 | 4.48 | | Pine, star arrangement | 24th July 07 |
| PG25 | | 103.00 | 1.73 | 0.89 | 18.88 | 9.68 | 28.55 | 1.95 | 1.83 | 0.94 | 2.77 | | Pine, 3cm needles, in smaller bunch | 24th July 07 |
| PG26 | | 101.00 | 1.73 | 0.90 | 18.94 | 9.79 | 28.73 | 1.94 | 1.88 | 0.97 | 2.84 | | Pine, 3cm needles, in smaller bunch | 24th July 07 |
| PG33 | | 99.00 | 1.90 | 1.73 | 18.88 | 25.76 | 44.64 | 0.73 | 1.91 | 2.60 | 4.51 | | pine, frozen, see pg 17, green strip | 24th July 07 |
| PG34 | | 100.00 | 1.90 | 1.70 | 18.97 | 25.17 | 44.13 | 0.75 | 1.90 | 2.52 | 4.41 | | pine, frozen, see pg 17, green strip | 24th July 07 |
| PG35 | | 101.00 | 2.06 | 1.09 | 22.43 | 12.03 | 34.46 | 1.86 | 2.22 | 1.19 | 3.41 | | Long needle frozen | 24th July 07 |

Appendix 1 (a). Example of the wet chemistry assay results to derive chlorophyll content in coniferous species in the New Forest.

Appendices

| Species | Model equation | R ² |
|-------------|-----------------------------------|----------------|
| Wheat | $y = 0.118x^2 + 0.919x + 7.925$ | 0.97 |
| Grass | $y = 0.019x^2 + 6.814x - 49.249$ | 0.80 |
| Maize | $y = 0.091x^2 + 1.594x + 32.41$ | 0.92 |
| Potato | $y = 5.384x + 76.35$ | 0.73 |
| Onion | $y = 8.365x - 75.42$ | 0.82 |
| Barley | $y = 26.40x - 693.4$ | 0.75 |
| Sugar Beet | $y = 8.70x + 5.62$ | 0.92 |
| Oak | $y = 10.08x - 77.61$ | 0.81 |
| Beech | $y = 0.047x + 26.52$ | 0.87 |
| Birch | $y = 0.002x^2 + 0.1299x - 17.599$ | 0.71 |
| Common lime | $y = 0.128x + 10.10$ | 0.79 |
| Sycamore | $y = 0.0545x + 17.331$ | 0.88 |
| Fern | $y = 13.47x - 91.50$ | 0.71 |

Appendix 1 (b). SPAD calibration equation derived from wet chemistry assay methods.

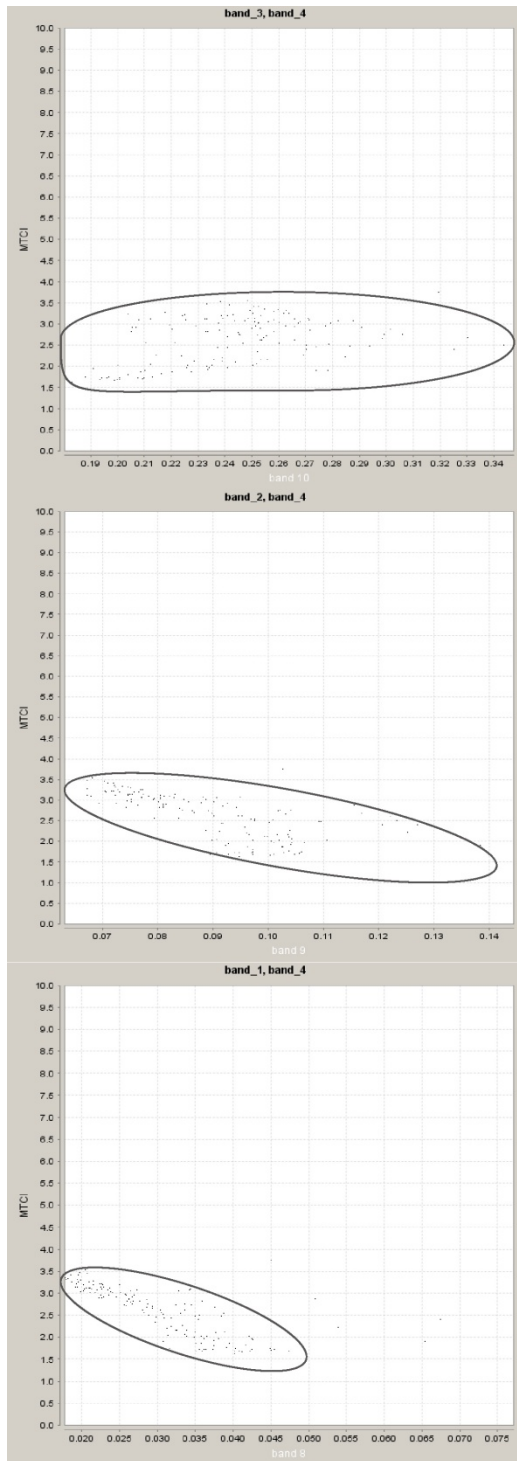
Appendix 2 – AZGCORR code

```
#
azgcorr -mUK99 osgb02.cgrf -p 2 2 -1 c192b011b.hdf -3 c192b013a_2m.hdf -eb
NFdem.bsq -edx 1 8000 8000 410000 90005 449995 130000 5 0 1 3 1 -1 -v
azgcorr -mUK99 osgb02.cgrf -p 2 2 -1 c192b021b.hdf -3 c192b023a_2m.hdf -eb
NFdem.bsq -edx 1 8000 8000 410000 90005 449995 130000 5 0 1 3 1 -1 -v
azgcorr -mUK99 osgb02.cgrf -p 2 2 -1 c192b031b.hdf -3 c192b033a_2m.hdf -eb
NFdem.bsq -edx 1 8000 8000 410000 90005 449995 130000 5 0 1 3 1 -1 -v
azgcorr -mUK99 osgb02.cgrf -p 2 2 -1 c192b041b.hdf -3 c192b043a_2m.hdf -eb
NFdem.bsq -edx 1 8000 8000 410000 90005 449995 130000 5 0 1 3 1 -1 -v
azgcorr -mUK99 osgb02.cgrf -p 2 2 -1 c192b051b.hdf -3 c192b053a_2m.hdf -eb
NFdem.bsq -edx 1 8000 8000 410000 90005 449995 130000 5 0 1 3 1 -1 -v
azgcorr -mUK99 osgb02.cgrf -p 2 2 -1 c192b061b.hdf -3 c192b063a_2m.hdf -eb
NFdem.bsq -edx 1 8000 8000 410000 90005 449995 130000 5 0 1 3 1 -1 -v
azgcorr -mUK99 osgb02.cgrf -p 2 2 -1 c192b071b.hdf -3 c192b073a_2m.hdf -eb
NFdem.bsq -edx 1 8000 8000 410000 90005 449995 130000 5 0 1 3 1 -1 -v

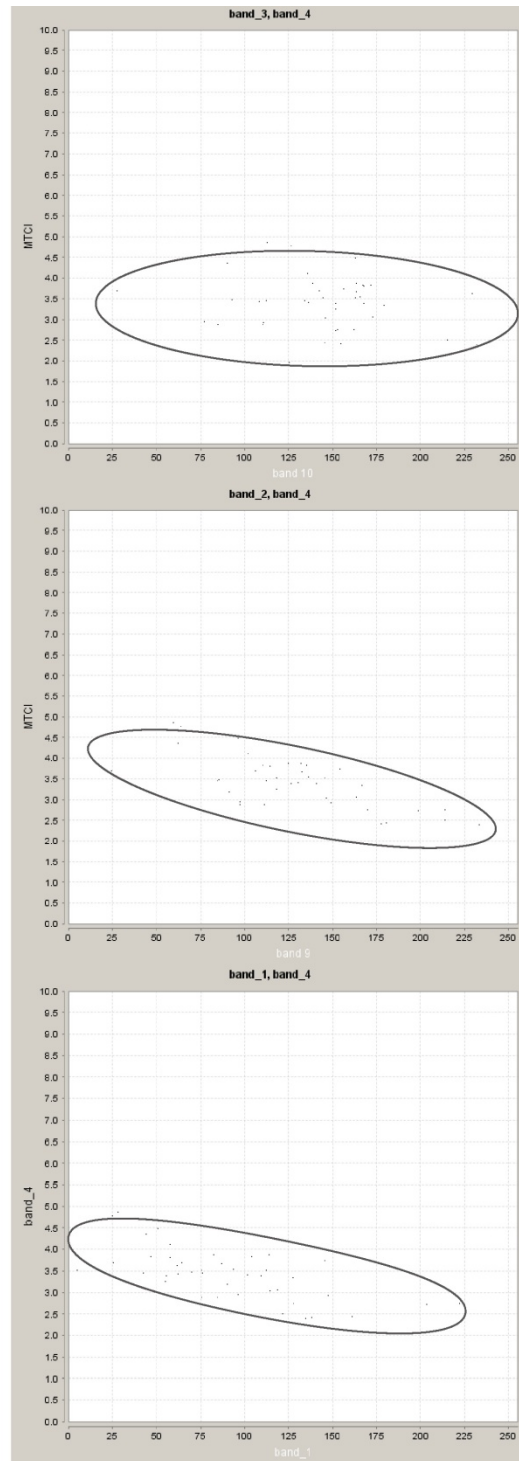
#
#Now generate GeoTIF colour composites of bands 9,6 and 4 for visual check
#Also useful for ENVI header data
#
#azexhdf -h c192b013a_2m.hdf -bl 9 6 4 -1 -G c192b013a_2m.tif
#
#
#Finally, create BIL files containing all of the bands
#
#azexhdf -h c192b013a_2m.hdf -B c192b013a_2m.bil
```

Appendix 3 – Radiometric variation between MERIS and CASI-2

a) MERIS



b) CASI



Appendix 3. The radiometric response from MERIS (a) and CASI (b) sensors for reflectance measured in bands 10, 9 and 8. Note that on the x axis MERIS units are in reflectance, CASI DN values

Appendix 4 - Publications

ALMOND, S.F., BOYD, D.S., CURRAN, P. J. and DASH, J.(2007). The response of UK vegetation to elevated temperatures in 2006: Coupling Envisat MERIS Terrestrial Chlorophyll Index (MTCI) and mean air temperature. *Challenges for Earth Observation: Technical and Commercial. Proceedings of the 2008 Annual Conference of the Remote Sensing and Photogrammetry Society (RSPSoc 2007)*, Remote Sensing and Photogrammetry Society, Nottingham(CD ROM).

ALMOND, S., BOYD, D.S., CURRAN, P.J., and DASH, J. (2008). Evaluation of the relationships between vegetation indices and canopy chlorophyll content for different view angle and soil backgrounds. *Proceedings of the 2008 Annual Conference of the Remote Sensing and Photogrammetry Society (RSPSoc 2008)*, 10-12 September 2008, University of Exeter. The Remote Sensing and Photogrammetry Society, Nottingham (CD ROM).

DASH, J., ALMOND, S., BOYD, D.S., and CURRAN, P.J. (2008). Multi-scale analysis and validation of the Envisat MERIS Terrestrial Chlorophyll Index (MTCI) in woodland and arable farmland. *Proceedings of the 2nd MERIS / (A)ATSR User Workshop*, Frascati, Italy, 22 - 26 September, 2008.

ALMOND, S., BOYD, D.S., DASH, J., CURRAN, P.J. (2009). Multi-scale analysis and validation of the Envisat MERIS Terrestrial Chlorophyll Index (MTCI) in woodland. *New Dimensions in Earth Observation. Proceedings of the 2009 Annual Conference of the Remote Sensing and Photogrammetry Society (RSPSoc 2009)*. Remote Sensing and Photogrammetry Society, Nottingham(CD ROM).

ALMOND, S., BOYD, D.S., CURRAN, P.J., DASH, J. and HILL, R. (2009). Phenological trends of vegetation in Southern England from Envisat MERIS Terrestrial Chlorophyll Index (MTCI) data. *International Journal of Remote Sensing*. Submitted.

Appendices

ALMOND, S., BOYD, D.S., CURRAN, P.J., DASH, J. and HILL, R. (2009). Multi-scale analysis and validation of the Envisat MERIS Terrestrial Chlorophyll Index (MTCI) in woodland and arable farmland. *Sensors*. Submitted.

Appendix 5 – SPSS Results

One-way ANOVA examining the effect of view angle on MTCI

Descriptives

| MTCI | | | | | | | | | |
|-------|----|--------|----------------|------------|----------------------------------|-------------|---------|---------|--|
| | N | Mean | Std. Deviation | Std. Error | 95% Confidence Interval for Mean | | Minimum | Maximum | |
| | | | | | Lower Bound | Upper Bound | | | |
| 1 | 4 | 1.8950 | .53929 | .26964 | 1.0369 | 2.7531 | 1.45 | 2.68 | |
| 2 | 4 | 1.8900 | .53260 | .26630 | 1.0425 | 2.7375 | 1.48 | 2.67 | |
| 3 | 4 | 1.8950 | .50613 | .25306 | 1.0896 | 2.7004 | 1.49 | 2.63 | |
| 4 | 4 | 1.8325 | .49406 | .24703 | 1.0463 | 2.6187 | 1.42 | 2.55 | |
| 5 | 4 | 1.8000 | .43962 | .21981 | 1.1005 | 2.4995 | 1.48 | 2.45 | |
| 6 | 4 | 1.8025 | .39920 | .19960 | 1.1673 | 2.4377 | 1.58 | 2.40 | |
| 7 | 4 | 1.8900 | .39657 | .19828 | 1.2590 | 2.5210 | 1.62 | 2.47 | |
| Total | 28 | 1.8579 | .42170 | .07969 | 1.6943 | 2.0214 | 1.42 | 2.68 | |

Test of Homogeneity of Variances

| MTCI | | | | |
|------------------|-----|-----|------|--|
| Levene Statistic | df1 | df2 | Sig. | |
| .109 | 6 | 21 | .994 | |

ANOVA

| MTCI | | | | | |
|----------------|----------------|----|-------------|------|-------|
| | Sum of Squares | df | Mean Square | F | Sig. |
| Between Groups | .048 | 6 | .008 | .035 | 1.000 |
| Within Groups | 4.754 | 21 | .226 | | |
| Total | 4.801 | 27 | | | |

Appendices

One-way ANOVA examining the effect of view angle on REP

Descriptives

REP

| | N | Mean | Std. Deviation | Std. Error | 95% Confidence Interval for Mean | | Minimum | Maximum |
|-------|----|----------|----------------|------------|----------------------------------|-------------|---------|---------|
| | | | | | Lower Bound | Upper Bound | | |
| 1 | 4 | 717.7125 | 2.05437 | 1.02718 | 714.4435 | 720.9815 | 716.13 | 720.73 |
| 2 | 4 | 717.4925 | 1.90041 | .95021 | 714.4685 | 720.5165 | 715.90 | 720.25 |
| 3 | 4 | 717.5750 | 1.78012 | .89006 | 714.7424 | 720.4076 | 716.19 | 720.16 |
| 4 | 4 | 717.3150 | 1.85563 | .92782 | 714.3623 | 720.2677 | 715.77 | 720.00 |
| 5 | 4 | 717.1975 | 1.59406 | .79703 | 714.6610 | 719.7340 | 716.10 | 719.55 |
| 6 | 4 | 717.2875 | 1.48296 | .74148 | 714.9278 | 719.6472 | 716.46 | 719.51 |
| 7 | 4 | 717.7500 | 1.39052 | .69526 | 715.5374 | 719.9626 | 716.59 | 719.69 |
| Total | 28 | 717.4757 | 1.54529 | .29203 | 716.8765 | 718.0749 | 715.77 | 720.73 |

Test of Homogeneity of Variances

REP

| Levene Statistic | df1 | df2 | Sig. |
|------------------|-----|-----|------|
| .140 | 6 | 21 | .989 |

ANOVA

REP

| | Sum of Squares | df | Mean Square | F | Sig. |
|----------------|----------------|----|-------------|------|------|
| Between Groups | 1.120 | 6 | .187 | .062 | .999 |
| Within Groups | 63.354 | 21 | 3.017 | | |
| Total | 64.474 | 27 | | | |

Appendices

One-way ANOVA examining the effect of view angle on NDVI

Descriptives

NDVI

| | N | Mean | Std. Deviation | Std. Error | 95% Confidence Interval for Mean | | Minimum | Maximum |
|-------|----|-------|----------------|------------|----------------------------------|-------------|---------|---------|
| | | | | | Lower Bound | Upper Bound | | |
| 1 | 4 | .7725 | .05500 | .02750 | .6850 | .8600 | .72 | .85 |
| 2 | 4 | .7700 | .05354 | .02677 | .6848 | .8552 | .71 | .84 |
| 3 | 4 | .7750 | .04655 | .02327 | .7009 | .8491 | .72 | .83 |
| 4 | 4 | .7750 | .04203 | .02102 | .7081 | .8419 | .73 | .83 |
| 5 | 4 | .7775 | .04113 | .02056 | .7121 | .8429 | .73 | .83 |
| 6 | 4 | .7900 | .03742 | .01871 | .7305 | .8495 | .75 | .84 |
| 7 | 4 | .7950 | .04123 | .02062 | .7294 | .8606 | .75 | .85 |
| Total | 28 | .7793 | .04127 | .00780 | .7633 | .7953 | .71 | .85 |

ANOVA

Test of Homogeneity of Variances

NDVI

| Levene Statistic | df1 | df2 | Sig. |
|------------------|-----|-----|------|
| .135 | 6 | 21 | .990 |

NDVI

| | Sum of Squares | df | Mean Square | F | Sig. |
|----------------|----------------|----|-------------|------|------|
| Between Groups | .002 | 6 | .000 | .170 | .982 |
| Within Groups | .044 | 21 | .002 | | |
| Total | .046 | 27 | | | |

Appendices

One-way ANOVA examining the effect of view angle on EVI

Descriptives

EVI

| | N | Mean | Std. Deviation | Std. Error | 95% Confidence Interval for Mean | | Minimum | Maximum |
|-------|----|--------|----------------|------------|----------------------------------|-------------|---------|---------|
| | | | | | Lower Bound | Upper Bound | | |
| 1 | 4 | 2.1275 | .29792 | .14896 | 1.6534 | 2.6016 | 1.72 | 2.43 |
| 2 | 4 | 2.1100 | .29360 | .14680 | 1.6428 | 2.5772 | 1.73 | 2.44 |
| 3 | 4 | 2.1350 | .28781 | .14390 | 1.6770 | 2.5930 | 1.75 | 2.44 |
| 4 | 4 | 2.1250 | .29011 | .14506 | 1.6634 | 2.5866 | 1.75 | 2.45 |
| 5 | 4 | 2.1125 | .28826 | .14413 | 1.6538 | 2.5712 | 1.77 | 2.47 |
| 6 | 4 | 2.1075 | .22515 | .11257 | 1.7492 | 2.4658 | 1.83 | 2.38 |
| 7 | 4 | 2.1300 | .23409 | .11705 | 1.7575 | 2.5025 | 1.84 | 2.40 |
| Total | 28 | 2.1211 | .24301 | .04592 | 2.0268 | 2.2153 | 1.72 | 2.47 |

Test of Homogeneity of Variances

EVI

| Levene Statistic | df1 | df2 | Sig. |
|------------------|-----|-----|------|
| .062 | 6 | 21 | .999 |

ANOVA

EVI

| | Sum of Squares | df | Mean Square | F | Sig. |
|----------------|----------------|----|-------------|------|-------|
| Between Groups | .003 | 6 | .000 | .006 | 1.000 |
| Within Groups | 1.592 | 21 | .076 | | |
| Total | 1.594 | 27 | | | |

Appendices

One-way ANOVA examining the effect of view angle on OSAVI

Descriptives

OSAVI

| | N | Mean | Std. Deviation | Std. Error | 95% Confidence Interval for Mean | | Minimum | Maximum |
|-------|----|-------|----------------|------------|----------------------------------|-------------|---------|---------|
| | | | | | Lower Bound | Upper Bound | | |
| 1 | 4 | .9325 | .04573 | .02287 | .8597 | 1.0053 | .88 | .99 |
| 2 | 4 | .9375 | .04500 | .02250 | .8659 | 1.0091 | .88 | .99 |
| 3 | 4 | .9400 | .03916 | .01958 | .8777 | 1.0023 | .89 | .98 |
| 4 | 4 | .9400 | .03559 | .01780 | .8834 | .9966 | .89 | .97 |
| 5 | 4 | .9400 | .03559 | .01780 | .8834 | .9966 | .89 | .97 |
| 6 | 4 | .9475 | .03862 | .01931 | .8860 | 1.0090 | .91 | .99 |
| 7 | 4 | .9550 | .03416 | .01708 | .9006 | 1.0094 | .92 | 1.00 |
| Total | 28 | .9418 | .03539 | .00669 | .9281 | .9555 | .88 | 1.00 |

Test of Homogeneity of Variances

OSAVI

| Levene Statistic | df1 | df2 | Sig. |
|------------------|-----|-----|------|
| .103 | 6 | 21 | .995 |

ANOVA

OSAVI

| | Sum of Squares | df | Mean Square | F | Sig. |
|----------------|----------------|----|-------------|------|------|
| Between Groups | .001 | 6 | .000 | .138 | .989 |
| Within Groups | .033 | 21 | .002 | | |
| Total | .034 | 27 | | | |

Appendices

One-way ANOVA examining the effect of view angle on MERIS REP

Descriptives

MERIS REP

| | N | Mean | Std. Deviation | Std. Error | 95% Confidence Interval for Mean | | Minimum | Maximum |
|-------|----|----------|----------------|------------|----------------------------------|-------------|---------|---------|
| | | | | | Lower Bound | Upper Bound | | |
| 1 | 4 | 721.7075 | 2.85419 | 1.42710 | 717.1658 | 726.2492 | 719.43 | 725.81 |
| 2 | 4 | 721.6850 | 2.76493 | 1.38246 | 717.2854 | 726.0846 | 719.32 | 725.53 |
| 3 | 4 | 721.7225 | 2.73443 | 1.36721 | 717.3714 | 726.0736 | 719.20 | 725.46 |
| 4 | 4 | 721.4550 | 2.54863 | 1.27431 | 717.3996 | 725.5104 | 719.54 | 725.10 |
| 5 | 4 | 721.1575 | 2.50948 | 1.25474 | 717.1644 | 725.1506 | 719.04 | 724.76 |
| 6 | 4 | 721.3000 | 2.46666 | 1.23333 | 717.3750 | 725.2250 | 718.55 | 724.55 |
| 7 | 4 | 721.8200 | 1.91797 | .95898 | 718.7681 | 724.8719 | 720.52 | 724.67 |
| Total | 28 | 721.5496 | 2.26861 | .42873 | 720.6700 | 722.4293 | 718.55 | 725.81 |

Test of Homogeneity of Variances

MERIS REP

| Levene Statistic | df1 | df2 | Sig. |
|------------------|-----|-----|------|
| .094 | 6 | 21 | .996 |

ANOVA

MERIS REP

| | Sum of Squares | df | Mean Square | F | Sig. |
|----------------|----------------|----|-------------|------|-------|
| Between Groups | 1.485 | 6 | .248 | .038 | 1.000 |
| Within Groups | 137.473 | 21 | 6.546 | | |
| Total | 138.958 | 27 | | | |